COMPARATIVE STUDY OF THE STRUCTURAL, CHEMICAL AND PHYSICAL PROPERTIES OF ACTIVATED SLUDGE FLOC FROM DIFFERENT FULL-SCALE WASTEWATER TREATMENT SYSTEMS

by

Mee Chu Cheung

A thesis submitted in conformity with the requirements
for the degree of Master of Applied Science
Graduate Department of Chemical Engineering and Applied Chemistry
University of Toronto

ABSTRACT

To better understand bioflocculation and the role of extracellular polymeric substances (EPS) on sludge properties, a comparative study with respect to the EPS composition, floc size and density, and ultra-structure of the floc matrix has been conducted. Four full-scale activated sludge systems treating domestic sewage, poultry processing wastes, petroleum refinery wastes and potato processing wastes were studied. The systems studied represent a range of configurations and effluents treated. The sludge properties during both functional and dysfunctional periods in one treatment system were also studied. In addition, the relation between sludge settling and EPS composition was investigated. Protein was found to be the dominant component in the extracted EPS followed by carbohydrate, DNA and acidic polysaccharide regardless of the types of wastewater and operating conditions. These four components formed a more or less constant percentage composition in the organic matrix with 77-81% protein, 11-15% carbohydrate, 4-9% DNA and 3-5% acidic polysaccharide. DNA and acidic polysaccharide were the most labile components in EPS. The level of EPS is inversely associated with the MCRT (sludge age) of the systems. Hence, the operating conditions such as sludge age may be more important than the microbial community alone as a factor in affecting the composition of EPS. The higher levels of DNA and acidic polysaccharide in EPS may be associated with better sludge settling as the correlation coefficients between the levels of DNA and acidic polysaccharide in EPS with sludge volume index (SVI) were - 0.61 and -0.71, respectively. The levels of protein and carbohydrate during the dysfunctional periods of system treating potato processing wastewater (system-Po) were 56% and 71% higher than functional periods. The higher levels of protein and carbohydrate may be associated with a higher bound water content and surface charge of the floc. Low F/M ratio may account for the higher level of EPS and abundant growth of the filaments during the dysfunctional periods of system-Po. The α-mannopyranosyl, α-glucopyranosyl, N-acetylglucosamine and N-acetylneuraminic acid residues were present at the floc matrices from all systems studied. However, the spatial distribution of these residues was different among them. A significantly lower amount of N-acetylglucosamine and N-acetylneuraminic acid residues was observed in the matrix of flocs from the system treating poultry processing wastewater. This indicates a possible role of N-acetylglucosamine and N-acetylneuraminic acid in bioflocculation.

ACKNOWLEDGMENTS

I am grateful to my two supervisors, Professor Steven N. Liss and Professor D. Grant Allen, for being the special teachers to guide me through this research work. I would like to especially thank Professor Liss, who supported me financially through the Natural Sciences and Engineering Research Council of Canada Strategic Grant for this work and for my participation at the IAWQ Second International Conference in California, U.S.A., 1997. Moreover, his advice and patience in revising my writing is very appreciated.

I would like to extend my sincere appreciation to:

- Ian Droppo and Gary Leppard of National Water Research Institute, Ontario for their tremendous help and advice in making this degree possible. Special thanks go to Ian for the numerous rides to collect the samples and to NWRI in those cold days.
- Alex Dobson of Main Treatment Plant, Toronto; Bob Gillespie of Petro-Canada, Oakville; Craig Oldham of Maple Lodge Farm, Brampton; and Wally Williams of Cavendish Farms, Prince Edward Island for their assistance in providing the samples and operating data.
- John Robertson of Beak Consultants and Betz Dearborn Inc. for their recommendation about the plants for study.
- Derrick Flannigan and Marcia M. West of McMaster University, Ontario for their technical support in transmission electron microscopy.
- Kaiguo Mo of the Biotechnology Laboratory at Ryerson Polytechnic University for his assistance in applying the phenotypic fingerprinting technique.
- Alan Sheppard of the Biotechnology Laboratory at Ryerson Polytechnic University for his assistance in filaments identification.
- Rob Irish of Writing Centre and Peter Austin of Statistics Consulting Service of University of Toronto for their advice in these two technical area.
- Liao, Jennine, Renata, Valerie and Cory of the Biotechnology Laboratory at Ryerson Polytechnic University for their friendship and advice to my work.
- A very special thank goes to my husband, Tim and my family members. Without their understanding and moral support, this endeavor would have never been possible.

TABLE OF CONTENTS

LIST OF FIGURES

LIST OF TABLES

NOMENCLATURE

ρ_e	Effective density of floc [g/cm^3]
ρ_w	Density of water [g/cm^3]
ρ_f	Wet density of floc [g/cm^3]
μ	Dynamic viscosity of the water [Pa-s]
g	Acceleration of gravity [m/s^2]
AR	Aspect ratio
BNR	Biological nutrient removal
BOD	Biochemical oxygen demand [mg/L]
CER	Cation exchange resin
CHO	Carbohydrate
CM	Correlative microscopy
COM	Conventional optical microscopy
ConA	Conconavalin A
DNA	Deoxyribonucleic acid
DO	Dissolved oxygen [mg/L]
EPS	Extracellular polymeric substances
ESD (D)	Equivalent spherical diameter [μm]
FF (ϕ)	Form factor
FITC	Florescein isothiocyanate
F/M	Food-to-microorganism ratio [g BOD/ g VSS / day]
HRT	Hydraulic retention time [hour]

MCRT	Mean cell residence time [day]
MLSS	Mixed liquor suspended solids [mg/L]
MLVSS	Mixed liquor volatile suspended solids [mg/L]
Re	Reynold number
RR	Ruthenium red
SCLM	Scanning confocal laser microscopy
SVI	Sludge volume index [ml/g]
TEM	Transmission electron microscopy
UA	Uranyl acetate
v	Floc settling velocity [mm/s]
WGA	Wheat germ agglutinin

CHAPTER 1 INTRODUCTION

Separation of the suspended solids from treated effluent in biological wastewater treatment systems is a crucial step prior to the discharge of final treated water to the environment. However, Pujol and Canler (1992) estimated that at least 70% of operating systems continue to experience difficulties with settling of suspended solids in activated sludge systems which are one of the most common biological wastewater treatment processes employed. A brief survey of different treatment systems in Canada shows the prevalence of this problem (Table 1.1). Different settling strategies have been employed by plant operators to achieve a quality final effluent where the standard is established by law. Regardless of the recognition of this costly problem, it continues to be an important issue in the operation of wastewater treatment plants.

Table 1.1. Survey on settling problem from different activated sludge treatment systems.

Types of activated sludge system	Municipal	Poultry processing	Petroleum refinery	Potato processing
Prevalence	Rarely (< 1/yr.)	Once a yr.	Rarely (< 1/yr.)	Constantly
Seasonal problem	Summer	Winter	No	Constantly
Time required to resolve the problem	1 month	2-3 weeks	No data	Not resolved until new modification being installed

Conventional studies on activated sludge floc settling have strictly treated the floc as a spherical physical entity. The conditions that affect the floc in wastewater treatment systems are usually considered in the context of the bulk mixed liquor or by optical microscopy. Recently, the extracellular polymeric substances (EPS) which form the matrix of activated sludge flocs have been shown to be important in flocculation and settling (Forster and Dallas-Newton, 1980; Urbain *et al.*, 1993). The chemical properties of the surface matrix are thought to be important

in determining the strength of binding between the floc particles. However, the precise role of EPS in relation to bioflocculation and its effect on floc settling are still not completely understood. In addition, previous studies have described the relationship between floc settling and physical properties of the floc, such as size, shape and density in a gross scale which is larger than 1 micron (Magara and Nambu, 1976; Li and Ganczarczyk, 1987). Recently, the importance of microorganisms and bioorganic material to floc development and properties has been well recognized (Unz and Farrah, 1976; Buffle and Leppard 1995a and 1995b). Therefore, the study of floc properties at the fine scale (submicron) becomes more important in understanding the flocculation process.

Comprehensive studies of different activated sludge treatment systems are necessary in order to develop sound control strategies for sludge settlement. The microbial community of different activated sludge system is considered to be different depending on the wastewater composition (Tezuka, 1969). These differences in microbial community affect the sludge properties which determine the criteria for efficient and functional operation. However, studies on the properties of activated sludge from different treatment systems are still lacking.

1.1 Objectives

In an effort to better understand bioflocculation and the role of EPS on the properties of activated sludge floc, a comparative study of several full-scale activated sludge systems has been conducted. The objectives of this study were as follows:

(1) compare the characteristics of floc with respect to EPS composition, floc size and density, and structural properties among different activated sludge treatment systems;
(2) compare the characteristics of floc during functional and dysfunctional settling periods;
(3) investigate the relation between the EPS composition and sludge settling.

CHAPTER 2 LITERATURE REVIEW

The objective of biological wastewater treatment is to remove the organic matter or other constituents in the wastewater. This task is accomplished biologically using microorganisms, principally bacteria. These microorganisms cleanse the wastewater by using the organic material present as a food source to grow and regenerate. The biomass produced is either maintained in suspension in water as suspended-growth or attached in some solid medium as fixed-film. Activated sludge process is one of the most commonly used suspended-growth biological wastewater treatment processes.

2.1 Activated sludge process

An activated sludge reactor contains an aerated mass of sludge floc, surrounded by the influent wastewater, to form mixed-liquor. Activated sludge floc is made up of aggregates of microorganisms, inorganic and organic colloidal material and large particulate material which are all held together in a compact organic matrix. The termed "activated" comes from the fact that significant quantities of bacteria, fungi and protozoa which are recycled to the reactor to increase the biomass concentration. Hence, recycle of biomass can be considered as a main characteristic feature of the activated sludge process.

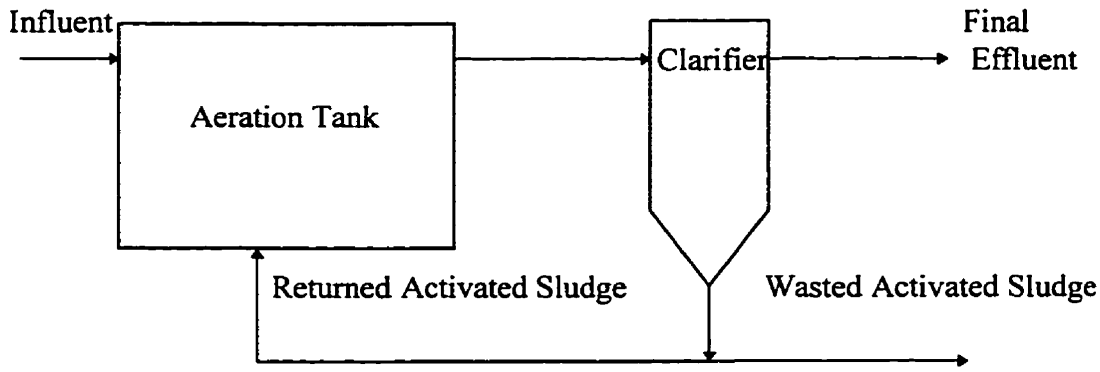

Figure 2.1. Schematic of typical activated sludge reactor (Metcalf & Eddy, 1991).

Many variations of the original process are in use today, but fundamentally they are all similar. A schematic diagram of the typical process is shown in Figure 2.1. The mixed-liquor flows through large aeration tanks which allow for a long detention time (hydraulic retention time - HRT) of between 4 to 6 hours. Oxygen is dissolved (DO) into the mixed liquor by bubble diffusers within the tank or by mechanical surface mixers which mix the liquor with air. Following this aeration period the mixed-liquor is directed to a secondary settling tank (clarifier) where the solids flocculate and settle by gravitation to form a sludge. This step is termed clarification. A portion of this sludge is sent back to the beginning of the process as return activated sludge (RAS). The period in which biomass is retained in the reactor is termed mean cell residence time (MCRT). The sludge produced in excess of the process requirements, termed as waste activated sludge (WAS), is discharged from the treatment system and handled as solid waste (Metcalf & Eddy, 1991).

Effective separation of the biomass in the settling tank is important to the operation for two reasons. Firstly, in order to ensure sufficient biomass is recycled to the aeration tank, the biomass is required to settle from the treated water and form a thickening biomass. Secondly, the discharging of suspended solids is responsible for the organic content and high turbidity in recipient water. It is important to note that unless the biomass produced from the organic matter is removed from the wastewater, complete and efficient treatment of the wastewater has not been accomplished.

2.2 Activated sludge floc and bioflocculation

Effective settling is dependent on production of individual flocs having specific physical, chemical and structural characteristics. The overall floc structure is negatively charged. The negative charge is the result of interaction between microorganisms (mainly bacteria), inorganic particles (silicate, calcium phosphate and iron oxides), multivalent cations and extracellular polymeric substances which is either from cellular metabolism and lysis or from the wastewater itself (Urbain *et al.*, 1992). This agglomeration of the active biomass is called bioflocculation. It is affected by the biological, physical and chemical properties of the treatment system. However,

the exact mechanisms of this phenomenon and the factors affecting these mechanisms are not fully understood.

A sludge surface model and filamentous backbone model have been proposed for the mechanism of bioflocculation. Tenney and Stumm (1965) proposed that polymers exposed on the microbial surface might act to adsorb and bridge between cell surfaces and therefore initiate floc formation. The bridging that occurs between bacterial cells and other particulate materials is suggested to form a heterogeneous aggregate. Tenney and Verhoff (1973) suggested further that this attachment was reversible with some type of equilibrium relationship. Forster and Dallas-Newton (1980) proposed a model on the possible structure of activated sludge floc (Figure 2.2). This model suggests that a range of inter-polymer reactions, hydrogen bonding, ionic structures and physical enmeshing is involved. The backbone model (Figure 2.3) states that the filamentous organisms form a matrix and provide a "backbone" for the build-up of the floc which was subsequently formed with the assistance of various polymer bridges between particles and smaller flocs (Sezgin *et al.*, 1978; Horan, 1990).

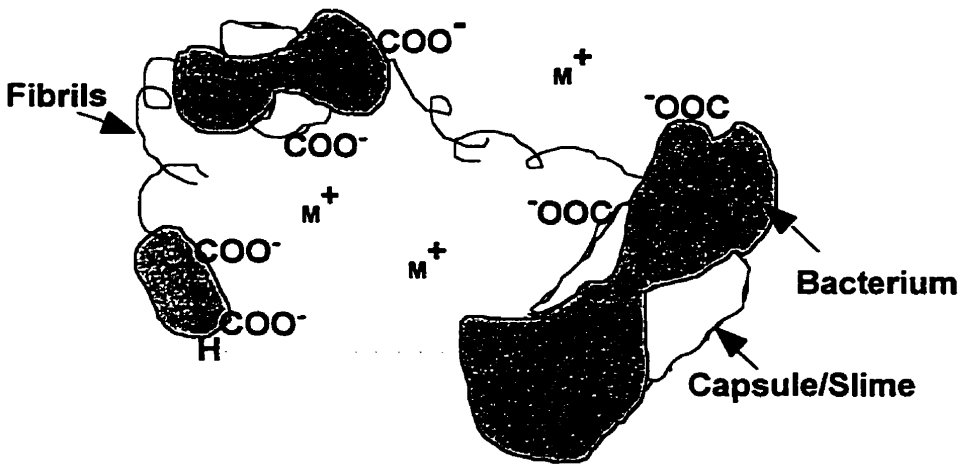

Figure 2.2. Sludge surface model for flocculation of activated sludge floc (Forster and Dallas-Newton, 1980).

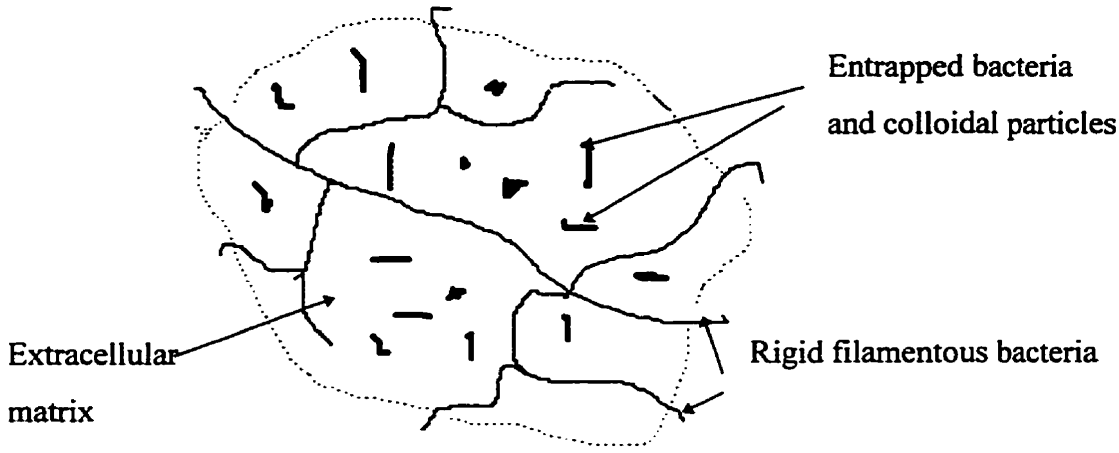

Figure 2.3. A typical activated sludge floc with filamentous bacteria (Horan, 1990).

Both of the models have much in common and are not mutually exclusive. Generally, the concept that bioflocculation is the result of the interaction of naturally produced, high molecular weight, long chain polysaccharide bridges which bring individual cells into an aggregate is widely accepted (Tenney and Verhoff, 1973; Horan, 1990). This polysaccharide is found within the extracellular matrix of the floc.

2.3 Settling problems - dysfunctional systems

Settling problems continue to be an important issue in the operation of wastewater treatment systems as mentioned in Chapter 1. Bulking is the main settling problem. A bulking sludge is one that has poor settling characteristics and poor compactability. Two principal types of sludge-bulking problems have been identified. One is filamentous bulking which is caused by the excessive growth of filamentous microorganisms (Pipes and Jones, 1963; Pipes, 1966; Rao and Washington, 1968). The other is non-filamentous bulking or viscous bulking (Jenkins, 1992). Pipes (1967) suggested that the non-filamentous bulking was caused by the presence of excessive amount of bound water in the floc particles. In addition, abundant growth of zoogloeal colonies has been observed associated with non-filamentous bulking (Novak *et al*,

1994). Jenkins (1992) suggests that viscous bulking is most probably related to the morphological characteristics of the flocs and the presence of a large amount of exocellular slime produced by particular bacteria including Zoogloea.

The precise reason for the variations in the settlement characteristics of the biomass is still unclear. Since changes in the nutritional balance are known to stimulate the production of surface biopolymers in pure bacterial cultures, similar processes are expected to occur in activated sludge. Surface polymers also control surface charge which has been shown previously to be related to settling (Forster, 1971). Therefore, the change in nature of sludge surface due to the variation in nutritional balance of the bacteria or in microbial populations is expected. Forster (1985) proposed a S-model to explain the cause of bulking (Figure 2.4).

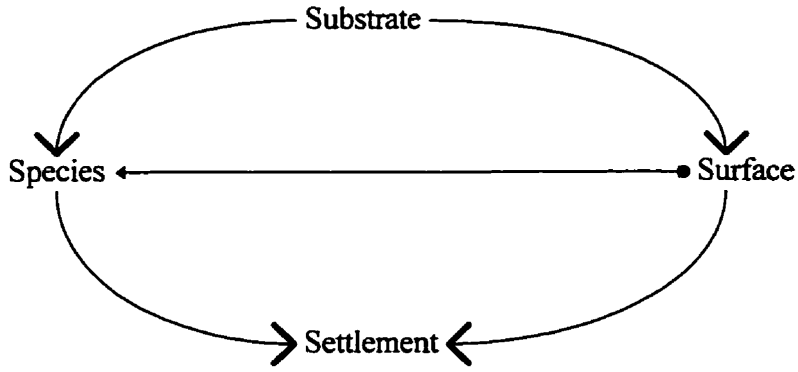

Figure 2.4. A sequence of generalized interaction related to the causes of sludge bulking (Forster, 1985).

2.4 Extracellular polymeric substances (EPS)

Extracellular polymeric substances (EPS) within the floc matrix and on the surface of floc have been shown to be important in flocculation and settling (Forster, 1971; Forster and Dallas-Newton, 1980; Vallom and McLoughlin, 1984; Goodwin and Forster, 1985; Morgan *et al.*, 1990; Urbain *et al.*, 1993). EPS are produced by bacteria and typically can be attached to the cell

as a capsule, or secreted to the surrounding medium as a slime. Sutherland (1972) and Wilkinson (1958) proposed that the EPS had an important protective function, aiding survival and dispersal of bacteria species. EPS represents a small fraction of the activated sludge mass. It generally accounts for less than 14 % of the sludge dry weight even with a drastic extraction procedure such as heat treatment which may cause cell lysis and the intracellular material would be measured as EPS (Beccari *et al.*, 1980; Clarke and Forster, 1982). EPS may have a role in bridging the microbes. Buffle and Leppard (1995) showed a mathematical simulation of a bridging flocculation process between colloids and macromolecules in the size range of 1 nm to 1 μm. Microbes and EPS could themselves be considered as colloids and macromolecules, respectively. Generally, capsular surface polymer is believed to have an effect on flocculation and settling. Slime is either loosely bound to the cell, or is totally free from it (Pelczar *et al.*, 1977; Sato and Ose, 1980). Therefore, it would be unlikely to assist the settling process, and in fact may hinder it by shielding the colloid (Deinema and Zevenhuizen, 1971). The terms surface polymers, biopolymers, exopolymers, extracellular polymers, extracellular polysaccharides and extracellular polymeric substances have been used to describe these substances by different investigators. Extracted EPS are the substances which can be removed from the cell surface of microorganisms (and in particular, bacteria) without disrupting the cell.

2.4.1 Characteristics of EPS

EPS play a significant role in flocculation and can be described as high molecular weight compounds (M.W. > 10,000) produced by microorganisms (Morgan *et al.*, 1990). Since the flocculation results from the attachment of polymeric materials between microbial surfaces, the length of the polymer segment must be sufficient to bridge the cell separation to induce the flocculation (Tenney and Verhoff, 1973). Moreover, the surface interactions which are involved in determining the settlement properties of sludge have an ionogenic (and presumably hydrophilic) nature with a part that is strongly hydrophobic (Goodwin and Forster, 1985). Hence, EPS with an ionogenic nature is considered to be important for flocculation. Since the surface charge is governed by the exact chemical composition of the sludge surface, it is important to study the constituents of the EPS.

2.4.2 Constituents of EPS

The chemical composition of EPS is reported to be very heterogeneous (Frølund *et al.*, 1996). The general categories of organic polymers present in extracted EPS include polysaccharide, protein, RNA and DNA, and lipids (Tenney and Verhoff, 1973; Goodwin and Forster, 1985). The extracted EPS observed in different studies, generally accounts for approximately 15 - 33 % of the sludge suspended solids (Urbain *et al.*, 1993). The molecular weights of these organic polymers are all greater than 10^4 amu and their sizes are larger than 0.001 μm as shown in Figure 2.5. As mentioned in the previous section, the high molecular weight macromolecules are considered to be responsible for the flocculation. Goodwin and Forster (1985) reported that lipid had a significant effect on sludge settlement even though lipids contained little ionogenic material and would not be expected to contribute to surface charge. However, lipids appear as the components of the cell membrane and cell wall in the form of lipoproteins and glycolipids. Thus, they are considered to be important at the cell membrane level rather than the intercellular level for flocculation. Moreover, RNA is not likely to be stable in the extracellular matrix (Leppard, 1997). Therefore, the effect of the level of protein, polysaccharides and DNA in extracellular matrix on flocculation is expected to be more significant.

Polysaccharides. Polysaccharides are thought to be the most important chemical component for flocculation. The EPS extracted from the activated sludge has been mainly of a polysaccharide nature (Brown and Lester, 1979). Hence, the vast majority of research related to EPS in activated sludge has been mainly concerned with the polysaccharide fraction. Horan and Eccles (1986) reported that all the polysaccharide fractions were of high molecular weight, ranging from 3 x 10^5 to 2 x 10^6 amu. The polysaccharides consist of both neutral and acidic sugars. The principal ionogenic component of such polysaccharides was reported to be glucuronic acid (Forster, 1971; Steiner *et al.*, 1976; Horan and Eccles, 1986). This surface acid contributes to the net negative charge commonly found in exopolysaccharides (Sutherland, 1972). At neutral pH values this compound will carry a strong negative charge which allows the sludge to behave as a polyelectrolyte (Horan, 1990). Hence, ionic bonding is suggested to be involved in the mechanism of flocculation (Forster and Dallas-Newton, 1980). When the polysaccharide is

composed of exclusively neutral sugars, hydrogen bonding through regions of electron density must be considered as a mechanism by which floc is formed (Friedman *et al.*, 1968).

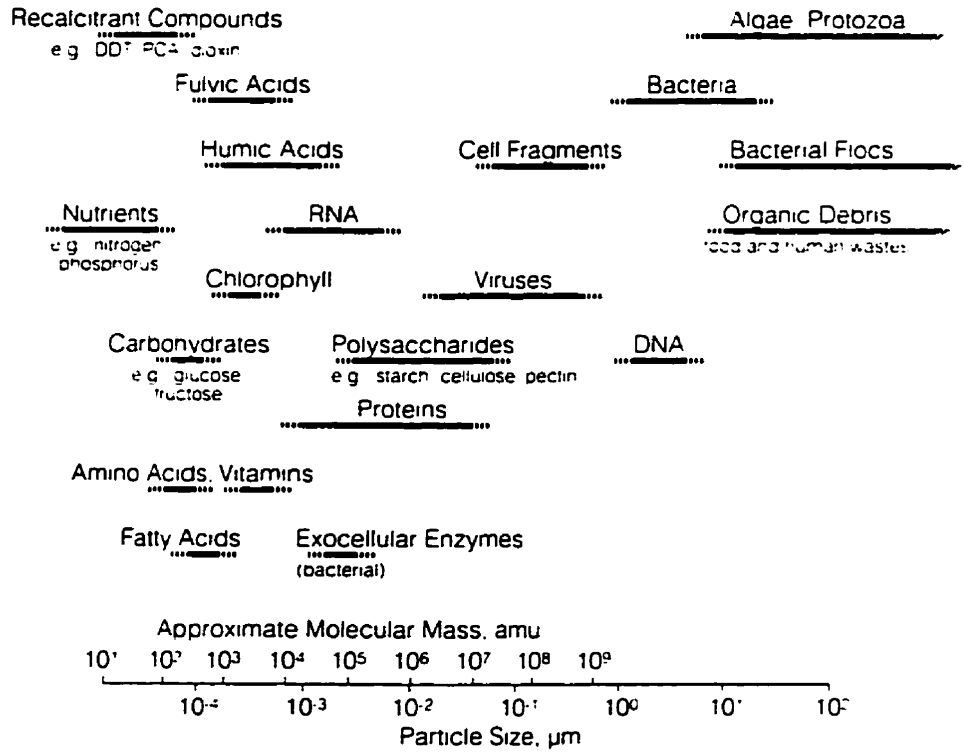

Figure 2.5. Particle sizes and approximate molecular masses of wastewater organics (Levine *et al.*, 1985).

Proteins. In addition to polysaccharides in EPS, the significance of protein for flocculation has also been shown. Many studies have reported that the exocellular protein concentration in activated sludge systems was greater than the exocellular polysaccharide concentration (Tenney and Verhoff, 1973; Brown and Lester, 1980; Urbain *et al.*, 1993). Removal of surface protein has been shown to cause the deflocculation of bacterial suspensions (Kato *et al.*, 1971). Tenney and Verhoff (1973) showed that the extracted biopolymers were capable of causing agglutination of inorganic colloids such as alumina and hypothesized that these biopolymers could belong to a class of proteins known as transport enzymes. Higgins and Novak (1997)

reported that incubation of a laboratory activated sludge with a proteolytic enzyme resulted in deflocculation of the suspension.

DNA. DNA in EPS may have a role in flocculation. Palmgren and Nielsen (1996) have demonstrated that DNA can be found in 3 fractions of the cell culture: as intracellular DNA, as DNA associated with the cell surface/in the capsular biopolymer, and as extracellular dissolved DNA in the slime polymers released by the cells. They found that the extracellular DNA can accumulate independently of the cell biomass and can be protected by capsular polymers. Therefore, they have suggested that DNA may have an influence on the activated sludge composition and stability. Other studies also indicate that large amounts of DNA can accumulate in the extracellular polymeric matrix of sludge flocs (Frølund *et al.*, 1996; Urbain *et al.*, 1992). Previous studies in wastewater treatment processes and in aquatic and sediment environments have used the amount of DNA present as a measure of the number of bacteria present in the system (Thomanetz, 1982; Liebeskind and Dohmann, 1994). Paul and David (1989) have suggested that the extracellular DNA is independent of the biomass but more dependent on physio-chemical factors. Vallom and McLaughlin (1984) have also postulated a role for DNA released during sludge autolysis, suggesting that it acts as a bridge to bind individual cells through surface charge. DNA in the sludge matrix is thought to be protected against enzymatic degradation by the formation of metal ion complexes. This hypothesis gives a possible indication of the role of nucleic acids in floc formation (Forster, 1976).

2.4.3 Extraction of EPS

The extraction procedure is important in determining the composition of extracted EPS in activated sludge. Many attempts have been made to extract and quantify sludge EPS because of the recognition of involvement of EPS in bioflocculation. A good extraction procedure is an effective extraction with the lowest extent of cell lysis and less disruption to the EPS (Gehr and Henry, 1983). Several extraction methods have been investigated including mechanical, chemical and thermal techniques in comparative studies (Kiff and Thompson, 1979; Brown and Lester, 1980; Gehr and Henry, 1973). The shearing effect of ultra-centrifugation is not an

effective method for activated sludge (Novak and Haugan, 1981), whereas chemical and heating procedures are too harsh on cell structure and can lead to cell lysis (Urbain *et al.*, 1993). Goodwin and Forster (1985) reported that temperature had little effect on the polysaccharide fraction. However, a greater sensitivity to the extraction temperature was found in the proteinaceous fraction. The extraction technique using cation exchange resin (CER) as described by Frølund *et al.* (1996) is considered to be a mild EPS extraction method. This resin removes cations from the sludge matrix leading to breakup of the flocs and a subsequent release of EPS. There is, however, still no unified method established for the quantitation of EPS of activated sludge. However, comparative studies can be useful if the extraction technique is standardized initially (Goodwin, 1988).

2.5 Physical properties of floc

Physical properties of sludge floc have long been recognized as having significant influence on the effective separation of solids from the treated effluent. Glasgow and Hsu (1984) have studied the physical characteristics of floc including size, strength, density and permeability. However, floc size and density are particularly important parameters and are measured in many studies related to activated sludge (Magara and Nambu, 1976; Klimpel *et al.* 1986; Andreadakis, 1993). In addition, the shape of sludge flocs is reported to be related to the settling properties (Eriksson and Hardin, 1984; Watanabe *et al.*, 1990).

2.5.1 Floc size and shape

Sampling and stabilization. In order to retain the specific size distribution and the geometric properties of floc for observation, physical stabilization of the floc is required. A major characteristic of a microbial suspension is its intrinsic instability due to the microbial activity and continuing aggregation and disaggregation processes. Therefore, the storage time should be short and the sample processing should be unobtrusive in order to retain the geometric properties of floc for study. Rapid dilution of mixed liquor sample has been used by different investigators to retain the form of the flocs. However, this prepared sample can only be observed immediately and is

inappropriate for storage and transportation as the water evaporates quickly. Of course, the geometric characteristics of floc are different in dried floc. Moreover, this method allows the microbial activities to continue inside the floc. These microbial activities might change the geometric forms of the flocs as well. Ganczarczyk *et al.* (1992) recommended a stabilization method by embedding in agar. Due to the rapid solidification and no requirement for intensive mixing in using the agar, the original morphological properties of the particle can be preserved for a long period of time and thus the opportunity for change in particle size distribution is minimized (Zahid and Ganczarczyk, 1990). Droppo *et al.* (1996a, b) described a method of using low melting point agarose to physically stabilize microbial flocs prior to further sample handling. The authors found this method not to significantly influence floc size distribution.

Floc size. Floc size has long been recognized as an important parameter affecting the sludge settling (Horan, 1990; Jenkins *et al.*, 1993; Ganczarczyk, 1994). Activated sludge flocs are dispersed in aeration tanks due to the turbulence generated in the aeration tanks, the duration of the aeration time and the concentration and composition of the wastewater and biomass (Ganczarczyk, 1967). Hence, a dynamic equilibrium of the sizes of the flocs is formed due to continuous aggregation and disaggregation (Parker *et al.*, 1971). Flocs are described as highly irregular in shape, porous and three dimensional. Since flocs are non-spherical and are generally observed as two dimensional projections, there is no simple means of specifying size or shape (Bache *et al.*, 1991). Most of the methods assume one or two principal axes and with a sphere-like shape. Longest dimension, breadth, equivalent spherical diameter, cross-sectional area and perimeter have been used to characterize the floc size by Li and Ganczarczyk (1986). Equivalent spherical diameter (ESD) is the term used by a number of investigators for floc size measurement due to its compatibility with Stokes' law when calculating floc density determination (Andreadakis, 1993; Droppo and Ongley, 1992; Magara *et al.*, 1976). Moreover, ESD is also the traditional parameter of presenting grain-size distribution. Floc sizes can range from a few μm to mm. The mathematical expression of ESD is as follows:

$$ESD = (4 \bullet Area / \pi)^{1/2} \qquad \text{(Eq. 2.1)}$$

where Area is the measured floc area.

The sizes of floc particles are presented as a size distribution curve. Both the sample mean (Forster and Choudhry, 1972) and sample median (Rao *et al.*, 1991) derived from these curves have been used to represent the typical floc size of a sample. However, sample median is a robust statistic which is an accurate measure of central tendency regardless of whether or not the distribution is symmetrical. In contrast, sample mean is a good measure of the central tendency only if the distribution is symmetrical.

Many methods have been developed to measure the floc size. These methods include photographic techniques (Magara *et al.*, 1976; Tambo and Watanable, 1979), Coulter counter technique (Andreadakis, 1993; Smith and Coackley, 1984), microscopic observation (Sezgin *et al.*, 1978; Pipes, 1979) and automated image analysis technique (Glasgow *et al.*, 1983; Li and Ganczarczyk, 1986; Droppo and Ongley, 1992). However, the Coulter counter method is destructive due to its impact on breakage and compression of larger flocs. Moreover, the shape of floc cannot be measured by this technique. On the other hand, the photographic technique does not allow the measurement of very small floc. Since an accurate representation of the size distribution depends on the ability to detect small particle sizes, the photographic technique may overestimate the importance of the larger floc (i.e. provides a larger floc size distribution) (Andreadakis, 1993). An automated image analysis system consists of a microscope and a computerized digitizer which allow for an accurate, reproducible and fast measurement of floc size and other geometric parameters (e.g. floc shape).

Floc shape. The effect of four morphological parameters including form factor, three-dimensional aspect ratio, roundness and fractal dimension on sludge settling was studied by Grijspeerdt and Verstraete (1997). Form Factor (FF) and Aspect Ratio (AR) were concluded to be the most suited morphological parameters to estimate the settleability of activated sludge. The terms shape factor, form factor, and circularity have been used by different investigators to describe the deviation of an object from a circle; however, they carry the same mathematical expression for calculation (Eq. 2.2). Form Factor is used after Grijspeerdt and Verstraete (1997). FF is the ratio of floc area to the area of a circle with the same perimeter as the floc, and it is particularly sensitive to the "roughness" of the boundaries. It is equal to 1.0 for a circular

floc and close to 0.0 for a linear floc. AR is sensitive to the extension of an object. The more elongated it is the larger the value for this parameter. A circle has an AR of 1.0. The mathematical definitions for FF and AR are as follows:

$$FF = 4\ \pi\ \text{Area} / \text{Perimeter}^2 \qquad \text{(Eq. 2.2)}$$

where Area = measured floc area, Perimeter = measured perimeter of floc particle.

$$AR = 1.0 + 4 / \pi\ (\text{Length} / \text{Width} - 1.0) \qquad \text{(Eq. 2.3)}$$

where Length = measured longest dimension of floc particle,

Width = measured shortest dimension of floc particle.

2.5.2 Floc settling velocity

Floc settling velocity is a function of the floc size, wet density and viscosity of the settling medium as described by Stokes' equation (Eq. 2.4).

$$v = D^2\ (\rho_f - \rho_w)\ g / (18\ \mu) \qquad \text{(Eq. 2.4)}$$

where v = settling velocity, D = equivalent spherical diameter of particle (ESD),

ρ_f = wet density, ρ_w = density of the water,

μ = dynamic viscosity (kinematic viscosity x ρ_w).

In addition, settling velocity is also affected by the shape and settling orientation. Lerman (1979) reported that the effect of fluid drag force on the settling velocity of a non-spherical particle was larger than that on a spherical particle. Therefore, the fastest settling rate is for a particle of spherical shape, followed by cylindrical, needle-like, and disc-like. Settling velocity of individual floc is important for the determination of wet density as discussed in Section 2.5.3.

Li and Ganczarczyk (1987) used a power function of the form $v = A L^n$, and a linear function of the form $v = A + BL$, to correlate the settling velocity of floc to its size as longest dimension (L). A, B and n are the equation coefficients determined experimentally. They concluded that the power function better described the relationship for very small floc than did the linear function. The power function predicts that the velocity will be zero when the floc size approaches zero whereas the linear function does not. Lee *et al.* (1996) managed to measure the settling velocity and size for a total of 1385 floc particles and reported the power coefficient of between 0.7 - 0.8. A linearized settling velocity equation (Eq. 2.4) in the form of power function is as follows:

$$\log v = \log A + 2 \log D \qquad \text{(Eq.2.5)}$$

where v = settling velocity, D = ESD, A = constant.

Different imaging techniques have been developed in order to capture the image of settling floc for size and settling velocity measurement. For photographic techniques, only one or a few flocs are introduced into the column when a picture is to be taken. However, the shallow depth of field limits the chance to obtain a sharp floc image. Therefore, the adoption of a very thin sedimentation column (Magara *et al.*, 1976; Tambo and Watanabe, 1979) helps to place the settling flocs within the focal plane. However, it complicates sample introduction (Li and Ganczarczyk, 1987). Hermanowicz and Ganczarczyk (1983) measured the floc size of the particle before it was dropped into the settling column. However, this requires the floc being manipulated more and it is not ideal for an easily perturbed structure like floc. A multi-exposure photographic technique using a stroboscope was employed by Li and Ganczarczyk (1987). This technique is effective in measuring floc size and settling velocity, but it lacks the precision in measuring fine floc. Klimpel *et al.* (1986) used a cinematographic technique to measure the larger floc (>100 μm), and the multi-exposure technique to measure the smaller floc (<100 μm). With the advance in imaging technology, video imaging has been used for settling velocity determination (Lee, 1994; Droppo *et al.*, 1997). This allows the tape to be replayed. Droppo *et al.* (1997) described a setup which interfaced the video camera with image

analysis software. The settling velocity was derived by digitally overlaying two video frames of a known time interval apart. In this way the same particle appears on the newly combined image twice and the distance of settling and the particle size can be digitized.

2.5.3 Floc density

Floc density is an important physical characteristic for floc settling. Together with floc size and shape, the wet density of a floc particle determines the separation efficiency of suspended solids from wastewater in the clarifier.

Density determination. Obtaining the bulk density of a floc is difficult due to the hydration water associated with its surface. Different methods have been used in previous studies. One of the methods is an indirect method involving the determination of the bound water content of the sludge by the dilatometric technique (Forster and Lewin, 1972; Barber and Veenstra, 1986). Another method is the interference microscopy method described by Andreadakis (1993) to measure the dry mass of activated sludge. However, density determinations for floc based on the observations of terminal settling velocity are usually used because of its simplicity and the low testing cost (Magara *et al.*, 1976; Tambo and Watanabe, 1979; Glasgow and Hsu, 1984; Li and Ganczarczyk, 1987; Droppo *et al.*, 1997).

By applying Stokes' equation (Eq.2.4), the floc wet density can be calculated based on the measurement of settling velocity. However, this method is based on the assumption of a single impermeable spherical particle in a laminar region (Reynolds Number < 0.5). It is still not ideal for the determination of floc density because of the heterogeneous structure and irregular shape of the floc (Burban *et al.*, 1990). Therefore, this approach is regarded only as an approximation. Settling velocity (v) and spherical diameter (D) are derived from the image analysis system. Water density (ρ_w) and viscosity (μ) are constants for a given water temperature. Wet density (ρ_f) can be calculated from Eq. 2.6.

$$\rho_f = 18\, v\, \mu / (D^2\, g) + \rho_w \qquad \text{(Eq. 2.6)}$$

where v = settling velocity, D = equivalent spherical diameter of particle (ESD),

ρ_f = wet density of floc, ρ_w = density of the water,

μ = dynamic viscosity (kinematic viscosity x ρ_w).

The density of a floc is expressed by various names as apparent, envelope, effective and piece density (Geldart, 1990). The concept of an effective density as defined by Tambo and Watanabe (1979) is used. The mathematical expression of effective density (ρ_e) is shown as follows:

- $\rho_e = \rho_f - \rho_w$ (Eq. 2.7)

Combining Eq. 2.4 and 2.6, the effective density (ρ_e) can be expressed as follows:

$$\rho_e = 18\, v\, \mu / (D^2 g) \quad \text{(Eq. 2.8)}$$

A linearized effective density (Eq. 2.8) expressed in power function is as follows:

$$\log \rho_e = \log A - 2 \log D \quad \text{(Eq. 2.9)}$$

where A is a constant.

Modified Stokes' law. Different floc density models related to the settling velocity and particle diameter have been proposed by investigators (Magara *et al.*, 1976; Tambo and Watanabe, 1979; Andreadakis, 1993). However, precaution should be taken to adopt these kinds of empirical models for density calculation as assumptions and limitations might be included. Námer and Ganczarczyk (1993) adopted a correction factor which incorporated the settling shape factor and the consideration of flow regime for the determination of the hydrodynamic properties of the flocs studied. This study indicated the necessity of taking the shape factor into the estimation of settling velocity and effective density. The Reynolds Number (Re) of a particle is calculated as Eq. 2.10 to determine the flow regime of floc.

$$\mathrm{Re} = D\, v\, \rho_w / \mu \quad \text{(Eq. 2.10)}$$

where D = ESD, v = settling velocity, ρ_w = density of the fluid,

μ = dynamic viscosity of the fluid.

For non-spherical floc (after Pettyjohn and Christiansen, 1948), if Re is in Stokes' regime (Re < 0.2), the correction factor k_s for Stokes' regime is as follows:

$$k_s = 0.843 \log (\phi / 0.065) \qquad \text{(Eq. 2.11)}$$

$$\rho_e = \rho_f - \rho_w = 18 \mu v / (k_s g D^2) \qquad \text{(Eq. 2.12)}$$

where g = acceleration of gravity (9.81 ms^{-2}), ϕ = Form Factor (FF).

If Re is in Newton's regime ($1000 < Re < 3 \times 10^5$), the correction factor k_n for Newton's regime is as follows:

$$k_n = 5.31 - 4.88 \phi \qquad \text{(Eq. 2.13)}$$

$$\rho_e = 3 k_n \rho_w v^2 / 4 g D^2 \qquad \text{(Eq. 2.14)}$$

If Re is in transition range ($0.2 < Re < 1000$) the correction factor k (after Geldart, 1990) is as follows:

$$k \approx [k_s - (0.43 / k_n)^{1/2}] \bullet (1000 - Re) / (1000 - 0.2) + (0.43 / k_n)^{1/2} \qquad \text{(Eq. 2.15)}$$

$$\rho_e = 18 \mu v / (k g D^2) \qquad \text{(Eq. 2.16)}$$

2.6 Structural properties of extracellular matrix

A number of workers have associated the formation of polysaccharide capsular matrices or exocellular fibrils with microbial flocculation (Forster, 1971a; Wallen and Davies, 1972; Friedman *et al.*, 1968). Much of the EPS appear as distinct fibrils in electron micrographs

(Leppard, 1992b). It is readily recognized in TEM images by its distinctive ribbon-like shape. Fibrils are colloidal in nature and can leave the surfaces of living cells without any concomitant damage to the cells (Decho, 1990). The fibrils observed by electron microscopy are largely in polysaccharides whose monomeric composition tends to be rich in uronic acid. Individual fibrils, whether branched or not, have a diameter typically in the range of 0.002 to 0.01 μm. Visual observations of natural flocs with high-resolution electron-optical microscopy techniques have revealed cross-linkages of floc particles by bridges of fibrils (Leppard, 1992b).

2.6.1 Correlative microscopy (CM)

Leppard (1992a) described a strategy called correlative microscopy (CM) which used different kinds of microscopes to obtain different information. For examining a sample of floc particle in micrometer to submicron fibril structure in an extracellular matrix, a series of microscopes is used in sequence to bridge the gap between the resolution of an aided eye (near 100μm) and that of a transmission electron microscope (near 0.001 μm). This allows one to detect, assess and minimize artifacts that might arise from using one technique only. Often multiple samples are required for multiple microscopic studies. However, correlation of the observations from multiple samples may be erroneous. Droppo *et al.* (1996a, b) described a floc stabilization technique using low melting point agarose to allow a single sample to be analyzed by different microscopes. In addition, Liss *et al.* (1996) conducted a study of natural and engineered flocs structure using CM including conventional optical microscopy (COM), scanning confocal laser microscopy (SCLM) and transmission electron microscopy (TEM). They described a minimal perturbation approach within a four-fold multipreparatory technique to prepare the sample for the examination using TEM. Correlating this information including sizing and morphological parameters of the floc itself and the fibril in extracellular matrix down to about 1 nm in the least dimension, the structural characteristics of floc can be described directly and more completely. The description and the method of sample preparation for each type of microscopy are included in Section 3.5.

CHAPTER 3 EXPERIMENTAL

This study has involved a comprehensive examination of sludge from four different types of full-scale activated sludge systems (Figure 3.1). Three of these treated industrial wastewater and include a poultry processing wastewater - Maple Lodge Farm, Brampton, ON; petroleum refinery wastewater - Petro-Canada, Oakville, ON; and potato processing wastewater - Prince Edward Island. A municipal system treating domestic sewage - Main Treatment Plant, Toronto, ON, was studied as well. Each wastewater treatment plant was sampled bi-weekly for a six-month period.

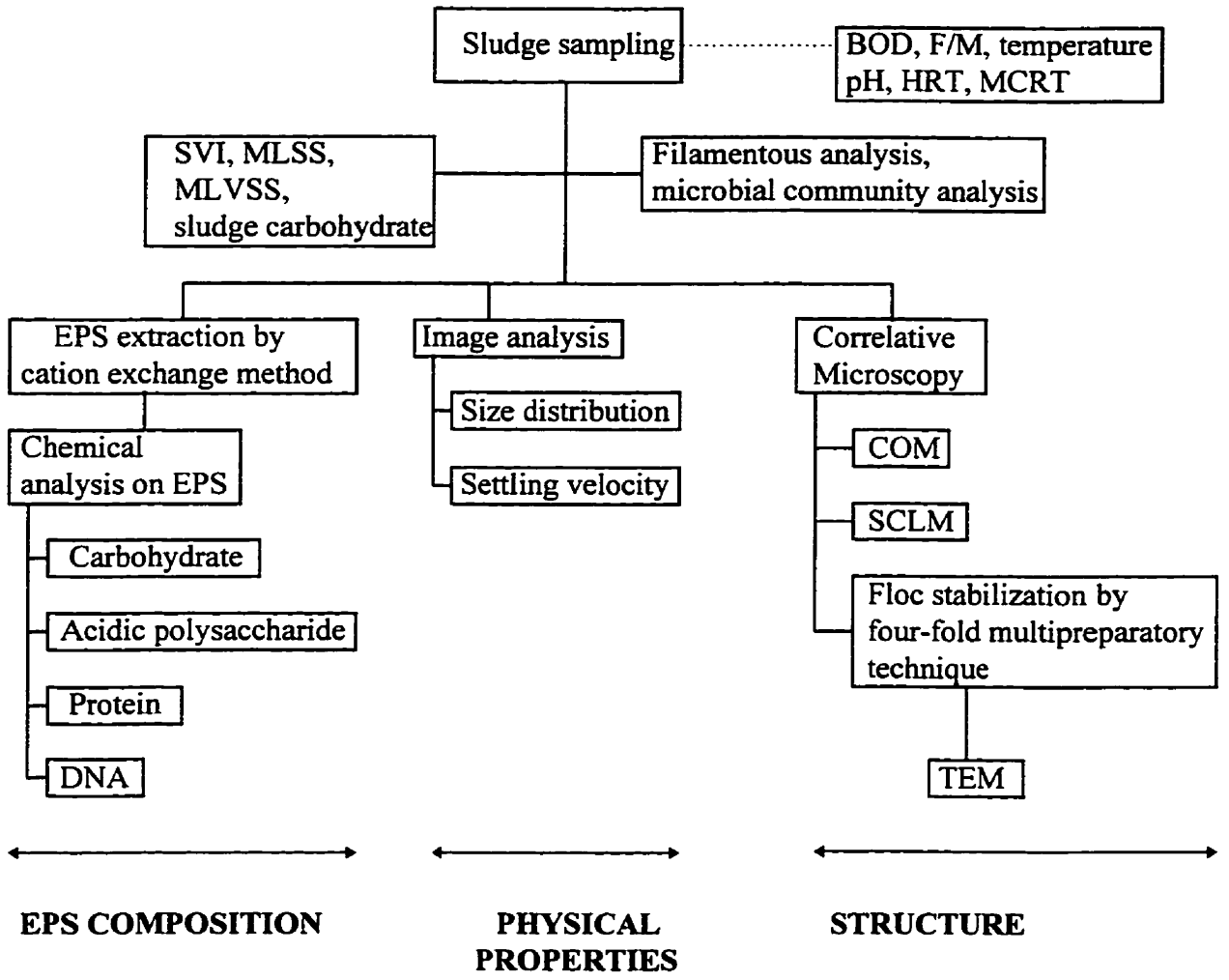

Figure 3.1. Experimental approach for correlative study on sludge floc. The dotted line represents the operating data provided by the treatment plants.

3.1 Sludge sampling

The mixed-liquor samples from the system treating domestic sewage (system-Dm) and petroleum refinery wastewater (system-Pm) were collected in person. The samples from systems treating poultry processing wastewater (system-Py) and potato processing wastewater (system-Po) were sent by courier. About two litres of mixed-liquor sample was collected each time and the sampling bottle was filled to about 80 % leaving some head space for air. The samples from system-Dm were analyzed on the same day as sampling. The samples from system-Py and system-Pm were analyzed on the next day after sampling. The samples from system-Po were analyzed at one day after the sampling day. For those samples not analyzed at the time of sampling, they were stored at 4° C for one day. The effect of storage time on the chemical properties of sludge was studied by Bura *et al.* (1997) and is discussed in Section 4.3.2.

3.2 Standard wastewater analysis

As environmental conditions are known to influence sludge settling, the informstion on operating conditions of treatment systems is important to know. Mixed-liquor suspended solids (MLSS), mixed-liquor volatile suspended solids (MLVSS) and sludge volume index (SVI) were measured according to standard methods (APHA, 1985). The data for mean cell residence time (MCRT or sludge age), hydraulic retention time (HRT), pH, biochemical oxygen demand (BOD) were obtained directly from the plant personnel. Food to microorganism ratio (F/M) was calculated from the BOD, HRT and MLVSS data provided.

Suspended solids concentration. Mixed-liquor suspended solids (MLSS) are composed of active and non-active microbial mass, non-biodegradable organic mass, and inorganic mass. Mixed-liquor volatile suspended solids (MLVSS) represents the organic fraction of the solids and are used traditionally as an index of biomass content in the modeling and operation of activated sludge systems. An aliquot of well-mixed mixed-liquor (5 mL) was filtered through a weighed standard glass-fibre filter (Whatman, 47 mm dia.) and the residue retained on the filter was dried to a constant weight at 103 - 105 °C in about 1 h. The increase in weight of the filter

represented the MLSS. The residue was then ignited at 550 °C for about 1 h. The remaining solids represented the fixed solids while the lost on ignition was the MLVSS. All these determinations were done in triplicate and the results were expressed in mg/L. MLSS and MLVSS are defined as:

$$\text{MLSS mg/L} = \frac{\text{(A - B) mg x 1000}}{\text{sample vol. (mL)}} \qquad \text{(Eq. 3.1)}$$

$$\text{MLVSS mg/L} = \frac{\text{(A - C) mg x 1000}}{\text{sample vol. (mL)}} \qquad \text{(Eq. 3.2)}$$

where A = weight of filter + dried residue after 105 °C, mg
B = weight of filter, mg
C = weight of filter + residue after ignition at 550 °C, mg

Sludge Volume Index (SVI). SVI is typically used to monitor the settling characteristics of activated sludge. It is the volume in mL per g of a suspension after 30-minute settling. 'Bulking' has been taken somewhat arbitrarily as occurring when SVI values exceeded 150 - 170 mL/g. One litre of mixed liquor sample was put into a 1-L graduated cylinder. The cylinder was covered and inverted several times to distribute the solids. The volume occupied by the suspension after 30 minutes was recorded. MLSS was determined as described in the above section. SVI is defined as:

$$\text{SVI mL/g} = \frac{\text{settled sludge volume (mL/L) x 1000}}{\text{SS (mg/L)}} \qquad \text{(Eq. 3.3)}$$

30-min settling test. This test is also used to monitor the settling characteristics of activated sludge. It is the percentage of sludge blanket settled in a 1-litre graduated cylinder after 30 minutes. The 30-min settling test is defined as:

$$\text{settling \%} = \frac{\text{height of sludge blanket after 30 minutes}}{\text{height of sludge before settling}} \times 100\% \qquad \text{(Eq. 3.4)}$$

Food and microorganism ratio (F/M). F/M ratio is one of the most commonly used parameters for the design and control of the activated sludge process. It can be considered as a measure of amount of substrate (BOD) supplied to a unit mass of microorganism. F/M ratio is defined as:

$$\text{F/M g BOD/g VSS/ d}^{-1} = \frac{So}{\theta X} \qquad \text{(Eq. 3.5)}$$

where So = influent BOD or COD concentration, mg/L (g/m^3)
θ = hydraulic retention time, d
X = concentration of microorganisms (VSS) in aeration tank, mg/L (g/m^3)

3.3 Microbial community analysis

Phenotypic fingerprinting. The BIOLOG method described by Victorio *et al.* (1996) was used as a community-level characterization of microbial biomass. It provides a sensitive and ecologically meaningful measure of heterotrophic community structure. In addition, it eliminates any bias that may be associated with cultural methods as reported by the same authors.

An aliquot (1 mL) of activated sludge sample was added into a blender. A portion of water (99 mL) was added in order to make a 100 times dilution. One drop of TWEEN 80 (0.01% v/v) and 10 µL of sodium pyrophosphate (0.01% v/v) were added into the blender. The suspension was homogenized using a Waring blender for 30 seconds. The recovered microbial fraction was washed three times with saline (0.85% NaCl) by centrifugation at 15,000 *g* for 15 minutes in order to remove contaminating organic material present on the cell surface and in the liquid phase of the biomass samples. Aliquots of 150 µL of prepared microbial suspension were inoculated into each well of Biolog GN microplate (BIOLOG Inc.). All plates were incubated for 12-18 h at

30°C and read spectrophotometrically at 590 nm with the Biolog microplate reader in conjunction with Biolog's Microlog 3.50 software. The Biolog GN microplate contains 95 different carbon substrates and a control well without a carbon source (Garland and Mills, 1991). Substrate, dye and nutrients are supplied in each well in a dried-film form which is reconstituted upon addition of sample. The metabolic response in each well is based on the reduction of tetrazolium dye which acts as an indicator of sole-carbon source utilization. The fingerprinting patterns of metabolic response were created by subtracting the color intensity of each well from that of the control well. The data were analyzed as described below.

Data analysis. The relationships among and within samples on the basis of optical densities of each well were determined by principal component analysis (PCA), using the STATISTICA software package (Statsoft, Tulsa, OK). This technique projects the original data onto new axes (principal components (PCs)) which reflect intrinsic patterns in the multidimensional data. Each PC extracts a portion of the variance in the original data, with the greatest amount of variance extracted by the first axis. Relationships among samples are readily observed by plotting samples in two dimensions on the basis of their scores for the first two principal components (Garland and Mills, 1991).

3.4 EPS composition

Extraction of EPS from sludge matrix is required prior to further chemical analysis of its composition. Prior to extraction, sludge was washed to remove the effluent polymer. The EPS was extracted using the cation exchange resin (CER) with the extraction strategy recommended by Frølund *et al.*, 1996. The CER used was DOWEX (Supelco 1-3443). The CER was washed for 1 h in extraction buffer prior to use.

3.4.1 EPS extraction

After the sludge sample was transported to the laboratory, an aliquot (200 mL) was settled for 1.5 h at 4°C. A 100 mL portion of the supernatant was decanted in order to thicken the suspended solids concentration. A thickened sludge with a MLSS of about 5 to 8 g/L was obtained. A 50

mL portion of thickened sludge was centrifuged at low speed (Model HN-S, International Equipment Co.) for 10 min. and the supernatant was decanted in order to remove the bulk wastewater. A washing step using 0.1 mg/L saline was performed and the sludge was centrifuged at low speed for 10 min.. The sludge pellet was resuspended to their original volume using an extraction buffer consisting of 2 mM Na_3PO_4, 4mM NaH_2PO_4, 9mM NaCl and 1mM KCl at pH 7.

The washed thickened sludge was mixed with the CER whose amount depended on the MLVSS (approximately 70 g CER/g VSS). The CER/sludge suspension was kept at 4°C and stirred at about 600 rpm for an hour. The extracted EPS was harvested by centrifugation at 4°C using 12,000g for 15 min.. The supernatant was collected and used for chemical analyses. The rest of the washed sludge was used for the determination of MLSS, MLVSS, and sludge carbohydrate.

3.4.2 Chemical analyses of sludge and EPS

Colorimetric methods were used for all the chemical analyses of extracted EPS. A series of standard solutions in different concentration was used to calibrate the standard curve for each measurement. Distilled water was used as the blank solution. Absorbance was read against the blank at different specified wavelengths. The concentration of each components studied in extracted EPS was obtained from the calibrated standard curve. All these determinations were done in triplicate and the results were expressed in mg (equivalent of standard) per g of VSS. Spectrometry and fluorometry were carried out by SP6-500 UV spectrophotometer (PYE UNICAM) and Turner fluorometer respectively. All chemicals used were analytical grade from Sigma Chemical Co. or Aldrich Chemical, Inc..

Carbohydrates measurement. The anthrone method (Gaudy, 1962) was used for the determinations of carbohydrate concentration in extracted EPS and sludge. Glucose solutions at concentrations of 20, 30 40 and 50 mg/L were used as standards. The anthrone reagent was prepared by dissolving 0.2 g of anthrone in 100 mL of 95 per cent sulphuric acid and stored in refrigerator until ice cold (about 4°C). An aliquot (5 mL) from each of the standard, blank and sample solutions was placed in test tubes. All tubes were placed in an ice water bath to

equilibrate. Anthrone reagent (5 mL, ice cold freshly prepared) was put into each tube. Each tube was capped with a glass marble, mixed thoroughly and placed in a boiling water bath for exactly 15 minutes. At the end of this period, the tubes were removed and placed in cool water. After reaching room temperature (about 23°C), the intensity of color developed in solution was measured as absorbance at 620 nm and the carbohydrate concentration was determined by spectrophotometry.

Acidic polysaccharides measurement. A *m*-hydroxydiphenyl sulphuric acid method (Blumenkrantz and Asboe-Hansen, 1973) as modified by Filisetti-Cozzi and Carpita (1991) was used for the determination of acidic polysaccharide concentration in extracted EPS. Glucuronic acid solutions at concentrations of 20, 30, 40, 50 mg/L were used as standards. An aliquot (0.8 mL) from each of standard, blank and sample solutions was placed in test tubes. 4M sulfamic acid (80 μL, pH=1.6 adjusted with KOH) was added to each tube and mixed thoroughly. Analytical grade (96.4 %) sulphuric acid containing 75 mM sodium tetraborate (4.8 mL) was added to each tube and stirred by vortex mixing. Each tube was capped with a glass marble and heated to approximately 100°C in a boiling water bath for 20 minutes. At the end of this period, the tubes were chilled in an ice bath to room temperature (about 23°C). After cooling, 0.15% (w/v) *m*-hydroxydiphenyl in 0.5% (w/v) NaOH (160 μL) was overlaid and then stirred in vigorously by vortex mixing. A pink colour was fully developed in solution after 5 to 10 minutes and was stable for about one hour. The intensity of color was measured as absorbance at 525 nm and the acidic polysaccharide concentration was determined by spectrophotometry.

Protein measurement. The Lowry method described by Lowry *et al.* (1951) using the Folin reagent was used for the determination of protein concentration in extracted EPS. Bovine serum albumin solutions at concentrations of 200, 400, 600 and 800 mg/L were used as standards. Reagent A was prepared by dissolving 20 g of Na_2CO_3 in 1 litre of 0.1 N NaOH. Reagent B was prepared by dissolving 0.5 g of $CuSO_4.5H_2O$ in 100 mL of a 1% (w/v) aqueous solution of sodium tartrate. Reagent C was prepared by mixing reagent A and B at a ratio of 50 to 1 respectively just before used. An aliquot (1mL) from each of standard, blank and sample solutions was placed in test tubes. Reagent C (5 mL) was added to each tube and mixed well. The mixture was allowed to

stand for 10 minutes at room temperature. Folin reagent (0.5 mL, concentrated Folin and Ciocalteau was diluted by deionized distilled water at a ratio of 18 to 90 respectively) was then added to the mixture and mixed immediately. The intensity of color developed in solution was measured as absorbance at 750 nm and the protein concentration was determined by spectrophotometry.

DNA measurement. The DAPI (4, 6-diaminodino-2-phenylindole) method as described by Brunk *et al.* (1979) and modified by Frølund *et al.* (1995) was used for the determination of DNA concentration in extracted EPS. DNA (from Salmon testes) at concentrations of 1, 2.5, 5 and 7.5 mg/L were used as standards. An aliquot (200 μL) from each of the standard, blank and sample solutions was placed in test tubes. DAPI reagent (5 mL, 0.2 mg/L DAPI in 100mM NaCl, 10mM EDTA, 1mM TRIS, pH=7) was added to each tube. The fluorescence developed in the solution was measured directly (excitation at 360 nm and emission at 450 nm) by fluorometry and the DNA concentration was determined.

3.5 Physical properties of floc

The size and shape factor of floc particle were determined using an image analysis system (Droppo and Ongley, 1992; Droppo *et al.*, 1996a). The image analysis system is a combination of microscopy, photography and digitization. The system set up and the procedures for floc sampling, stabilization and measurement are described in the following sections.

3.5.1 Floc size distribution

Sampling and stabilization. The sample was settled within a plankton chamber as described by Droppo and Ongley (1992). The chamber (Hydro-Bios Kiel) contained three removable components: 1) a 3 mL reservoir with removable circular microscope slide upon which the specimen comes to rest after settling; 2) a 50 mL settling column; 3) a top cap to provide a hydrostatic seal over the chamber (Figure 3.2).

Figure 3.2. Plankton chamber components (A= 3-mL reservoir, B= settling column, C= top cap, D= square glass plate 4.2 x 4.2 cm).

In order to minimize the particle-particle interaction and overlapping during settling for high biomass concentration samples (Droppo and Ongley, 1992), dilution was done by sub-sampling using a wide-mouth pipette (4 mm diameter) which was able to minimize the floc breakage (Mueller *et al.*, 1967; Li and Ganczarczyk, 1986). The settling column was put on top of the reservoir and fully filled with deionized distilled water. Two drops of a sludge sample were introduced into the chamber by a wide-mouth pipette. The chamber was sealed with the top cap for subsequent settling. After the particles had settled, excess water was removed by sliding the settling column off the reservoir. The remaining water in the reservoir was drained out by allowing the water to seep out through the tissue paper placed around its rim. About 0.5 mL agarose solution (0.75 w/v, low melting point electrophoresis grade) was immediately added to cover the whole reservoir floor starting from the outer edge. The agarose solidified in 1 to 2 minutes. The stabilized specimen was contained in a clear, highly porous, resilient medium which allowed the microscopic observation directly or further manipulation such as staining.

For storage, the reservoir was covered by a glass plate and wrapped with parafilm. It was kept at 4°C to prevent dehydration.

Size measurement. The agarose embedded sample was analyzed directly for size distribution using a Zeiss Axiovert 100 inverted conventional optical microscope interfaced with a Sony CCD B&W video camera, and IBM computer with Northern Exposure™ (Empix Imaging Inc.) image analysis software (Figure 3.3A and 3.3B). A magnification of 25x (eyepiece 10x) was used to digitize the images and the minimum equivalent spherical diameter (ESD) measured was 8 μm. The entire slide was viewed and about 1000 particles were digitized with their size as ESD and other morphological parameters such as form factor, longest dimension, breadth, aspect ratio and roundness. Form factor (FF) and aspect ratio (AR) were used in this study to describe the morphological characteristics of floc.

3.5.2 Settling velocity determination

Setup for settling velocity determination. To determine settling velocity, flocs were allowed to settle in a quiescent water column and the settling flocs were monitored by obtaining images using a CCD camera attached to a microscope and an VCR (Droppo *et al.*, 1997). The settling test is similar to the photographic techniques used by many researchers (Magara *et al.*, 1976; Li and Ganczarczyk, 1987) but offers a better image resolution and control for gravitational settling flocs. The videographic technique also allows the replay of the recorded settling floc image conveniently. The videographic technique makes use of a CCD video camera (Sony), stereoscopic microscope (Olympus) and a SVHS VCR to capture images of settling flocs (Figure 3.4A and 3.4B). The settling chamber (2.5 litres capacity) was made of an acrylic sheet of 6 mm thickness with a dimension of 10 cm length by 5 cm width by 50 cm height. The distance of settling until detection by the microscope was approximately 35 cm which was required for the floc particles reaching the terminal velocities.

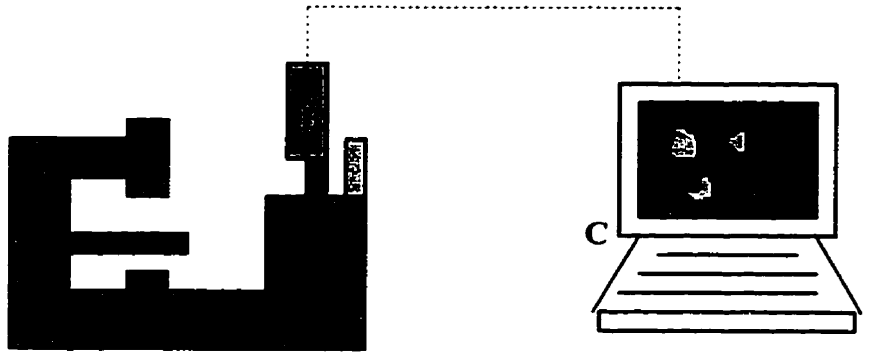

Figure 3.3A. The schematic setup of floc size determination (A= inverted microscope, B= colour video camera, C= computer with Northern Exposure Image Analysis).

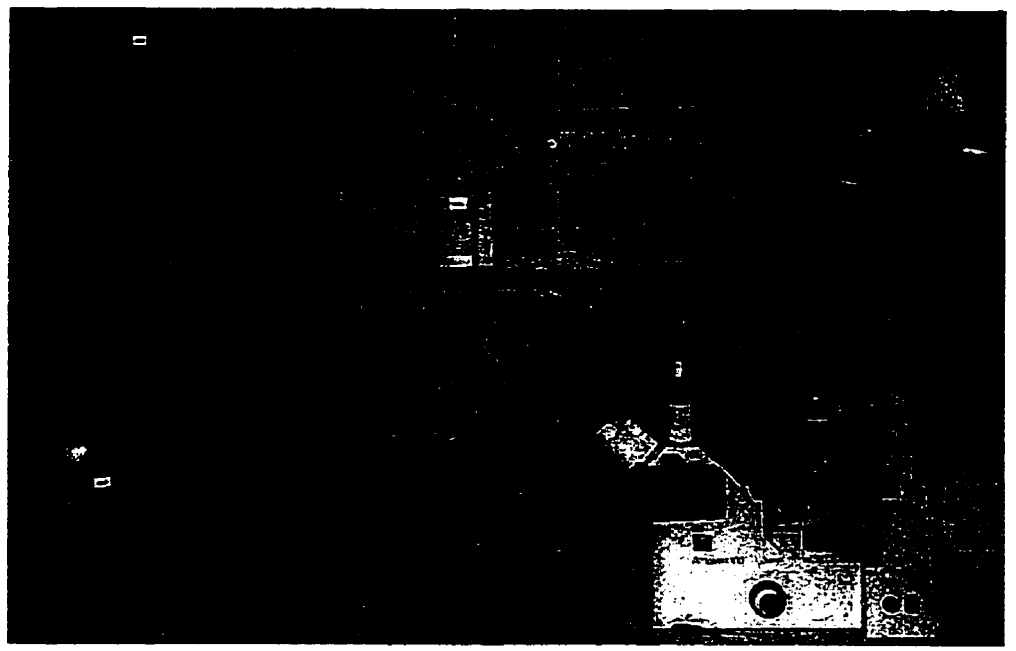

Figure 3.3B. The experimental setup for floc size determination.

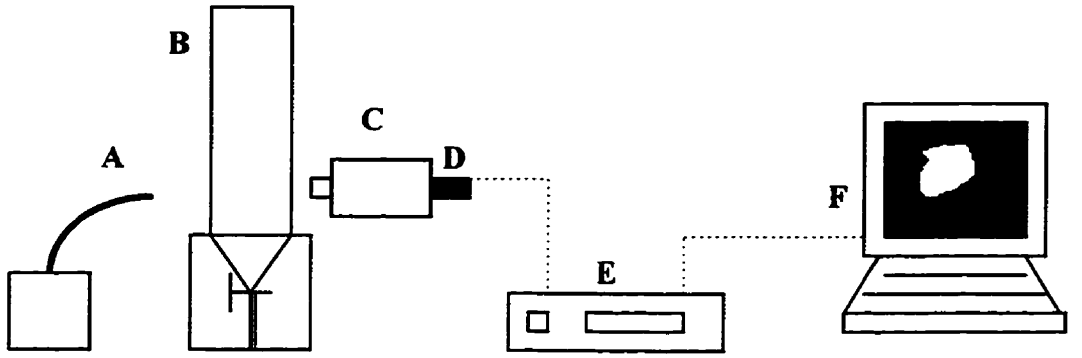

Figure 3.4A. The schematic setup of settling velocity determination (A= fibre optical light, B= insulated settling column, C= stereoscopic microscope, D= B/W video camera, E= SVHS VCR, F= computer with Northern Exposure™).

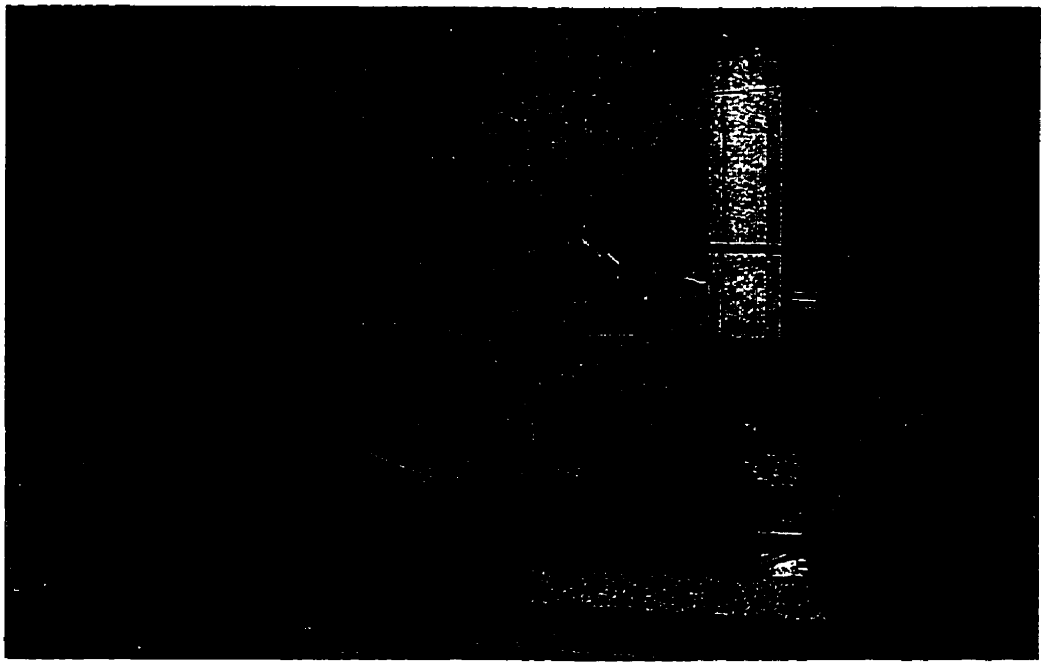

Figure 3.4B. The experimental setup for settling velocity determination.

Settling velocity measurement. A drop (ca. 0.2 mL) of a gently-mixed sample was sampled by a wide-mouth pipette (4 mm diameter) and introduced into the settling column filled with tap water as the settling medium. The particles were video taped and recorded on a video recorder as they passed through the field of view of the microscope. The temperature of the water was recorded in order to determine the water density and viscosity. The video tape was then used for the image analysis determination of settling velocity and particle size using Northern Exposure™ (Empix Imaging Inc.) image analysis software. Settling velocity was derived by digitally overlaying two video frames (each representing 1/30 sec.) of a known time interval apart (15 frames). The data was automatically stored in a spread sheet where density was then derived mathematically according to Eq. 2.8 of Section 2.5.3. Approximately 100 particles were measured for each sample.

3.6 Correlative microscopy (CM)

The information on floc structure was obtained by correlative microscopy including conventional optical microscopy (COM), scanning confocal laser microscopy (SCLM) and transmission electron microscopy (TEM) as described by Liss *et al.*, 1996.

3.6.1 Conventional optical microscopy (COM)

Conventional optical microscopy is the most popular tool being used in the laboratories of wastewater treatment systems or the research institutes to study the gross morphological characteristics of the floc particles such as size and shape or identify the types of microorganisms (e.g. protozoa) present in wastewater.

A Zeiss Axiovert 100 inverted microscope interfaced with a Northern Exposure Image Analysis system was used for gross particle size analysis (see Section 3.4.1). The images of floc particles were recorded at different magnifications of 25x, 50x, 100x, 200x and 400x (eyepiece 10x). In addition, a reflected light microscope (Oympus BH2-RFC) with phase contrast was used for studying the gross structure at magnifications of 100x and 400x (eyepiece 10x). The floc sample

was stained with 0.1% (w/v) ruthenium red which stained the acidic polysaccharides and DNA in the floc matrix and provided better contrast for microscopic observation.

3.6.2 Scanning confocal laser microscopy (SCLM)

The strength of using SCLM over COM is that it allows an *in situ* observation of the three-dimensional disposition of various particles within the floc (Liss *et al.*, 1996). Light from above and below the plane of focus is not included when the image is formed, the image can be considered as an optically thin section with a thickness approaching the theoretical resolution of COM (~0.2 μm). This optically thin section in SCLM greatly reduces the interference from out-of-focus cell material and gives a more accurate image. Since no dehydration and embedding is required as in TEM, it allows the examination of living material over a time course without altering the growth and metabolism of living cells. In addition, it can be used with fluorescent molecular probes (e.g. lectin stains) to study the spatial distribution of cell viability, pH gradient, polysaccharides, protein, RNA, lipids, and other components of living cells. This tool has been used recently to study the microbial floc (Zartarian *et al.*, 1994). Therefore, it was shown to be a useful tool in bridging the resolution gap between COM and TEM.

The samples were stained with fluorescent molecular probes prior to using SCLM. The agarose-embedded samples were sliced into several pieces for five different fluorescent stains (Table 3.1). FITC is a general protein stain which produces an image representing the overall morphological structure. ConA and WGA are lectin stains and they indicate the presence of specific polysaccharide residues. Gram stain stains the cell wall structure to obtain the major difference of bacterial groups. Live/Dead stain indicates the bacterial viability. All of these fluorescent stains were from Molecular Probes, Inc., USA. Images of stained flocs were obtained by SCLM using a Zeiss Micro System LSM (model LSM 10 BioMed). The SCLM is equipped with an argon laser with emission lines at 418 and 514 nm.

Staining for SCLM. Lectins are proteins or glycoproteins of non-immune origin that agglutinate cells and/or precipitate complex carbohydrates. They bind specific configurations of sugar

molecules (Table 3.1), and thus serve to identify cellular components. The staining procedure for the lectin stains used in this study was similar. The buffered dyes were prepared as follows: FITC (0.25 mg/mL of 10 mM Tris, pH=9); ConA (0.25 mg/mL of 0.1 M sodium bicarbonate in 1 mM Mn^{2+} and 1 mM Ca^{2+}, pH= 8.3) and WGA (0.25 mg/mL of 0.1 M sodium bicarbonate, pH= 8.3). Agarose-embedded samples were put into microfuge tubes with about 1 mL of buffered dyes. The samples were stained for 15 minutes in the dark at room temperature (about 23°C). The stained samples were washed with corresponding buffers three times (allowing for 5 minutes between washes). The washed samples were put into silicone wells mounted on the regular glass slides. They were sealed with cover slips and silicone and observed by SCLM immediately or next day.

Table 3.1. List of fluorescent stains used with SCLM.

Fluorescent stain	Detection specific	Filter
Live/Dead	live and dead cells	FITC/TR
Gram stain	Gram sign living cells	---
Fluorescein isothiocyanate (FITC)	protein	FITC
Wheat germ agglutinin (WGA)* TR conjugated	N-acetylglucosamine and N-acetylneuraminic acid residues	TR
Concanavalin A (ConA)* TR conjugated	α-mannopyranosyl and α-glucopyranosyl residues	FITC

TR= Texas Red™, Molecular Probes, Inc., USA.
* = Lectin stains

For Live/Dead stain and Gram stain, two individual bottles labeled by the manufacturer as Component A and B were included in each stain package. The staining procedure for these two stains is similar. A portion of reagent (3 μL) from Component A and B of each stain were mixed

in a microfuge tube thoroughly. An amount of 3 μL from this mixture was added to another microfuge tube where a piece of floc sample was kept. The tube was mixed gently and incubated in the dark at room temperature (about 23°C) for 15 minutes. The stained sample was put into a silicone well mounted on the regular glass slide. It was sealed with a cover slip and silicone and observed by SCLM immediately.

3.6.3 Transmission Electron microscopy (TEM)

Transmission electron microscopy has been used to study the extracellular fibrils of biomass (Eighmy *et al.*, 1983; Leppard, 1986; Strycek *et al.*, 1992). The resolution of SCLM is not a significant improvement over the COM while the TEM greatly improves the resolution (Caldwell *et al.*, 1992). TEM possesses little depth of focus but a much better resolution (down to 1 - 2 nm), allowing the observation of the ultrastructural details within the floc matrix. A TEM image can show the material generally considered to be "colloidal" compounds (i.e. size < 0.45 μm).

Four-fold multipreparatory technique. Fibril aggregates can change drastically according to mode of preparation for TEM. Matrix shrinkage may occur due to the solvent dehydration. This brings the individual fibrils much closer together than they were in their unperturbed state and creates misleading 3-D spatial composition analysis. In order to overcome specific artifacts inherent to each mode of preparation when used independently, samples were stabilized by four different treatments correlatively (Figure 3.5) as described previously by Liss *et al.* (1996). The artifactual shrinkage due to the dehydration step in glutaraldehyde fixation is overcome by preparing the sample using the Nanoplast procedure. The low contrast in matrix structure when using Nanoplast is corrected by addition of uranyl acetate as an enbloc stain. A sub-sampling of the agarose-embedded floc (see Section 3.5.1 for stabilization method) was cut into four equal sections. A different treatment was applied to each section. The treatments are described in the following.

Glutaraldehyde and ruthenium red. Tube A of 2% glutaraldehyde (Glutaraldehyde EM, 8% stock solution, Marivac Ltd.) and tube B of 2% glutaraldehyde with 0.05% ruthenium red (RR) were

prepared as follows: 8% glutaraldehyde (2.5 mL) was put into each of two 15-mL centrifuge tubes (tube A and B). Na-cacodylate buffer (1 mL, 1M, pH=7.1) and distilled water (6.5 mL) were added to each tube. The RR powder (0.005 g) was added to tube B and mixed thoroughly.

A vial (Vial 1) with 1 % osmium tetraoxide (OsO_4, 4 % stock solution) and a second vial (Vial 2) with 1% OsO_4 plus 0.05% RR were prepared as follows: 4 % OsO_4 (1 mL) and distilled water (3 mL) were put into each vials. The RR powder (0.002 g) was added to Vial 2 and mixed thoroughly.

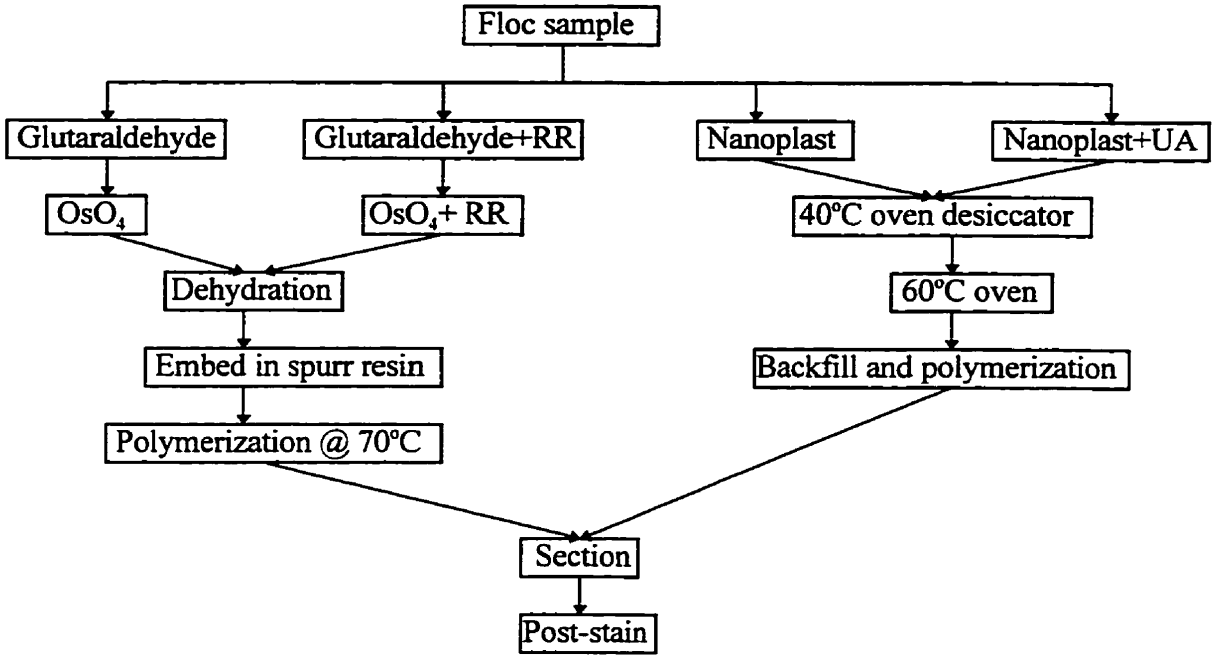

Figure 3.5. Four-fold multipreparatory technique for ultra-structural analysis of floc (Liss *et al.*, 1996). UA= uranyl acetate, RR= ruthenium red.

The agarose-embedded samples were put into tube A and B which were then incubated in ice for an hour (max. 2 h) and mixed periodically. The samples were then washed with 0.1 M Na-cacodylate buffer for three times (allowing for 5 minutes between washes). After washing, the contents from Vial 1 and 2 were put into tubes A and B respectively. Tubes A and B were incubated again in ice for an hour (shaking for every 15 minutes interval). These samples in tube A and B were rinsed twice with a minimum of 5 mL cold distilled water (the tubes were still kept

in ice and waited for 5 minutes between rinse). These samples were then dehydrated by mixing with about 5 mL of 50 % methanol for 10 minutes (mixed 2 - 3 times). This step was repeated by using methanol series at increasing concentrations as follows: 70%, 90% and 100%. The samples were then placed in increasing concentrations of Spurr resin (Spurr, 1969) and placed into molds. The resin was polymerized at 70°C for 8 h.

Nanoplast and uranyl acetate. A third vial (Vial 3) with Nanoplast (JBS-supplies) and a fourth vial (Vial 4) with Nanoplast and uranyl acetate were prepared as follows: Nanoplast resin (2 mL, medium-hard set: 10 g resin and 0.225 g catalyst) was put into an additional vial. Catalyst powder (0.045 g) was put into this vial and mixed thoroughly by a magnetic stir bar. Half of the well-mixed solution was put into Vial 3. Uranyl acetate (UA) powder (0.005 g) was put into the remaining solution in the vial and mixed well. After UA completely dissolved into the solution, it was put into Vial 4. Agarose embedded samples were put into Vial 3 and 4. Both vials were kept dark and cool and mixed on a spinner for overnight. After overnight mixing, the samples were put into micromold capsules and kept in a desiccator which was then placed in an oven at 40°C. After 48 h, the capsules were removed from the desiccator and heated for a further 48 h, at 60°C. The capsules containing the samples were then backfilled with Spurr resin and polymerized at 70°C for 8 h.

After polymerization, all samples were sectioned identically using a diamond knife mounted in an ultramicrotome (RMC Ultramicrotome MT-7). Ultrathin sections were mounted on copper grids. The Spurr sections were counter-stained with UA and lead citrate. The Nanoplast sections were counter-stained with 1% aqueous UA. Observations of the prepared samples were made in transmission mode (TEM) on ultrathin sections with a JEOL 1200 Ex II TEMSCAN scanning transmission electron microscope at an accelerated voltage of 80 kV.

3.7 Statistical analysis

The physical and chemical properties of sludge from each system were compared with that from the other three systems studied using 2-tailed t-test (Mendenhall and Sincich, 1992) to test the

hypothesis that there is no significant difference between systems. If the corresponding probability for the calculated t-statistic was $\geq$ 95%, then the null hypothesis was rejected and the characteristics were concluded to be different between systems.

The physical and chemical properties of sludge from functional and dysfunctional periods within a system were compared using ANOVA to test the hypothesis that there is no significant difference between periods. If the corresponding probability for the calculated F-statistic was $\geq$ 95%, then the null hypothesis was rejected and the characteristics were concluded to be different between periods.

The relation among the solids concentration, sludge settling and EPS composition was studied by computing the coefficient of correlation between variables. The null hypothesis that there is no correlation between variables was tested using the following test statistic (Norcliffe, 1982):

$$t = r\,((N-2)/(1-r^2))^{1/2} \qquad \text{(Eq. 3.6)}$$

where N = no. of samples

r = correlation coefficient

If the corresponding probability for the calculated t-statistic was $\geq$ 95%, then the null hypothesis was rejected and the variables were concluded to be correlated.

CHAPTER 4 RESULTS AND DISCUSSION

The primary goal of this work was to compare the activated sludge from different types of treatment systems. The characteristics of sludge from functional and dysfunctional settling periods within a system were compared as well. In addition, the relation among the solids concentration of sludge, sludge settling and the composition of extracellular polymeric substances (EPS) was investigated. To fulfill these objectives, mixed-liquor samples were collected regularly from four full-scale treatment systems for a six-month period. These systems treated different types of wastewater including domestic sewage (Dm), poultry processing wastewater (Py), petroleum refinery wastewater (Pm) and potato processing wastewater (Po). The operating conditions of the systems studied were very different as well. For instance, the mean cell residence time (MCRT) of the systems studied ranged between 4 to 25 days.

The characteristics of sludge were studied according to the following four categories: settling properties (SVI and 30-min settling test); chemical properties (EPS composition and sludge carbohydrate); physical properties (floc size and shape, settling velocity and effective density); and structural properties (spatial distribution of EPS and ultrastructure of extracellular matrix). The solids concentration of sludge expressed as mixed-liquor suspended solids (MLSS) and mixed-liquor volatile suspended solids (MLVSS) were determined as well. The data concerning operating conditions including the temperature, pH, hydraulic retention time (HRT), food-to-microorganisms ratio (F/M ratio) and MCRT were provided by the plant personnel.

The characteristics of sludge (except the structural properties) from each system were compared with that from the other three systems studied using a 2-tailed t-test to test the hypothesis that there is no significant difference between systems. If the corresponding probability for the calculated t-statistic was $\geq 95\%$, then the null hypothesis was rejected and the characteristics were concluded to be different between systems. The characteristics of sludge from functional and dysfunctional periods within a system were compared using ANOVA to test the hypothesis that there is no significant different between periods. If the corresponding probability for the

calculated F-statistic was $\geq$ 95%, then the null hypothesis was rejected and the characteristics were concluded to be different between periods. The relation among the solids concentration, sludge settling and EPS composition was studied by computing the coefficient of correlation between variables. The correlation coefficient (r) was tested using Eq. 3.6 as test statistic:

$$t = r\,((N-2)/(1-r^2))^{1/2} \qquad \text{(Eq. 3.6)}$$

where N is the number of samples, to test the null hypothesis that there is no correlation between variables. If the corresponding probability for the calculated t-statistic was $\geq$ 95%, then the null hypothesis was rejected and the variables were concluded to be correlated.

The results are represented in six sections. Descriptions of the treatment process of each system studied is described in Section 4.1. The operating conditions of each system are compared with the recommended conditions and the other systems studied. The comparison of settling properties of sludge among the systems studied is presented in Section 4.2. The comparison of chemical composition of sludge among the systems studied is presented in Section 4.3. The effect of operating conditions on chemical composition of sludge is discussed followed by the effect of chemical composition on settling properties. The relation among the solids concentration, EPS composition and settling properties is discussed. The comparison of physical properties of floc among the systems studied is presented in Section 4.4. The effect of floc size and shape on sludge settling is discussed followed by the effect of chemical composition on settling velocity and effective density. The comparison of sludge properties between functional and dysfunctional periods of system-Po is presented in Section 4.5. Finally, the qualitative comparison of ultrastructure of extracellular matrix and spatial distribution of EPS of floc among the systems studied is presented in Section 4.6. A summary of results and discussion is presented at the end of each section.

4.1 Operating conditions of system and evaluation

4.1.1 Characteristics of wastewater composition

Mixed-liquor samples were collected from four full-scale activated sludge wastewater treatment systems treating domestic sewage (Dm), poultry processing wastewater (Py), petroleum refinery wastewater (Pm) and potato processing wastewater (Po). The configuration of treatment system, process design and operating conditions for each of these systems reflected the characteristics of the wastewater and the requirements to effectively handle the very different wastes (Table 4.1).

Table 4.1. General characteristics of different types of wastewater.

Types of wastewater	General description	Major organic composition	Toxic compounds	BOD[1] mg/l
Domestic sewage (Dm)	Composition varies with time	Carbohydrates, fats, oils and grease	No data	198
Poultry processing wastes (Py)	High in dissolved and suspended matter	Blood, proteins and fats	No data	895
Petroleum refinery wastes (Pm)	High in dissolved salts from field, odor, hot	Oils and grease	Phenol, sulphur compounds, ammonia	na[2]
Potato processing wastes (Po)	High in suspended solids, colloidal and dissolved organic matter	Proteins and carbohydrates	No data	4926[3]

[1] Average BOD values of influent to the activated sludge systems over the past 10 months. [2]na: Not available as it was not measured by the treatment plant. [3] Average COD values of influent to the treatment plant.

The industrial wastewaters had a high nitrogen content. Poultry and potato processing wastewater had a high protein nitrogen. The petroleum refinery wastewater had a high

ammonia-nitrogen. Removal of nitrogen from wastewater prior to disposal is required as nitrogen is a nutrient to the microorganisms and can have an impact on receiving water quality. Therefore, removal of nitrogen in the industrial treatment systems studied was also considered to be as important as COD removal.

4.1.2 Operating conditions

The system capacity, temperature and pH of the activated sludge systems treating these four types of wastewater are described briefly. The capacities of systems studied ranged between 4400 to 818,000 m^3 of influent per day (Table 4.2). The municipal treatment system treating domestic sewage (system-Dm) had the largest capacity. The temperatures of three of the treatment systems including the system treating poultry processing wastewater (system-Py), the system treating potato processing wastewater (system-Po) and the system-Dm varied from a low of 6°C in the winter to a high of 31°C in the summer. The temperature of the system treating petroleum refinery wastewater (system-Pm) was at a higher constant temperature of 38°C due to a higher temperature of wastewater from the refinery process. The pH of mixed-liquor in all the systems studied were within the neutral range and generally fell between 7 and 8. Process modifications, HRT, MCRT and F/M ratio reflect the characteristics of the type of wastewater being treated and are described in the following section.

Step-feed process. For system-Dm and system-Pm, a step-feed process was employed (Figure 4.1). Since system-Dm treats both domestic and industrial sewage, the composition of wastewater can potentially vary with time (Figure 4.2). System-Pm treats the petroleum refinery wastewater containing by-product chemicals which are toxic to the living biomass in an activated sludge system (Figure 4.3). Therefore, shock load due to the varying organic strength and toxic chemicals in the wastewater may exist. In the step-feed process, the wastewater is fed to the aeration tanks at several points to equalize the F/M ratio. This modification has the advantages of lowering the peak oxygen demand and reducing the possibility of shock load (Meltcalf and Eddy, 1991). The flow diagrams of municipal and petroleum refinery wastewater treatment plants are shown in Appendix A (Figure A.1 and A.3).

Table 4.2. Operating conditions and recommended design parameters of the treatment systems.

Process types	Types of wastewater	Plant capacity (m^3/d)	Temperature[1] (°C)	pH	Other operating parameters	Operating condition	Recommended range[2]
Continuous, step-feed	Domestic sewage (Dm)	818,000	15 - 27	7 - 8	MCRT[3]	4	5 - 15
					HRT[4]	4	3 - 5
					F/M[5]	0.5 - 0.9	0.2 - 0.4
					MLSS[6]	2300	2000 - 3500
	Petroleum refinery wastes (Pm)	4,400	38	8	MCRT	20	5 - 15
					HRT	8	3 - 5
					F/M	na[7]	0.2 - 0.4
					MLSS	4320	2000 - 3500
Continuous, extended aeration	Poultry processing wastes (Py)	8,300	6 - 27	7	MCRT	25	20 - 30
					HRT	84	18 - 36
					F/M	0.05 - 0.15	0.05 - 0.15
					MLSS	3620	3000 - 6000
Continuous, complete-mix, BNR[8] for nitrogen removal	Potato processing wastes (Po)	7,900	26 - 31	7 - 7.6	MCRT	8 - 10	5 - 15
					HRT	28	3 - 5
					F/M	na	0.2 - 0.6
					MLSS	2800	2500 - 4000

[1] Range over 12 months period, [2] Metcalf and Eddy (1991), [3] Mean cell residence time [d], [4] Hydraulic retention time [h], [5] Food-to-microorganisms ratio [kg BOD/kg VSS per day, [6] Mixed-liquor suspended solids [mg/l.], [7]na: not available as it was not measured by the treatment plant, [8] Biological Nitrogen Removal.

Of the treatment systems studied, system-Dm had the shortest HRT and MCRT, 4 hours and 4 days, respectively. System-Pm was operated at a long MCRT of 20 days. A long MCRT favours the growth of nitrifying bacteria for the removal of ammonia in the wastewater (Petro-Canada, 1997).

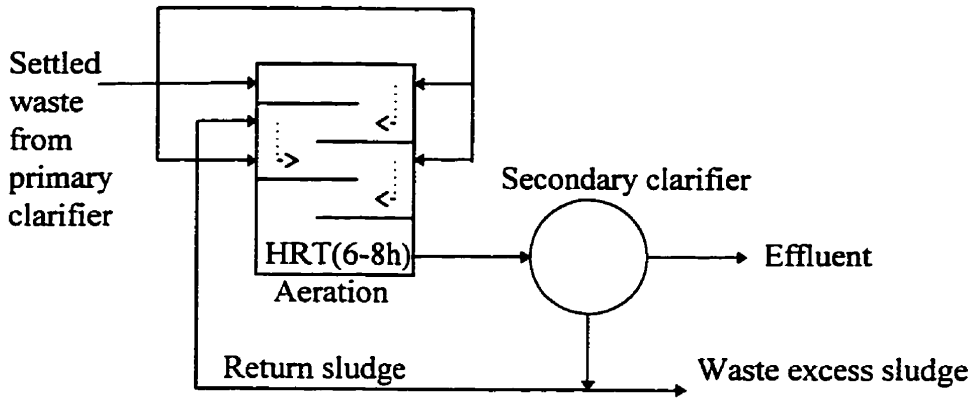

Figure 4.1. A typical flow diagram for step-feed process (Jones, 1974).

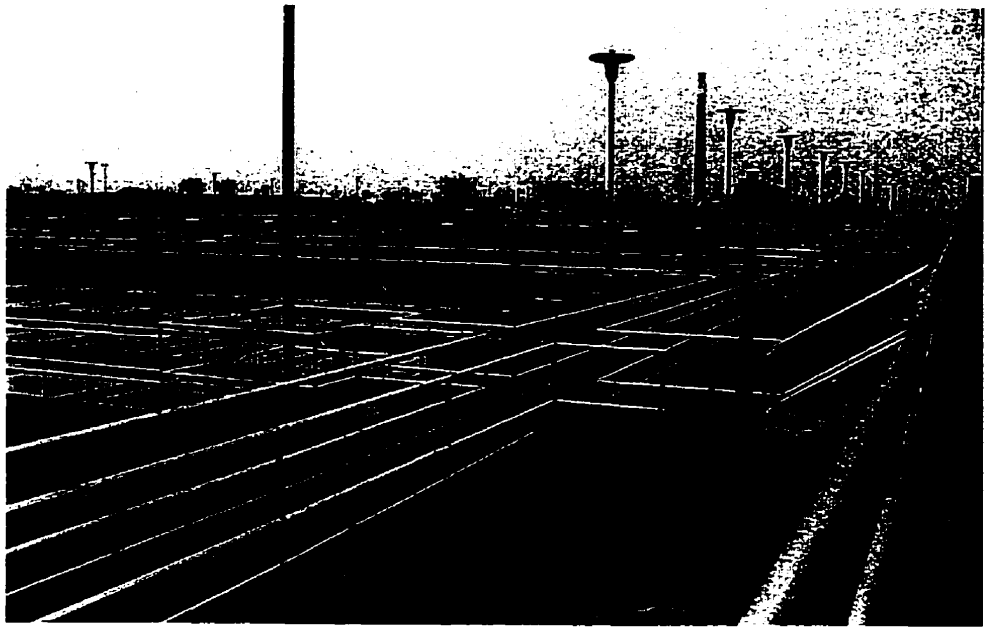

Figure 4.2. The aeration tanks and clarifier of system-Dm.

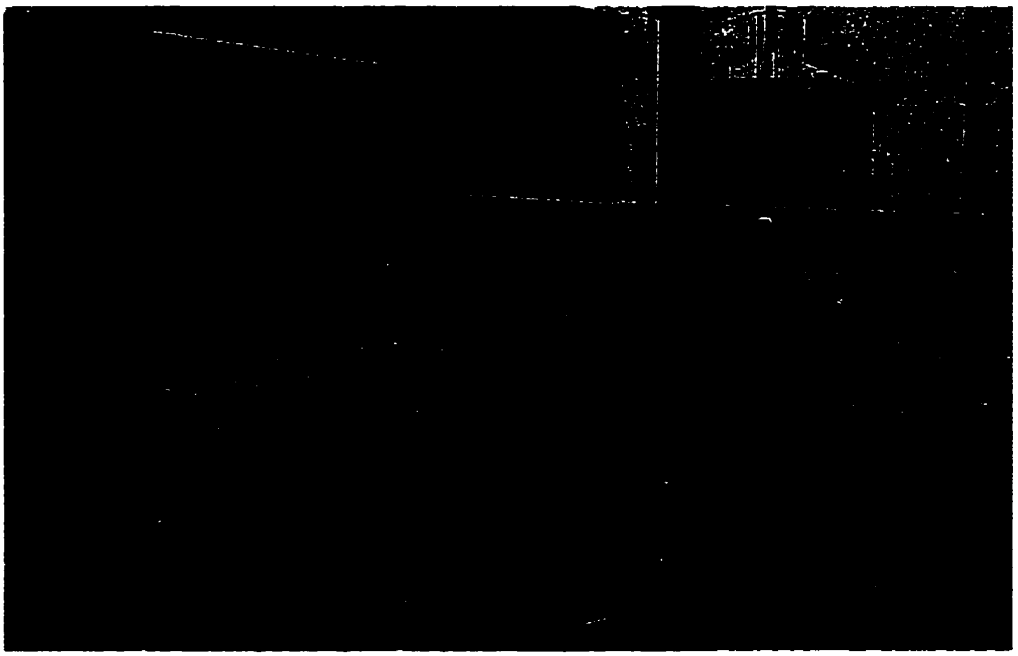

Figure 4.3. The aeration tank of system-Pm (covered completely due to the strong sulphide odor in the wastewater).

Extended aeration. System-Py was an extended aeration system which was operated at a long HRT (84 hours) and MCRT (25 days) for the removal of the protein nitrogen in the wastewater (Figure 4.4). A flow diagram of the treatment plant is shown in Appendix A (Figure A.2). The HRT and MCRT of the system were the longest time frames included in this study. The biomass in the extended aeration system is typically in the endogenous respiration phase of the growth curve. This condition presumably requires a low organic loading and a long aeration time (Metcalf and Eddy, 1991). The F/M ratio of system-Py ranged between 0.05 to 0.15 kg BOD/kg VSS per day which is much lower than system-Dm whose F/M ratio ranged between 0.5 to 0.9 kg BOD/kg VSS per day. Under this low organic loading, a small volume of sludge is generated.

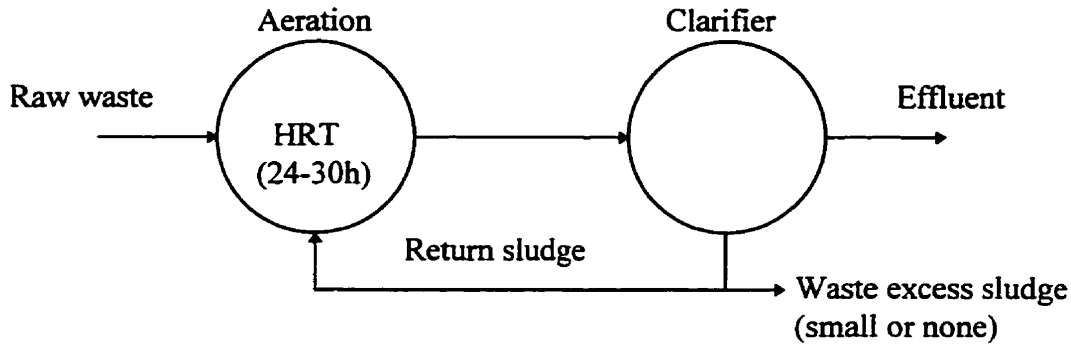

Figure 4.4. A typical flow diagram for an extended aeration process (Jones, 1974).

Biological Nutrient Removal. System-Po is a biological nutrient removal (BNR) process designed for the removal of protein nitrogen (Figure 4.5). A flow diagram of the treatment plant is shown in Appendix A (Figure A.4). Protein nitrogen is transformed into ammonia-nitrogen by bacterial decomposition and hydrolysis. The removal of ammonia-nitrogen from wastewater is accomplished in two conversion steps. In the first step, nitrification, the oxygen demand of ammonia is reduced by converting it to nitrates, which takes place in an aerobic zone. However, the nitrogen has merely changed forms and has not been removed. In the second step, denitrification, nitrate is converted to a gaseous product in an anoxic (without oxygen) zone (Metcalf and Eddy,1991). The BNR process includes an anoxic zone for the removal of nitrogen. The HRT and MCRT of system-Po were 28 hours and 8 - 10 days, respectively.

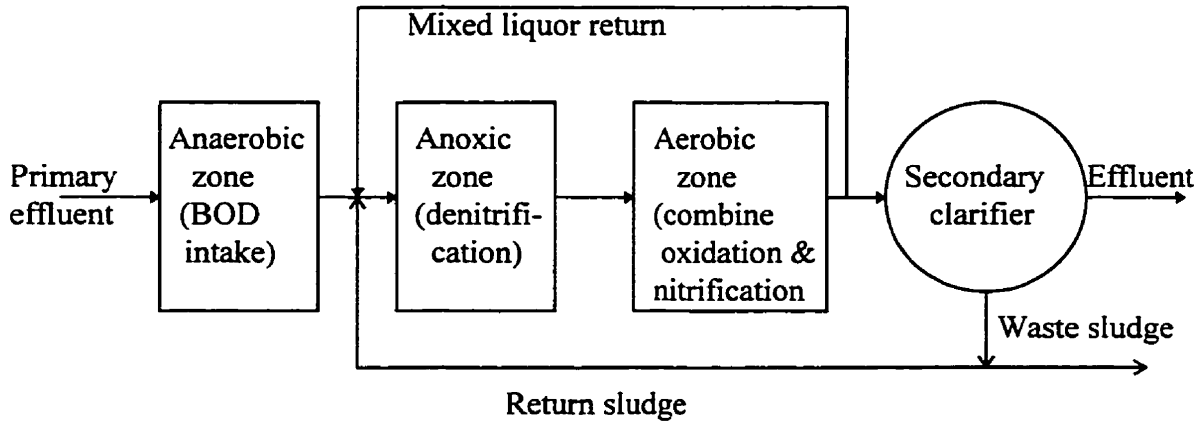

Figure 4.5. A typical flow diagram for BNR process (Metcalf and Eddy,1991).

4.1.3 Evaluation of the operating conditions

The MLSS of all systems except system-Pm were kept within the recommended range (Table 4.2). Keeping the MLSS within this range is necessary in order to maintain the optimum sludge-blanket level for an efficient operation in the clarifier. The MLSS can be monitored by regulating other operating parameters such as MCRT, HRT and F/M ratio. The MCRT of system-Dm was 4 days which was slightly lower than the recommended range of 5 - 15 days for the step-feed process (Metcalf and Eddy,1991). The lower MCRT reduced the biomass concentration in the system and increased the F/M ratio. The F/M ratio of system-Dm was between 0.5 - 0.9 kg BOD/kg VSS per day which was higher than the recommended range of 0.2 - 0.4 kg BOD/kg VSS per day. The higher F/M ratio increased the biomass production. As a result, the MLSS of system-Dm were kept within the recommended range of 2000-3500 mg/L. The F/M ratio of system-Py was kept at a recommended range of 0.05 - 0.15 kg BOD/kg VSS per day by increasing the HRT to 84 hours where the recommended range is 18 - 36 hours for the extended aeration process. The HRT is often used to regulate the F/M ratio of the system. The MLSS of system-Py were kept within the recommended range of 3000-6000 mg/L. The HRT of system-Po was 28 hours which was higher than the recommended range of 3 - 5 hours. The HRT is regulated according to the organic strength of influent. The organic strength of influent to system-Po was not measured; therefore, the F/M ratio of the system could not be determined. Nevertheless, the MLSS of system-Po were kept within the recommended range of 2500 - 4000 mg/L.

The MLSS of system-Pm were 4320 mg/L which was about 23% higher than maximum limit of recommended range of 2000 - 3500 mg/L. The higher MLSS were due to the higher MCRT and HRT. The MCRT and HRT were 20 days and 8 hours, respectively, which were higher than the recommended ranges for the step-feed process. The recommended ranges of MCRT and HRT are 5 - 15 days and 3 - 5 hours, respectively. The higher MCRT favours the growth of nitrifying bacteria for ammonia removal. However, this higher MCRT also led to the increase of biomass concentration in the system and poor sludge settling observed during the course of the study. The average height of settled sludge after 30 minutes was 87% ± 11% which was the highest among the systems studied.

In summary, the systems studied represented a range of configurations and different types of wastewater composition. The distinct operating conditions such as MCRT (sludge age) and microbial community of each system could possibly affect the sludge properties. The effect of sludge age on EPS composition is discussed in Section 4.3. The characterization of microbial communities is reported in Section 4.4.2.

4.2 Settling properties of sludge

The sludge settling and sludge properties from different systems are compared and discussed in the following sections. A summary of these properties is shown in Table 4.3.

SVI and settling test. The sludge of system-Dm settled better than the other systems. The settling of sludge was measured as SVI and 30-min settling test. The average SVI of system-Dm was 87 mL/g which is significantly lower than the other systems (Figure 4.6 and Table 4.4). The average SVI of the other three systems were similar and in the range of 215 - 219 mL/g. No significant differences were found. However, the limitations in applying SVI to indicate the settleability should be noted. The index value that is characteristic of a good settling sludge varies with the characteristics and concentration of the mixed-liquor solids, so observed values for a given system are not comparable to other systems. For example, if the solids did not settle at all but occupied the entire 1000 mL at the end of 30 minutes, the maximum index value would be obtained and would vary from 1000 for a MLSS of 1000 mg/L to a 100 for a MLSS of 10,000 mg/L (Metcalf and Eddy,1991). For such conditions, the computation has no meaning other than determination of limiting values. Therefore, the 30-min settling test was used to indicate the height of settled sludge in a 1-litre graduated cylinder after 30 minutes. The 30-min settling test for system-Dm was 21% which was significantly lower than that of the other systems (Figure 4.7 and Table 4.4). The 30-min settling test of the system-Po was 66% which was lower than that for system-Py and system-Pm whose 30-min settling test were 83 and 87%, respectively. Although the differences in the settling test between the industrial systems studied

were not significant, this test still indicates that the sludge of system-Po settled relatively better than system-Py and system-Pm.

Table 4.3. The settling properties of sludge from different treatment systems.

Treatment systems	No. of samples analyzed	SVI (mL/g)			30-min settling test (%)		
		Range	Mean	SD%	Range	Mean	SD%
System-Dm	17	77-98	87	8	13-36	21	24
System-Py	8	143-254	219	15	57-96	83	17
System-Pm	7	162-307	216	25	71-97	87	11
System-Po	10	125-319	215	31	29-100	66	44

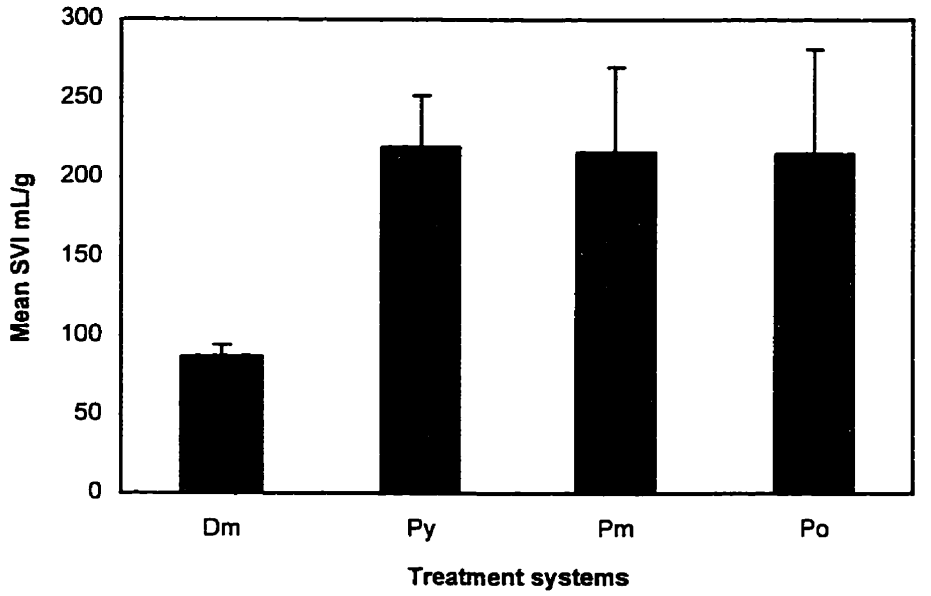

Figure 4.6. The mean SVI of sludge from different treatment systems.

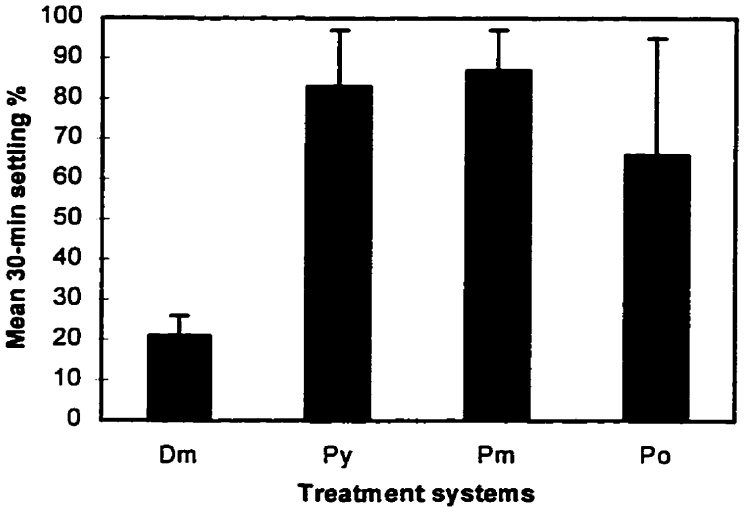

Figure 4.7. The mean 30-min settling test of sludge from different treatment systems.

Table 4.4. Comparison of settling properties of sludge from different treatment systems.[1]

Treatment systems	Settling properties[2,3]	
	SVI	30-min.settling test
Dm-Py	sd	sd
Dm-Pm	sd	sd
Dm-Po	sd	sd
Py-Pm	nsd	nsd
Py-Po	nsd	nsd
Pm-Po	nsd	nsd

[1]Results of the statistical comparison using t-test can be found in Appendix I. No. of sludge samples analyzed are as follows: Dm (17), Py (8), Pm (7) and Po (10).
[2] sd: significant difference of the means between two systems using 2-tailed t-test at $\alpha = 0.05$.
[3] nsd: no significant difference of the means between two systems using 2-tailed t-test at $\alpha = 0.05$.

For the industrial systems, the high SVI and 30-min settling test indicated poor settling. However, the systems were still regarded as normal by plant personnel. This high level of settled sludge was partly due to the high MLSS. However, lowering MLSS may not be desirable for many plants as this may cause the loss of nitrification and increase waste sludge production (WEAO, 1997).

Turbidity. Turbidity of the supernatant of settled sludge from system-Dm and system-Pm were lower. Turbidity, a measure of the light-transmitting properties of water, is another test used to indicate the quality of waste discharges and natural waters with respect to colloidal and residue suspended matter (Metcalf and Eddy, 1991). It is determined quantitatively by measuring the intensity of light scattered by a sample. However, only a qualitative observation of turbidity of the supernatant following sludge settling was done in this study. A clear supernatant was observed usually in settled sludge for system-Dm and system-Pm. Occasionally sludge from system-Py and system-Po was observed to rise or float to the surface after a relatively short settling period (rising sludge). The likely cause of this phenomenon is denitrification, in which nitrites and nitrates in the wastewater are converted to nitrogen gas. As nitrogen gas is formed in the sludge layer, much of it is trapped in the sludge mass that becomes buoyant and rises to the surface (Metcalf and Eddy, 1991). Turbidity of the supernatant in system-Py was relatively higher than the other systems as pin-point flocs were observed occasionally.

In summary, the sludge of system-Dm settled better than the industrial systems in terms of SVI, 30-min settling test and turbidity. Although the SVI and 30-min settling test indicate poor settling of sludge from industrial systems, the systems were still regarded as normal by plant personnel. This indicates the concern of fulfilling other operation objectives such as the BOD and nutrient removal besides the clarification of treated effluent.

4.3 EPS composition

Extraction of EPS from sludge matrix is required prior to the chemical analysis of its composition. Prior to extraction, the sludge was washed to remove the effluent polymer so that only the capsular polymer was extracted. The extraction strategy recommended by Frølund *et al.* (1995) using the cation exchange resin (CER) was employed. This extraction strategy is discussed in Section 4.3.1. The EPS composition and the effect of sludge age on it are reported and discussed in Section 4.3.2. The characteristics of EPS composition from each system were compared using a 2-tailed t-test to test the hypothesis that there is no significant difference between systems. If the corresponding probability for the calculated t-statistic was $\geq 95\%$, then the null hypothesis was rejected and the characteristics were concluded to be different between systems. The relation

between the EPS composition and other sludge and settling properties is discussed in Section 4.3.3. The correlation coefficient (r) was tested using Eq. 3.6 to test the null hypothesis that there is no correlation between variables. If the corresponding probability for the calculated t-statistic was $\geq 95\%$, then the null hypothesis was rejected and the variables were concluded to be correlated.

4.3.1 Evaluation of extraction technique

Cell lysis and EPS degradation through the extraction procedure using cation exchange resin (CER) were not significant according to the study of Frølund *et al.* (1996). The same study used the High Performance Size Exclusion Chromatography (HPSEC) to investigate the extracted EPS and revealed that the extraction using CER did not significantly degrade the EPS. They reported that some cell lysis was identified during extraction for extraction time greater than 1 - 2 h by observing a decrease in cell number. However, the lysis was not considered a significant problem for contaminating the EPS. Moreover, they recommended a mild extraction strategy with minimum induced cell lysis by using a short extraction time (0.5 - 1 h), 600 rpm stirring intensity and approximately 70 g CER/g VSS . This mild extraction strategy was employed in this study. Therefore, the concerns about the cell lysis and EPS degradation were minimized.

This extraction method is suitable to be used for the sludge from different treatment systems according to Frølund *et al.* (1996) and the standard deviations of the test on reproducibility ranged between 4 - 17 %. Frølund *et al.* (1996) reported that the sludge from two different types of treatment plants responded very similarly to this CER extraction. Therefore, this extraction method is suitable to be used for study of the sludge from different types of treatment plants. The reproducibility of this extraction technique was tested by two extractions on sludge taken from same sample. The standard deviations (SD %) of protein and DNA were about 5 % while carbohydrate and acidic polysaccharide were 13 and 17 % respectively (Table 4.5). This indicates that the precision in extraction of protein and DNA is higher than polysaccharides. It may be due to the reason that the components in EPS show a different accessibility for extraction (Frølund *et al.*, 1996). Their study reported that DNA and uronic acid were rapidly extracted while protein was the most difficult compound to extract. Therefore, the level of

acidic polysaccharide may be more sensitive to any possible random error incurred between two extractions. However, only two extractions were done to test the reproducibility in this study and this is not enough to get a good measure of error. Moreover, sludge is a very heterogeneous biomass and sub-samples from the same sample can still be very different. Therefore, the reproducibility reported in this study can only be a very rough approximation. More tests should be done to get a better determination of the reproducibility of this extraction technique in further studies. The levels of EPS are compared to the published data of Frølund *et al.* (1996) since the same extraction technique was used in both studies. A lower level of EPS was found in this study (Table 4.6). It may be due to a lower mixing intensity of 600 rpm used in this study while a mixing intensity of 900 rpm was used in their study.

Table 4.5. Reproducibility of the CER extraction method[1].

	EPS composition mg/gVSS			
	Protein	CHO	DNA	Acidic Poly.
1st Trial	63.89	5.07	2.88	1.74
2nd Trial	60.00	6.13	2.69	2.22
Mean	61.95	5.60	2.79	1.98
SD %	4	13	5	17

[1] Extraction condition: 57 g CER/g VSS at 600 rpm for 1 h.

Table 4.6. Comparison of EPS composition with published data using the CER extraction method.

	CHO in sludge	EPS composition mg/gVSS			
	mg/gVSS	Protein	CHO	DNA	Acidic Poly.
This study[1]	152 - 237	37 - 79	6 - 10	2 - 4	2 - 4
Frølund *et al.*, 1996[2]	179 - 181	90 - 95	15 - 20	10 - 11	3 - 4

[1] Extraction conditions: 70 g CER/g VSS at 600 rpm for 1 hour. Results from sludge of four different treatment systems.
[2] Extraction conditions: 65 - 85 g CER/g VSS at 900 rpm for 1 hour.

The results of extracted EPS from the standardized extraction technique are more useful for a comparative study. Data on composition of extracted EPS from different studies is sometimes controversial since there is no unified method for extraction as discussed in Section 3.4.1. In addition, the extraction method employed in this study is sensitive to the amount of CER added, stirring intensity and extraction time. Therefore, the level of extracted EPS is susceptible to changing in any of these extraction conditions. Hence, standardizing the extraction method and conditions initially are necessary.

4.3.2 EPS composition of sludge from different systems

Protein was found to be the dominant component in the extracted EPS followed by carbohydrate, DNA and acidic polysaccharide generally regardless of the types of wastewater and operating conditions (Figure 4.8). This sequence of dominance of components in EPS agrees with the result reported by Vallom and McLoughlin (1984) but differs from Pavoni *et al.* (1972) who reported that carbohydrate was the major constituent followed by RNA, protein and DNA. Vallom and McLaughlin (1984) accounted for the difference in the substrate used in each study. Protein was found to be the major constituent in extracted EPS while it was used as a substrate to acclimate the sludge. Carbohydrate was reported as the major constituent when it was used as the substrate. However, the substrate attached to the sludge might bias the level of particular component in extracted EPS since no washing step prior to extraction was done in those studies. Prior to extraction, sludge washing is important to the removal of the organic content of sewage and the slime layer. The same recommendation is given from the work of Gehr and Henry (1983) and Frølund *et al.* (1995). This helps to focus on the level of floc-bound EPS. Vallom and McLoughlin (1984) reported that the four general constituent polymers DNA, RNA, carbohydrate and protein accounted for at least 88 $\pm$ 4 % of the polymeric groups present at the onset of flocculation.

Table 4.7. The EPS composition of sludge from different treatment systems.

Types of treatment systems		System-Dm			System-Py			System-Pm			System-Po		
No. of samples analysed			17			8			7			10	
		Range	Mean	SD %	Range	Mean	SD %	Range	Mean	SD %	Range	Mean	SD %
Sludge properties	MLSS (g/l)	1.553 - 4.020	2.304	26	3.310 - 4.110	3.616	11	2.660 - 5.813	4.319	23	2.223 - 3.680	2.795	21
	MLVSS (g/l)	0.9833 - 2.467	1.489	20	2.137 - 3.090	2.750	11	2.300 - 4.753	3.564	28	1.827 - 3.000	2.274	18
	VSS/SS (%)	61 - 68	65	3	74 - 78	76	1	80 - 87	83	4	78 - 84	82	2
	CHO in sludge (mg/gVSS)	152.2 - 308.2	202.3	25	113.8 - 201.3	152.3	22	102.1 - 255.5	177.2	28	122.7 - 441.2	236.7	49
EPS composition	Protein (mg/gVSS)	56.63 - 125.9	79.38 (80.8)[1]	20 (6)	24.40 - 53.36	37.06 (75.9)	24 (7)	28.50 - 77.98	51.19 (80.6)	29 (5)	29.19 - 88.19	55.59 (76.5)	32 (11)
	CHO (mg/gVSS)	5.067 - 22.79	10.32 (10.8)[2]	39 (31)	4.525 - 7.507	5.874 (12.6)	15 (25)	4.980 - 11.66	7.656 (12.5)	26 (28)	5.295 - 17.60	10.35 (14.8)	39 (42)
	DNA (mg/gVSS)	2.005 - 5.668	4.146 (4.2)[3]	24 (26)	2.710 - 4.958	3.945 (8.5)	20 (33)	1.180 - 4.408	2.176 (3.7)	46 (57)	0.6955 - 5.480	2.694 (3.7)	74 (62)
	Acidic Poly. (mg/gVSS)	1.741 - 7.370	4.081 (4.2)[4]	25 (31)	0.7655 - 3.476	1.489 (3.0)	60 (50)	0.4826 - 4.002	1.967 (3.1)	51 (55)	1.931 - 5.656	3.49 (4.9)	29 (29)
	Total EPS (mg/gVSS)	70.69 - 152.5	97.69 (100)	19	36.58 - 64.49	48.37 (100)	19	37.98 - 89.72	62.99 (100)	25	50.27 - 112.6	72.13 (100)	29
	Extractable CHO (%)	1.8 - 12.7	5.3	43	3.0 - 4.9	4.0	18	2.9 - 4.9	4.3	30	2.3 - 5.8	4.4	23

[1] The percentage composition of protein [%]. [2] The percentage composition of carbohydrate [%]. [3] The percentage composition of DNA [%].
[4] The percentage composition of acidic polysaccharide [%].

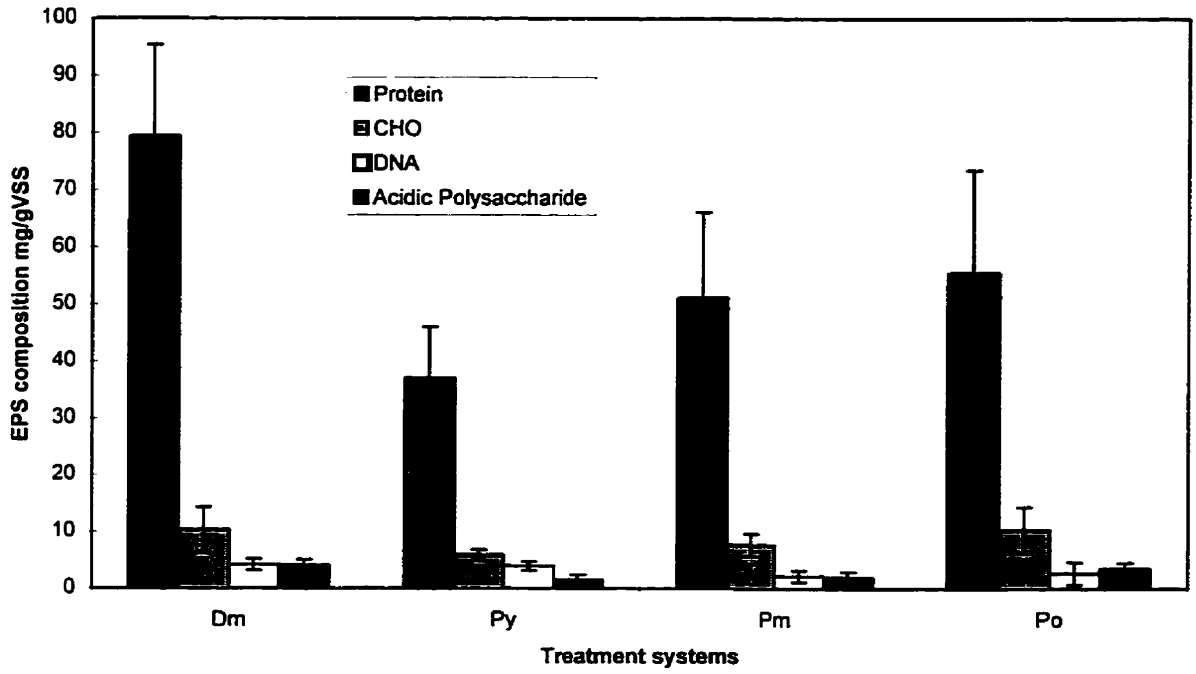

Figure 4.8. EPS composition of sludge from different treatment systems.

Table 4.8. Comparison of EPS composition of sludge from different treatment systems.[1]

Treatment systems	EPS composition[2,3]				
	Protein	CHO	DNA	Acidic Poly.	Total EPS
Dm-Py	sd	sd	nsd	sd	sd
Dm-Pm	sd	nsd	sd	sd	sd
Dm-Po	sd	nsd	sd	nsd	sd
Py-Pm	nsd	nsd	sd	nsd	nsd
Py-Po	sd	sd	nsd	sd	sd
Pm-Po	nsd	nsd	nsd	sd	nsd

[1]Results of the statistical comparison using t-test can be found in Appendix I. No. of sludge samples analyzed are as follows: Dm (17), Py (8), Pm (7) and Po (10).
[2]sd: significant difference of the means between two systems using 2-tailed t-test at $\alpha = 0.05$.
[3]nsd: no significant difference of the means between two systems using 2-tailed t-test at $\alpha = 0.05$.

DNA and acidic polysaccharide were the most labile components in EPS. The standard deviations (SD %) of the levels of acidic polysaccharide in system-Py and system-Pm was 60 and 51 % respectively. These deviations were the highest among the other components in EPS (Table 4.3). The standard deviation of the level of DNA in system-Po was 74 % which was the highest deviation among the other components in EPS. Therefore, the levels of acidic polysaccharide and DNA in EPS within a system varied quite remarked (SD > 50%). Bura *et al.* (1997) reported more than 30 % loss of uronic acid and a 10 % loss of DNA after the storage of sludge at 4 °C for one day. In fact, it was only possible to analyze samples from system-Dm immediately after sampling. Samples from other systems were stored for about one day before analysis due to the remote locations from the plants to the laboratory. This storage time may account for the larger deviations in measurement for these two components. Moreover, the samples came from uncontrolled systems. The sludge could be very different even though they came from the same system.

EPS and sludge age. The highest level of EPS was found with the youngest sludge. The level of EPS in sludge from system-Dm was the highest followed by the sludge from system-Po, system-Pm and system-Py (Figure 4.9). The significance of difference in the total EPS among the systems is shown in Table 4.8. This is in same order as increasing sludge age as the sludge age of system-Dm, system-Po, system-Pm and system-Py were 4, 9, 20 and 25 days respectively. However, the level of DNA of system-Py was exceptionally high at 3.945 mg/g VSS which is significantly higher than the system-Po and system-Pm (Table 4.5). It may be due to the long retention of solids in the system-Py whose MCRT was 25 days and hence increased the proportion of cells degraded by endogenous respiration and subjected to cell lysis. However, this cell lysis did not cause an increase in the levels of other components in EPS except DNA. Palmgren and Nielsen (1996) studied the accumulation of DNA in the exopolymeric matrix of activated sludge and suggested that inhibition of DNAses and protection of DNA by metal ions are the most probable reasons why the DNA is retained in the matrix but the other lytic material might be degraded by the bacteria.

The level of EPS in sludge is inversely associated with the MCRT of system ranging between four to 25 days. The bacterial storage polymers accumulate when the F/M ratio is low under endogenous respiration phase, a phase which could be expected to be dominant in activated sludge systems with the longer periods of aeration (Forster, 1976). Pavoni *et al.* (1972) reported that EPS production increased with the sludge age up to 7 days and the optimum was found during the endogenous growth stages of bacteria. However, this study did not show the sludge age in which this optimum production of EPS would persist. Instead, Bank *et al.* (1976) studied viability of sludge in several plants with results indicating that the viability of bacteria decreased with the increasing MCRT up to 7 days. Gulas *et al.* (1979) observed a decline in polymeric mass with increasing sludge ages. Vallom and McLoughlin (1984) reported that the EPS composition decreased with the longer length of the endogenous phase, which possibly reflects the slow degradation of the polymers present in the system. Therefore, the viability and level of EPS may be associated inversely with sludge age.

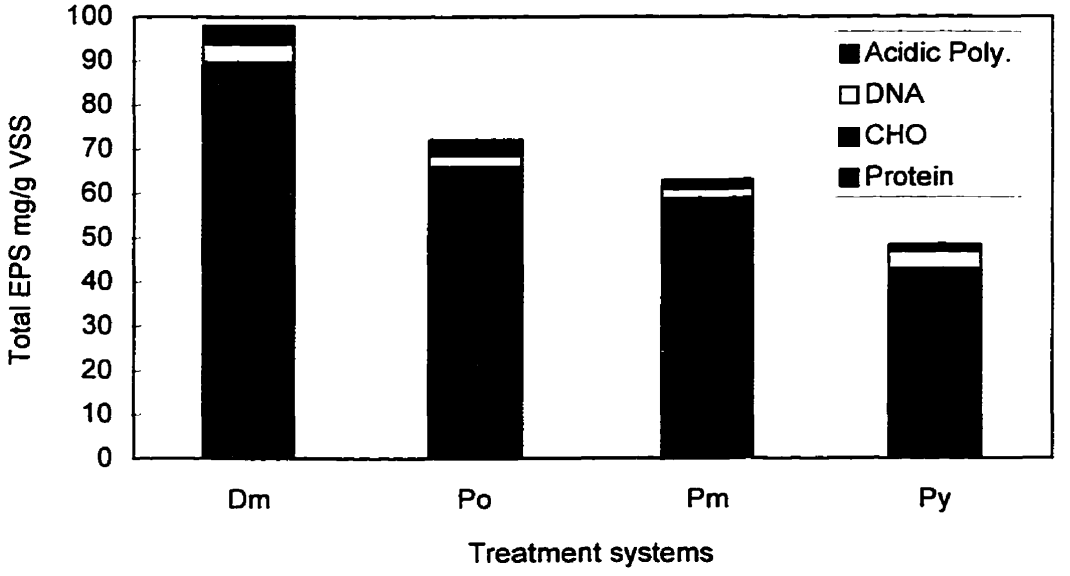

Figure 4.9. Total EPS of sludge from different treatment systems.

Percentage composition. The levels of protein, polysaccharide and DNA formed a more or less constant percentage composition in the organic matrix generally. The percentage composition of EPS in the systems varied between 77 - 81% protein, 11 - 15% carbohydrate, 4 - 9% DNA

and 3 - 5% acidic polysaccharide (Figure 4.10). The percentage composition of EPS in sludge from system-Dm are not significantly different from sludge of system-Po and system-Pm regardless the difference in wastewater composition (Table 4.9). Because of the difference in substrate, it is reasonable to assume that the predominant bacterial species differ in different microbial communities. Pavoni *et al.* (1972) studied bacterial growth on four different substrates and suggest that the precise composition of various exocellular polymers differ according to microbial dominance but all have constituents in common. The same kind of argument is supported by Tenney and Verhoff (1973). However, this study reveals that the level of EPS does vary with system but the percentage composition does not vary significantly regardless of the differences in wastewater composition. This agrees with the study by Urbain *et al.* (1993) where they found that the levels of protein, polysaccharide and DNA formed a more or less constant ratio in the organic matrix.

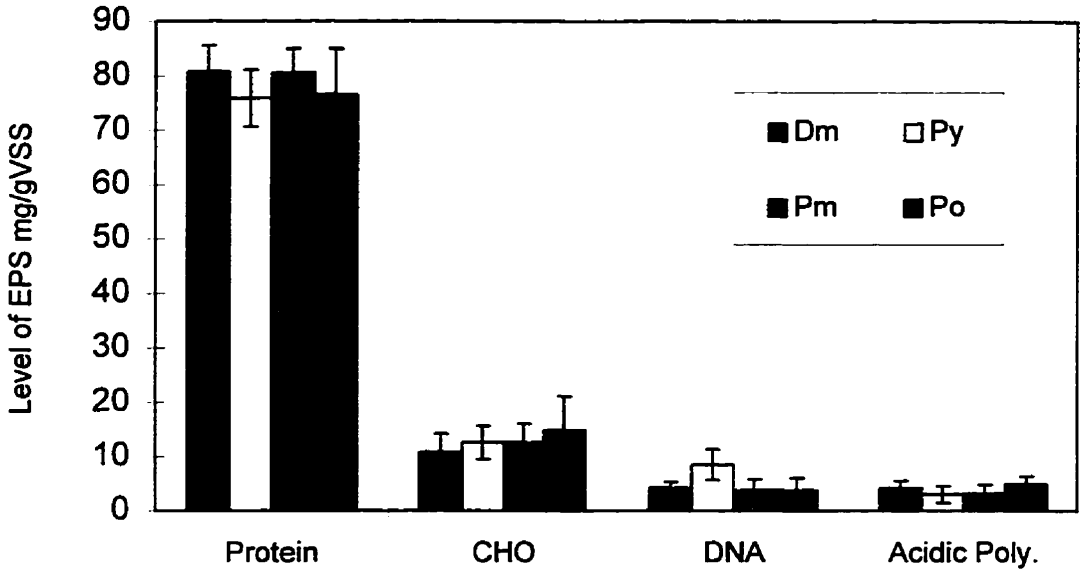

Figure 4.10. The percentage composition in EPS of different treatment systems.

Table 4.9. Comparison of percentage composition in EPS of different treatment systems.[1]

Treatment systems	Percentage composition[2,3]			
	Protein	CHO	DNA	Acidic Poly.
Dm-Py	sd	nsd	sd	nsd
Dm-Pm	nsd	nsd	nsd	nsd
Dm-Po	nsd	nsd	nsd	nsd
Py-Pm	nsd	nsd	sd	nsd
Py-Po	nsd	nsd	sd	sd
Pm-Po	nsd	nsd	nsd	sd

[1]Results of the statistical comparison using t-test can be found in Appendix I. No. of sludge samples analyzed are as follows: Dm (17), Py (8), Pm (7) and Po (10).
[2] sd: significant difference of the means between two systems using 2-tailed t-test at $\alpha = 0.05$.
[3] nsd: no significant difference of the means between two systems using 2-tailed t-test at $\alpha = 0.05$.

The operating conditions such as sludge age is much more important than microbial community alone as a factor in affecting the percentage composition of EPS. The percentage composition of EPS in sludge from system-Dm are not significantly different from the sludge of system-Po and system-Pm regardless the differences in microbial communities as discussed in Section 4.4.2. On the other hand, the percentage composition of DNA in system-Py was 9% which is significantly higher than system-Dm regardless of the similarity in their microbial communities as discussed in Section 4.4.2 (Figure 4.18). This may be due to the long retention of solids and cell lysis in system-Py as discussed previously.

4.3.3 Relationship of settling, sludge properties and EPS composition

The relationships between the settling properties, sludge properties and EPS composition of sludge from system-Dm were investigated further using linear correlation (Mendenhall and Sincich,1992). The SVI of sludge from system-Dm was lower than 100 mL/g and the 30-minute settling was about 20% as discussed at Section 4.2. Sludge with this settling properties is described as good settling as SVI value of 150 mL/g is considered to be a limit before bulking (Forster, 1985). The linear correlation matrix of settling properties, sludge properties and EPS

composition was set up as shown in Table 4.10 and significant linear relationships between variables were tested statistically at a 0.95 probability level (Norcliffe, 1982).

Table 4.10 Linear coefficients of correlation statistically significant at a 0.95 probability level ($\alpha = 0.05$, no. of samples = 11, no. of variables = 10).

	SVI	MLSS	MLVSS	VSS/SS%	CHO_{sludge}	Ext-CHO	$Protein_{EPS}$	CHO_{EPS}	DNA_{EPS}	AP_{EPS}
SVI	1.00	-	-	-	-	-	-	-	-	-
MLSS	-	1.00	-	-	-	-	-	-	-	-
MLVSS	-	0.99	1.00	-	-	-	-	-	-	-
VSS/SS%	-	-	-	1.00	-	-	-	-	-	-
CHO_{sludge}	-	0.69	0.68	-	1.00	-	-	-	-	-
Ext-CHO	-	-	-	-	-	1.00	-	-	-	-
$Protein_{EPS}$	-	-	-	-	-	-	1.00	-	-	-
CHO_{EPS}	-	-	-	-	0.73	-	-	1.00	-	-
DNA_{EPS}	-0.61	-	-	-	-	-	-	-	1.00	-
AP_{EPS}	-0.71	-	-	-	-	-	-	0.65	-	1.00

The significant tests on the correlation coefficients are shown in Appendix 1.

EPS and SVI. The higher levels of DNA and acidic polysaccharide in EPS may be associated with better sludge settling. The levels of DNA and acidic polysaccharide were inversely correlated to SVI with the correlation coefficients of - 0.61 and - 0.71 respectively (Figure 4.11). This suggests a positive role of DNA and acidic polysaccharide on settling. However, the data originated from full-scale system was not subject to the degree of control which can be achieved in laboratory experiments. Therefore, this is a trend rather than a precise relationship. These results are compared with other studies and contradictions are found (Table 4.11). The relation between DNA and SVI agrees with the result from Vallom and McLoughlin (1986). They reported that the flocculation occurred during the same stage that lysis took place. The same study suggests that DNA can act as a bridge to bind individual cells. However, this disagrees with Urbain *et al.* (1993) who reported an increase in SVI with a high level of DNA in EPS. The strongly flocculated activated sludge had a higher content of DNA in the floc matrix than the more loosely flocculated and the not flocculated systems reported by Polmgren and Nielsen (1996). Even thought the mechanism of how DNA acts as a floc agent is still not clear yet, this study supports its positive role on flocculation. In addition, acidic polysaccharide plays an important role at the surface of non-bulked sludge is suggested by Forster (1971). Acidic polysaccharides

such as uronic acids are described as glue-like component of the exopolymer (Fazio *et al.*, 1982; Dade *et al.*, 1991). This favours the sludge flocculation and settling.

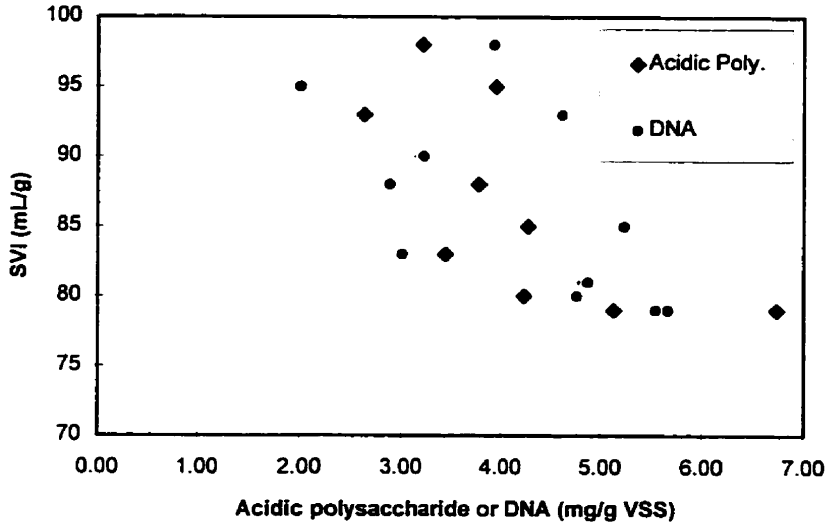

Figure 4.11. Relations between the levels of DNA and acidic polysaccharide in EPS with SVI for sludge from system-Dm.

Table 4.11. Relationship between EPS composition and sludge settling in different studies.

Study	CHO in sludge ↑	EPS composition			
		Protein ↑	CHO or polysaccharide ↑	DNA ↑	Acidic polysaccharide ↑
This study				SVI ↓	SVI ↓
Forster, 1971	SVI ↑				
Goodwin & Forster, 1985			SVI ↓		
Vallom & McLoughlin, 1986				Settling better	
Urbain *et al.*, 1993		SVI ↑	SVI ↑	SVI ↑	

The correlation coefficients of the levels of protein and carbohydrate with SVI are not significant in this study. The effect of polysaccharide on SVI is contradicted in previous studies. An increase in SVI with a higher level of protein in EPS was reported by Urbain *et al.* (1993).

However, other studies such as Kato *et al.* (1971) and Higgins and Novak (1997) reported deflocculation by removal of surface protein. This study indicates a non-significant correlation coefficient between protein and carbohydrate on settling.

Carbohydrate in sludge and EPS. The level of carbohydrate in EPS is directly associated with the level of sludge carbohydrate. The correlation coefficient between the level of carbohydrate in EPS and sludge carbohydrate is 0.73 (Figure 4.12). Since the carbohydrate in sludge includes the total amount of intracellular and extracellular carbohydrate, higher extracellular carbohydrate content will increase the level of sludge carbohydrate. However, determining the amount of intracellular and extracellular carbohydrate separately is difficult; therefore, this is a rough estimation that the sludge carbohydrate is higher when more carbohydrate in EPS is extracted.

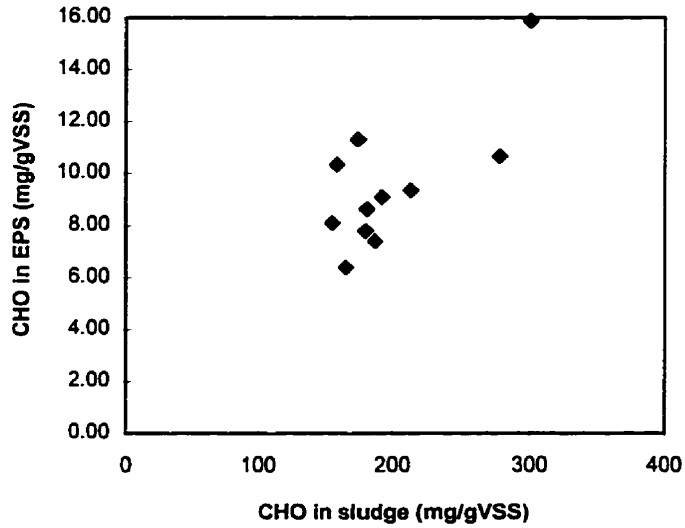

Figure 4.12. The relation between carbohydrate in sludge and EPS for sludge from system-Dm.

Sludge carbohydrate and MLSS. More carbohydrate might be stored in younger sludge. The level of sludge carbohydrate increased when the MLSS (or MLVSS) increased. The correlation coefficients between the level of sludge carbohydrate with MLSS and MLVSS are 0.69 and 0.68

respectively (Figure 4.13) . The levels of sludge carbohydrate from system-Dm and system-Po were higher than that of system-Pm and system-Py (Figure 4.14). The sludge ages of system-Dm and system-Po were younger than system-Pm and system-Py as just discussed previously indicating that more carbohydrate might be stored in these sludges. On the other hand, one of the general characteristics of young sludge is the high generation of MLVSS (WEAO, 1997). Therefore, a higher MLVSS (MLSS) could be related to a younger sludge which could store more carbohydrate.

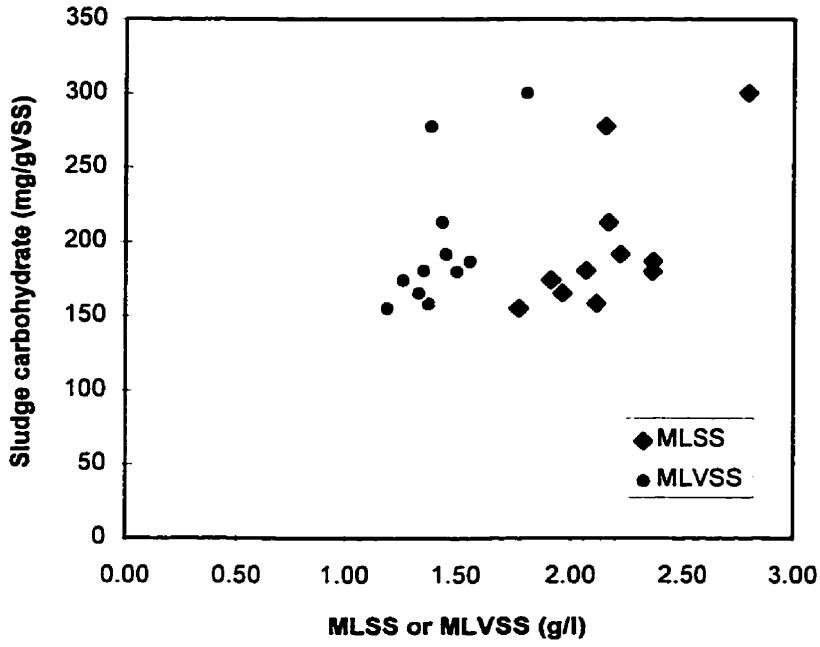

Figure 4.13. The relation between sludge carbohydrate and MLSS or MLVSS for sludge from system-Dm.

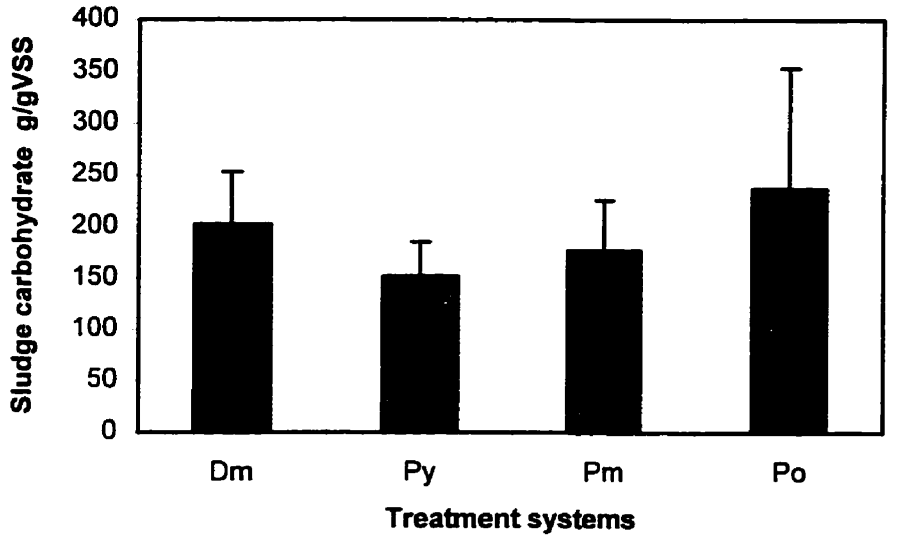

Figure 4.14. The mean carbohydrate composition in sludge from different treatment systems.

Percentage of volatile suspended solids. The percentage of volatile suspended solids (VSS/SS%) is quite constant within a system but different among the systems. The percentage of volatile suspended solids which represents the fraction of organic content in the sludge is calculated from the ratio of MLVSS to MLSS. Since the MLSS is so closely correlated to MLVSS with a correlation coefficient of 0.99 that the VSS/SS% should be quite constant within a system (Figure 4.15). This is supported by a small standard deviation of the VSS/SS% within a system (< 5 %) (Figure 4.16). Meanwhile, the VSS/SS% were significantly different among the systems studied (Table 4.12). The VSS/SS% of system-Dm was the lowest at 65 %.

Table 4.12. Comparison of the percentage of volatile suspended solids of sludge from different treatment systems.[1]

Treatment systems	Dm-Py	Dm-Pm	Dm-Po	Py-Pm	Py-Po	Pm-Po
VSS/SS %[2,3]	sd	sd	sd	sd	sd	nsd

[1]Results of the statistical comparison using t-test can be found in Appendix I. No. of sludge samples analyzed are as follows: Dm (17), Py (8), Pm (7) and Po (10).
[2]sd: significant difference of the means between two systems using 2-tailed t-test at $\alpha = 0.05$.
[3]nsd: no significant difference of the means between two systems using 2-tailed t-test at $\alpha = 0.05$.

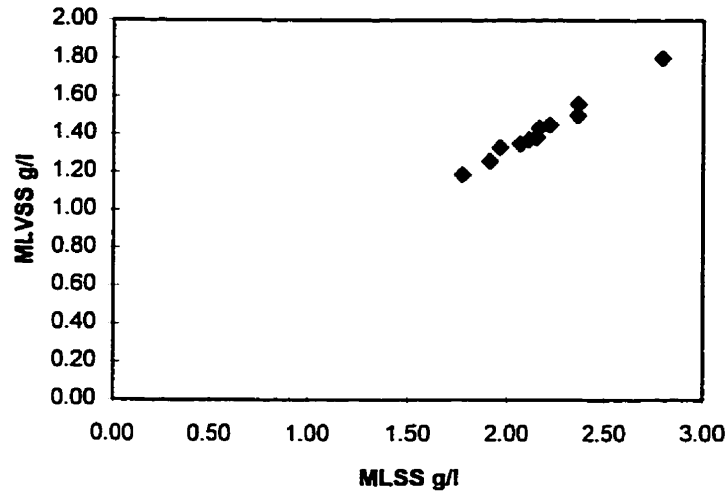

Figure 4.15. The relation between MLVSS and MLSS for sludge from system-Dm.

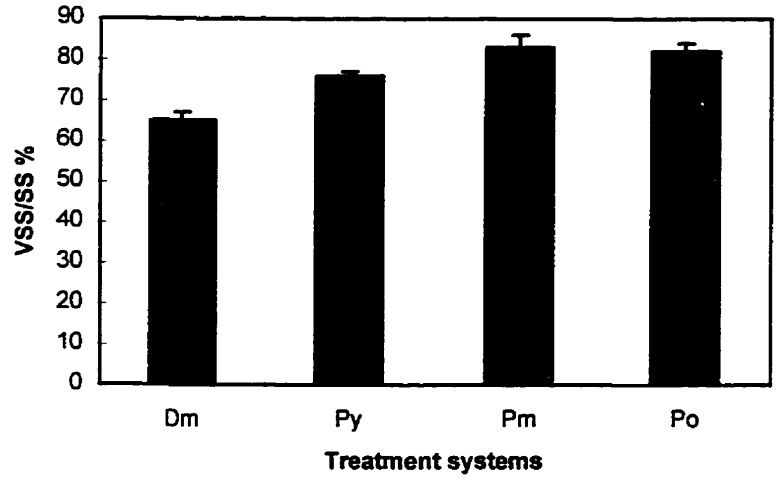

Figure 4.16. The percentage of volatile suspended solid concentration in sludge.

Polysaccharide in EPS. The relation between the carbohydrate and acidic polysaccharide in EPS is unclear. Although the correlation coefficient between carbohydrate and acidic polysaccharide in EPS was fairly high at 0.65, this correlation was attributable to one observation (Figure 4.17). More samples are required to determine this correlation.

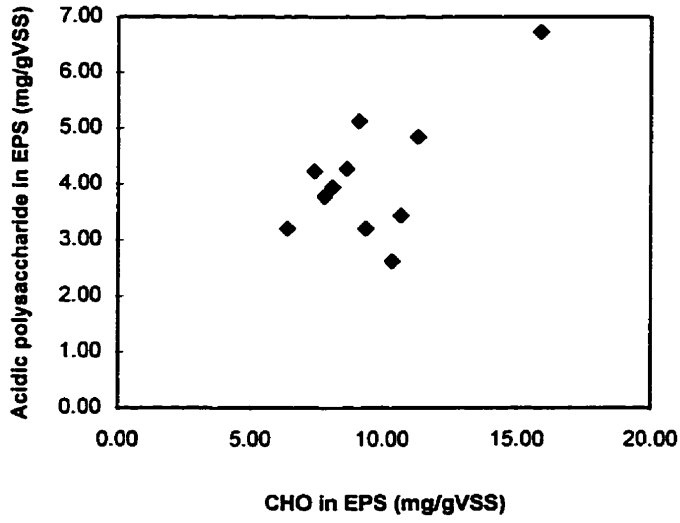

Figure 4.17. The relation between the level of acidic polysaccharide and carbohydrate in EPS for sludge from system-Dm.

4.3.4 Summary of the characteristics of EPS composition in sludge

Protein was found to be the dominant component in the extracted EPS followed by carbohydrate, DNA and acidic polysaccharide regardless of the types of wastewater and operating conditions. These four components formed a more or less constant percentage composition in the organic matrix with 77-81% protein, 11-15% carbohydrate, 4-9% DNA and 3-5% acidic polysaccharide. DNA and acidic polysaccharide were the most labile components in EPS. The level of EPS is inversely associated with the MCRT (sludge age) of system. Hence, the operating conditions such as sludge age is much more important than microbial community alone as a factor in affecting the composition of EPS. Higher levels of DNA and acidic polysaccharide in EPS may be associated with better sludge settling as the correlation coefficient between DNA and acidic polysaccharide with SVI was greater than 0.61 at 95% probability level. Moreover, the level of carbohydrate in EPS is directly associated with the level of sludge carbohydrate as the correlation coefficient between carbohydrate in sludge and EPS was 0.73 at 95% probability level. In addition, the percentage of volatile suspended solids (VSS/SS%) is quite constant within a system (SD < 5%) but different among the systems.

4.4 Physical properties of floc

The morphology of floc was studied using the conventional optical microscopy (COM). The results are reported in Section 4.4.1. The characterization of microbial biomass at a community-level was studied using the BIOLOG method described by Victorio *et al.* (1996). The results are reported in Section 4.4.2. The size and shape of floc were determined using the conventional optical microscope interfaced with a CCD camera and a computer. The sizes and shapes of approximately 1000 particles were analysed for each sample. The settling velocity of floc was determined using a CCD video camera interfaced with a microscope and an VCR to capture the images of settling flocs in a settling column as described by Droppo *et al.* (1997). Approximately 100 settling particles were analysed for each sample. The Northern Exposure™ image analysis software was used to digitize the images for the measurement of sizes, shapes and settling velocities of flocs. The results on physical properties of flocs are reported and discussed in Section 4.4.3 and 4.4.4. These physical properties of flocs from each system were compared using a 2-tailed t-test to test the hypothesis that there is no significant difference between systems. If the corresponding probability for the calculated t-statistic was $\geq 95\%$, then the null hypothesis was rejected and the characteristics were concluded to be different between systems.

4.4.1 Morphology of floc

The flocs from system-Dm were firm, round and compact with a few filamentous organisms inside the flocs (Figure 4.18A). These filaments formed a network inside the flocs as described by the backbone model (Sezgin *et al.*, 1978; Horan, 1990). Good settling is usually associated with this type of floc (WEAO, 1997). The flocs from system-Py and system-Po were firm, irregular and diffused with filaments bridging with the other flocs (Figure 4.18B and 4.18D). These filaments were commonly observed in flocs from these two systems (Table 4.13). The dominant type of filamentous organisms in system-Py was Nostocoida *limicola* (see Appendix H). These bridging filaments may cause the compaction problem in sludge settling. The flocs from system-Pm were firm, irregular and diffused with a few filamentous organisms inside the flocs (Figure 4.18C).

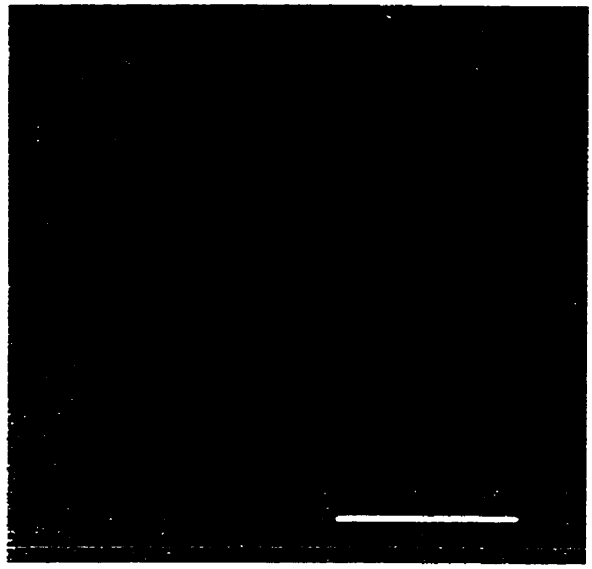

A. System-Dm

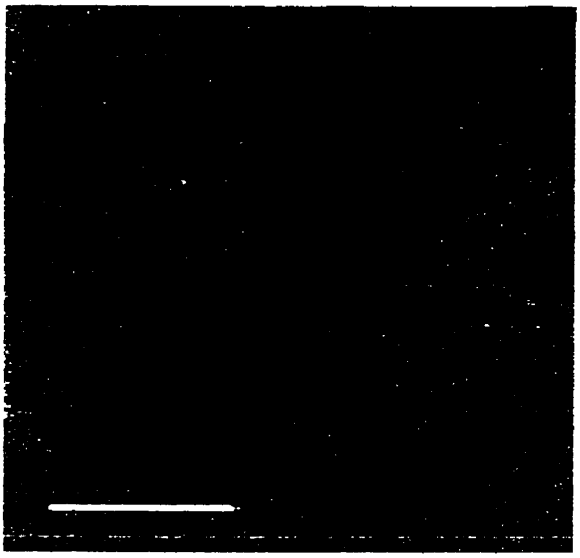

B. System-Py

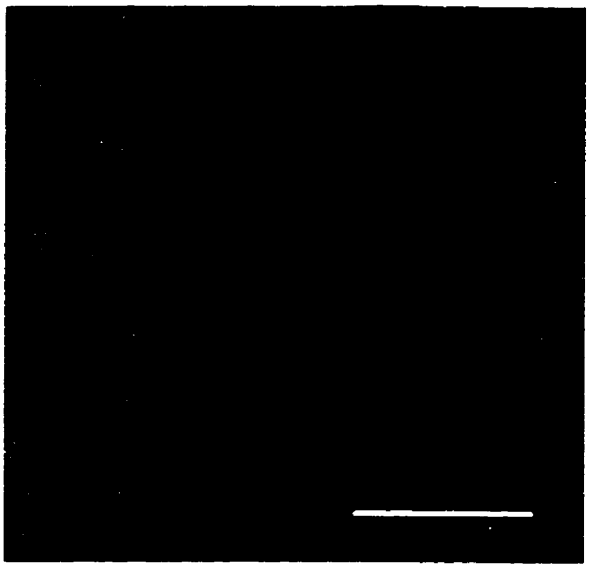

C. System-Pm

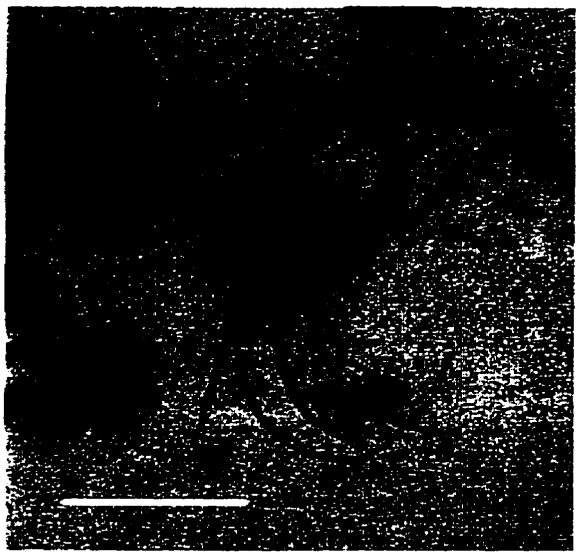

D. System-Po

Figure 4.18. Appearance of flocs from different treatment systems. The scale bars represent 200 microns.

Table 4.13. The microscopic analysis of flocs from different treatment systems.

Treatment systems	Dm	Py	Pm	Po
Morphology of floc	Firm, round, compact	Firm, irregular, diffused	Firm, irregular, diffused	Firm, irregular, diffused
Filament effect on floc structure	Little or none	Bridging	Little or none	Bridging
Filament abundance*	Few	Common	Few	Very common

*Few: filament present but only observed in an occasional floc.
Common: filaments observed in all flocs, but at low density (e.g., 1-5 filaments per floc).
Very common: filaments observed in all flocs at medium density (e.g., 5-20 per floc).

4.4.2 Microbial community characterization

The microbial communities were different among the systems studied. An unstable microbial community was observed during the poor settling period of system-Pm. The microbial communities of system-Dm and system-Py were relatively alike and stable as the coordinates for samples from system-Dm and system-Py clustered together on the plot of principal component analysis (Figure 4.19). The microbial community of system-Pm was very different from that of other systems as the coordinates of samples from this system located far away from that of the other systems. Moreover, the microbial community of system-Pm was very unstable as remarkable change in the coordinates (Pm-1 and Pm-2) was observed within one week. The sludge settling of this system was poor as the height of settled sludge was more than 90 % during this period (Table 4.14). However, the heights of settled sludge from other systems were at reasonable good with a range between 16 - 40 % during the study periods. This indicates an unstable microbial community during the poor settling period.

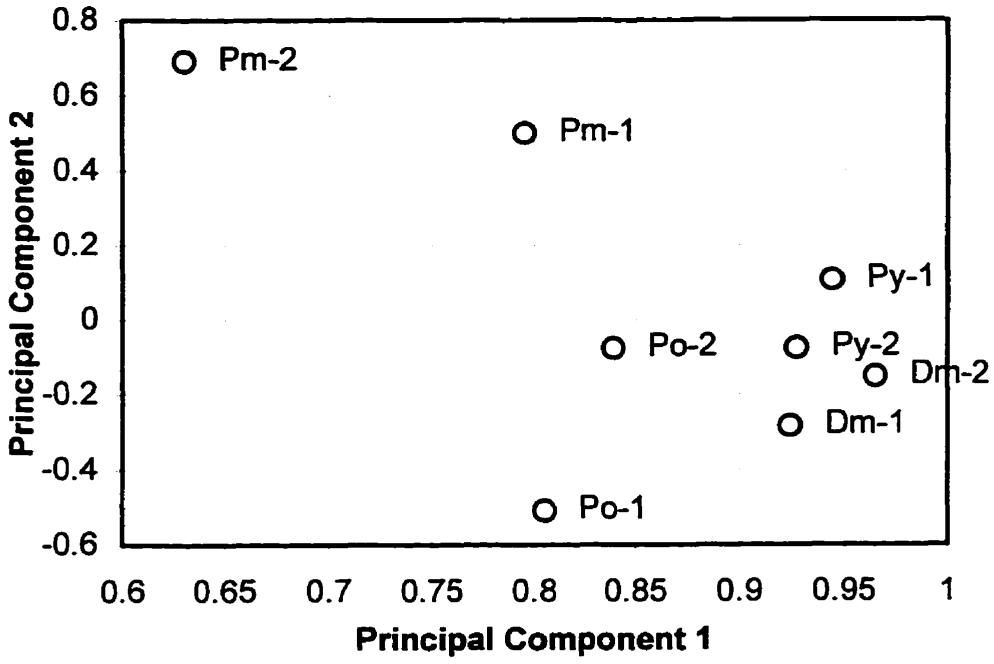

Figure 4.19. Community-level characterization of microbial biomass from different treatment systems. The distance between two coordinates indicates the similarity of microbial communities between two sludge samples.

Table 4.14. The settling properties of sludge corresponding to the samples used for microbial community characterization.

Samples	Duration between samplings	SVI (mL/g)	30-min settling test (%)
Dm-1		95	16
Dm-2	1 week	90	19
Py-1		130	32
Py-2	1 week	108	40
Pm-1		162	93
Pm-2	1 week	166	94
Po-1		125	29
Po-2	2 weeks	116	33

4.4.3 Size and shape of floc

The size of floc was measured as equivalent spherical diameter (ESD). The shape of floc was measured as form factor (FF) and aspect ratio (AR). The median measurement of these properties was used to characteristize the samples. Sample median gives a better central tendency estimation of a population than the sample mean when the shape of the population distribution is not normal. The median by number and by volume were calculated. The means of sample medians of sludge from different treatment systems are compared statistically using a 2-tailed t-test at $\alpha = 0.05$.

Floc size. Most of the floc particles were very small while a few of them were very large in size. The median ESD by number of flocs from different treatment systems ranged between 37.4 - 58.7 μm (Table 4.15). This result agrees with most of the other studies (Li and Ganczarczyk, 1988; Andreadakis, 1993). The median ESD by volume of flocs from different systems ranged between 212.0 - 471.2 μm. This indicates that most of the flocs were very small while a few of them were very large in size. This characteristic of floc size is consistent with other studies which reported that more than 87 % of floc particles were small with a size less than 75 μm (Knocke and Zentkouich, 1986; Sadalgekar *et al.*, 1988).

Table 4.15. Size properties of the flocs from different treatment systems.

Treatment systems	No. of samples	Median ESD (by no.) μm			Median ESD (by volume) μm		
		Range	Mean	SD %	Range	Mean	SD %
System-Dm	8	28 - 85	59	34	320 - 840	470	43
System-Py	9	21 - 61	45	34	100 - 560	300	51
System-Pm	7	14 - 61	37	48	220 - 570	350	44
System-Po	7	41 - 68	56	18	170 - 320	210	23

A higher level of EPS may be associated with a larger floc size. The median ESD by number of floc from system-Dm and system-Po were 58.7 and 56.1 μm, respectively (Figure 4.20). These are significantly larger than the other systems (Table 4.16). Meanwhile, the levels of EPS of sludge from these two systems were higher as well. Therefore, a higher level of EPS may be associated with a larger floc size. On the other hand, the median ESD by volume of flocs from system-Po was 212.0 μm which is the smallest among the systems studied. The range of median ESD by volume for flocs from system-Po was 169.8 - 317.7 μm (Table 4.15). This indicates a more compact distribution (i.e. fewer extreme particles). This is different from the general characteristic of floc size that most of the floc particles are very small with a few very large in size.

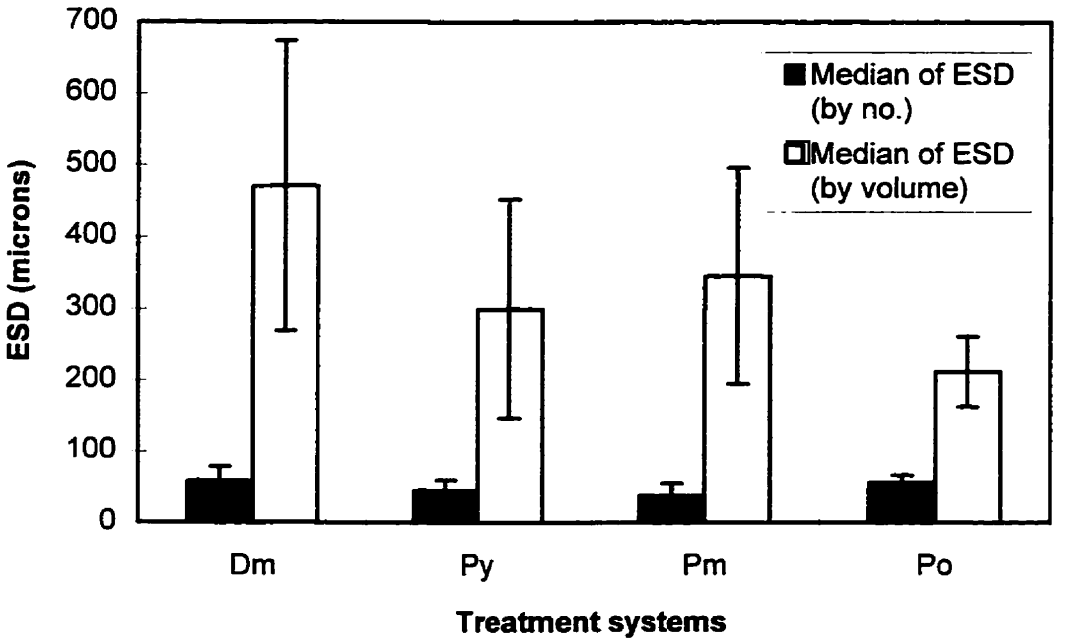

Figure 4.20. The median ESD of flocs from different treatment systems.

Table 4.16. Comparison of size and shape properties of flocs from different systems.[1]

	Median ESD (by no.)[2,3]	Median ESD (by volume)	Median Form Factor	Median Aspect Ratio
Dm-Py	nsd	nsd	nsd	nsd
Dm-Pm	sd	nsd	nsd	nsd
Dm-Po	nsd	nsd	sd	nsd
Py-Pm	nsd	nsd	nsd	nsd
Py-Po	sd	nsd	sd	nsd
Pm-Po	sd	nsd	sd	nsd

[1]Results of the statistical comparison using t-test can be found in Appendix I. No. of sludge samples analyzed are as follows: Dm (8), Py (9), Pm (7) and Po (7).
[2] sd: significant difference of the means between two systems using 2-tailed t-test at $\alpha = 0.05$.
[3] nsd: no significant difference of the means between two systems using 2-tailed t-test at $\alpha = 0.05$.

Floc shape. The shape properties of flocs from system-Dm were not significantly different from the industrial systems regardless of the difference in sludge settleability. Moreover, the floc shape was quite uniform within a system. The shape properties of flocs were represented by the form factor (FF) and aspect ratio (AR). Both FF and AR indicate the flocs were non-spherical shape. The median FF of flocs from different systems ranged between 0.52 - 0.61 (1.0 = perfect circle) (Table 4.17). The median FF of system-Po was 0.61 and is significantly higher than that in the other systems (Figure 4.21 and Table 4.16). The high value in FF of flocs from system-Po is unexpected since an abundance of filaments extending out from the flocs was observed (i.e. visually making the floc more elongated). This misleading result may be due to the difficulty in measuring the very fine filaments by the image analysis system. It may be due to the median AR of floc particles from different systems ranged between 1.8 - 2.0 (1.0 = perfect circle) and were not significantly different among the systems studied. Grijspeerdt and Verstraete (1997) reported the FF and AR of sludge floc ranged between 0.5 - 0.8 and 2.5 - 4.5 respectively. They also concluded that the more the floc shape approached that of a sphere, the better it settled. However, the median FF and AR of the flocs from system-Dm were not significantly different from industrial systems regardless of the significant difference in sludge

settleability. This indicates that factors other than FF and AR may have an effect on sludge settleabilty. The deviations (SD %) in the measurement of FF and AR within a system ranged between 3 - 13 %. This low deviation indicates the FF and AR was quite uniform within a system. The effect of level of EPS on floc shape cannot be determined.

Table 4.17. Shape properties of the flocs from different treatment systems.

Treatment systems	No. of samples	Median Form Factor			Median Aspect Ratio		
		Range	Mean	SD %	Range	Mean	SD %
System-Dm	8	0.46 - 0.62	0.52	12	1.4 - 2.0	1.9	11
System-Py	9	0.47 - 0.59	0.53	8	1.9 - 2.0	2.0	3
System-Pm	7	0.44 - 0.65	0.52	13	1.4 - 2.0	1.8	11
System-Po	7	0.57 - 0.69	0.61	7	1.8 - 2.0	1.9	5

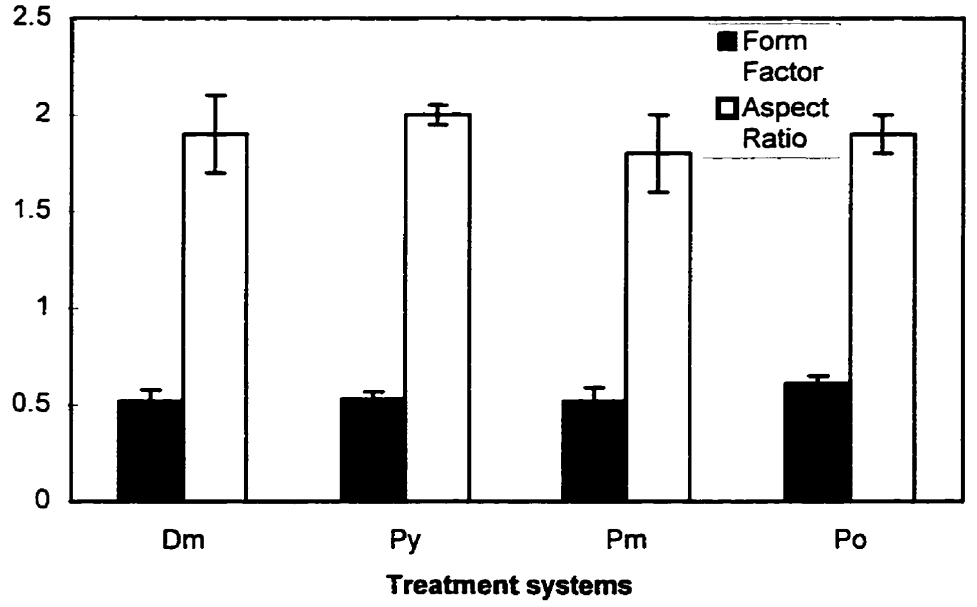

Figure 4.21. Shape properties of flocs from different treatment systems.

4.4.4 Settling velocity and density of floc

Settling velocity. A smaller increase in settling velocity with increasing size for floc than that for solid sphere reflects the porous nature of floc. According to Stokes' law, settling velocity (v) is a function of ESD (D). A linearized form of settling velocity equation $v = A\ D^m$ is established (Eq. 4.1):

$$\log v = \log A + m \log D \qquad \text{(Eq. 4.1)}$$

Therefore, the slope of a plot of log v versus log D indicates the change of log settling velocity with log ESD (Figure 4.22). Since the mass of a solid sphere increases with ESD, therefore the settling velocity increases with ESD. The slope for a single, impermeable particle in laminar region is two. However, a floc has been proposed as a highly porous aggregate made of many primary particles (Li and Ganczarczyk, 1992). Hence a floc grows as additional individual aggregates attach to the central floc structure. This linkage creates additional pores. Therefore, the change in log settling velocity with log ESD of a floc was less than that for a solid sphere due to the porous nature and irregular shape of floc. This is consistent with the results obtained in this study. The mean slopes of flocs from different treatment systems studied ranged between 0.54 - 0.87 (Table 4.18). Li and Ganczarczyk (1987) reported a slope of 0.55 in the study of the correlation between settling velocity and longest dimension.

Table 4.18. The means of slopes of linearized settling velocity equation of flocs.[1]

Treatment systems	No. of samples	log v = log A + m log D*		
		Range of slopes	Mean of slopes	SD %
Dm	8	0.25 - 1.35	0.87	54
Py	8	0.31 - 1.29	0.75	51
Pm	6	0.11 - 1.39	0.72	81
Po	9	0.13 - 0.97	0.54	63

[1] Approximately 100 floc particles from each sample were analyzed. The results of statistical comparison are shown in Appendix I.
*v = settling velocity (mm/s), A = constant, m = slope, D = ESD (microns).

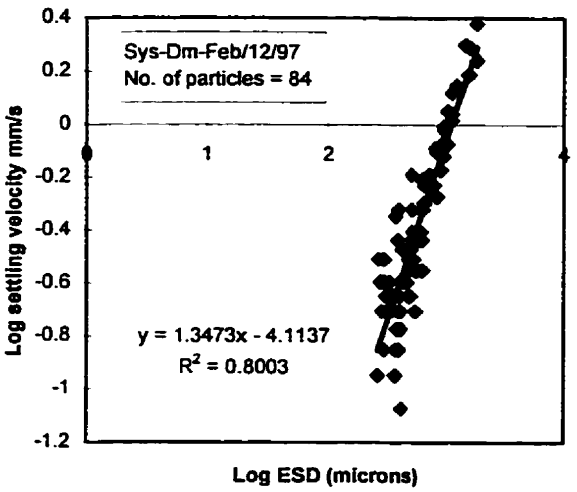

A. System-Dm

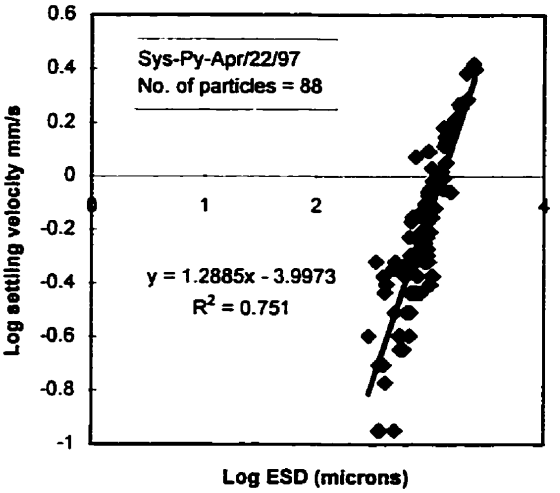

B. System-Py

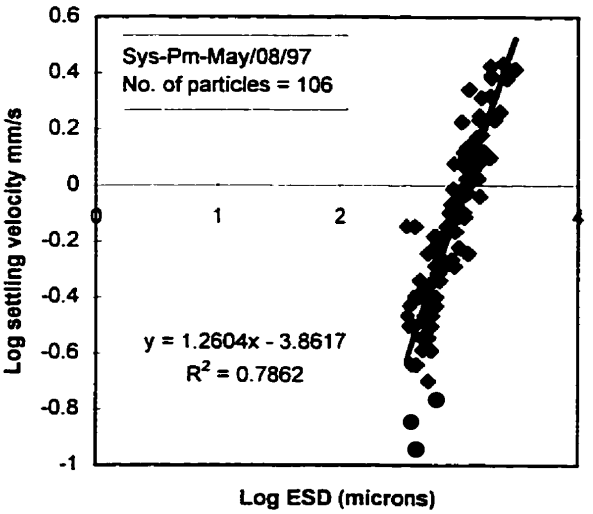

C. System-Pm

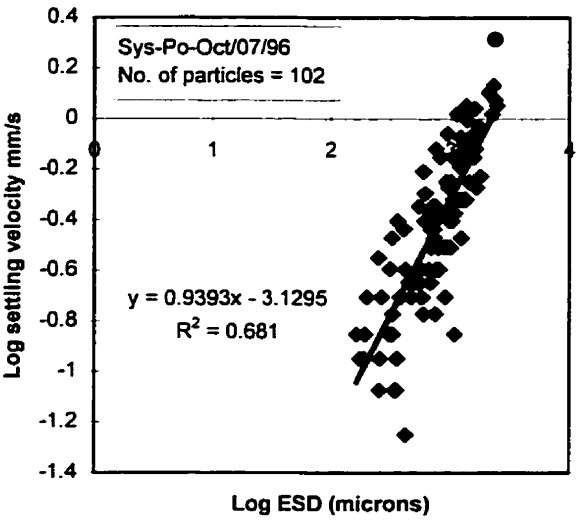

D. System-Po

Figure 4.22. The linearized settling velocity with ESD of flocs from different treatment systems.

Effective floc density. The flocs from system-Dm might be less porous than that of other systems studied. The effective density (ρ_e) of floc particle is a function of ESD (D) as discussed in Section 2.5.2, a linearized effective density equation for floc particles is established (Eq. 4.2):

$$\log \rho_e = \log A - m \log D \qquad \text{(Eq. 4.2)}$$

Therefore, the slope of a plot of log ρ_e versus log D means the change of log effective density with log ESD (Figure 4.23). The density of a solid sphere is constant. However, the density of a porous and heterogeneous object such as floc is not constant. A floc grows as additional individual aggregates attach to the central floc structure as just described. This increased porosity leads to an increase in water content that reduces the effective density. Therefore, the effective density decreases with increasing ESD of the floc. The mean slope of flocs from system-Dm was - 1.00 which is the smallest among the systems studied (Table 4.19). This means that the change in log effective density with log ESD of the flocs from system-Dm was the smallest. Therefore, the flocs from system-Dm might be less porous. Both the porosity of floc and the density of biomass may affect the density of floc. Since the levels of sludge carbohydrate and EPS of sludge from system-Dm were the highest as discussed in Section 4.3.2, the biomass of system-Dm could be more dense than that of the other systems studied. In addition, the SCLM images described in Section 4.6.1 provides a qualitative evidence that the internal floc structure of system-Dm was compact.

The mean slope of flocs from system-Py was - 1.27 which is the greatest. This means that the change in log effective density with log ESD of the flocs from system-Py is the greatest among the systems studied. The flocs of system-Py might be more porous. This porosity may be explained by the commonly present filaments which formed loose aggregate. Both the COM images described in Section 4.4.1 and the SCLM images described in Section 4.6.1 provide the qualitative evidence to support this.

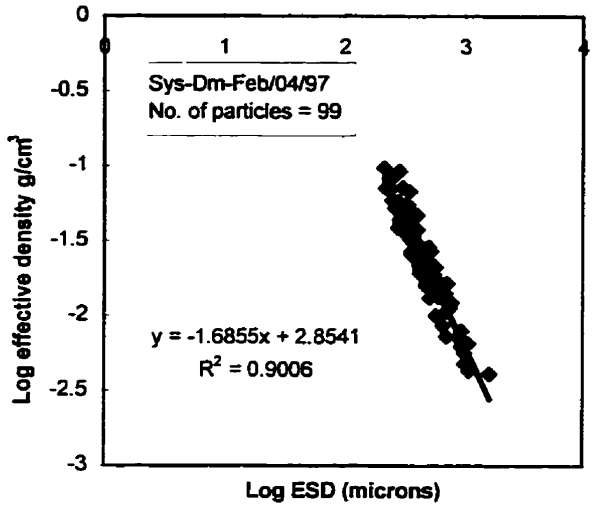

A. System-Dm

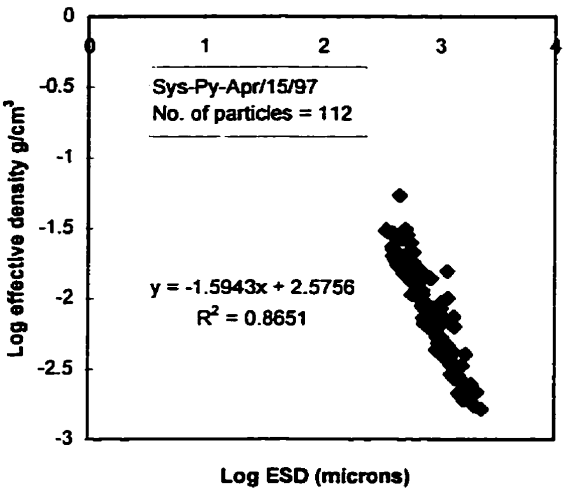

B. System-Py

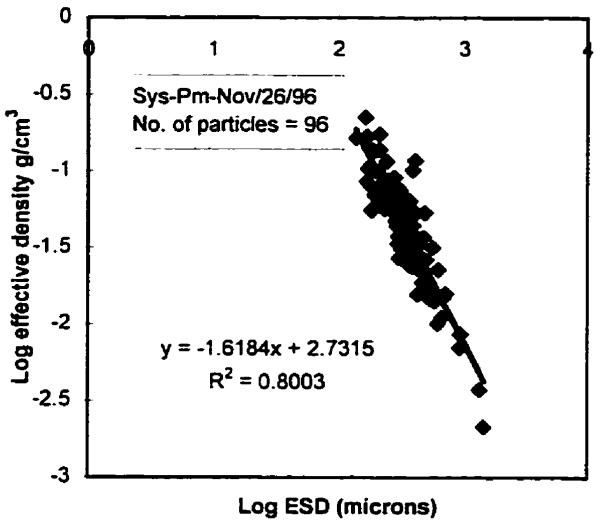

C. System-Pm

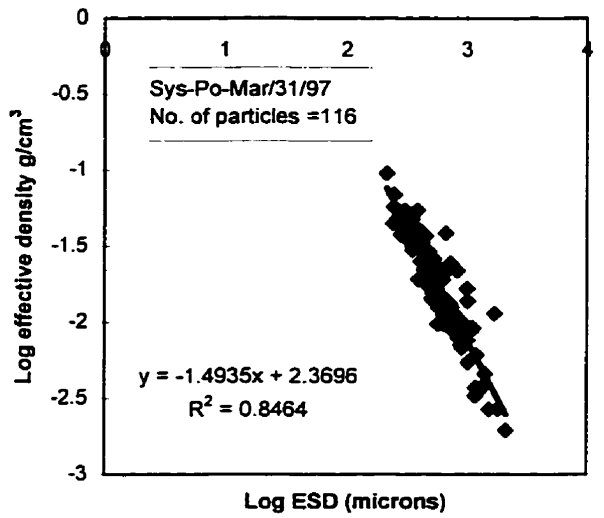

D. System-Po

Figure 4.23. The linearized effective density with ESD of flocs from different treatment systems.

Table 4.19. The means of slopes for linearized effective density equation of flocs.[1]

Treatment systems	No. of samples	log (Eff. den.) = log A + m log (ESD)*		
		Range of slopes (negative)	Mean of slopes	SD %
Dm	8	0.49 - 1.69	-1.00	47
Py	8	0.84 - 1.65	-1.27	26
Pm	6	0.69 - 1.63	-1.24	35
Po	9	0.70 - 1.61	-1.24	23

[1] Approximately 100 floc particles from each sample were analysed. The results of statistical comparison are shown in Appendix I.
* Eff. den. = effective density (g/cm^3), A = constant, m = slope, ESD = ESD (microns).

4.4.5 The deviations in measurement using image analysis technique

Since floc is a highly heterogeneous aggregate, a large number of particles should be analysed in order to get the representative data for the physical properties. The physical properties including median ESD, FF, AR and the mean slopes of linearized settling velocity and linearized effective density plots are compared statistically among the systems using a 2-tailed t-test (see Appendix I). However, the significant difference can only be found in the comparison of median ESD by number and median FF. The differences of the other physical properties among the systems studied were not statistically significant. These results could be due to the following reasons. Firstly, a high standard deviation (SD %) incurred in the measurement. The deviations of median ESD ranged between 18 - 51 % (Table 4.15). The deviations of mean slope of linearized settling velocity plot were more than 50 % (Table 4.18). The deviations of mean slope of linearized effective density plot ranged between 20 - 50 % (Table 4.19). These large deviations in measurement may be due to the highly heterogeneous nature of flocs. A very large number of particles should be analysed in order to evaluate representative data set. However, approximately 100 particles per sample were analysed for determination of settling velocity in this study. This may not be enough to get a good estimation. However, there is a limited time frame for analysis of each sample. This means that the sample must be analysed as soon as possible after sampling. Moreover, it is quite time consuming in using this technique. Therefore, the number of particles analysed were limited. In addition, the deviations could be due to the variation in the characteristics of samples which came from the uncontrolled systems

in this study. This means that the samples could be very different at different sampling days even though they came from the same systems.

Secondly, the data may be condensed too much by the method employed for statistical comparison. The mean of medians was used for the statistical comparison of size and shape properties while the mean of slopes was used for statistical comparison of the change in settling velocity and effective density with ESD. These mean values may not reflect the characteristics of the entire population. A better method for statistical comparison should be sought in further studies. Although the differences in the physical properties were not statistically significant, they still can indicate a trend among the systems studied.

In summary, a large number of particles per sample should be analysed in order to get the representative data on the physical properties of small, porous and heterogeneous objects such as floc by applying the image analysis technique. Moreover, a statistical method by comparing the entire population of particles may provide more information to interpret the results.

4.4.6 Summary of physical properties of floc

Most of the floc particles were very small while a few of them were very large in size. A higher level of EPS may be associated with a larger floc size. The floc shape was quite uniform within a system. The microbial communities were different among the systems studied. An unstable microbial community was observed during the poor settling period of system-Pm.

The flocs from system-Dm were firm, round and compact with a few filamentous organisms inside the flocs. The shape properties of flocs from system-Dm was not significantly different from the industrial systems regardless of the difference in sludge settleability. The flocs from system-Dm were more dense due to a higher level of sludge carbohydrate and EPS, and a compact floc structure. The flocs from system-Po and system-Py were less dense due to the porous floc structure caused by the presence of abundant filaments which formed a loose aggregate.

4.5 Functional and dysfunctional periods in system-Po

Poor sludge settling was a constant problem to the operation of system-Po as mentioned in Chapter 1. The system had undergone a modification halfway through this study. The sludge settling has improved significantly and the operation has run normally since then. The sludge from both periods was analyzed. The characteristics of sludge from functional and dysfunctional periods within a system were compared using ANOVA to test the hypothesis that there is no significant different between periods. If the corresponding probability for the calculated F-statistic was $\geq$ 95%, then the null hypothesis was rejected and the characteristics were concluded to be different between periods.

4.5.1 Settling and EPS composition

The MLSS during dysfunctional (poor settling) periods was 34% higher than that during functional periods. The MLSS during dysfunctional and normal period were 3.4 and 2.5 g/L respectively (Table 4.20). The 30 min settling test was 99 % and 52 % during the dysfunctional and functional periods respectively.

The levels of protein and carbohydrate in EPS during dysfunctional periods were 56 % and 71% higher than that during functional periods (Figure 4.24). The levels of DNA and acidic polysaccharide in EPS were 26 % higher while the level of sludge carbohydrate was 59 % higher than the functional periods. However, the percentage composition of EPS between two periods was not significantly different (Figure 4.25).

The significantly higher levels of protein and carbohydrate during dysfunctional periods may be associated with the poor settling through a higher bound water content and surface charge of the floc. Kiff (1978) reported that the higher level of extracted carbohydrate with an increased water retention capacity was observed in poorly settled sludge. The high bound water content in the sludge may be associated with the poor flocculation. In addition, Wu *et al.* (1984) found that the settling properties deteriorated due to the increase in cell protein content and surface charge at both nitrogen-rich or nitrogen-restricted sludge. Therefore, the study on the effect of cell and extracellular protein on surface charge and flocculation is recommended for further studies.

Table 4.20. Comparison of settling, sludge properties and EPS composition of sludge from system-Po during functional and dysfunctional periods.[1]

		Functional			Dysfunctional			
No. of samples		7			3			
		Range	Mean	SD %	Range	Mean	SD %	ANOVA[2,3]
Settling properties	SVI (ml/g)	125-267	197	30	175-319	257	29	nsd
	30-min (%)	29-91	52	41	99-100	99	1	sd
Sludge properties	MLSS (g/L)	2.223-3.220	2.539	14	2.860-3.680	3.393	14	sd
	MLVSS (g/L)	1.827-2.590	2.088	14	2.230-3.000	2.708	15	sd
	VSS/SS (%)	80-84	82	1	78-82	80	3	nsd
	CHO in sludge (mg/gVSS)	122.7-409.8	197.7	54	220.3-441.2	314.6	36	nsd
EPS composition (mg/gVSS)	Protein	29.19-57.08	47.59	21	50.78-88.19	74.26	28	sd
	CHO	5.30-14.24	8.54	35	10.52-17.7	14.59	25	sd
	DNA	0.6955-4.808	2.502	67	0.7099-5.480	3.143	76	nsd
	Acidic Poly.	1.931-4.673	3.240	33	3.180-5.656	4.073	34	nsd
	Total EPS	50.27-75.09	61.87	16	73.04-112.6	96.07	21	sd
	Extractable CHO (%)	2.3 - 5.8	4.30	28	4.0 - 5.5	4.80	17	nsd

[1] The results of statistically comparison using ANOVA is shown in Appendix I.
[2] sd: significant difference of the means between two systems using 2-tailed t-test at $\alpha = 0.05$.
[3] nsd: no significant difference of the means between two systems using 2-tailed t-test at $\alpha = 0.05$.

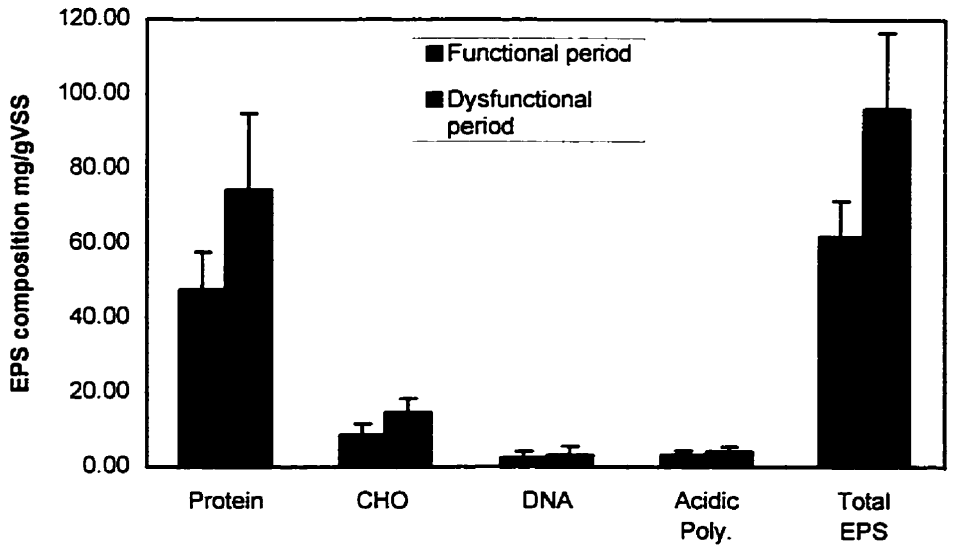

Figure 4.24. The EPS composition of sludge from system-Po during functional and dysfunctional periods.

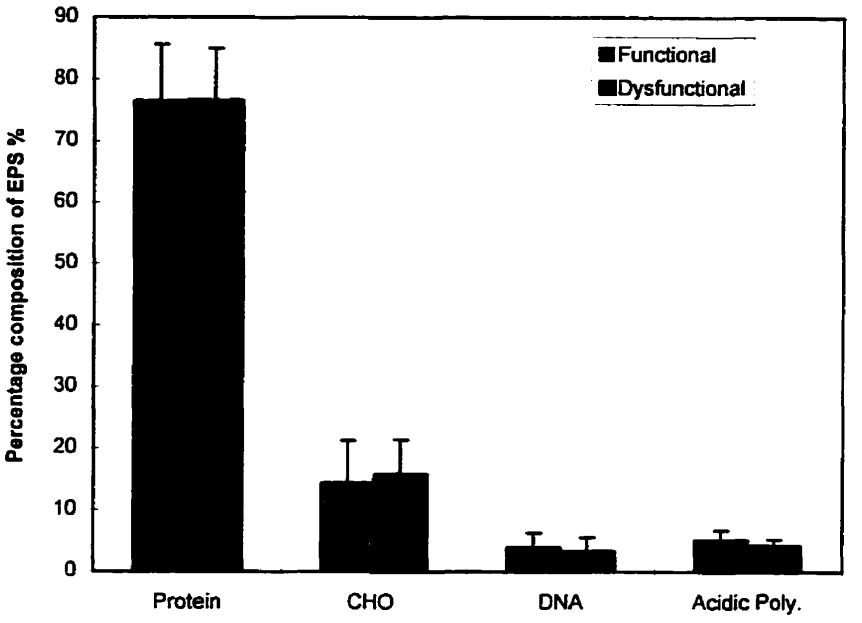

Figure 4.25. The percentage composition of EPS of sludge from system-Po during dysfunctional and normal periods.

The low F/M ratio may account for the higher level of EPS during dysfunctional periods. The F/M ratio was low during the dysfunctional periods of system-Po. Exopolymers are thought to be secreted under nutrient-limiting conditions in the phases of growth, and that they are the biopolymers responsible for flocculation (Tenny and Stumm, 1965; Bush and Stumm, 1968; Pavoni *et al.*, 1972). Low F/M ratio storage polymers can be expected to accumulate in the endogenous phase (Forster, 1976). This may account for the higher level of EPS during the periods of low F/M ratio. Although the results of EPS composition from different studies are not easily comparable, a positive linear relationship between SVI and EPS composition was observed in most cases (Magara *et al.*, 1976; Kiff , 1978; Urbain *et al.*, 1993). Therefore, this higher level of EPS may partly account for the poor settling during this periods.

Besides the possible change on the surface properties, abundant growth of the filamentous microorganisms increased the MLSS in the system and decreased the compactibility of sludge. This contributes to poor settling as well. Some of the filaments were identified as related to the low F/M filaments by the operators in plant. In a filamentous sludge the individual flocs are

held apart in a huge three dimensional matrix hindering both the downwards motion of the solids and the upward flow of liquid (Figure 4.26). This may cause the compaction problem in sludge.

Figure 4.26. Appearance of flocs from system-Po during dysfunctional periods (Scale bar = 200 microns).

4.5.2 Floc size and shape

A number of floc particles were very large in size during the dysfunctional periods while the shape properties were not significantly difference between the periods. The median ESD by number and by volume during the dysfunctional periods were 19% and 472% larger than that during the functional periods (Table 4.21). The significantly larger in median ESD by volume during the dysfunctional periods indicates that a number of floc particles were huge in size during the dysfunctional periods. The differences in the median FF and AR between these two periods was not significant.

Table 4.21. Comparison of size and shape properties of flocs from system-Po during functional and dysfunctional periods.[1]

	Functional			Dysfunctional			
No. of samples		7			2		
	Range	Mean	SD %	Range	Mean	SD %	ANOVA[2,3]
Median ESD (by no.) μm	41.0 - 68.8	56.1	18	64.4 - 68.9	66.7	5	nsd
Median ESD (by volume) μm	169.8 - 317.7	212.0	23	1166.9 - 1259.7	1213.3	5	sd
Median Form Factor	0.57 - 0.69	0.61	7	0.64 - 0.67	0.66	3	nsd
Median Aspect Ratio	1.8 - 2.0	1.9	5	1.9 - 2.1	2.0	100	nsd

[1] The results of statistically comparison using ANOVA is shown in Appendix I.
[2] sd: significant difference of the means between two systems using 2-tailed t-test at $\alpha = 0.05$.
[3] nsd: no significant difference of the means between two systems using 2-tailed t-test at $\alpha = 0.05$.

In summary, the MLSS, EPS composition and sludge carbohydrate were higher during the dysfunctional periods. The levels of protein and carbohydrate during dysfunctional periods were 56% and 71% higher than functional periods. The higher level of protein and carbohydrate may be associated with a higher bound water content and surface charge of the flocs. Abundant growth of the filamentous microorganisms increased the MLSS and decreased the compactibility of sludge. A number of floc particles were very large in size during the dysfunctional periods as the median ESD by volume was six times larger than that during functional periods. The shape properties were not significantly difference between the periods. Low F/M ratio may account for the higher level of EPS and abundant growth of the filaments during the dysfunctional periods. However, the percentage composition of EPS between two periods was not significantly different.

4.6 Correlative microscopy

The floc structure is observed using conventional optical microscopy (COM), scanning confocal laser microscopy (SCLM) and transmission electron microscopy (TEM). The floc structure observed by COM has been described in Section 4.4.1. The internal morphology and spatial distribution of EPS in extracellular matrix of the floc was observed using SCLM coupled with

various fluorescent stains. The TEM images reveal the patterns of fibrils in extracellular matrix. The observations by SCLM and TEM are described in the following sections.

4.6.1 Spatial distribution of EPS

Fluorescein isothiocyanate (FITC). The internal floc structure was non-homogeneous as revealed by SCLM images of flocs stained by FITC. FITC is a general protein stain which produces an image representing the overall morphological structure. This amorphous floc structure was observed at the images of flocs from all systems (Figure 4.27). The images of flocs from system-Dm reveal a round and compact floc structure (Figure 4.27A). Filamentous organisms are seen at the core of flocs. The images of flocs from industrial systems reveals an irregular and diffused floc structure (Figure 4.27B - 4.27D). These results agree with the observation using COM. The filamentous organisms were commonly seen in the images of flocs from system-Po (just like the one shown at the upper right corner of Figure 4.27D). These filaments extended far beyond the flocs. However, another filament-like object is seen at the lower right corner of the same image. It is suspected to be a piece of potato peeling rather than a filamentous organism, because of its irregular shape.

Concanavalin A (ConA). The α-mannopyranosyl and α-glucopyranosyl residues were present at the floc matrices from all systems but the spatial distribution was different among the systems as revealed by images of flocs stained with ConA (Figure 4.28). The difference in the spatial distribution may be associated with the sludge age of the flocs. ConA is a lectin stain that indicates the presence of specific polysaccharide residues. ConA is specific for α-mannopyranosyl and α-glucopyranosyl residues. The patterns of distribution of these residues around the flocs from the treatment systems studied and their association with sludge age are described in the following.

(1) Flocs from system-Dm and system-Po

An even distribution of these residues within the floc matrices is observed in the images of flocs from system-Dm and system-Po (Figure 4.28A and 4.28D). A floc grows as

additional individual aggregates attach to the central floc structure (Li and Ganczarczyk, 1992). Therefore, the bacterial age at the core of floc was older than that at the periphery of floc. However, the sludge ages of system-Dm and system-Po were relatively young at 4-day and 10-day old respectively. Therefore, the difference of bacterial age at the core and the periphery of floc was not significant. The bacterial age could affect the production of EPS as a higher level of EPS was observed at younger sludge as discussed in Section 4.3.2. Hence, the secretion of EPS by the bacteria was quite even within the floc matrices of samples from these two systems.

(2) Flocs from system-Py and system-Pm

The distribution of these residues was less dense at the core but more dense around the periphery of the floc matrix of system-Py (Figure 4.28B). This may be due to a significantly older bacterial age at the core than at the periphery of flocs since the sludge age of system-Py was old (25-day). Therefore, more EPS was secreted by the bacteria at the periphery than that at the core of flocs. Some dense spots of residues were found within the floc matrix of system-Pm (Figure 4.28C). The particular reason for this pattern of distribution is still unknown yet.

Wheat germ agglutinin (WGA). The N-acetylglucosamine and N-acetylneuraminic acid residues were present within the floc matrices from all systems but a significantly less dense distribution was present within the matrix of system-Py as revealed by the images of flocs stained with WGA (Figure 4.29). WGA is a lectin stain specific for N-acetylglucosamine and N-acetylneuraminic acid residues. These polysaccharide residues were detected in the extracellular matrices of flocs from all systems. This is consistent with the study by Sutherland (1972) who states that the presence of glucose, N-acetylglucosamine and N-acetylgalactosamine in bacterial polymers is wide-spread. A significantly less dense distribution of N-acetylglucosamine and N-acetylneuraminic acid residues was observed within the matrix of floc from system-Py (Figure 4.29B). This observation is supported by the significantly low level of EPS in system-Py as found by chemical analysis. Steiner *et al.* (1976) reported that there was a decrease in surface charge when either muramic acid, N-acetyl hexosamine or a combination of both was removed from

the sludge surface. Although the types of polysaccharide studied are different in both studies, the results in this study indicates a possible role of N-acetylglucosamine and N-acetylneuraminic acid in bioflocculation. Further studies on the role of these two compounds in bioflocculation are recommended.

4.6.2 Ultrastructure of floc matrix

The ultrastructure of floc matrix was found to be different among the systems studied. The heterogeneous nature of components inside the flocs and their random dispersion are clearly seen in the TEM images. The ultrathin sections of samples stained by ruthenium red reveal a complex three-dimensional network of extracellular polysaccharide fibrils with different diameters and arrangements within the matrices of flocs (Table 4.22). The well-define, ribbon-like fibrils with diameters ranging between 2 - 15 nm were observed in matrices of all system generally. However, these fibrils cannot be commonly seen at the images of flocs from system-Pm. The range of diameter of fibrils observed is similar to the range of diameter of fibrils at 2 - 10 nm as reported by Leppard (1992b). The characteristics of this material are consistent with the descriptions of Type II polymers which are thought to link microorganisms within 2.5 to 13 μm particles (Jorand *et al.*, 1995). Similar Type II polymers were observed by Droppo *et al.* (1996b). The ultrastructure of floc matrices of the treatment systems studied is described in the following.

(1) Flocs from system-Dm

The TEM images of flocs from system-Dm reveal a more extensive, uniform and dense matrix structure than that of the other systems studied (Figure 4.30). This agrees with a higher level of EPS found by chemical analysis at system-Dm.

(2) Flocs from system-Py and system-Po

Two distinct layers was found in the matrices of system-Py and system-Po: a) the dense inner layer and b) the less dense outer layer. The fibril matrix of flocs from system-Py was not extensive as that for system-Po (Figure 4.31 and 4.33). This agrees with a lower level of EPS

found by chemical analysis at system-Py than that of system-Po. A number of filamentous microorganisms were found in images of flocs from system-Po (Figure 4.33B). However, no ribbon-like fibrils around these microorganisms were observed.

(3) Flocs from system-Pm

The well-defined fibrils or network was not commonly observed in the images of flocs from system-Pm. A thin, dense, slime-like material of about 18 - 36 nm in thickness surrounding the cell was observed (Figure 4.32). Layers of material which seemed to be overlapping one another forming an envelope of about 55 nm in thickness enclosing the cell was found (Figure 4.32A). These layers of material were quite uniform in thickness and spatial arrangement. This material could be lipid.

Table 4.22. Summary of the observations of ultrastructure of floc matrices from different treatment systems.

Treatment systems	Form of fibrils	Diameter of fibrils	Description of extracellular matrix
Dm	- well-defined - ribbon-like - no spatial arrangement	7 - 15 nm	- thick and extensive - uniformly dense
Py	- well-defined - ribbon-like - bundle of fibrils form a thicker filaments	2 - 8 nm	- two distinct layers : a) dense inner layer b) less dense outer layer
Pm	- well-defined, ribbon-like fibrils not commonly seen	---	- thin, dense, slime-like material - layers of material overlapping one another forming an envelope
Po	- well-defined fibrils - ribbon-like	3 - 8 nm	- two distinct layers : a) dense inner layer b) less dense outer layer

4.6.3 Summary of the spatial distribution of EPS and the ultrastructure of matrix

The internal floc structure was heterogeneous. The α-mannopyranosyl, α-glucopyranosyl, N-acetylglucosamine and N-acetylneuraminic acid residues were present at the floc matrices from all systems studied. However, the spatial distribution of these residues was different among the systems studied. The difference in the spatial distribution may be associated with the sludge age of the flocs. A significantly less dense distribution of N-acetylglucosamine and N-acetylneuraminic acid residues was observed at the matrix of system-Py. This indicates a possible role of N-acetylglucosamine and N-acetylneuraminic acid in bioflocculation.

The ultrastructure of floc matrix is different among the systems studied. A complex three-dimensional network of extracellular polysaccharide fibrils with different diameters and arrangements within the matrices of flocs was observed. The heterogeneous nature of components inside the flocs and their random dispersion are clearly seen as well.

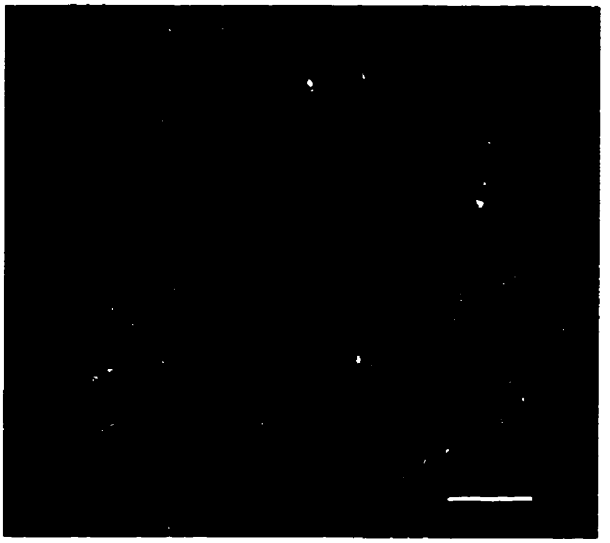

A. System-Dm

B. System-Py

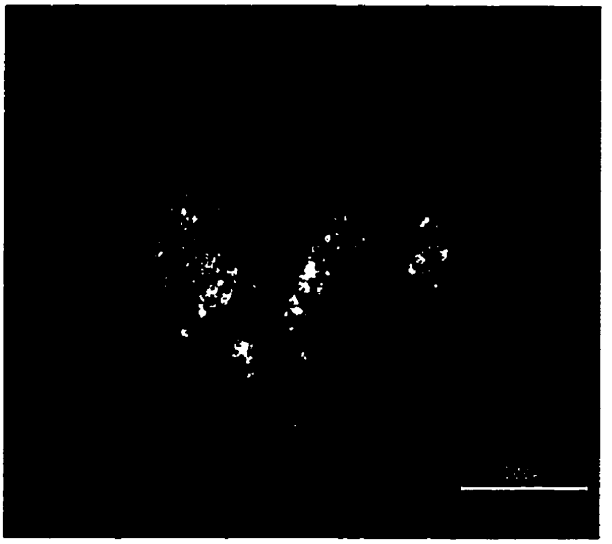

C. System-Pm

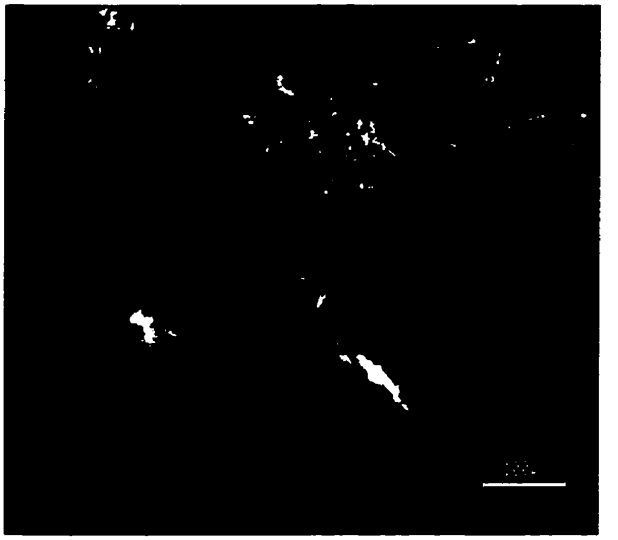

D. System-Po

Figure 4.27. SCLM images of flocs stained by fluorescein isothiocyanate (FITC). The scale bars for A and B = 100 microns.

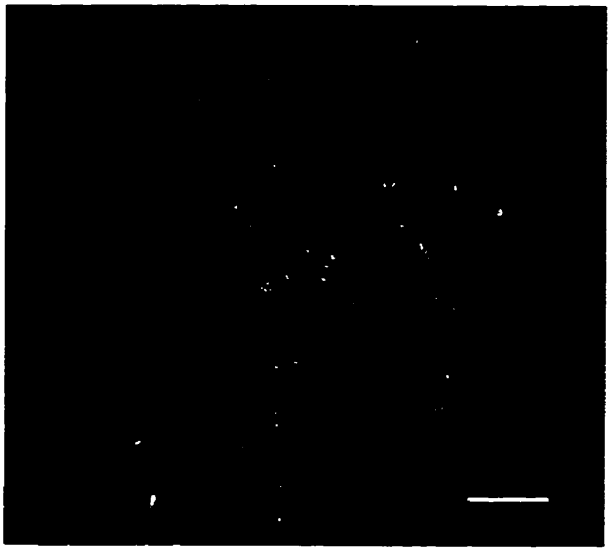

A. System-Dm

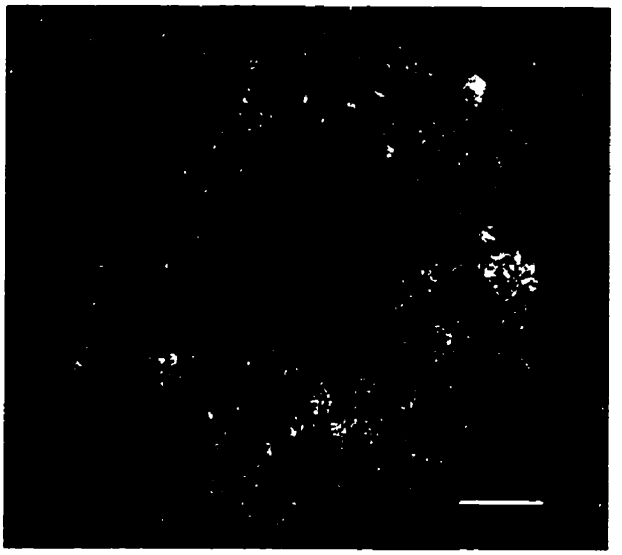

B. System-Py

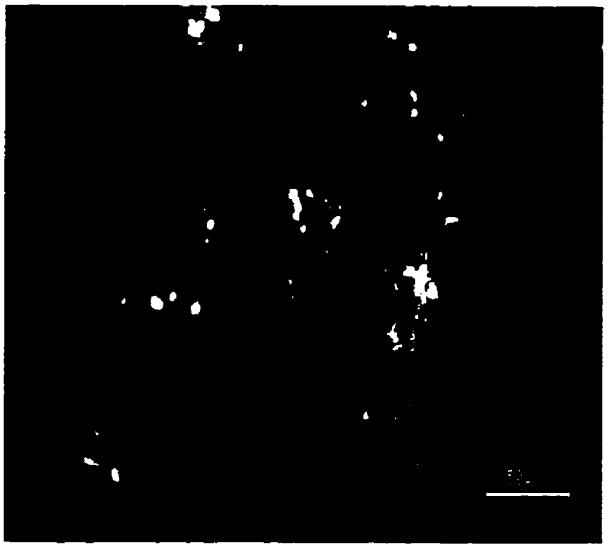

C. System-Pm

D. System-Po

Figure 4.28. SCLM images of flocs stained by Concanavalin A (ConA). The scale bars for A and B = 100 microns.

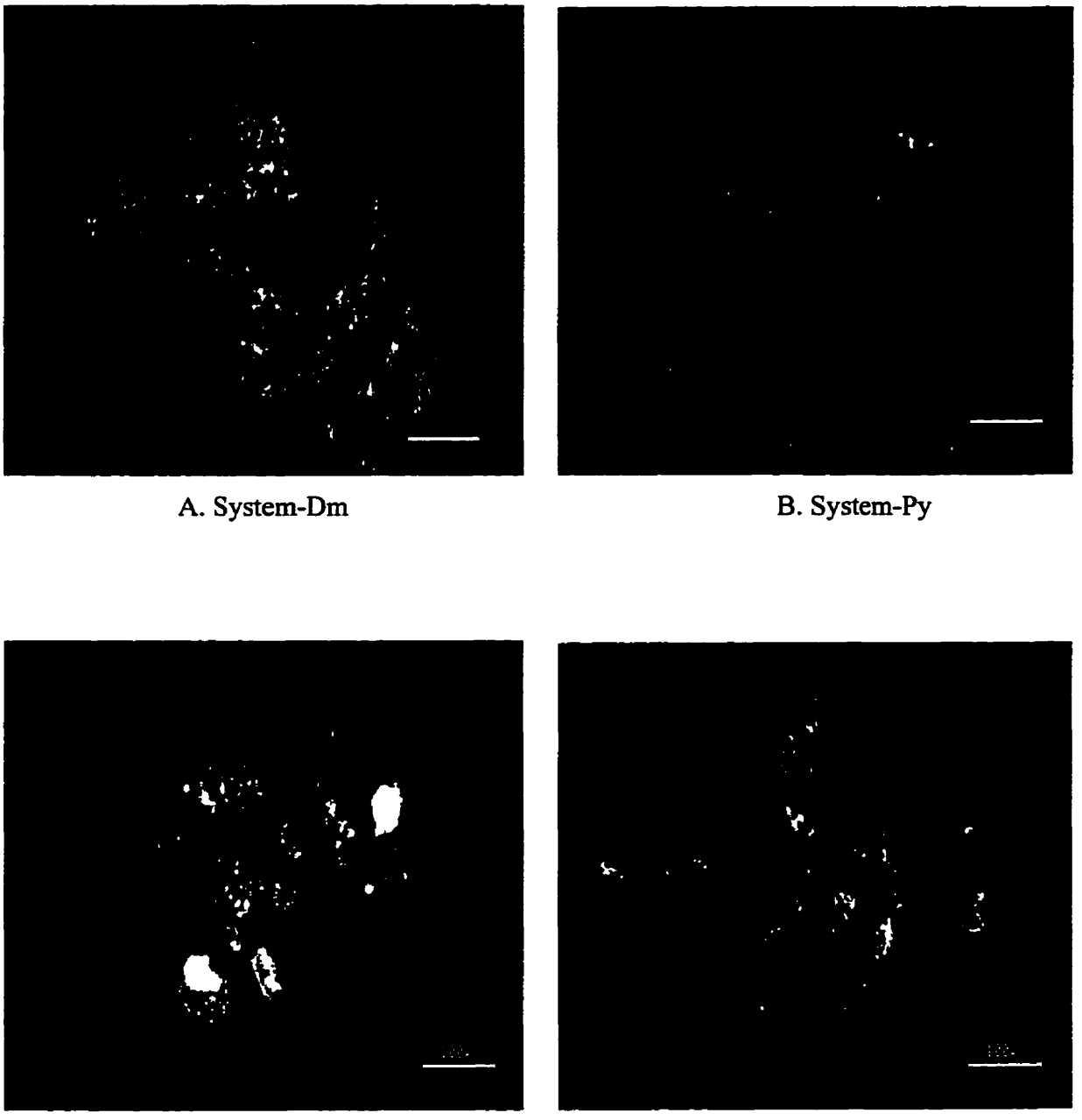

A. System-Dm

B. System-Py

C. System-Pm

D. System-Po

Figure 4.29. SCLM images of flocs stained by wheat germ agglutinin (WGA). The scale bars for A and B = 100 microns.

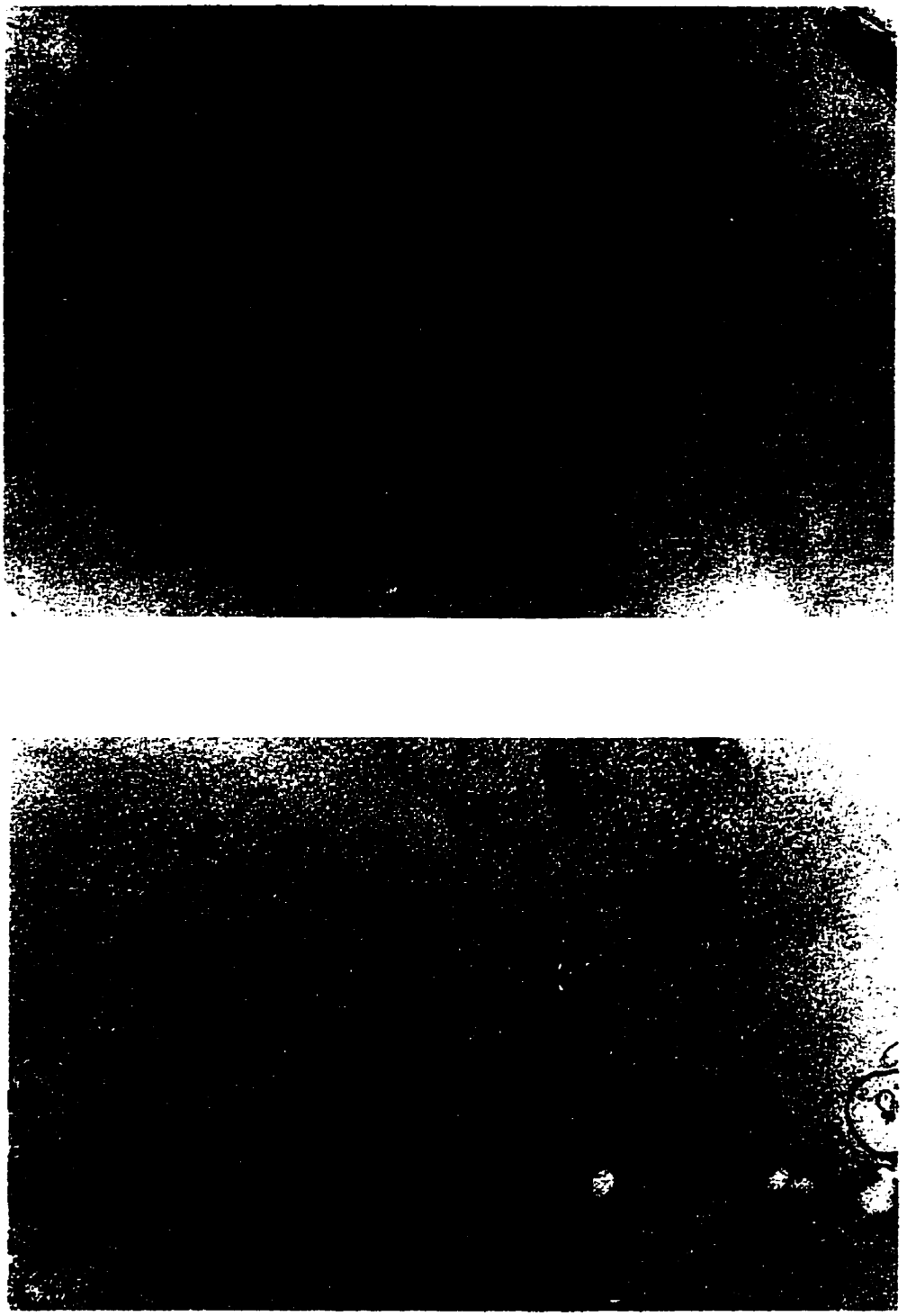

Figure 4.30. TEM images of flocs from system-Dm. Sample was stained by ruthenium red in glutaraldehyde. The scale bars represent 200 nm.

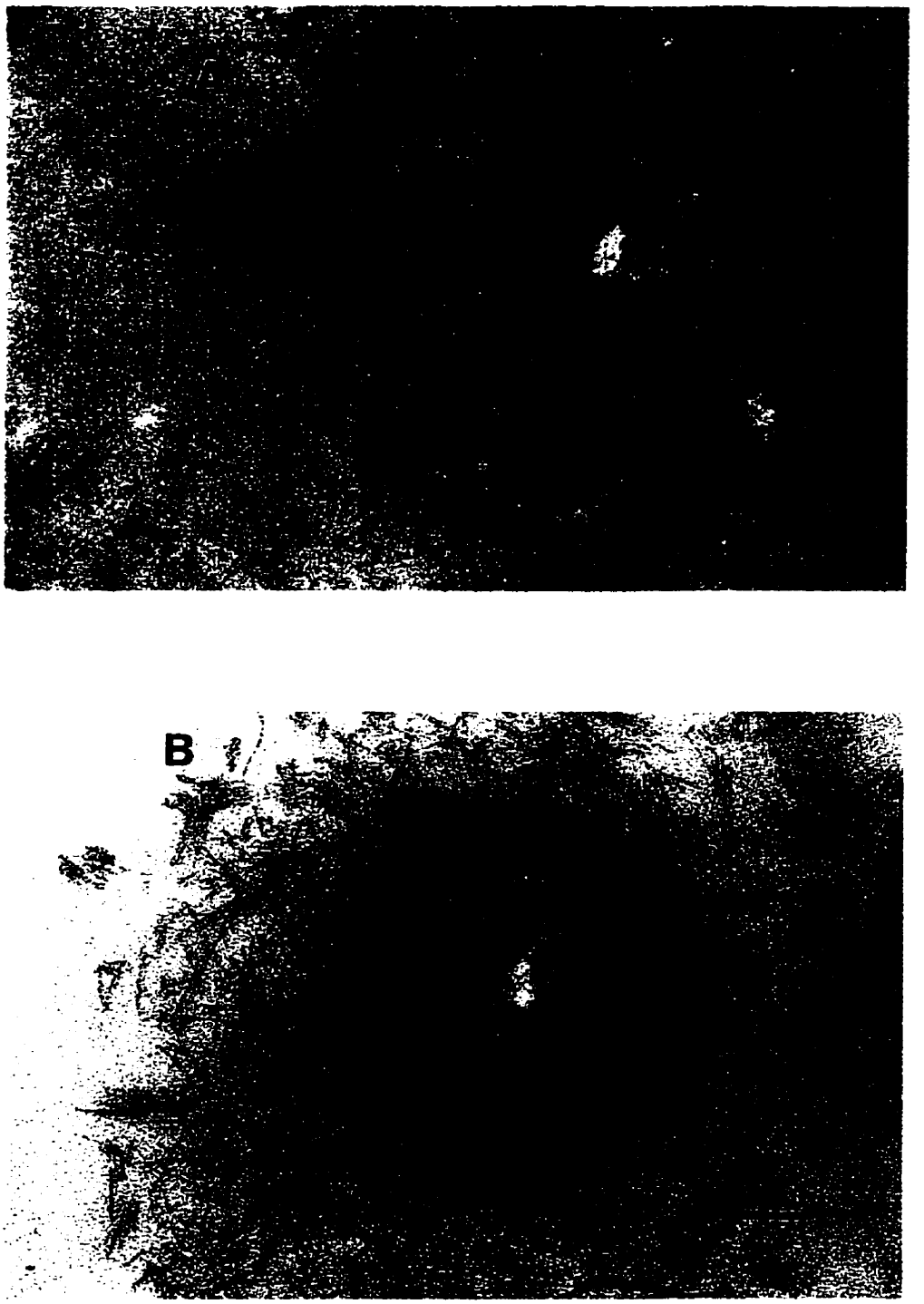

Figure 4.31. TEM images of flocs from system-Py. Sample was stained by ruthenium red in glutaraldehyde. The scale bars represents 200 nm.

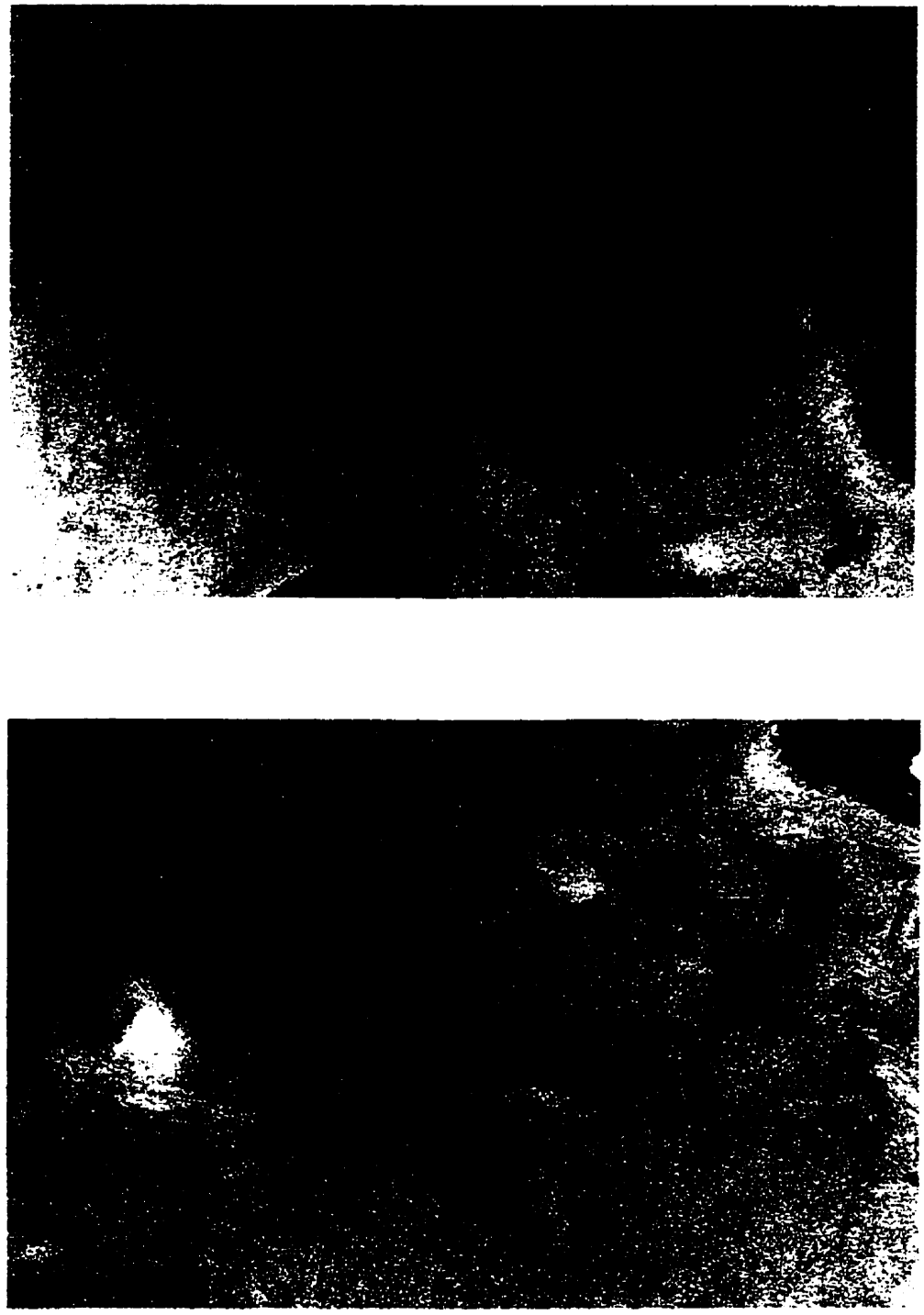

Figure 4.32. TEM images of flocs from system-Pm. Sample was stained by uranyl acetate in Nanoplast. The scale bars represent 200 nm.

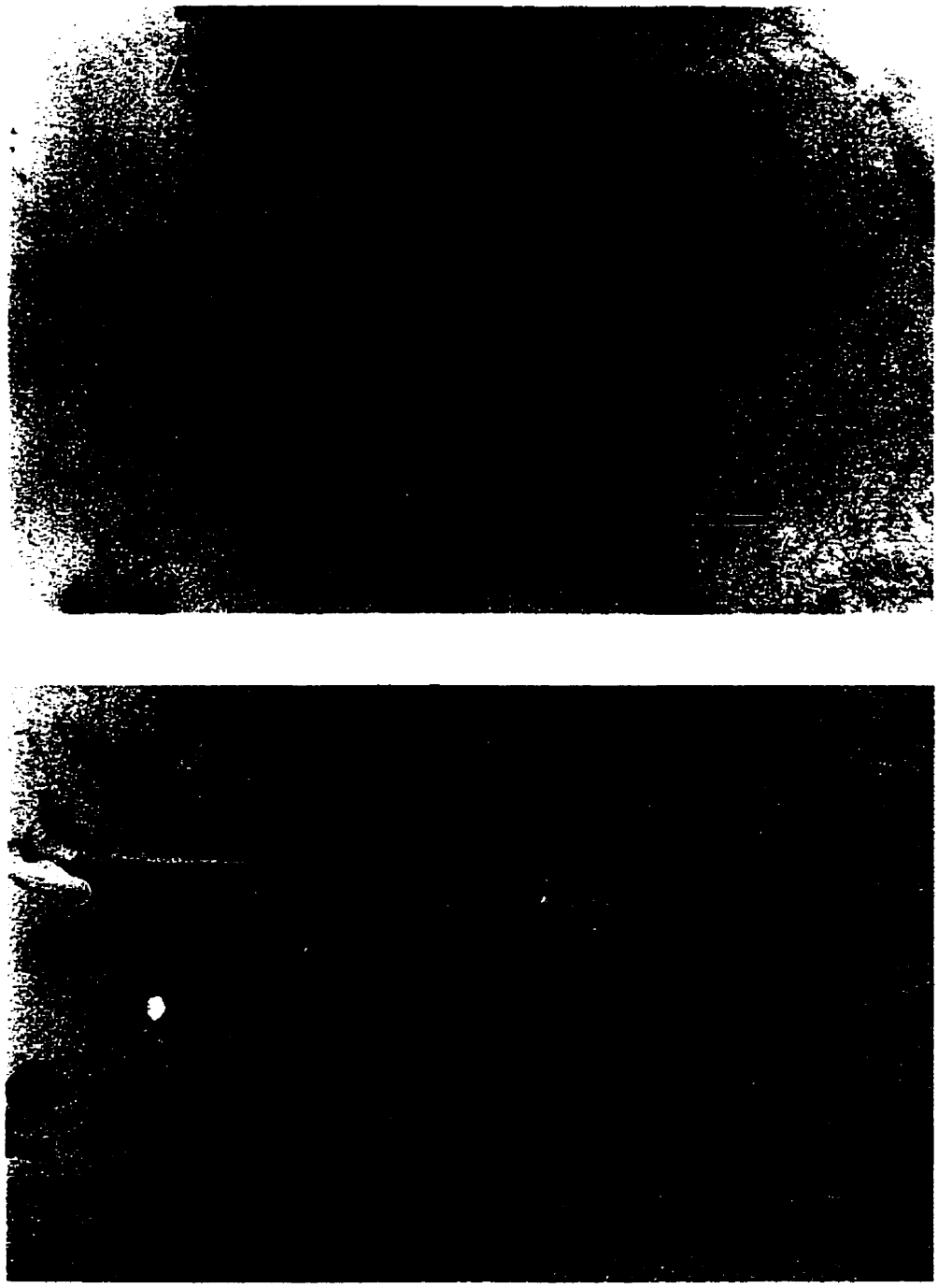

Figure 4.33. TEM images of flocs from system-Po. Sample was stained by ruthenium red in glutaraldehyde. The scale bars represent 200 nm.

4.7 Significance of Results

The full-scale systems studied represented a range of configurations and different types of wastewater. The distinct operating conditions such as MCRT (sludge age) and the microbial community of each system could possibly affect the sludge properties. Because the variations in operating conditions affect the physiological state of bacteria and the microbial communities, as a result, the floc development is affected also. Although the explanation for an observation may not be concluded easily due to the uncontrolled study conditions, the study on full-scale systems can provide important observations based on actual operation. These observations may provide a guideline for further study using controlled systems. For instance, the relation between sludge age and EPS was observed in this study. This may lead to the further study to investigate the sludge age for an optimum production of EPS to achieve an effective sludge settling.

The results concerning the characteristics of EPS indicate the possibility of designing operating conditions for the development of an optimum floc which is not only able to remove the substrate in the wastewater but also settle well. This study reveals the quantitative and qualitative characteristics of EPS composition from sludge in full-scale systems. Protein was found to be the dominant component in the extracted EPS followed by carbohydrate, DNA and acidic polysaccharide generally regardless of the types of wastewater and operating conditions. These four components formed a more or less constant percentage composition in the organic matrix. The level of EPS is inversely associated with the MCRT (sludge age) of system. Hence, an operating condition such as sludge age is much more important than microbial community alone as a factor in affecting the composition of EPS. In addition, DNA and acidic polysaccharide were the most labile components in EPS; the higher levels of these components may be associated with better sludge settling. Another observation found that the spatial distribution of EPS was different among the systems studied. The difference in the spatial distribution may be associated with the sludge age of the flocs. A possible role of N-acetylglucosamine and N-acetylneuraminic acid in the bioflocculation was observed as

significantly less of these compounds was found in the extracellular matrix of flocs from system treating poultry processing wastewater.

Observation of the sludge properties during functional and dysfunctional periods of the system treating potato processing wastewater reveals that there is not only biological change in sludge properties such as abundant growth of filaments but also physical and chemical changes. The MLSS, EPS composition and sludge carbohydrate were higher during the dysfunctional periods. The significantly higher levels of protein and carbohydrate may be associated with a higher bound water content and surface charge of the floc. The floc size expressed as median ESD by volume was six times larger than the functional periods. Therefore, all these properties should be considered in developing appropriate control strategy to improve sludge settlement.

CHAPTER 5 CONCLUSIONS AND RECOMMENDATIONS

In an effort to better understand bioflocculation and the role of EPS on the properties of activated sludge floc, a comparative study of four full-scale activated sludge systems has been conducted. Specific conclusions that can be drawn from this study are as follows:

1. Protein was found to be the dominant component in the extracted EPS followed by carbohydrate, DNA and acidic polysaccharide generally regardless of the types of wastewater and operating conditions.
2. These four components formed a more or less constant percentage composition in the organic matrix with 77-81% protein, 11-15% carbohydrate, 4-9% DNA and 3-5% acidic polysaccharide.
3. DNA and acidic polysaccharide were the most labile components in EPS.
4. The higher levels of DNA and acidic polysaccharide in EPS may be associated with better sludge settling as the correlation coefficient between DNA and acidic polysaccahride with SVI was greater than 0.61 (95% probability level).
5. The level of EPS is inversely associated with the MCRT (sludge age) of system. Hence, an operating condition such as sludge age is much more important than microbial community alone as a factor in affecting the composition of EPS.
6. The level of carbohydrate in EPS is directly associated with the level of sludge carbohydrate as the correlation coefficient was 0.71 (95% probability level).
7. The percentage of volatile suspended solids (VSS/SS%) is quite constant (SD < 5%) within a system but different among the systems.
8. The levels of protein and carbohydrate in EPS during dysfunctional periods of system-Po were 56% and 71% higher than functional periods. These higher levels of protein and carbohydrate may be associated with a higher bound water content and surface charge of the floc.
9. Low F/M ratio may account for the higher level of EPS and abundant growth of the filaments during the dysfunctional periods of system-Po.
10. The α-mannopyranosyl, α-glucopyranosyl, N-acetylglucosamine and N-acetylneuraminic acid residues were present at the floc matrices from all systems studied. However, the spatial distribution of these residues was different among the systems studied. The difference in the spatial distribution may be associated with the sludge age of the flocs.

11. A significantly less amount of N-acetylglucosamine and N-acetylneuraminic acid residues was observed at the floc matrix of system-Py. This indicates a possible role of N-acetylglucosamine and N-acetylneuraminic acid in the bioflocculation.
12. The ultrastructure of floc matrix is different among the systems studied. A complex three-dimensional network of extracellular polysaccharide fibrils with different diameters and arrangements within the matrices of flocs was observed.

Recommendations for future study:

1. The effect of sludge age on EPS composition conducted under controlled conditions should be studied. This can provide a better understanding of the optimum operating conditions which can achieve an efficient substrate removal and solid-liquid separation. The range of MCRT studied should extend to 25 days as a longer MCRT has been used by full-scale system for nitrogen removal.
2. The effect of EPS composition on bound water, surface charge and hydrophobicity during dysfunctional period should be studied as EPS is thought to have an effect on the surface properties of floc.
3. The levels of protein and carbohydrate in sludge and EPS should be determined as well. The higher levels of protein and carbohydrate in EPS were found to be associated with poor settling during the dysfunctional periods.
4. The role of particular types of polysaccharides such as N- acetylglucosamine and N-acetylneuraminic acid on the bioflocculation should be investigated.
5. A statistical method based on the comparison of the entire population should be sought for the comparison of physical properties of flocs.

REFERENCES

Andreadakis A.D. (1993) Physical and chemical properties of activated sludge floc. *Wat. Res.* **27**, 1707-1714.

APHA (1985) Standard Methods for the Examination of Water and Wastewater, 16 ed., Washington, DC.

Bache D.H., Hossain M.D., Al-Ani S.H. and Jackson P.J. (1991) Optimum coagulation conditions for a colored water in terms of floc size, density and strength. *Water Supply* **29**, 93-102.

Barber J.B. and Veenstra K.W. (1986) Evaluation of biological sludge properties influencing volume reduction. *J. Wat. Pollut. Control Fed.* **58**, 149-156.

Brown M.J. and Lester J.N. (1979) Metal removal in activated sludge: the role of bacterial extracellular polymers. *Water Res.* **13**, 817-837.

Brown M.J. and Lester J.N. (1980) Comparison of bacterial extracellular polymer extraction methods. *Appl. Environ. Microbiol.* **40**, 179-185.

Buffle J. and Leppard G.G. (1995a) Characterization of aquatic colloids I and II. *Environmental Sci. Technol.* **29**, 2169-2175.

Buffle J. and Leppard G.G. (1995b) Characterization of aquatic colloids I and II. *Environmental Sci. Technol.* **29**, 2176-2184.

Bura R., Cheung M., Liao B., Finlayson J., Lee B.C., Droppo I., Leppard G.G. and Liss S.N. (1997) Composition of extracellular polymeric substances in the activated sludge floc matrix. *Proceedings Second International Conference on Microorganisms in Activated Sludge and Biofilm Processes, Berkeley, California, USA.*

Burban P.-Y, Xu Y.-J., McNeil J. and Nick W. (1990) Settling speeds of flocs in fresh water and seawater. *J. Geophys. Res.* **95** (C10), 18213-18220.

Caldwell D.E., Korber D.R. and Lawrence J.R. (1992) Image analysis in microbiology. In *Advances in Microbial. Ecology* **12**, 1-67.

Costerton J.W. and Irvin R.T. (1981) The bacterial glycocalyx in nature and disease. *A Rev. Microbiol.* **35**, 299-324.

Chudoba J. (1989) Glycocalyx contra filamentous backbone. *IAWPRC Specialist Group in Activated Sludge Population Dynamics Newsletter* **December**, 1989.

Decho A.W. (1990) Microbial exopolymer secretions in ocean environments: their role(s) in food webs and marine processes. *Oceanogr. Mar. Biol. Annu. Resv.* **28**, 73-153.

Deinema M.H, and Zevenhuizen L.P.T.M. (1971) Formation of cellular fibrils by Gram-negative bacteria and their role in bacterial floccculation. *Arch. Mikrobiol.* **78**, 42-57.

Droppo I.G., and Ongley E.D. (1992) The State of Suspended Sediment in the Freshwater Fluvial Environment: A method of Analysis. *Wat. Res.* **26**, 65-72.

Droppo I.G., Flannigan D.T., Leppard G.G., Jaskot C. and Liss S.N. (1996a) Floc stabilization for multiple microscopic techniques. *Appl. Environ. Microbiol.* **62**, 3508-3515.

Droppo I.G., Flannigan D.T., Leppard G.G. and Liss S.N. (1996b) Microbial floc stabilization and preparation for structural analysis by correlative microscopy. *Wat. Sci. Tech.* **34**, 155-162.

Droppo I.G., Leppard G.G., Flannigan D.T. and Liss S.N. (1997) The freshwater floc: a functional relationship of water and organic and inorganic floc constituents affecting suspended sediment properties. *Water, Air and Soil Pollution* **99**, 43-54.

Dudman W.F. and Wilkinson J.F. (1956) The composition of the extracellular polysaccharides of Aero-bacter-Klebsiella strains. *Biochem. J.* **62**, 289-295.

Duguid J.P. and Wilkinson J.F. (1953) The influence of cultural conditions on polysaccharide production by Aerobacter *aerogenes*. *J. Gen. Microbiol.* **9**, 174-189.

Eighmy T.T., Maratea D. and Bishop P.L. (1983) Electron microscopic examination of wastewater biofilm formation and structural components. *Appl. Environ. Microbiolog.* **45**, 1921-1931.

EPA (1974) *Process Design Manual for Sludge Treatment and Disposal*, Program No. 1-74 -006.

Eriksson L and Härdin A.M. (1984) Settling properties of activated sludge related floc structure. *Wat. Sci. Tech.* **16**, 55-68.

Filisetti-Cozzi T.M.C.C. and Carpita N.C. (1991) Measurement of uronic acids without interference from neutral sugars. *Analytical Biochemistry* **197**, 157-162.

Forster C.F. (1971) Activated sludge surfaces in relation to the sludge volume index. *Water Res.* **5**, 861-870.

Forster C.F. (1976) Bioflocculation in the activated sludge process. *Water SA* **2**, 119-125.

Forster C.F. (1985) Factors involved in the settlement of activated sludge - I. Nutrients and surface polymers. *Water Res.* **14**, 1257 - 1264.

Forster C.F. and Choudhry N.M. (1972) Physio-chemical studies on activated sludge bioflocculation. *Effluent and Water Treatment Journal* **12**, 127-131.

Forster C.F. and Dallas-Newton J. (1980) Activated sludge settlement - some suppositions and suggestions. *Wat. Pollut. Control* **79**, 338-351.

Forster C.F. and Lewin D.C. (1972) Polymer interactions at activated sludge surfaces. *Effluent Wat. Treatment Journal* **Oct.**, 520-525.

Frølund B., Griebe T. and Nielsen P.H. (1995) Enzymatic activity in activated sludge floc matrix. *Appl. Microbiol. Biotechnol.* **43**, 755-761.

Frølund B., Palmgren R., Keiding K., Nielsen P.H. (1996) Extraction of extracellular polymers from activated sludge using a cation exchange resin. *Wat. Res.* **30**, 1749-1758.

Friedman B.A., Dugan P.R. and Pfister R.M. and Remsen, C.C. (1968) Fine structure and composition of the Zoogloeal matrix surrounding *Zoogloea ramigera*. *J. Bacteriology*. **96**, 2144-2153.

Friedman B.A., Dugan P.R. and Pfister R.M. and Remsen, C.C. (1969) Structure of exocellular polymers and their relationship to bacterial flocculation. *J. Bact.* **98**, 1328-1334.

Ganczarczyk J.J. (1967) Nominal diameter of floc related to oxygen transfer: discussion. *J.sanit. Engng, Am. Soc. civ. Engr.* **93**, 36-38.

Ganczarczyk J.J. (1994) Microbial aggregates in wastewater treatment. *Wat. Sci. Tech.* **30**, 87-95.

Ganczarczyk J.J., Zahid W.M. and Li D.H. (1992) Physical stabilization and embedding of microbial aggregates for light microscopy studies. *Wat. Res.* **26**, 1695-1699.

Garland J.L. and Mills A.L. (1991) Classification and characterization of heterotrophic microbial communities on the basis of pattern of community-level sole-carbon-source utilization. *Appl. Environ. Microbiol.* **57**, 2351-2359.

Gaudy A.F. (1962) Colorimetric determination of protein and carbohydrate. *Industrial Water and Wastes* **Jan.-Feb.**, 17-22.

Gehr R. and Henry J.G. (1983) Removal of extracellular material - techniques and pitfalls. *Water Res.* **17**, 1743-1748.

Geldart D. (1990) Estimation of basic properties for use in fluid-particle process calculation. *Powder Technol.* **60**, 1-13.

Glasgow L.A. (1989) Effects of the physiochemical environment on floc properties. *Chem. Eng. Progress* **Aug.**, 51-55.

Glasgow L.A. and Hsu J.-P. (1984) Floc characteristics in water and wastewater treatment. *Particulate Sci. Technol.* **2**, 285-303.

Goodwin J.A.S. (1988) Surface chemistry in the activated sludge process. Ph.D. thesis, University of Birmingham.

Goodwin J.A.S. and Forster C.F. (1985) A further examination into the composition of activated sludge surfaces in relation to their settling characteristics. *Water Res.* **19**, 527 - 533.

Grijspeerdt K. and Verstraete W. (1997) Image analysis to estimate the settleability and concentration of activated sludge. *Water Res.* **31**, 1126-1134..

Hattingh W.H.J. and Siebert M.L. (1967) Determination of the deoxyribonucleic acid (DNA) content of anaerobic sludge. *Water Res.* **1**, 197-203.

Hermanowicz S.W. and Ganczarczyk J.J. (1983) Some fluidization characteristics of biological beds. *Biotechnol. Bioengng.* **25**, 1321-1330.

Higgins M.J. and Novak J.T. (1997) Characterization of exocellular protein and its role in bioflocculation. *J. Environmental Engineering* **May**, 479-485.

Horan H.J. (1990) *Biological Wastewater Treatment Systems - Theory and Operation*, Wiley.

Horan H.J. and Eccles C.R. (1986) Purification and characterization of extracellular polysaccharides from activated sludges. *Wat. Res.* **20**, 1427-1432.

Jenkins D. (1992) Towards a comprehensive model of activated sludge bulking and foaming. *Wat. Sci. Tech.* **25**, 215-230.

Jenkins D., Richards M.G. and Daigger G.T. (1993) *Manual on the causes and control of activated sludge bulking and foaming*. Lewis Publishers, Chelsea, Mich..

Jorand F., Zartarian F., Thomas F., Block J.C., Bottero J.Y., Villemin G., Urbain V. and Manem J. (1995) Chemical and structural (2D) linkage between bacteria within activated sludge flocs. *Wat. Res.* **29**, 1639-1647.

Kato A., Izaki K. and Takahashi H. (1971) Floc-forming bacteria isolated from activated sludge. *J. of General and Applied Microbiology* **17**, 439-456.

Kiff R.J. and Thompson R.T. (1979) Physical methods for the extraction of bacterial exopolymers from activated sludge biomass. *Biotechnol. Lett.* **1**, 183-186.

Klimpel R.C., Dirican C. and Hogg R. (1986) Measurement of agglomerate density in flocculated fine particle suspensions. *Particulate Sci. Technol.* **4**, 45-59.

Lee D.J. (1994) Floc structure and bound water content in excess activated sludges . *J. Chin. I. Ch. E.* **25**, 201-207.

Lee D.J., Chen G.W. Liao C.Y. and Hsieh C.C. (1996) On the free-settling test for estimating activated sludge floc density. *Wat. Res.* **30**, 541-550.

Leppard G.G. (1997) Personal communication.

Leppard G.G. (1992a) Size, morphology and composition of particulates in aquatic ecosystems: Solving speciation problems by correlative electron microscopy, *Analyst* **117**, 595-603.

Leppard G.G. (1992b) Evaluation of electron microscope techniques for the description of aquatic colloids. In *Environmental Particles* **Vol.1**, Lewis Publishers, Boca Raton, pp. 231-289.

Leppard G.G. (1986) The fibrillar matrix component of lacustrine biofilms. *Wat. Res.* **20**, 697-702.

Lerman A. (1979) *Geochemical processes: Water and Sediment Environment*, Wiley, N.Y..

Levine A.D., Tchobanoglous G. and Asano T. (1985) Characterization of the size distribution of contaminants in wastewater: Treatment and reuse implications. *J.Water Pollut. Control Fed.* **57**, 805-816.

Li D.H. and Ganczarczyk J.J. (1986) Application of image analysis system for activated sludge flocs. *Wat. Poll. Res. J. Canada* **21**, 130-140.

Li D.H. and Ganczarczyk J.J. (1987) Stroboscopic determination of settling velocity, size, porosity of activated sludge flocs. *Wat. Res.* **21**, 257-262.

Liebeskind M. and Dohmann M. (1994) Improved method of activated sludge biomass determination. *Water Sci. Tech.* **29**, 7-13.

Liss S.N., Droppo I.G., Flannigan D.T. and Leppard G.G. (1996) Floc architecture in wastewater and natural riverine systems. *Environ. Sci. Technol.* **30**, 680-686.

Lowry O.H., Rosenbrough N.J., Farr A.L. and Randall R.J. (1951) Protein measurement with the Folin phenol reagent. *J. Biol. Chem.* **193**, 265.

Magara Y., Nambu S. and Utowsa K. (1976) Biochemical and physical properties of activated sludge on settling characteristics. *Wat. Res.* **10**, 71-77.

Maruyama A.; Oda M. and Higashihara T. (1993) Abundance of virus-sized non-DNase-digestible DNA (coated DNA) in eutrophic seawater. *Appl. Environ. Microbiol.* **59**, 712 -717.

Mendenhall W. and Sincich T. (1992) Statistics for Engineering and the Sciences 3 ed., Maxwell Macmillian Canada, Inc.

Metcalf and Eddy Inc. (1991) *Wastewater Engineering - Treatment, disposal and Reuse*. 3 ed., McGraw-Hill.

Morgan J.W., Forster C.F. and Evison L. (1990) A comparative study of the nature of biopolymers extracted from anaerobic and activated sludges. *Water Res.* **24**, 743-750.

Mueller J.A., Morand J. and Boyle W.C. (1967) Floc sizing technique. *Appl. Microbiol.* **15**, 124-134.

Námer J. and Ganczarczyk J.J. (1993) Settling properties of digested sludge particle aggregates. *Wat. Res.* **27**, 1285-1294.

Nemerow N.L. (1978) *Industrial water pollution - origins, characteristics and treatment.* Addison-Wesley.

Norcliffe G.B. (1982) Inferential Statistics for Geographer 2 ed., Hutchinson and Co. Ltd., London.

Novak J.T. and Haugar B.E. (1981) Polymer extraction from activated sludge. *J. Wat. Pollut. Control Fed.* **53**, 1420-1425.

Novak L., Larrea L., Wanner J. and Garcia-Heras J.L. (1994) Non-filamentous activated sludge bulking caused by *Zooglea*. *Wat. Sci. Tech.* **29**, 301-304.

Palmgren R. and Nielsen P.H. (1996) Accumulation of DNA in the exopolymeric matrix of activated sludge and bacteria cultures. *Wat. Sci. Tech.* **34**, 233-240.

Parker D.S., Kaufman W.J. and Jenkins D. (1971) Physical conditioning of activated sludge flocs. *J. Wat. Pollut. Control Fed.* **43**, 1817-1833.

Paul J.H. and David A. (1989) Production of extracellular nucleic acids by genetically altered bacteria in aquatic-environment microcosms. *Appl. Environ. Microbiol.* **55**, 1865-1869.

Pavoni J.L., Tenney M.W. and Echelberger W.F. Jr. (1972) Bacterial exocellular polymers and biological flocculation. *J. Wat. Pollut. Control Fed.* **44**, 414-431.

Pelczar M.J.Jr., Reid R.O. and Chan E.C.F. (1977) "Capsules". In *Microbiology*, 4th ed., , McGraw-Hill, New York, pp. 87-89.

Petro-Canada (1997) Personal communication with the officer in the department of Environmental Management for Refinery.

Pettyjohn E.A. and Christiansen E.B. (1948) Effect of particle shape on free settling rates of isometric particles. *Chem. Engng. Prog.* **44**, 157-172.

Pipes W.O. (1967) Bulking of activated sludge. *Advances in Appl. Microbiology* **9**, 185-234.

Pujol R. and Canler J.P. (1992) Biosorption and dynamics of bacterial populations in activated sludge. *Wat. Res.* **26**, 209-212.

Rao S.S., Droppo I.G., Taylor C.M. and Burnison B.K. (1991) Freshwater bacterial aggregate development : Effect of dissolved organic matter. *Wat. Poll. Res. J. Canada* **26**, 163-171.

Sato T. and Ose Y. (1980) Floc-forming substances extracted from activated sludge by sodium hydroxide solution. *Water Res.* **14**, 333-338.

Sezgin M., Jenkins D. and Parker D.S. (1978) A unified theory of filamentous activated sludge bulking. *J. Wat. Pollut. control Fed.* **50**, 362.

Smith P.G. and Coackley P. (1984) Diffusivity, tortuosity and pore structure in activated sludge. *Wat. Res.* **18**, 117-122.

Spurr A.R. (1969) A low-viscosity epoxy resin embedding medium for electron microscopy. *J. Ultrastruct. Res.* **26**, 31-43.

Steiner A.E., McLaren D.A. and Forster C.F. (1976) The nature of activated sludge flocs. *Water Res.* **10**, 25-30.

Strycek T., Acreman J., Kerry A., Leppard G., Nermut M. and Kushner D. (1992) Extracellular fibril production by freshwater algae and Cyanobacteria. *Microb. Ecol.* **23**, 53-74.

Sutherland I.W. (1972) Bacterial exopolysaccharides. *Adv. Microb. Physiol* **8**, 143-213.

Tago Y. and Aida K. (1977) Exocellular mucopolysaccharide closely related to bacterial floc formation. *Appl. Environ. Microbiol.* **34**, 308-314.

Tambo N. and Watanabe Y. (1979) Physical characteristics of floc I - the focal density function and aluminum floc. *Wat. Res.* **13**, 409-419.

Tenney M.W. and Stumm W.J. (1965) Chemical flocculation and microorganisms in biological waste treatment. *J. Wat. Poll. Control Fed.* **39**, 1370-1388.

Tenney M.W. and Verhoff F.H. (1973) Chemical and autoflocculation of microorganisms in biological wastewater treatment. *Biotechnology and Bioengineering* **15**, 1045-1073.

Tezuka Y. (1969) Cation-dependent flocculation in a *Flavobacterium* species predominant in activated sludge. *Appl. Microbiology* **17**, 222-226.

Thomanetz E. (1982) Untersuchungen zur charakterisierung and quanitiativen erfassung der biomass von belebten schlammen. *Stuttgarter Berichte zur Siedlungswasserwirtschaft* **74**, R. Oldenbourg, Munchen, Germany.

Unz R.F. and Farrah S.R. (1976) Exopolymer production and flocculation by *Zoogloea* MP6. *Appl. Environ. Microbiol* **31**, 623-626.

Urbain V., Block J.C., and Manen J. (1992) Bioflocculation in activated sludge: an analytical approach. *Water Sci Tech.*. **25**, 441-443.

Urbain V., Block J.C. and Manem J. (1993) Bioflocculation in activated sludge : an analytical approach. *Wat. Res.* **27**, 829-838.

Vallom J.K. and McLoughlin A.J. (1984) Lysis as a factor in sludge flocculation. *Wat. Res.* **18**, 1523-1528.

Victorio L., Gilbride K.A., Allen D.G. and Liss S.N. (1996) Phenotypic fingerprinting of microbial communities in wastewater treatment systems. *Wat. Res.* **30**, 1077-1086.

Wallen L.L. and Davis E.N. (1972) Biopolymers of activated sludge. *Environ. Sci. Tech.* **6**, 161-164.

Watanabe S., Baba K., Matuzaki H., Hiraoka M. and Tsumura K. (1990) Operation condition diagnosis system for activated sludge processes based on microorganism image information. In *Advances in Water Pollution control*, Pergamon Press, London, pp. 683-690.

WEAO (1997) Wastewater Microbiology Seminar - Technical Symposium. Water Environment Association of Ontario.

Wilkinson J.F. (1958) The extracellular polysaccharides of bacteria. *Bacteriol. Rev.* **22**, 46-73.

Wilkinson J.F., Duguid J.P. and Edmunds P.N. (1954) The distribution of polysaccharide production in aerobacter and escherichia strains and its relation to antigenic character. *J. Gen. Microbiol.* **11**, 59-72.

Zahid W.M. and Ganczarczyk J.J. (1990) Suspended solids in biological filter effluents. *Wat. Res.* **24**, 215-220.

Zartarian F., Mustin C., Bottero J.Y., Villemin G., Thomas F., Aillères L., Champerois M., Grulois P. and Manem J. (1994) Spatial arrangement of components of activated sludge flocs. *Wat. Sci. Tech.* **30**, 243-250.

APPENDIX A

FLOW DIAGRAMS OF WASTEWATER TREATMENT PLANTS

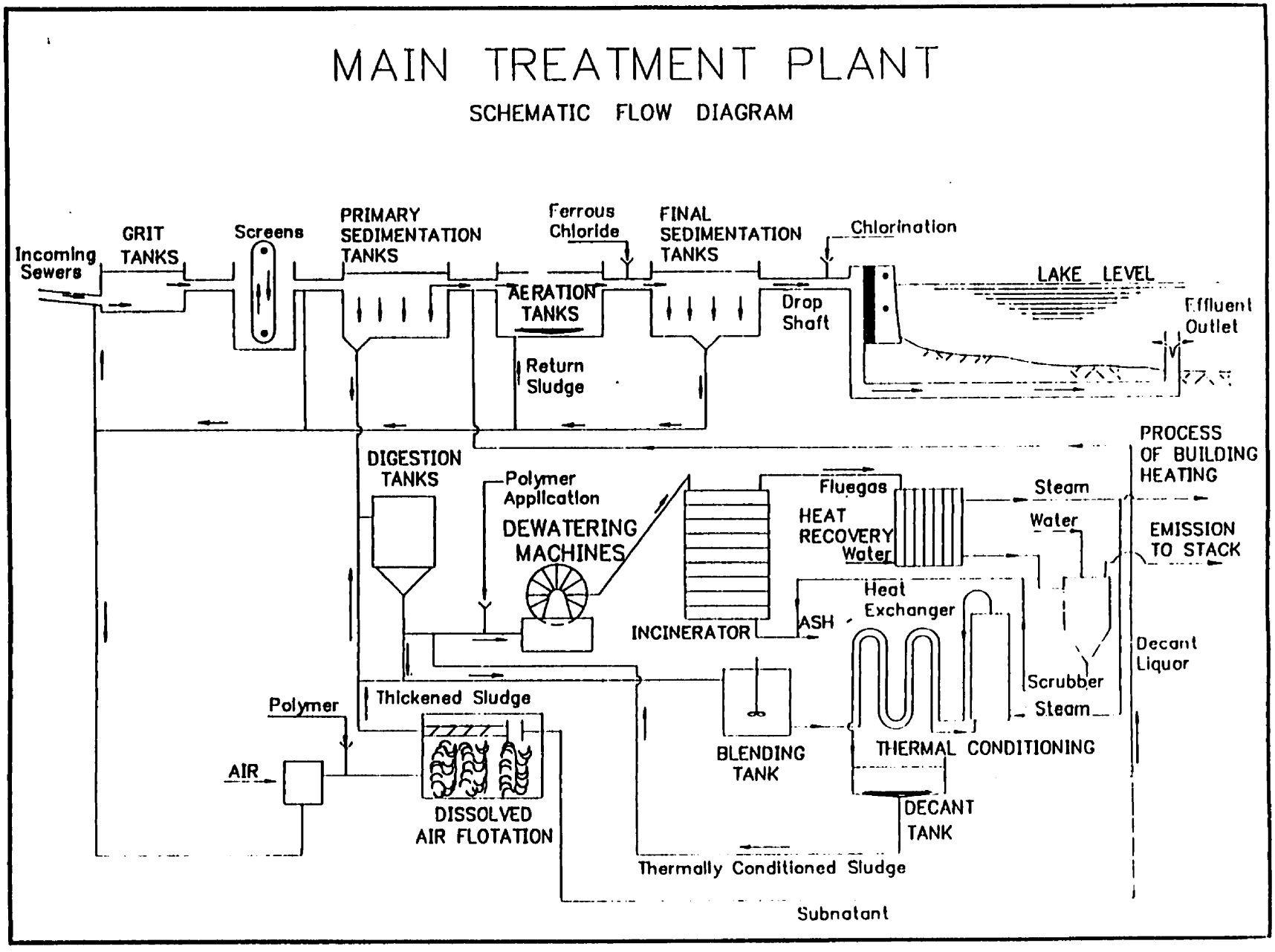

Figure A.1. Schematic flow diagram of municipal wastewater treatment plant (courtesy of Toronto Main Treatment Plant).

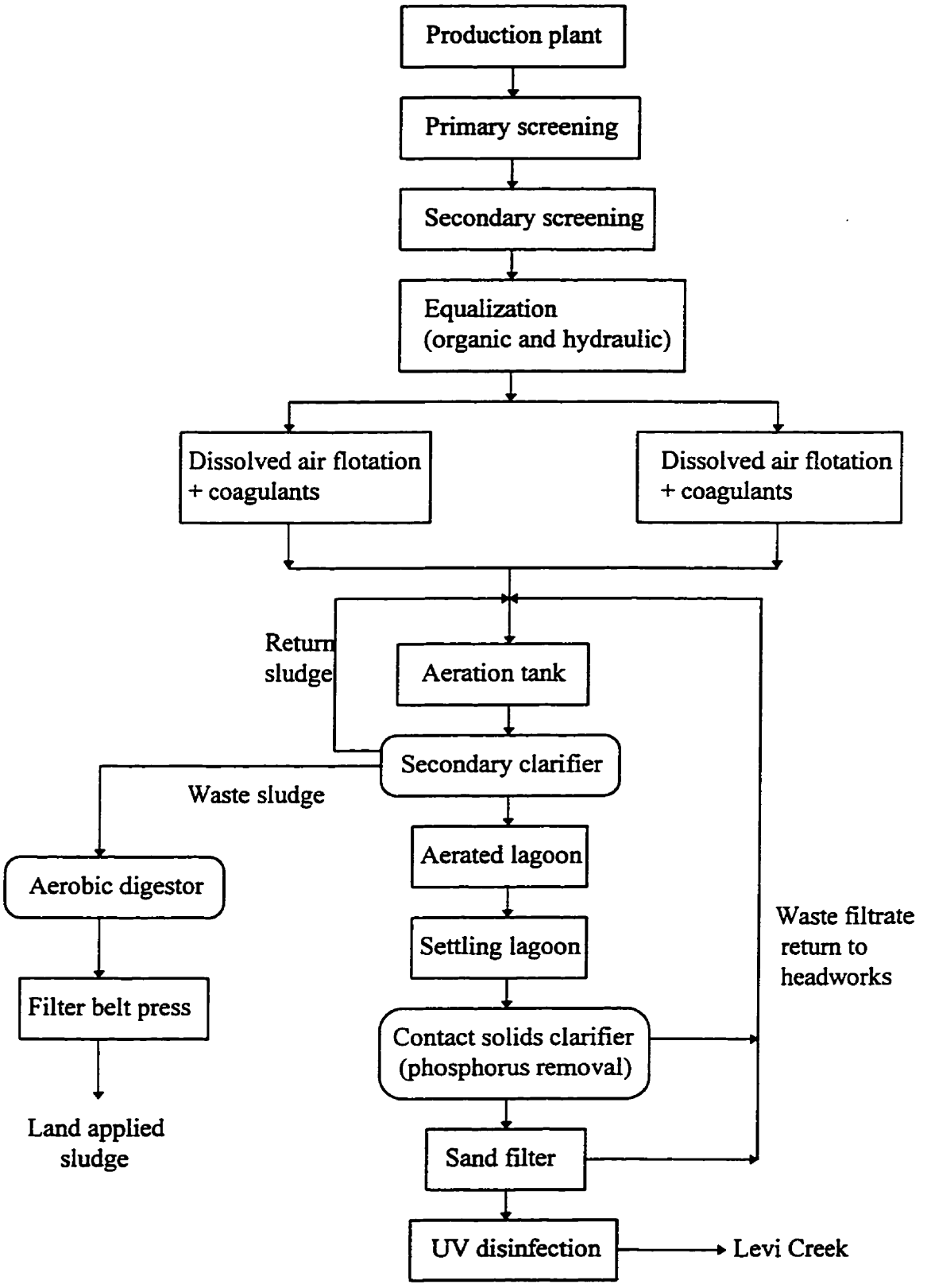

Figure A.2. Schematic flow diagram of poultry processing wastewater treatment plant (courtesy of Maple Lodge Farms Ltd.).

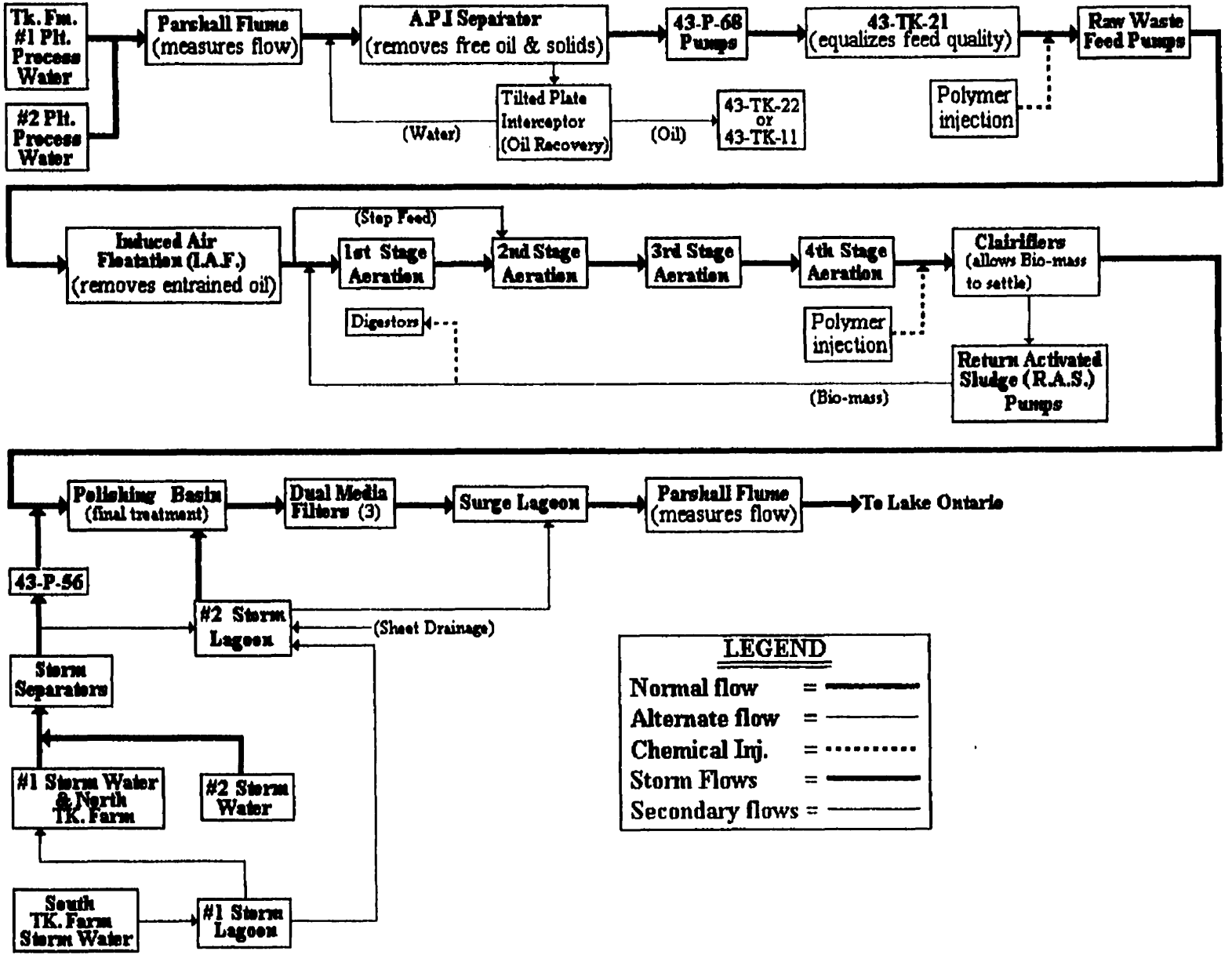

Figure A.3 Schematic flow diagram of petroleum refinery wastewater treatment plant (courtesy of Petro-Canada).

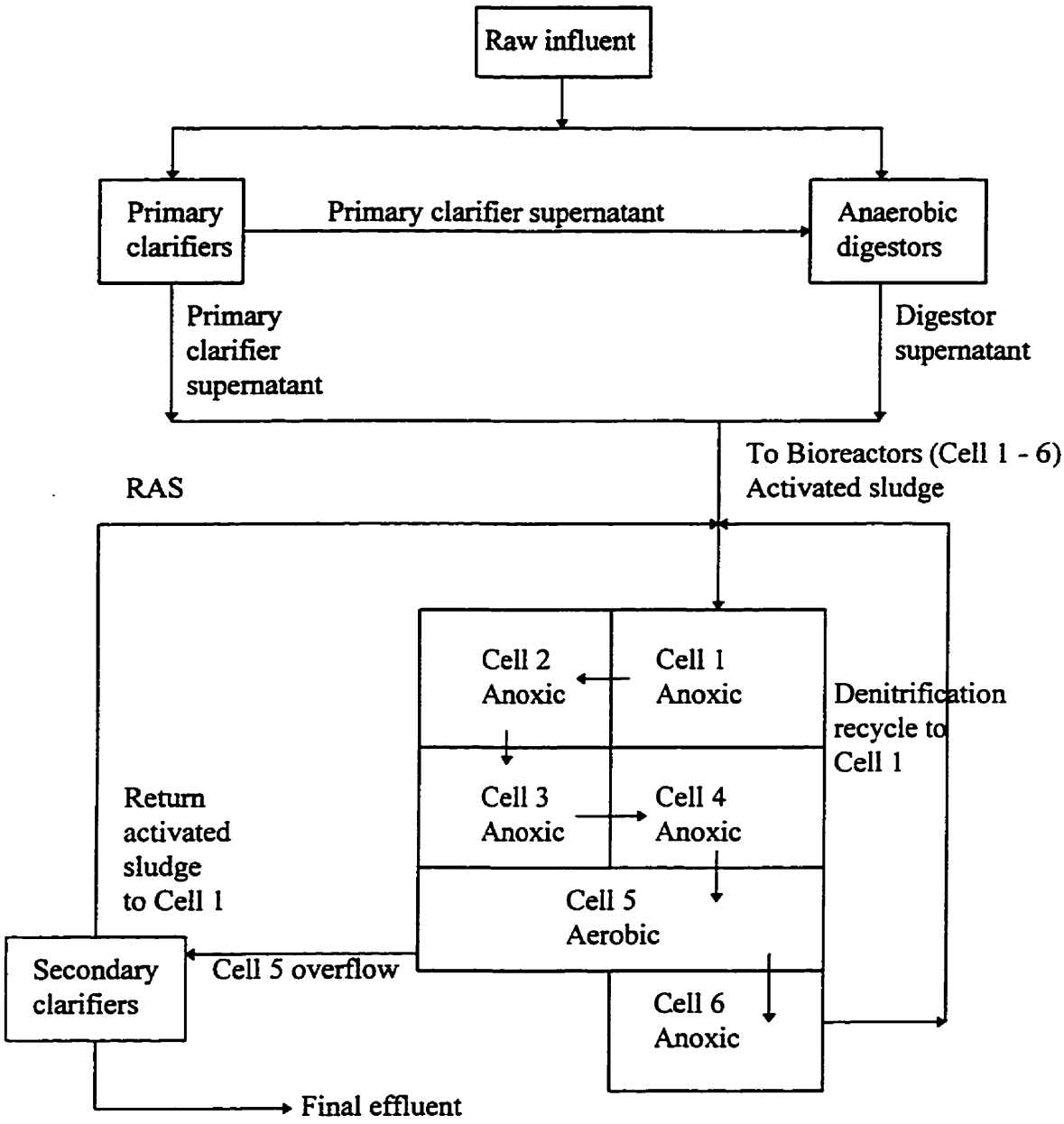

Figure A.4. Schematic flow diagram of potato processing wastewater treatment plant.

APPENDIX B

DATA OF CHEMICAL ANALYSIS OF SLUDGE

Table B.1. Chemical properties of activated sludge samples from municipal wastewater treatment plant.

Sampling date	SVI ml/g	30-min settling %	MLSS g/L	MLVSS g/L	VSS %	CHO in sludge mg/gVSS	Extractable CHO %	EPS composition mg/gVSS				
								CHO	Acidic Poly.	Protein	DNA	Total EPS
Nov. 6, 96	83	26	2.938	1.820	61	250.2	6.6	16.58	5.062	125.9	4.969	152.5
Nov. 20, 96	94	36	4.020	2.467	61	179.6	12.7	22.79	7.370	80.06	4.382	114.6
Feb. 12, 97	77	13	1.553	0.983	63	152.2	6.9	10.46	3.051	72.88	3.221	89.61
Feb. 19, 97	93	23	2.310	1.500	65	159.1	3.2	5.067	1.741	63.89	2.884	73.58
Mar. 24, 97	91	19	2.093	1.310	63	206.7	4.9	10.05	2.635	85.24	3.866	101.8
Apr. 7, 97	93	19	2.110	1.373	65	158.5	6.5	10.35	2.630	74.07	4.612	91.66
Apr. 11, 97	85	19	2.063	1.350	65	180.7	4.8	8.642	4.277	58.85	5.232	77.00
Apr. 14, 97	79	17	2.217	1.450	65	191.9	4.7	9.103	5.131	80.08	5.668	99.98
Apr. 16, 97	81	16	1.910	1.260	66	174.1	6.5	11.32	4.850	79.37	4.873	100.4
Apr. 23, 97	98	22	2.163	1.433	66	213.2	4.4	9.360	3.208	86.07	3.924	102.6
Apr. 28, 97	96	24	2.400	1.610	67	308.2	1.8	5.458	Nil	91.61	5.436	102.5
May 7, 97	95	16	1.770	1.187	67	155.1	5.2	8.105	3.949	56.63	2.005	70.69
May 12, 97	88	21	2.360	1.500	64	179.8	4.3	7.802	3.778	86.11	2.881	100.6
May 14, 97	90	19	1.960	1.330	68	165.4	3.9	6.405	3.208	81.45	3.222	94.29
May 16, 97	80	21	2.363	1.560	66	186.9	4.0	7.410	4.234	86.54	4.761	102.9
May 21, 97	83	18	2.150	1.383	64	277.7	3.8	10.68	3.443	65.88	3.007	83.01
May 23, 97	79	23	2.793	1.803	65	300.4	5.3	15.88	6.735	74.88	5.547	103.0

Shaded area indicates the samples collected from Aeration Tank #6.

Table B.2. Chemical properties of activated sludge samples from poultry processing wastewater treatment plant

Sampling date	SVI ml/g	30-min settling %	MLSS g/L	MLVSS g/L	VSS %	CHO in sludge mg/gVSS	Extractable CHO %	EPS composition mg/gVSS				
								CHO	Acidic Poly.	Protein	DNA	Total EPS
Dec. 9, 96	230	96	3.873	3.003	78	154.7	4.9	7.507	1.123	39.41	3.831	51.87
Jan. 13, 97	235	96	3.673	2.830	77	117.9	4.7	5.491	1.291	53.36	4.348	64.49
Jan. 28, 97	143	57	3.520	2.690	76	113.8	4.0	4.525	1.569	41.10	2.710	49.90
Feb. 11, 97	237	87	3.690	2.820	76	129.4	4.6	5.935	1.093	32.11	4.958	44.10
Feb. 25, 97	215	72	3.310	2.523	76	136.3	3.9	5.311	0.874	27.30	3.789	37.27
Apr. 1, 97	225	88	3.927	2.903	74	188.3	3.5	6.525	0.766	24.40	4.887	36.58
Apr. 15, 97	211	90	4.110	3.090	75	176.6	3.2	5.645	3.476	40.18	3.067	52.37
Apr. 22, 97	254	74	2.823	2.137	76	201.3	3.0	6.054	1.721	38.61	3.966	50.35

Shaded area indicates the samples collected during poor settling period.

Table B.3. Chemical properties of activated sludge samples from petroleum refinery wastewater treatment plant.

Sampling date	SVI ml/g	30-min settling %	MLSS g/L	MLVSS g/L	VSS %	CHO in sludge mg/gVSS	Extractable CHO %	EPS composition mg/gVSS				
								CHO	Acidic Poly.	Protein	DNA	Total EPS
Oct. 15, 96	230	76	3.087	2.693	87	102.1	6.3	6.482	4.002	77.98	1.260	89.72
Oct. 29, 96	259	71	2.660	2.300	87	255.5	4.6	11.66	1.152	50.73	1.180	64.72
Nov. 26, 96	307	86	2.800	2.337	83	172.1	4.9	8.443	2.445	59.48	1.611	71.98
Apr. 3, 97	215	97	4.520	3.677	81	Nil	Nil	9.176	1.299	47.37	4.408	62.25
Apr. 24, 97	176	95	5.813	4.653	80	182.5	4.1	7.403	2.199	51.22	2.277	63.10
May 1, 97	162	93	5.627	4.533	81	161.8	3.1	4.980	0.483	43.02	2.663	51.15
May 8, 97	166	94	5.727	4.753	83	189.4	2.9	5.451	2.192	28.50	1.836	37.98

Shaded area indicates the samples collected during poor settling period.

Table B.4. Chemical properties of activated sludge samples from potato processing wastewater treatment plant.

Sampling date	SVI ml/g	30-min settling %	MLSS g/L	MLVSS g/L	VSS %	CHO in sludge mg/gVSS	Extractable CHO %	EPS composition mg/gVSS				
								CHO	Acidic Poly.	Protein	DNA	Total EPS
Oct. 7, 96	267	66	2.853	2.393	84	139.4	3.8	5.295	2.832	50.84	0.736	59.70
Oct. 22, 96	264	90	3.220	2.590	80	409.8	2.3	9.336	1.931	39.58	0.696	51.54
Nov. 4, 96	175	99	2.860	2.230	78	220.3	4.8	10.52	3.180	88.19	0.710	102.6
Nov. 18, 96	278	100	3.640	2.893	80	441.2	4.0	17.60	5.656	83.82	5.480	112.6
Dec. 2, 96	319	98	3.680	3.000	82	282.3	5.5	15.64	3.382	50.78	3.239	73.04
Feb. 17, 97	201	47	2.370	1.950	82	122.7	4.7	5.812	1.937	51.71	1.006	60.47
Mar. 31, 97	125	29	2.223	1.827	82	Nil	Nil	14.23	3.722	29.19	3.131	50.27
Apr. 14, 97	220	56	2.357	1.937	82	171.7	4.3	7.364	4.111	47.75	3.549	62.77
Apr. 21, 97	178	47	2.410	2.000	83	166.3	5.8	9.722	3.477	57.08	4.808	75.09
Apr. 28, 97	125	29	2.337	1.917	82	176.3	4.6	8.022	4.673	56.95	3.589	73.23

Shaded area indicates the samples collected during poor settling period.

APPENDIX C

DATA OF FLOC SIZE DISTRIBUTION

Table C.1.1 - C.1.9	Samples from municipal wastewater treatment plant (system-Dm)
Table C.2.1 - C.2.10	Samples from poultry processing wastewater treatment plant (system-Py)
Table C.3.1 - C.3.8	Samples from petroleum refinery wastewater treatment plant (system-Pm)
Table C.4.1 - C.4.10	Samples from potato processing wastewater treatment plant (system-Po)

Table C.1.1. Summary of the medians ESD of sludge from system-Dm.

Sampling date	No. of particles	ESD (by no.) Range	ESD (by no.) Median	ESD (by volume) Median
6-Nov	1006	3.6 - 507.5	28	326.7
20-Nov	583	9.4 - 702.7	38.7	352.5
4-Dec	577	9.3 - 977.6	46.7	721.5
10-Dec	558	8.4 - 798.8	60.3	476.6
22-Jan	601	9.4 - 1184.7	59.6	843.4
29-Jan	662	9.4 - 718.1	73.1	415.0
4-Feb	726	10.2 - 670.0	85.4	318.2
12-Feb	737	9.4 - 647.5	77.7	315.7

Table C.1.2. Size distribution of sample from system-Dm on Nov. 6, 1996.

Size classes μm	Frequency	Frequency %	Cumulative frequency %	Spherical volume	Volume %	Cumulative volume %
< 8.3	219	21.77	21.77	22813.4315	0.00	0.00
8.3 - 9.6	18	1.79	23.56	6680.02549	0.00	0.00
9.6 - 11.1	31	3.08	26.64	17786.0433	0.00	0.01
11.1 - 12.9	31	3.08	29.72	28866.3981	0.00	0.01
12.9 - 15	25	2.49	32.21	33859.354	0.00	0.02
15 - 17.4	39	3.88	36.08	85308.3823	0.01	0.03
17.4 - 20.1	49	4.87	40.95	169248.503	0.02	0.05
20.1 - 23.3	41	4.08	45.03	218065.888	0.03	0.08
23.3 - 27	42	4.17	49.20	352424.025	0.05	0.13
27 - 31.3	44	4.37	53.58	580316.135	0.08	0.21
31.3 - 36.3	65	6.46	60.04	1296694.94	0.18	0.39
36.3 - 42.1	53	5.27	65.31	1744771.07	0.24	0.63
42.1 - 48.8	61	6.06	71.37	3022108.56	0.42	1.05
48.8 - 56.6	34	3.38	74.75	2606226.98	0.36	1.41
56.6 - 65.6	44	4.37	79.13	5087745.24	0.71	2.12
65.6 - 76	33	3.28	82.41	5860688.97	0.81	2.93
76 - 88.1	39	3.88	86.28	11197748.4	1.55	4.48
88.1 - 102.1	29	2.88	89.17	12785651.4	1.77	6.26
102.1 - 118.4	28	2.78	91.95	19395662.1	2.69	8.95
118.4 - 137.5	21	2.09	94.04	22713490.8	3.15	12.10
137.5 - 158.8	12	1.19	95.23	20499364.5	2.84	14.94
158.8 - 184.5	10	0.99	96.22	25777667.2	3.57	18.51
184.5 - 214.5	10	0.99	97.22	37087337.9	5.14	23.66
214.5 - 249.2	10	0.99	98.21	66760376.1	9.26	32.91
249.2 - 289.5	6	0.60	98.81	61308470.5	8.50	41.41
289.5 - 336.5	5	0.50	99.30	78248468.3	10.85	52.27
336.5 - 391	1	0.10	99.40	28297660.3	3.92	56.19
391 - 454.4	2	0.20	99.60	76356047.5	10.59	66.78
454.4 - 528	4	0.40	100.00	239577801	33.22	100.00
528 - 614	0	0.00	100.00	0	0.00	100.00
614 - 713.8	0	0.00	100.00	0	0.00	100.00
713.8 - 829.8	0	0.00	100.00	0	0.00	100.00
829.8 - 964.7	0	0.00	100.00	0	0.00	100.00
964.7 - 1121.5	0	0.00	100.00	0	0.00	100.00
1121.5 - 1303.8	0	0.00	100.00	0	0.00	100.00
1303.8 - 1515.7	0	0.00	100.00	0	0.00	100.00
Total	1006	100.00		721139350	100.00	
Median (μm)			[redacted]			[redacted]

Table C.1.3. Size distribution of sample from system-Dm on Nov. 20, 1996.

Size classes μm	Frequency	Frequency %	Cumulative frequency %	Spherical volume	Volume %	Cumulative volume %
< 8.3	0	0.00	0.00	0	0.00	0.00
8.3 - 9.6	1	0.17	0.17	432.078783	0.00	0.00
9.6 - 11.1	3	0.51	0.69	1851.70413	0.00	0.00
11.1 - 12.9	6	1.03	1.72	5753.74831	0.00	0.00
12.9 - 15	11	1.89	3.60	15347.6155	0.00	0.00
15 - 17.4	28	4.80	8.40	63257.3663	0.01	0.02
17.4 - 20.1	30	5.15	13.55	103650.601	0.02	0.04
20.1 - 23.3	44	7.55	21.10	239629.247	0.05	0.09
23.3 - 27	62	10.63	31.73	516017.997	0.11	0.20
27 - 31.3	48	8.23	39.97	615625.463	0.13	0.33
31.3 - 36.3	37	6.35	46.31	754209.527	0.16	0.49
36.3 - 42.1	44	7.55	53.86	1352352.16	0.29	0.78
42.1 - 48.8	33	5.66	59.52	1645872.54	0.35	1.13
48.8 - 56.6	53	9.09	68.61	4038662.68	0.86	1.99
56.6 - 65.6	36	6.17	74.79	4372316.82	0.93	2.92
65.6 - 76	28	4.80	79.59	5021510.37	1.07	3.99
76 - 88.1	28	4.80	84.39	8219521.69	1.75	5.74
88.1 - 102.1	18	3.09	87.48	8009936.3	1.71	7.45
102.1 - 118.4	12	2.06	89.54	8732822.36	1.86	9.31
118.4 - 137.5	21	3.60	93.14	22049974.9	4.70	14.00
137.5 - 158.8	8	1.37	94.51	13706180.2	2.92	16.92
158.8 - 184.5	13	2.23	96.74	34059441.8	7.25	24.18
184.5 - 214.5	7	1.20	97.94	30145653.2	6.42	30.60
214.5 - 249.2	5	0.86	98.80	31012867	6.60	37.20
249.2 - 289.5	1	0.17	98.97	11015144.8	2.35	39.55
289.5 - 336.5	3	0.51	99.49	42820617.8	9.12	48.67
336.5 - 391	1	0.17	99.66	21374917.3	4.55	53.22
391 - 454.4	1	0.17	99.83	37964283.6	8.09	61.30
454.4 - 528	0	0.00	99.83	0	0.00	61.30
528 - 614	0	0.00	99.83	0	0.00	61.30
614 - 713.8	1	0.17	100.00	181700241	38.70	100.00
713.8 - 829.8	0	0.00	100.00	0	0.00	100.00
829.8 - 964.7	0	0.00	100.00	0	0.00	100.00
964.7 - 1121.5	0	0.00	100.00	0	0.00	100.00
1121.5 - 1303.8	0	0.00	100.00	0	0.00	100.00
1303.8 - 1515.7	0	0.00	100.00	0	0.00	100.00
Total	583	100.00		469558092	100.00	
Median (μm)			[redacted]			[redacted]

Table C.1.4. Size distribution of sample from system-Dm on Dec. 4, 1996.

Size classes µm	Frequency	Frequency %	Cumulative frequency %	Spherical volume	Volume %	Cumulative volume %
< 8.3	0	0.00	0.00	0	0.00	0.00
8.3 - 9.6	2	0.35	0.35	854.59162	0.00	0.00
9.6 - 11.1	2	0.35	0.69	1415.63302	0.00	0.00
11.1 - 12.9	5	0.87	1.56	4658.1567	0.00	0.00
12.9 - 15	2	0.35	1.91	2602.8957	0.00	0.00
15 - 17.4	24	4.16	6.07	52178.126	0.00	0.00
17.4 - 20.1	17	2.95	9.01	59992.6309	0.00	0.00
20.1 - 23.3	29	5.03	14.04	154639.568	0.01	0.01
23.3 - 27	40	6.93	20.97	338975.556	0.01	0.02
27 - 31.3	45	7.80	28.77	589860.268	0.02	0.05
31.3 - 36.3	47	8.15	36.92	967438.162	0.04	0.09
36.3 - 42.1	42	7.28	44.19	1370473.72	0.05	0.14
42.1 - 48.8	41	7.11	51.30	2029490.24	0.08	0.22
48.8 - 56.6	43	7.45	58.75	3217793.76	0.13	0.35
56.6 - 65.6	35	6.07	64.82	4159723.67	0.17	0.52
65.6 - 76	40	6.93	71.75	7480469.11	0.30	0.81
76 - 88.1	33	5.72	77.47	9336197.35	0.37	1.19
88.1 - 102.1	22	3.81	81.28	9903360.18	0.39	1.58
102.1 - 118.4	15	2.60	83.88	10268208.2	0.41	1.99
118.4 - 137.5	19	3.29	87.18	20779865.5	0.83	2.82
137.5 - 158.8	18	3.12	90.29	28833257.7	1.15	3.97
158.8 - 184.5	9	1.56	91.85	22725818.6	0.91	4.88
184.5 - 214.5	11	1.91	93.76	48386999.6	1.93	6.80
214.5 - 249.2	8	1.39	95.15	54415761.5	2.17	8.97
249.2 - 289.5	5	0.87	96.01	53789548.9	2.14	11.12
289.5 - 336.5	2	0.35	96.36	37406761.5	1.49	12.61
336.5 - 391	6	1.04	97.40	139637998	5.57	18.18
391 - 454.4	3	0.52	97.92	118837011	4.74	22.91
454.4 - 528	4	0.69	98.61	273702207	10.91	33.83
528 - 614	4	0.69	99.31	374578481	14.93	48.76
614 - 713.8	0	0.00	99.31	0	0.00	48.76
713.8 - 829.8	2	0.35	99.65	470444413	18.76	67.52
829.8 - 964.7	1	0.17	99.83	325515322	12.98	80.50
964.7 - 1121.5	1	0.17	100.00	489207110	19.50	100.00
1121.5 - 1303.8	0	0.00	100.00	0	0.00	100.00
1303.8 - 1515.7	0	0.00	100.00	0	0.00	100.00
Total	577	100.00		2508198888	100.00	
Median (µm)			[redacted]			[redacted]

Table C.1.5. Size distribution of sample from system-Dm on Dec. 10, 1996.

Size classes μm	Frequency	Frequency %	Cumulative frequency %	Spherical volume	Volume %	Cumulative volume %
< 8.3	0	0.00	0.00	0	0.00	0.00
8.3 - 9.6	1	0.18	0.18	309.170409	0.00	0.00
9.6 - 11.1	3	0.54	0.72	2147.21854	0.00	0.00
11.1 - 12.9	1	0.18	0.90	1043.45013	0.00	0.00
12.9 - 15	12	2.15	3.05	17722.8985	0.00	0.00
15 - 17.4	13	2.33	5.38	28386.6514	0.00	0.00
17.4 - 20.1	17	3.05	8.42	55021.2955	0.00	0.00
20.1 - 23.3	27	4.84	13.26	139012.946	0.01	0.01
23.3 - 27	28	5.02	18.28	238972.113	0.01	0.02
27 - 31.3	26	4.66	22.94	334527.279	0.02	0.04
31.3 - 36.3	36	6.45	29.39	731463.258	0.03	0.07
36.3 - 42.1	28	5.02	34.41	880223.949	0.04	0.11
42.1 - 48.8	28	5.02	39.43	1419676.4	0.07	0.18
48.8 - 56.6	36	6.45	45.88	2813580.67	0.13	0.31
56.6 - 65.6	45	8.06	53.94	5212732.38	0.24	0.55
65.6 - 76	33	5.91	59.86	6001764.06	0.28	0.83
76 - 88.1	27	4.84	64.70	7313888.59	0.34	1.17
88.1 - 102.1	24	4.30	69.00	11064898.7	0.51	1.68
102.1 - 118.4	18	3.23	72.22	12387040.1	0.57	2.26
118.4 - 137.5	27	4.84	77.06	27839147.8	1.29	3.55
137.5 - 158.8	22	3.94	81.00	38372140.3	1.78	5.33
158.8 - 184.5	26	4.66	85.66	68646580.3	3.18	8.51
184.5 - 214.5	19	3.41	89.07	78308525.3	3.63	12.14
214.5 - 249.2	20	3.58	92.65	126339508	5.86	18.00
249.2 - 289.5	12	2.15	94.80	122666948	5.69	23.69
289.5 - 336.5	5	0.90	95.70	81287211.7	3.77	27.46
336.5 - 391	11	1.97	97.67	264177943	12.25	39.71
391 - 454.4	5	0.90	98.57	205734028	9.54	49.25
454.4 - 528	1	0.18	98.75	53395306.9	2.48	51.73
528 - 614	3	0.54	99.28	244799606	11.35	63.08
614 - 713.8	2	0.36	99.64	321932083	14.93	78.01
713.8 - 829.8	2	0.36	100.00	474104833	21.99	100.00
829.8 - 964.7	0	0.00	100.00	0	0.00	100.00
964.7 - 1121.5	0	0.00	100.00	0	0.00	100.00
1121.5 - 1303.8	0	0.00	100.00	0	0.00	100.00
1303.8 - 1515.7	0	0.00	100.00	0	0.00	100.00
Total	558	100.00		2156246273	100.00	
Median (μm)			[redacted]			[redacted]

Table C.1.6. Size distribution of sample from system-Dm on Jan. 22, 1997.

Size classes µm	Frequency	Frequency %	Cumulative frequency %	Spherical volume	Volume %	Cumulative volume %
< 8.3	0	0.00	0.00	0	0.00	0.00
8.3 - 9.6	1	0.17	0.17	432.078783	0.00	0.00
9.6 - 11.1	4	0.67	0.83	2567.44365	0.00	0.00
11.1 - 12.9	7	1.16	2.00	6797.19844	0.00	0.00
12.9 - 15	3	0.50	2.50	4819.48972	0.00	0.00
15 - 17.4	15	2.50	4.99	35135.9098	0.00	0.00
17.4 - 20.1	19	3.16	8.15	65018.6084	0.00	0.00
20.1 - 23.3	16	2.66	10.82	87588.7303	0.00	0.00
23.3 - 27	35	5.82	16.64	286543.807	0.01	0.01
27 - 31.3	30	4.99	21.63	380809.507	0.01	0.02
31.3 - 36.3	30	4.99	26.62	627721.129	0.01	0.04
36.3 - 42.1	45	7.49	34.11	1458784.18	0.03	0.07
42.1 - 48.8	39	6.49	40.60	1918719.84	0.05	0.12
48.8 - 56.6	47	7.82	48.42	3548293.72	0.08	0.20
56.6 - 65.6	34	5.66	54.08	4136627.87	0.10	0.30
65.6 - 76	34	5.66	59.73	6126387.9	0.15	0.44
76 - 88.1	33	5.49	65.22	9533718.63	0.23	0.67
88.1 - 102.1	36	5.99	71.21	16802466.3	0.40	1.07
102.1 - 118.4	20	3.33	74.54	14306439.3	0.34	1.41
118.4 - 137.5	24	3.99	78.54	27257146	0.65	2.06
137.5 - 158.8	17	2.83	81.36	31288966.7	0.74	2.80
158.8 - 184.5	20	3.33	84.69	53127807.2	1.26	4.07
184.5 - 214.5	23	3.83	88.52	97310018.7	2.31	6.38
214.5 - 249.2	23	3.83	92.35	158134565	3.76	10.14
249.2 - 289.5	15	2.50	94.84	155732018	3.70	13.84
289.5 - 336.5	11	1.83	96.67	177903833	4.23	18.07
336.5 - 391	5	0.83	97.50	115732567	2.75	20.82
391 - 454.4	2	0.33	97.84	81845378.8	1.95	22.77
454.4 - 528	3	0.50	98.34	173990051	4.14	26.90
528 - 614	2	0.33	98.67	210420066	5.00	31.90
614 - 713.8	2	0.33	99.00	287524272	6.84	38.74
713.8 - 829.8	2	0.33	99.33	394376684	9.38	48.11
829.8 - 964.7	2	0.33	99.67	786452030	18.70	66.81
964.7 - 1121.5	1	0.17	99.83	525657705	12.50	79.31
1121.5 - 1303.8	1	0.17	100.00	870533828	20.69	100.00
1303.8 - 1515.7	0	0.00	100.00	0	0.00	100.00
Total	601	100.00		4206615808	100.00	
Median (µm)			[redacted]			[redacted]

Table C.1.7. Size distribution of sample from system-Dm on Jan. 29, 1997.

Size classes µm	Frequency	Frequency %	Cumulative frequency %	Spherical volume	Volume %	Cumulative volume %
< 8.3	0	0.00	0.00	0	0.00	0.00
8.3 - 9.6	4	0.60	0.60	1728.31513	0.00	0.00
9.6 - 11.1	2	0.30	0.91	1135.96462	0.00	0.00
11.1 - 12.9	3	0.45	1.36	2623.39792	0.00	0.00
12.9 - 15	5	0.76	2.11	7254.95267	0.00	0.00
15 - 17.4	13	1.96	4.08	29718.2552	0.00	0.00
17.4 - 20.1	11	1.66	5.74	40180.3504	0.00	0.00
20.1 - 23.3	21	3.17	8.91	116587.625	0.00	0.01
23.3 - 27	34	5.14	14.05	277825.889	0.01	0.02
27 - 31.3	34	5.14	19.18	442470.891	0.02	0.04
31.3 - 36.3	31	4.68	23.87	622813.594	0.03	0.06
36.3 - 42.1	29	4.38	28.25	932123.645	0.04	0.10
42.1 - 48.8	38	5.74	33.99	1878996.15	0.08	0.18
48.8 - 56.6	33	4.98	38.97	2515995.79	0.10	0.29
56.6 - 65.6	42	6.34	45.32	4933113.26	0.21	0.49
65.6 - 76	46	6.95	52.27	8769731.56	0.37	0.86
76 - 88.1	38	5.74	58.01	11113064.7	0.46	1.32
88.1 - 102.1	48	7.25	65.26	21865524	0.91	2.23
102.1 - 118.4	32	4.83	70.09	22700264.4	0.95	3.18
118.4 - 137.5	33	4.98	75.08	37038924.4	1.54	4.72
137.5 - 158.8	34	5.14	80.21	58189703.8	2.42	7.14
158.8 - 184.5	39	5.89	86.10	104117736	4.34	11.48
184.5 - 214.5	17	2.57	88.67	66706245.8	2.78	14.26
214.5 - 249.2	20	3.02	91.69	132039665	5.50	19.76
249.2 - 289.5	12	1.81	93.50	133037490	5.54	25.31
289.5 - 336.5	10	1.51	95.02	145175179	6.05	31.36
336.5 - 391	14	2.11	97.13	325743398	13.57	44.93
391 - 454.4	8	1.21	98.34	322092797	13.42	58.35
454.4 - 528	5	0.76	99.09	326685167	13.61	71.96
528 - 614	5	0.76	99.85	479036706	19.96	91.92
614 - 713.8	0	0.00	99.85	0	0.00	91.92
713.8 - 829.8	1	0.15	100.00	193904197	8.08	100.00
829.8 - 964.7	0	0.00	100.00	0	0.00	100.00
964.7 - 1121.5	0	0.00	100.00	0	0.00	100.00
1121.5 - 1303.8	0	0.00	100.00	0	0.00	100.00
1303.8 - 1515.7	0	0.00	100.00	0	0.00	100.00
Total	662	100.00		2400018363	100.00	
Median (µm)			[redacted]			[redacted]

Table C.1.8. Size distribution of sample from system-Dm on Feb. 4, 1997.

Size classes µm	Frequency	Frequency %	Cumulative frequency %	Spherical volume	Volume %	Cumulative volume %
< 8.3	0	0.00	0.00	0	0.00	0.00
8.3 - 9.6	0	0.00	0.00	0	0.00	0.00
9.6 - 11.1	1	0.14	0.14	561.694929	0.00	0.00
11.1 - 12.9	4	0.55	0.69	3793.37078	0.00	0.00
12.9 - 15	5	0.69	1.38	6980.25014	0.00	0.00
15 - 17.4	14	1.93	3.31	29449.9601	0.00	0.00
17.4 - 20.1	15	2.07	5.37	52649.9174	0.00	0.00
20.1 - 23.3	18	2.48	7.85	104299.989	0.00	0.01
23.3 - 27	18	2.48	10.33	157619.185	0.01	0.01
27 - 31.3	23	3.17	13.50	306801.832	0.01	0.03
31.3 - 36.3	42	5.79	19.28	852151.062	0.04	0.06
36.3 - 42.1	39	5.37	24.66	1261788.56	0.05	0.12
42.1 - 48.8	29	3.99	28.65	1388261.28	0.06	0.17
48.8 - 56.6	40	5.51	34.16	3071499.49	0.13	0.30
56.6 - 65.6	40	5.51	39.67	4849388.17	0.20	0.50
65.6 - 76	37	5.10	44.77	7071054.82	0.29	0.80
76 - 88.1	48	6.61	51.38	13588128.4	0.57	1.36
88.1 - 102.1	39	5.37	56.75	17415363.4	0.73	2.09
102.1 - 118.4	42	5.79	62.53	30261929.1	1.26	3.35
118.4 - 137.5	45	6.20	68.73	49859017	2.08	5.43
137.5 - 158.8	37	5.10	73.83	65325712.8	2.72	8.15
158.8 - 184.5	45	6.20	80.03	118997203	4.96	13.11
184.5 - 214.5	35	4.82	84.85	146069110	6.09	19.19
214.5 - 249.2	35	4.82	89.67	222671875	9.28	28.47
249.2 - 289.5	26	3.58	93.25	255492809	10.65	39.12
289.5 - 336.5	27	3.72	96.97	427395608	17.81	56.93
336.5 - 391	11	1.52	98.48	279716061	11.65	68.58
391 - 454.4	5	0.69	99.17	213157280	8.88	77.46
454.4 - 528	3	0.41	99.59	169256769	7.05	84.52
528 - 614	1	0.14	99.72	92773167.5	3.87	88.38
614 - 713.8	2	0.28	100.00	278856918	11.62	100.00
713.8 - 829.8	0	0.00	100.00	0	0.00	100.00
829.8 - 964.7	0	0.00	100.00	0	0.00	100.00
964.7 - 1121.5	0	0.00	100.00	0	0.00	100.00
1121.5 - 1303.8	0	0.00	100.00	0	0.00	100.00
1303.8 - 1515.7	0	0.00	100.00	0	0.00	100.00
Total	726	100.00		2399993250	100.00	
Median (µm)			[redacted]			[redacted]

Table C.1.9. Size distribution of sample from system-Dm on Feb. 12, 1997.

Size classes μm	Frequency	Frequency %	Cumulative frequency %	Spherical volume	Volume %	Cumulative volume %
< 8.3	0	0.00	0.00	0	0.00	0.00
8.3 - 9.6	2	0.27	0.27	864.157565	0.00	0.00
9.6 - 11.1	4	0.54	0.81	2567.44365	0.00	0.00
11.1 - 12.9	5	0.68	1.49	4710.29818	0.00	0.00
12.9 - 15	7	0.95	2.44	9699.15936	0.00	0.00
15 - 17.4	11	1.49	3.93	23881.6231	0.00	0.00
17.4 - 20.1	20	2.71	6.65	68251.3579	0.00	0.01
20.1 - 23.3	30	4.07	10.72	159160.543	0.01	0.01
23.3 - 27	24	3.26	13.98	201026.425	0.01	0.02
27 - 31.3	39	5.29	19.27	506809.744	0.03	0.05
31.3 - 36.3	25	3.39	22.66	490502.02	0.02	0.07
36.3 - 42.1	44	5.97	28.63	1358445.35	0.07	0.14
42.1 - 48.8	33	4.48	33.11	1640459.7	0.08	0.22
48.8 - 56.6	51	6.92	40.03	4021168.41	0.20	0.42
56.6 - 65.6	32	4.34	44.37	3875719.4	0.19	0.62
65.6 - 76	37	5.02	49.39	6825087.07	0.34	0.96
76 - 88.1	37	5.02	54.41	10733862.8	0.54	1.50
88.1 - 102.1	47	6.38	60.79	21560503.9	1.08	2.57
102.1 - 118.4	45	6.11	66.89	31568660.9	1.58	4.15
118.4 - 137.5	39	5.29	72.18	42744990.3	2.14	6.29
137.5 - 158.8	39	5.29	77.48	65482869	3.27	9.56
158.8 - 184.5	36	4.88	82.36	94032897.6	4.70	14.26
184.5 - 214.5	38	5.16	87.52	157237404	7.86	22.11
214.5 - 249.2	30	4.07	91.59	197249235	9.86	31.97
249.2 - 289.5	23	3.12	94.71	220656364	11.02	42.99
289.5 - 336.5	16	2.17	96.88	251729688	12.58	55.57
336.5 - 391	11	1.49	98.37	275074166	13.74	69.31
391 - 454.4	7	0.95	99.32	250895229	12.54	81.85
454.4 - 528	4	0.54	99.86	221184447	11.05	92.90
528 - 614	0	0.00	99.86	0	0.00	92.90
614 - 713.8	1	0.14	100.00	142120687	7.10	100.00
713.8 - 829.8	0	0.00	100.00	0	0.00	100.00
829.8 - 964.7	0	0.00	100.00	0	0.00	100.00
964.7 - 1121.5	0	0.00	100.00	0	0.00	100.00
1121.5 - 1303.8	0	0.00	100.00	0	0.00	100.00
1303.8 - 1515.7	0	0.00	100.00	0	0.00	100.00
Total	737	100.00		2001459358	100.00	
Median (μm)			[redacted]			[redacted]

Table C.2.1. Summary of the medians ESD of sludge from system-Py.

Sampling date	No. of particles	ESD (by no.) Range	ESD (by no.) Median	ESD (by volume) Median
9-Dec	461	8.4 - 760.2	37.1	560.3
13-Jan	544	8.4 - 692.8	44.8	365.1
28-Jan	538	9.4 - 964.8	54.9	435.1
11-Feb	598	8.4 - 872.4	61.7	405.5
25-Feb	720	9.3 - 540.5	60.8	258.5
1-Apr	1022	4.3 - 263.1	22.4	102.3
8-Apr	1040	4.3 - 248.1	21.3	124.9
15-Apr	1095	8.4 - 359.7	52.7	188.7
22-Apr	1287	9.3 - 511.1	45.6	254.1

Table C.2.2. Size distribution of sample from system-Py on Dec. 9, 1996.

Size classes µm	Frequency	Frequency %	Cumulative frequency %	Spherical volume	Volume %	Cumulative volume %
< 8.3	0	0	0	0	0.00	0.00
8.3 - 9.6	4	0.87	0.87	1587.6	0.00	0.00
9.6 - 11.1	8	1.74	2.60	5224.2	0.00	0.00
11.1 - 12.9	15	3.25	5.86	14810.0	0.00	0.00
12.9 - 15	22	4.77	10.63	30541.2	0.00	0.01
15 - 17.4	20	4.34	14.97	44298.7	0.00	0.01
17.4 - 20.1	26	5.64	20.61	94024.4	0.01	0.02
20.1 - 23.3	24	5.21	25.81	127157.4	0.01	0.03
23.3 - 27	32	6.94	32.75	272782.3	0.03	0.06
27 - 31.3	40	8.68	41.43	526583.8	0.05	0.11
31.3 - 36.3	35	7.59	49.02	713484.9	0.07	0.19
36.3 - 42.1	34	7.38	56.40	1086821.2	0.11	0.30
42.1 - 48.8	33	7.16	63.56	1647553.0	0.17	0.46
48.8 - 56.6	25	5.42	68.98	1931058.5	0.20	0.66
56.6 - 65.6	24	5.21	74.19	2836472.7	0.29	0.95
65.6 - 76	22	4.77	78.96	4117324.9	0.42	1.36
76 - 88.1	19	4.12	83.08	5538135.2	0.56	1.93
88.1 - 102.1	12	2.60	85.68	5416757.4	0.55	2.47
102.1 - 118.4	17	3.69	89.37	11687843.0	1.19	3.66
118.4 - 137.5	9	1.95	91.32	9020995.4	0.91	4.57
137.5 - 158.8	5	1.08	92.41	7662742.1	0.78	5.35
158.8 - 184.5	3	0.65	93.06	8496046.5	0.86	6.21
184.5 - 214.5	8	1.74	94.79	32749226.6	3.32	9.53
214.5 - 249.2	9	1.95	96.75	58802034.8	5.96	15.50
249.2 - 289.5	4	0.87	97.61	39812276.2	4.04	19.53
289.5 - 336.5	1	0.22	97.83	17545209.3	1.78	21.31
336.5 - 391	2	0.43	98.26	47944356.3	4.86	26.18
391 - 454.4	3	0.65	98.92	103057495.7	10.45	36.63
454.4 - 528	1	0.22	99.13	61910132.3	6.28	42.90
528 - 614	2	0.43	99.57	186146576.0	18.88	61.78
614 - 713.8	1	0.22	99.78	146858678.5	14.89	76.67
713.8 - 829.8	1	0.22	100.00	230037739.4	23.33	100.00
829.8 - 964.7	0	0.00	100	0	0.00	100.00
Total	461	100		986135969.4	100.00	
Median (µm)			[illegible]			560.3

Table C.2.3. Size distribution of sample from system-Py on Jan. 13, 1997.

Size classes µm	Frequency	Frequency %	Cumulative frequency %	Spherical volume	Volume %	Cumulative volume %
< 8.3	0	0.00	0	0	0.00	0.00
8.3 - 9.6	10	1.84	1.84	3952.06271	0.00	0.00
9.6 - 11.1	7	1.29	3.13	4566.90499	0.00	0.00
11.1 - 12.9	8	1.47	4.60	7840.64858	0.00	0.00
12.9 - 15	15	2.76	7.35	20244.7726	0.00	0.00
15 - 17.4	28	5.15	12.50	64662.6645	0.00	0.01
17.4 - 20.1	21	3.86	16.36	70409.2954	0.01	0.01
20.1 - 23.3	25	4.60	20.96	130544.057	0.01	0.02
23.3 - 27	39	7.17	28.13	306614.545	0.02	0.05
27 - 31.3	36	6.62	34.74	479653.855	0.04	0.08
31.3 - 36.3	38	6.99	41.73	789475.511	0.06	0.14
36.3 - 42.1	31	5.70	47.43	951883.894	0.07	0.21
42.1 - 48.8	32	5.88	53.31	1581662.21	0.12	0.33
48.8 - 56.6	29	5.33	58.64	2276159.73	0.17	0.51
56.6 - 65.6	29	5.33	63.97	3544634.62	0.27	0.77
65.6 - 76	20	3.68	67.65	3782680.71	0.29	1.06
76 - 88.1	13	2.39	70.04	3852417.88	0.29	1.35
88.1 - 102.1	16	2.94	72.98	7238186.47	0.55	1.90
102.1 - 118.4	19	3.49	76.47	13088444.9	0.99	2.89
118.4 - 137.5	19	3.49	79.96	20849232	1.58	4.46
137.5 - 158.8	25	4.60	84.56	42953356.5	3.25	7.71
158.8 - 184.5	23	4.23	88.79	60793176.4	4.60	12.31
184.5 - 214.5	15	2.76	91.54	63777033.8	4.82	17.13
214.5 - 249.2	7	1.29	92.83	43637983.4	3.30	20.43
249.2 - 289.5	13	2.39	95.22	126436576	9.56	29.98
289.5 - 336.5	12	2.21	97.43	189657358	14.34	44.32
336.5 - 391	6	1.10	98.53	142955621	10.81	55.13
391 - 454.4	3	0.55	99.08	117425486	8.88	64.00
454.4 - 528	2	0.37	99.45	102071165	7.72	71.72
528 - 614	2	0.37	99.82	200003515	15.12	86.84
614 - 713.8	1	0.18	100.00	174120780	13.16	100.00
713.8 - 829.8	0	0.00	100.00	0	0.00	100.00
829.8 - 964.7	0	0.00	100	0	0.00	100.00
Total	544	100		1322875318	100.00	
Median (µm)			[illegible]			[illegible]

Table C.2.4. Size distribution of sample from system-Py on Jan. 28, 1997.

Size classes µm	Frequency	Frequency %	Cumulative frequency %	Spherical volume	Volume %	Cumulative volume %
< 8.3	0	0.00	0	0	0.00	0.00
8.3 - 9.6	1	0.19	0.19	432.0787826	0.00	0.00
9.6 - 11.1	4	0.74	0.93	2567.443648	0.00	0.00
11.1 - 12.9	3	0.56	1.49	2792.382076	0.00	0.00
12.9 - 15	11	2.04	3.53	15356.3592	0.00	0.00
15 - 17.4	20	3.72	7.25	45774.62768	0.00	0.00
17.4 - 20.1	17	3.16	10.41	57337.41043	0.00	0.01
20.1 - 23.3	33	6.13	16.54	176974.9951	0.01	0.02
23.3 - 27	42	7.81	24.35	346232.3899	0.02	0.04
27 - 31.3	33	6.13	30.48	418484.6085	0.03	0.07
31.3 - 36.3	31	5.76	36.25	619539.718	0.04	0.11
36.3 - 42.1	29	5.39	41.64	935445.8959	0.06	0.17
42.1 - 48.8	23	4.28	45.91	1124175.452	0.07	0.24
48.8 - 56.6	25	4.65	50.56	1861373.279	0.12	0.35
56.6 - 65.6	30	5.58	56.13	3519091.871	0.22	0.58
65.6 - 76	24	4.46	60.59	4477070.133	0.28	0.86
76 - 88.1	22	4.09	64.68	6395679.023	0.40	1.27
88.1 - 102.1	15	2.79	67.47	7115652.157	0.45	1.72
102.1 - 118.4	30	5.58	73.05	20958822.67	1.33	3.04
118.4 - 137.5	27	5.02	78.07	29651203.72	1.88	4.92
137.5 - 158.8	31	5.76	83.83	52558123.08	3.32	8.24
158.8 - 184.5	17	3.16	86.99	47448936.68	3.00	11.24
184.5 - 214.5	27	5.02	92.01	107429723.5	6.80	18.04
214.5 - 249.2	14	2.60	94.61	85761012.53	5.42	23.46
249.2 - 289.5	9	1.67	96.28	85610993.35	5.42	28.88
289.5 - 336.5	6	1.12	97.40	97911518.28	6.19	35.07
336.5 - 391	7	1.30	98.70	181406224.2	11.47	46.55
391 - 454.4	2	0.37	99.07	78493516	4.97	51.51
454.4 - 528	2	0.37	99.44	122500832.5	7.75	59.26
528 - 614	2	0.37	99.81	173846503	11.00	70.26
614 - 713.8	0	0.00	99.81	0	0.00	70.26
713.8 - 829.8	0	0.00	99.81	0	0.00	70.26
829.8 - 964.7	0	0.00	99.81	0	0.00	70.26
964.7 - 1121.5	1	0.19	100	470196213.6	29.74	100.00
Total	538	100		1580887603	100	
Median (µm)			[redacted]			[redacted]

Table C.2.5. Size distribution of sample from system-Py on Feb. 11, 1997.

Size classes μm	Frequency	Frequency %	Cumulative frequency %	Spherical volume	Volume %	Cumulative volume %
< 8.3	0	0.00	0	0	0.00	0.00
8.3 - 9.6	3	0.50	0.50	1173.32797	0.00	0.00
9.6 - 11.1	9	1.51	2.01	6146.14122	0.00	0.00
11.1 - 12.9	6	1.00	3.01	5753.74831	0.00	0.00
12.9 - 15	8	1.34	4.35	10912.519	0.00	0.00
15 - 17.4	13	2.17	6.52	28431.617	0.00	0.00
17.4 - 20.1	13	2.17	8.70	45538.7705	0.00	0.01
20.1 - 23.3	35	5.85	14.55	178427.448	0.01	0.02
23.3 - 27	36	6.02	20.57	290109.351	0.02	0.03
27 - 31.3	32	5.35	25.92	425892.039	0.02	0.06
31.3 - 36.3	32	5.35	31.27	629611.747	0.04	0.09
36.3 - 42.1	33	5.52	36.79	1039900.99	0.06	0.15
42.1 - 48.8	31	5.18	41.97	1480140.31	0.08	0.24
48.8 - 56.6	30	5.02	46.99	2279366.34	0.13	0.37
56.6 - 65.6	29	4.85	51.84	3426227.01	0.20	0.56
65.6 - 76	26	4.35	56.19	4652389.99	0.27	0.83
76 - 88.1	33	5.52	61.71	9348443.83	0.54	1.37
88.1 - 102.1	28	4.68	66.39	12600144.9	0.72	2.09
102.1 - 118.4	32	5.35	71.74	22963571	1.31	3.40
118.4 - 137.5	25	4.18	75.92	27206814.5	1.56	4.96
137.5 - 158.8	31	5.18	81.10	51989300.6	2.98	7.94
158.8 - 184.5	26	4.35	85.45	67800506.1	3.88	11.82
184.5 - 214.5	32	5.35	90.80	130934234	7.50	19.31
214.5 - 249.2	16	2.68	93.48	98338696	5.63	24.94
249.2 - 289.5	18	3.01	96.49	178403639	10.21	35.16
289.5 - 336.5	8	1.34	97.83	125435304	7.18	42.34
336.5 - 391	4	0.67	98.49	102656113	5.88	48.22
391 - 454.4	4	0.67	99.16	135782759	7.77	55.99
454.4 - 528	1	0.17	99.33	54295270.6	3.11	59.10
528 - 614	2	0.33	99.67	204938726	11.73	70.83
614 - 713.8	1	0.17	99.83	161776781	9.26	80.09
713.8 - 829.8	0	0.00	99.83	0	0.00	80.09
829.8 - 964.7	1	0.17	100	347702320	19.91	100.00
Total	598	100		1746672643	100.00	
Median (μm)			64.7			405.5

Table C.2.6. Size distribution of sample from system-Py on Feb. 25, 1997.

Size classes μm	Frequency	Frequency %	Cumulative frequency %	Spherical volume	Volume %	Cumulative volume %
< 8.3	0	0.00	0	0	0.00	0.00
8.3 - 9.6	5	0.69	0.69	2136.47405	0.00	0.00
9.6 - 11.1	4	0.56	1.25	2392.8957	0.00	0.00
11.1 - 12.9	4	0.56	1.81	3793.36191	0.00	0.00
12.9 - 15	14	1.94	3.75	19563.678	0.00	0.00
15 - 17.4	15	2.08	5.83	33393.7159	0.00	0.01
17.4 - 20.1	23	3.19	9.03	81160.8282	0.01	0.02
20.1 - 23.3	28	3.89	12.92	157138.757	0.02	0.04
23.3 - 27	32	4.44	17.36	268533.123	0.03	0.07
27 - 31.3	39	5.42	22.78	506371.937	0.06	0.13
31.3 - 36.3	44	6.11	28.89	868513.952	0.11	0.24
36.3 - 42.1	46	6.39	35.28	1386264.48	0.17	0.42
42.1 - 48.8	37	5.14	40.42	1772971.19	0.22	0.64
48.8 - 56.6	40	5.56	45.97	3000088.38	0.37	1.01
56.6 - 65.6	53	7.36	53.33	6302802.72	0.79	1.80
65.6 - 76	52	7.22	60.56	9688513.95	1.21	3.01
76 - 88.1	49	6.81	67.36	14002603.9	1.75	4.75
88.1 - 102.1	43	5.97	73.33	19258489.4	2.40	7.15
102.1 - 118.4	49	6.81	80.14	35211385.7	4.39	11.55
118.4 - 137.5	45	6.25	86.39	48768162.9	6.08	17.63
137.5 - 158.8	25	3.47	89.86	42523576.4	5.30	22.94
158.8 - 184.5	27	3.75	93.61	70116677.6	8.75	31.68
184.5 - 214.5	15	2.08	95.69	60455415.7	7.54	39.22
214.5 - 249.2	9	1.25	96.94	61461065.3	7.67	46.89
249.2 - 289.5	10	1.39	98.33	107600004	13.42	60.31
289.5 - 336.5	6	0.83	99.17	93238397.5	11.63	71.95
336.5 - 391	4	0.56	99.72	105402074	13.15	85.10
391 - 454.4	1	0.14	99.86	36822521.3	4.59	89.69
454.4 - 528	0	0.00	99.86	0	0.00	89.69
528 - 614	1	0.14	100.00	82657611.3	10.31	100.00
614 - 713.8	0	0.00	100.00	0	0.00	100.00
713.8 - 829.8	0	0.00	100.00	0	0.00	100.00
829.8 - 964.7	0	0.00	100	0	0.00	100.00
Total	720	100		801611624	100.00	
Median (μm)			[redacted]			[redacted]

Table C.2.7. Size distribution of sample from system-Py on Apr. 1, 1997.

Size classes µm	Frequency	Frequency %	Cumulative frequency %	Spherical volume	Volume %	Cumulative volume %
< 8.3	94	9.20	9.20	15849.1897	0.02	0.02
8.3 - 9.6	46	4.50	13.70	17027.2949	0.02	0.04
9.6 - 11.1	73	7.14	20.84	42531.5998	0.05	0.09
11.1 - 12.9	67	6.56	27.40	60440.2128	0.07	0.16
12.9 - 15	67	6.56	33.95	95208.6259	0.11	0.28
15 - 17.4	53	5.19	39.14	119012.912	0.14	0.42
17.4 - 20.1	71	6.95	46.09	241792.328	0.29	0.71
20.1 - 23.3	56	5.48	51.57	296155.82	0.35	1.06
23.3 - 27	61	5.97	57.53	507905.139	0.61	1.67
27 - 31.3	51	4.99	62.52	685097.858	0.82	2.49
31.3 - 36.3	52	5.09	67.61	1034368.58	1.24	3.72
36.3 - 42.1	65	6.36	73.97	2102800.03	2.51	6.23
42.1 - 48.8	49	4.79	78.77	2382308.05	2.85	9.08
48.8 - 56.6	56	5.48	84.25	4144431.91	4.95	14.03
56.6 - 65.6	53	5.19	89.43	6288659.45	7.51	21.55
65.6 - 76	37	3.62	93.05	6826457.96	8.16	29.70
76 - 88.1	27	2.64	95.69	7560138.65	9.03	38.73
88.1 - 102.1	19	1.86	97.55	9363954.12	11.19	49.92
102.1 - 118.4	9	0.88	98.43	6097185.39	7.28	57.21
118.4 - 137.5	10	0.98	99.41	10381248.9	12.40	69.61
137.5 - 158.8	3	0.29	99.71	4364088.77	5.21	74.82
158.8 - 184.5	0	0.00	99.71	0	0.00	74.82
184.5 - 214.5	0	0.00	99.71	0	0.00	74.82
214.5 - 249.2	2	0.20	99.90	11534911.2	13.78	88.60
249.2 - 289.5	1	0.10	100.00	9537814.53	11.40	100.00
289.5 - 336.5	0	0.00	100.00	0	0.00	100.00
336.5 - 391	0	0.00	100.00	0	0.00	100.00
391 - 454.4	0	0.00	100.00	0	0.00	100.00
454.4 - 528	0	0.00	100.00	0	0.00	100.00
528 - 614	0	0.00	100.00	0	0.00	100.00
614 - 713.8	0	0.00	100.00	0	0.00	100.00
713.8 - 829.8	0	0.00	100.00	0	0.00	100.00
829.8 - 964.7	0	0.00	100	0	0.00	100.00
Total	1022	100		83699388.6	100.00	
Median (µm)			[redacted]			[redacted]

Table C.2.8. Size distribution of sample from system-Py on Apr. 8, 1997.

Size classes μm	Frequency	Frequency %	Cumulative frequency %	Spherical volume	Volume %	Cumulative volume %
< 8.3	122	11.73	11.73	21025.8773	0.02	0.02
8.3 - 9.6	51	4.90	16.63	18634.1251	0.02	0.04
9.6 - 11.1	76	7.31	23.94	44001.8518	0.04	0.08
11.1 - 12.9	69	6.63	30.58	61224.1395	0.06	0.14
12.9 - 15	64	6.15	36.73	91971.0611	0.09	0.22
15 - 17.4	61	5.87	42.60	136253.144	0.13	0.35
17.4 - 20.1	57	5.48	48.08	201859.369	0.19	0.54
20.1 - 23.3	59	5.67	53.75	316610.274	0.30	0.84
23.3 - 27	56	5.38	59.13	473250.852	0.45	1.29
27 - 31.3	56	5.38	64.52	717831.579	0.68	1.97
31.3 - 36.3	74	7.12	71.63	1527481.71	1.44	3.41
36.3 - 42.1	52	5.00	76.63	1618194.66	1.53	4.94
42.1 - 48.8	51	4.90	81.54	2486374.82	2.35	7.29
48.8 - 56.6	33	3.17	84.71	2513481.5	2.37	9.66
56.6 - 65.6	38	3.65	88.37	4255486.61	4.02	13.68
65.6 - 76	36	3.46	91.83	6664433.1	6.30	19.98
76 - 88.1	21	2.02	93.85	5765062.43	5.45	25.43
88.1 - 102.1	19	1.83	95.67	9261852.56	8.75	34.18
102.1 - 118.4	19	1.83	97.50	13207493.4	12.48	46.66
118.4 - 137.5	10	0.96	98.46	10371268.3	9.80	56.46
137.5 - 158.8	6	0.58	99.04	9399315.92	8.88	65.34
158.8 - 184.5	5	0.48	99.52	12733993.4	12.03	77.37
184.5 - 214.5	4	0.38	99.90	15958500.7	15.08	92.45
214.5 - 249.2	1	0.10	100.00	7992306.74	7.55	100.00
249.2 - 289.5	0	0.00	100.00	0	0.00	100.00
289.5 - 336.5	0	0.00	100.00	0	0.00	100.00
336.5 - 391	0	0.00	100.00	0	0.00	100.00
391 - 454.4	0	0.00	100.00	0	0.00	100.00
454.4 - 528	0	0.00	100.00	0	0.00	100.00
528 - 614	0	0.00	100.00	0	0.00	100.00
614 - 713.8	0	0.00	100.00	0	0.00	100.00
713.8 - 829.8	0	0.00	100.00	0	0.00	100.00
829.8 - 964.7	0	0.00	100	0	0.00	100.00
Total	1040	100		105837908	100.00	
Median (μm)			21.3			124.9

Table C.2.9. Size distribution of sample from system-Py on Apr. 15, 1997.

Size classes µm	Frequency	Frequency %	Cumulative frequency %	Spherical volume	Volume %	Cumulative volume %
< 8.3	0	0.00	0.00	0	0.00	0.00
8.3 - 9.6	5	0.46	0.46	2014.92652	0.00	0.00
9.6 - 11.1	10	0.91	1.37	6055.29987	0.00	0.00
11.1 - 12.9	3	0.27	1.64	2928.57802	0.00	0.00
12.9 - 15	16	1.46	3.11	23501.3713	0.00	0.01
15 - 17.4	23	2.10	5.21	52305.2214	0.01	0.02
17.4 - 20.1	29	2.65	7.85	106683.913	0.02	0.03
20.1 - 23.3	42	3.84	11.69	231121.071	0.04	0.07
23.3 - 27	51	4.66	16.35	428551.648	0.07	0.15
27 - 31.3	81	7.40	23.74	1070767.97	0.19	0.33
31.3 - 36.3	63	5.75	29.50	1299552.64	0.23	0.56
36.3 - 42.1	82	7.49	36.99	2534319.46	0.44	1.00
42.1 - 48.8	95	8.68	45.66	4714205.06	0.82	1.82
48.8 - 56.6	87	7.95	53.61	6545610.95	1.14	2.96
56.6 - 65.6	98	8.95	62.56	11702644.1	2.04	5.00
65.6 - 76	78	7.12	69.68	14393110.2	2.50	7.50
76 - 88.1	71	6.48	76.16	20377864.6	3.54	11.04
88.1 - 102.1	75	6.85	83.01	33897448.7	5.90	16.94
102.1 - 118.4	58	5.30	88.31	39422963.5	6.86	23.79
118.4 - 137.5	41	3.74	92.05	45692756.8	7.95	31.74
137.5 - 158.8	25	2.28	94.34	42679941.2	7.42	39.17
158.8 - 184.5	20	1.83	96.16	51089556.9	8.89	48.05
184.5 - 214.5	18	1.64	97.81	80385851.7	13.98	62.03
214.5 - 249.2	13	1.19	99.00	83036741.6	14.44	76.47
249.2 - 289.5	8	0.73	99.73	82689919	14.38	90.86
289.5 - 336.5	2	0.18	99.91	28206418.8	4.91	95.76
336.5 - 391	1	0.09	100.00	24368234.9	4.24	100.00
391 - 454.4	0	0.00	100.00	0	0.00	100.00
454.4 - 528	0	0.00	100.00	0	0.00	100.00
528 - 614	0	0.00	100.00	0	0.00	100.00
614 - 713.8	0	0.00	100.00	0	0.00	100.00
713.8 - 829.8	0	0.00	100.00	0	0.00	100.00
829.8 - 964.7	0	0.00	100	0	0.00	100.00
Total	1095	100		574961070	100.00	
Median (µm)			[redacted]			[redacted]

Table C.2.10. Size distribution of sample from system-Py on Apr. 22, 1997.

Size classes μm	Frequency	Frequency %	Cumulative frequency %	Spherical volume	Volume %	Cumulative volume %
< 8.3	0	0.00	0.00	0	0.00	0.00
8.3 - 9.6	4	0.31	0.31	1709.17924	0.00	0.00
9.6 - 11.1	14	1.09	1.40	8740.43805	0.00	0.00
11.1 - 12.9	16	1.24	2.64	15173.4477	0.00	0.00
12.9 - 15	15	1.17	3.81	21143.7405	0.00	0.01
15 - 17.4	45	3.50	7.30	103601.619	0.01	0.02
17.4 - 20.1	51	3.96	11.27	184863.362	0.02	0.04
20.1 - 23.3	76	5.91	17.17	421702.252	0.05	0.09
23.3 - 27	68	5.28	22.46	572608.185	0.07	0.15
27 - 31.3	97	7.54	29.99	1235966.41	0.14	0.29
31.3 - 36.3	82	6.37	36.36	1659353.63	0.19	0.48
36.3 - 42.1	112	8.70	45.07	3618782.66	0.41	0.89
42.1 - 48.8	115	8.94	54.00	5628606.06	0.64	1.53
48.8 - 56.6	89	6.92	60.92	6850542.2	0.78	2.31
56.6 - 65.6	89	6.92	67.83	10381870.7	1.18	3.49
65.6 - 76	86	6.68	74.51	15924226	1.81	5.30
76 - 88.1	87	6.76	81.27	24955002.1	2.83	8.13
88.1 - 102.1	55	4.27	85.55	25144606	2.86	10.99
102.1 - 118.4	43	3.34	88.89	29369910.7	3.34	14.32
118.4 - 137.5	38	2.95	91.84	41692773.8	4.74	19.06
137.5 - 158.8	35	2.72	94.56	57551812.5	6.54	25.60
158.8 - 184.5	24	1.86	96.43	63371651.6	7.20	32.79
184.5 - 214.5	15	1.17	97.59	65151670.3	7.40	40.19
214.5 - 249.2	11	0.85	98.45	76741868.1	8.72	48.91
249.2 - 289.5	8	0.62	99.07	78777753.1	8.95	57.86
289.5 - 336.5	6	0.47	99.53	93511016.7	10.62	68.48
336.5 - 391	3	0.23	99.77	77301330.7	8.78	77.26
391 - 454.4	0	0.00	99.77	0	0.00	77.26
454.4 - 528	3	0.23	100.00	200200694	22.74	100.00
528 - 614	0	0.00	100.00	0	0.00	100.00
614 - 713.8	0	0.00	100.00	0	0.00	100.00
713.8 - 829.8	0	0.00	100.00	0	0.00	100.00
829.8 - 964.7	0	0.00	100	0	0.00	100.00
Total	1287	100		880398980	100.00	
Median (μm)			[redacted]			[redacted]

Table C.3.1. Summary of the medians ESD of sludge from ssytem-Pm.

Sampling date	No. of particles	ESD (by no.) Range	ESD (by no.) Median	ESD (by volume) Median
15-Oct	1008	1.9 - 417.8	14.3	263.7
29-Oct	998	1.9 - 350.8	28.2	236.8
26-Nov	449	4.8 - 363.0	18.2	301.1
3-Apr	1424	8.4 - 661.6	38.2	265.1
24-Apr	1121	8.4 - 461.7	50.0	224.3
1-May	977	8.4 - 978.1	61.7	551.0
8-May	1128	9.3 - 877.3	51.5	573.9

Table C.3.2. Size distribution of sample from system-Pm on Oct. 15, 1996.

Size classes μm	Frequency	Frequency %	Cumulative frequency %	Spherical volume	Volume %	Cumulative volume %
< 8.3	278	27.58	27.58	17050.7685	0.01	0.01
8.3 - 9.6	35	3.47	31.05	13213.6921	0.01	0.01
9.6 - 11.1	51	5.06	36.11	30892.276	0.01	0.03
11.1 - 12.9	96	9.52	45.63	86677.0277	0.04	0.07
12.9 - 15	64	6.35	51.98	90641.5174	0.04	0.11
15 - 17.4	55	5.46	57.44	126625.766	0.06	0.16
17.4 - 20.1	65	6.45	63.89	224182.324	0.10	0.26
20.1 - 23.3	55	5.46	69.35	299436.55	0.13	0.40
23.3 - 27	51	5.06	74.40	414889.231	0.19	0.58
27 - 31.3	66	6.55	80.95	842127.652	0.38	0.96
31.3 - 36.3	40	3.97	84.92	822371.539	0.37	1.32
36.3 - 42.1	36	3.57	88.49	1104343.68	0.49	1.82
42.1 - 48.8	24	2.38	90.87	1168539.81	0.52	2.34
48.8 - 56.6	15	1.49	92.36	1242482.16	0.55	2.89
56.6 - 65.6	6	0.60	92.96	655637.581	0.29	3.19
65.6 - 76	10	0.99	93.95	1843983.92	0.82	4.01
76 - 88.1	11	1.09	95.04	3364741.83	1.50	5.51
88.1 - 102.1	6	0.60	95.63	2581367.81	1.15	6.66
102.1 - 118.4	9	0.89	96.53	6561621.2	2.93	9.59
118.4 - 137.5	10	0.99	97.52	10941574.6	4.88	14.47
137.5 - 158.8	6	0.60	98.12	10376292.8	4.63	19.10
158.8 - 184.5	5	0.50	98.61	13291285	5.93	25.03
184.5 - 214.5	4	0.40	99.01	16990894.1	7.58	32.61
214.5 - 249.2	5	0.50	99.50	34877670.6	15.56	48.17
249.2 - 289.5	1	0.10	99.60	11383713.3	5.08	53.25
289.5 - 336.5	1	0.10	99.70	12888881.3	5.75	59.00
336.5 - 391	1	0.10	99.80	21212551	9.46	68.47
391 - 454.4	2	0.20	100.00	70674493.4	31.53	100.00
454.4 - 528	0	0.00	100.00	0	0.00	100.00
528 - 614	0	0.00	100.00	0	0.00	100.00
614 - 713.8	0	0.00	100.00	0	0.00	100.00
713.8 - 829.8	0	0.00	100.00	0	0.00	100.00
829.8 - 964.7	0	0.00	100	0	0.00	100.00
Total	1008	100		224128182	100.00	
Median (μm)			[redacted]			[redacted]

Table C.3.3. Size distribution of sample from system-Pm on Oct. 29, 1996.

Size classes μm	Frequency	Frequency %	Cumulative frequency %	Spherical volume	Volume %	Cumulative volume %
< 8.3	63	6.31	6.31	7893.49277	0.00	0.00
8.3 - 9.6	25	2.51	8.82	9482.96005	0.00	0.01
9.6 - 11.1	27	2.71	11.52	15251.6224	0.00	0.01
11.1 - 12.9	37	3.71	15.23	33807.4675	0.01	0.02
12.9 - 15	41	4.11	19.34	60740.4161	0.02	0.04
15 - 17.4	87	8.72	28.06	193179.494	0.06	0.10
17.4 - 20.1	54	5.41	33.47	184677.581	0.06	0.16
20.1 - 23.3	51	5.11	38.58	273241.016	0.09	0.25
23.3 - 27	82	8.22	46.79	689579.407	0.22	0.47
27 - 31.3	83	8.32	55.11	1045024.32	0.34	0.81
31.3 - 36.3	72	7.21	62.32	1464080.09	0.47	1.28
36.3 - 42.1	71	7.11	69.44	2159726.89	0.70	1.98
42.1 - 48.8	64	6.41	75.85	3193510.68	1.03	3.00
48.8 - 56.6	52	5.21	81.06	3964633.77	1.28	4.28
56.6 - 65.6	37	3.71	84.77	4434421.57	1.43	5.71
65.6 - 76	35	3.51	88.28	6331335.74	2.04	7.75
76 - 88.1	24	2.40	90.68	6682742.68	2.15	9.90
88.1 - 102.1	20	2.00	92.69	9026534.81	2.91	12.81
102.1 - 118.4	15	1.50	94.19	10355736.6	3.33	16.14
118.4 - 137.5	14	1.40	95.59	15702918.1	5.06	21.20
137.5 - 158.8	12	1.20	96.79	21118399	6.80	28.00
158.8 - 184.5	10	1.00	97.80	25741201.7	8.29	36.29
184.5 - 214.5	6	0.60	98.40	24938664.7	8.03	44.32
214.5 - 249.2	4	0.40	98.80	27509908.8	8.86	53.18
249.2 - 289.5	8	0.80	99.60	82123268.7	26.45	79.62
289.5 - 336.5	3	0.30	99.90	40678632.2	13.10	92.72
336.5 - 391	1	0.10	100.00	22598155.5	7.28	100.00
391 - 454.4	0	0.00	100.00	0	0.00	100.00
454.4 - 528	0	0.00	100.00	0	0.00	100.00
528 - 614	0	0.00	100.00	0	0.00	100.00
614 - 713.8	0	0.00	100.00	0	0.00	100.00
713.8 - 829.8	0	0.00	100.00	0	0.00	100.00
829.8 - 964.7	0	0.00	100	0	0.00	100.00
Total	998	100		310536749	100.00	
Median (μm)			28.2			236.8

Table C.3.4. Size distribution of sample from system-Pm on Nov. 26, 1996.

Size classes μm	Frequency	Frequency %	Cumulative frequency %	Spherical volume	Volume %	Cumulative volume %
< 8.3	33	7.35	7.35	6361.12891	0.00	0.00
8.3 - 9.6	30	6.68	14.03	11020.5926	0.01	0.01
9.6 - 11.1	35	7.80	21.83	20639.7409	0.01	0.02
11.1 - 12.9	43	9.58	31.40	38972.5395	0.02	0.04
12.9 - 15	35	7.80	39.20	50004.9985	0.03	0.07
15 - 17.4	39	8.69	47.88	88076.9557	0.05	0.11
17.4 - 20.1	28	6.24	54.12	94796.2896	0.05	0.16
20.1 - 23.3	24	5.35	59.47	124809.064	0.06	0.23
23.3 - 27	31	6.90	66.37	261789.716	0.14	0.36
27 - 31.3	21	4.68	71.05	267905.216	0.14	0.50
31.3 - 36.3	11	2.45	73.50	230908.953	0.12	0.62
36.3 - 42.1	15	3.34	76.84	471430.537	0.24	0.86
42.1 - 48.8	16	3.56	80.40	746355.511	0.39	1.25
48.8 - 56.6	8	1.78	82.18	619484.028	0.32	1.57
56.6 - 65.6	13	2.90	85.08	1553497.02	0.81	2.38
65.6 - 76	20	4.45	89.53	3645887.25	1.89	4.27
76 - 88.1	13	2.90	92.43	3925684.52	2.04	6.30
88.1 - 102.1	8	1.78	94.21	3554461.2	1.84	8.15
102.1 - 118.4	1	0.22	94.43	840663.477	0.44	8.58
118.4 - 137.5	7	1.56	95.99	7826932.01	4.06	12.64
137.5 - 158.8	2	0.45	96.44	3677715.54	1.91	14.55
158.8 - 184.5	2	0.45	96.88	6030997.96	3.13	17.67
184.5 - 214.5	4	0.89	97.77	16970198.1	8.80	26.47
214.5 - 249.2	3	0.67	98.44	17131104.8	8.88	35.35
249.2 - 289.5	1	0.22	98.66	12279715.2	6.37	41.72
289.5 - 336.5	4	0.89	99.55	64494813	33.44	75.16
336.5 - 391	2	0.45	100.00	47908495.3	24.84	100.00
391 - 454.4	0	0.00	100.00	0	0.00	100.00
454.4 - 528	0	0.00	100.00	0	0.00	100.00
528 - 614	0	0.00	100.00	0	0.00	100.00
614 - 713.8	0	0.00	100.00	0	0.00	100.00
713.8 - 829.8	0	0.00	100.00	0	0.00	100.00
829.8 - 964.7	0	0.00	100	0	0.00	100.00
Total	449	100		192872721	100.00	
Median (μm)			[redacted]			[redacted]

Table C.3.5. Size distribution of sample from system-Pm on Apr. 3, 1997.

Size classes μm	Frequency	Frequency %	Cumulative frequency %	Spherical volume	Volume %	Cumulative volume %
< 8.3	0	0.00	0.00	0	0.00	0.00
8.3 - 9.6	10	0.70	0.70	4074.96155	0.00	0.00
9.6 - 11.1	19	1.33	2.04	12416.9641	0.00	0.00
11.1 - 12.9	22	1.54	3.58	20590.0765	0.00	0.00
12.9 - 15	34	2.39	5.97	49357.1377	0.00	0.01
15 - 17.4	76	5.34	11.31	170904.192	0.02	0.03
17.4 - 20.1	69	4.85	16.15	237136.424	0.02	0.05
20.1 - 23.3	107	7.51	23.67	566762.765	0.06	0.10
23.3 - 27	101	7.09	30.76	832813.223	0.08	0.19
27 - 31.3	123	8.64	39.40	1614564.86	0.16	0.34
31.3 - 36.3	108	7.58	46.98	2149956.45	0.21	0.55
36.3 - 42.1	105	7.37	54.35	3245094.86	0.32	0.87
42.1 - 48.8	85	5.97	60.32	4194907.8	0.41	1.28
48.8 - 56.6	83	5.83	66.15	6425590.92	0.63	1.91
56.6 - 65.6	74	5.20	71.35	8727273.32	0.85	2.77
65.6 - 76	81	5.69	77.04	15010754.6	1.47	4.24
76 - 88.1	51	3.58	80.62	15110660.7	1.48	5.72
88.1 - 102.1	52	3.65	84.27	22770300.8	2.23	7.95
102.1 - 118.4	58	4.07	88.34	39621587.7	3.88	11.83
118.4 - 137.5	41	2.88	91.22	44933053.1	4.40	16.23
137.5 - 158.8	34	2.39	93.61	56654170.8	5.55	21.78
158.8 - 184.5	34	2.39	96.00	88730059.3	8.69	30.47
184.5 - 214.5	19	1.33	97.33	78640674	7.70	38.18
214.5 - 249.2	13	0.91	98.24	89738044	8.79	46.97
249.2 - 289.5	8	0.56	98.81	78552309.4	7.69	54.66
289.5 - 336.5	12	0.84	99.65	196881497	19.29	73.95
336.5 - 391	2	0.14	99.79	44763601.6	4.38	78.33
391 - 454.4	2	0.14	99.93	69606260.6	6.82	85.15
454.4 - 528	0	0.00	99.93	0	0.00	85.15
528 - 614	0	0.00	99.93	0	0.00	85.15
614 - 713.8	1	0.07	100.00	151609133	14.85	100.00
713.8 - 829.8	0	0.00	100.00	0	0.00	100.00
829.8 - 964.7	0	0.00	100	0	0.00	100.00
Total	1424	100		1020873550	100.00	
Median (μm)			[redacted]			265

Table C.3.6. Size distribution of sample from system-Pm on Apr. 24, 1997.

Size classes μm	Frequency	Frequency %	Cumulative frequency %	Spherical volume	Volume %	Cumulative volume %
< 8.3	0	0.00	0.00	0	0.00	0.00
8.3 - 9.6	13	1.16	1.16	5433.28501	0.00	0.00
9.6 - 11.1	11	0.98	2.14	7055.3572	0.00	0.00
11.1 - 12.9	14	1.25	3.39	12775.4272	0.00	0.00
12.9 - 15	27	2.41	5.80	39244.9405	0.00	0.01
15 - 17.4	47	4.19	9.99	106229.23	0.01	0.02
17.4 - 20.1	65	5.80	15.79	226816.437	0.02	0.04
20.1 - 23.3	58	5.17	20.96	321006.209	0.03	0.08
23.3 - 27	73	6.51	27.48	620961.899	0.07	0.14
27 - 31.3	60	5.35	32.83	779337.796	0.08	0.22
31.3 - 36.3	56	5.00	37.82	1123656.52	0.12	0.34
36.3 - 42.1	59	5.26	43.09	1836678.79	0.19	0.53
42.1 - 48.8	67	5.98	49.06	3288512.75	0.34	0.88
48.8 - 56.6	64	5.71	54.77	5030857.21	0.53	1.41
56.6 - 65.6	66	5.89	60.66	8173484.2	0.86	2.26
65.6 - 76	73	6.51	67.17	13507364.6	1.42	3.68
76 - 88.1	59	5.26	72.44	16942903.4	1.78	5.46
88.1 - 102.1	62	5.53	77.97	26971791.2	2.83	8.28
102.1 - 118.4	51	4.55	82.52	36351501.1	3.81	12.10
118.4 - 137.5	55	4.91	87.42	59900115.7	6.28	18.38
137.5 - 158.8	38	3.39	90.81	65213895.3	6.84	25.22
158.8 - 184.5	35	3.12	93.93	91294295	9.57	34.79
184.5 - 214.5	29	2.59	96.52	117783367	12.35	47.15
214.5 - 249.2	15	1.34	97.86	96349244.5	10.10	57.25
249.2 - 289.5	9	0.80	98.66	95628822.6	10.03	67.28
289.5 - 336.5	9	0.80	99.46	139435530	14.62	81.90
336.5 - 391	4	0.36	99.82	89340404.4	9.37	91.27
391 - 454.4	1	0.09	99.91	31678956	3.32	94.59
454.4 - 528	1	0.09	100.00	51538605.1	5.41	100.00
528 - 614	0	0.00	100.00	0	0.00	100.00
614 - 713.8	0	0.00	100.00	0	0.00	100.00
713.8 - 829.8	0	0.00	100.00	0	0.00	100.00
829.8 - 964.7	0	0.00	100	0	0.00	100.00
Total	1121	100		953508846	100.00	
Median (μm)			50.0			224.3

Table C.3.7. Size distribution of sample from system-Pm on May 1, 1997.

Size classes µm	Frequency	Frequency %	Cumulative frequency %	Spherical volume	Volume %	Cumulative volume %
< 8.3	0	0.00	0.00	0	0.00	0.00
8.3 - 9.6	17	1.74	1.74	6656.27412	0.00	0.00
9.6 - 11.1	14	1.43	3.17	8594.31681	0.00	0.00
11.1 - 12.9	12	1.23	4.40	11380.0857	0.00	0.00
12.9 - 15	11	1.13	5.53	15937.9613	0.00	0.00
15 - 17.4	37	3.79	9.31	83401.6639	0.00	0.00
17.4 - 20.1	41	4.20	13.51	148267.591	0.00	0.01
20.1 - 23.3	34	3.48	16.99	181531.178	0.01	0.01
23.3 - 27	37	3.79	20.78	316151.341	0.01	0.02
27 - 31.3	62	6.35	27.12	812489.852	0.02	0.04
31.3 - 36.3	43	4.40	31.53	898392.306	0.03	0.07
36.3 - 42.1	43	4.40	35.93	1346256.56	0.04	0.11
42.1 - 48.8	62	6.35	42.27	3107591.52	0.09	0.19
48.8 - 56.6	52	5.32	47.59	3808771.71	0.11	0.30
56.6 - 65.6	44	4.50	52.10	5285442.48	0.15	0.45
65.6 - 76	66	6.76	58.85	12245247.6	0.34	0.79
76 - 88.1	47	4.81	63.66	13499650.5	0.38	1.16
88.1 - 102.1	58	5.94	69.60	26067749	0.73	1.89
102.1 - 118.4	55	5.63	75.23	39191730.5	1.09	2.98
118.4 - 137.5	58	5.94	81.17	64278973.5	1.79	4.77
137.5 - 158.8	37	3.79	84.95	63510335	1.77	6.54
158.8 - 184.5	39	3.99	88.95	102141614	2.84	9.38
184.5 - 214.5	32	3.28	92.22	130031180	3.62	13.00
214.5 - 249.2	22	2.25	94.47	147745434	4.11	17.11
249.2 - 289.5	12	1.23	95.70	128527351	3.58	20.68
289.5 - 336.5	13	1.33	97.03	206442541	5.75	26.43
336.5 - 391	6	0.61	97.65	144423880	4.02	30.45
391 - 454.4	5	0.51	98.16	198444176	5.52	35.97
454.4 - 528	6	0.61	98.77	331966012	9.24	45.21
528 - 614	7	0.72	99.49	642536370	17.88	63.09
614 - 713.8	2	0.20	99.69	309570663	8.62	71.71
713.8 - 829.8	2	0.20	99.90	526621243	14.66	86.36
829.8 - 964.7	0	0.00	99.90	0	0.00	86.36
964.7 - 1121.5	1	0.10	100.00	490010802	13.64	100.00
Total	977	100.00		3593285816	100.00	
Median (µm)			[redacted]			[redacted]

Table C.3.8. Size distribution of sample from system-Pm on May 8, 1997.

Size classes µm	Frequency	Frequency %	Cumulative frequency %	Spherical volume	Volume %	Cumulative volume %
< 8.3	0	0.00	0.00	0	0.00	0.00
8.3 - 9.6	2	0.18	0.18	854.589621	0.00	0.00
9.6 - 11.1	12	1.06	1.24	7763.17205	0.00	0.00
11.1 - 12.9	7	0.62	1.86	7056.16627	0.00	0.00
12.9 - 15	14	1.24	3.10	19563.678	0.00	0.00
15 - 17.4	32	2.84	5.94	75047.4933	0.00	0.00
17.4 - 20.1	43	3.81	9.75	152263.414	0.01	0.01
20.1 - 23.3	42	3.72	13.48	223122.267	0.01	0.02
23.3 - 27	56	4.96	18.44	484579.801	0.02	0.04
27 - 31.3	68	6.03	24.47	885130.72	0.04	0.07
31.3 - 36.3	66	5.85	30.32	1325075.07	0.05	0.13
36.3 - 42.1	90	7.98	38.30	2840936.08	0.11	0.24
42.1 - 48.8	99	8.78	47.07	4833844.65	0.19	0.44
48.8 - 56.6	93	8.24	55.32	7179654.85	0.29	0.73
56.6 - 65.6	90	7.98	63.30	10800337.4	0.43	1.16
65.6 - 76	89	7.89	71.19	16433502.3	0.66	1.82
76 - 88.1	78	6.91	78.10	21529422.6	0.87	2.69
88.1 - 102.1	52	4.61	82.71	23350351.4	0.94	3.63
102.1 - 118.4	53	4.70	87.41	37298554.7	1.50	5.13
118.4 - 137.5	32	2.84	90.25	33914432.2	1.37	6.49
137.5 - 158.8	22	1.95	92.20	37226621.5	1.50	7.99
158.8 - 184.5	23	2.04	94.24	60829559.3	2.45	10.44
184.5 - 214.5	18	1.60	95.83	73510405.3	2.96	13.40
214.5 - 249.2	16	1.42	97.25	104035697	4.19	17.59
249.2 - 289.5	7	0.62	97.87	76122497.1	3.06	20.65
289.5 - 336.5	3	0.27	98.14	48687797.1	1.96	22.61
336.5 - 391	5	0.44	98.58	151022650	6.08	28.69
391 - 454.4	5	0.44	99.02	193455877	7.79	36.48
454.4 - 528	0	0.00	99.02	0	0.00	36.48
528 - 614	6	0.53	99.56	629892512	25.35	61.83
614 - 713.8	4	0.35	99.91	594870239	23.94	85.77
713.8 - 829.8	0	0.00	99.91	0	0.00	85.77
829.8 - 964.7	1	0.09	100.00	353507384	14.23	100.00
964.7 - 1121.5	0	0.00	100.00	0	0.00	100.00
Total	1128	100.00		2484522732	100.00	
Median (µm)			[redacted]			[redacted]

Table C.4.1. Summary of the medians ESD of sludge from system-Po.

Sampling date	No. of particles	ESD (by no.) Range	ESD (by no.) Median	ESD (by volume) Median
18-Nov	539	20.5 - 1384.7	64.4	1166.9
2-Dec	434	18.7 - 1433.9	68.9	1259.6
20-Jan	560	8.4 - 436.0	41.0	183.2
17-Feb	910	9.3 - 371.5	60.2	169.8
31-Mar	769	8.4 - 492.2	60.6	221.8
7-Apr	1195	9.4 - 492.3	47.3	197.9
14-Apr	1135	8.4 - 900.6	49.3	317.7
21-Apr	1175	9.3 - 545.4	65.7	195.6
28-Apr	1253	9.3 - 481.9	68.8	198.3

Shaded area represents the samples from dysfunctional period.

Table C.4.2. Size distribution of sample from system-Po on Nov. 18, 1996.

Size classes μm	Frequency	Frequency %	Cumulative frequency %	Spherical volume	Volume %	Cumulative volume %
< 8.3	0	0.00	0.00	0	0.00	0.00
8.3 - 9.6	0	0.00	0.00	0	0.00	0.00
9.6 - 11.1	0	0.00	0.00	0	0.00	0.00
11.1 - 12.9	0	0.00	0.00	0	0.00	0.00
12.9 - 15	0	0.00	0.00	0	0.00	0.00
15 - 17.4	0	0.00	0.00	0	0.00	0.00
17.4 - 20.1	0	0.00	0.00	0	0.00	0.00
20.1 - 23.3	3	0.56	0.56	14798.6232	0.00	0.00
23.3 - 27	7	1.30	1.86	54477.0376	0.00	0.00
27 - 31.3	12	2.23	4.08	163894.523	0.00	0.01
31.3 - 36.3	34	6.31	10.39	666346.256	0.02	0.02
36.3 - 42.1	44	8.16	18.55	1409570.42	0.03	0.05
42.1 - 48.8	55	10.20	28.76	2825101.99	0.06	0.12
48.8 - 56.6	67	12.43	41.19	5194732.89	0.12	0.23
56.6 - 65.6	52	9.65	50.83	6072273.71	0.14	0.37
65.6 - 76	51	9.46	60.30	9466164.11	0.21	0.58
76 - 88.1	46	8.53	68.83	12977118.3	0.29	0.88
88.1 - 102.1	34	6.31	75.14	15570001.4	0.35	1.23
102.1 - 118.4	41	7.61	82.75	29357880	0.66	1.89
118.4 - 137.5	28	5.19	87.94	29921692.6	0.67	2.56
137.5 - 158.8	16	2.97	90.91	26563294.8	0.60	3.16
158.8 - 184.5	12	2.23	93.14	31885837.2	0.72	3.88
184.5 - 214.5	4	0.74	93.88	17650965.1	0.40	4.28
214.5 - 249.2	6	1.11	94.99	41476431.7	0.93	5.21
249.2 - 289.5	9	1.67	96.66	86802356.2	1.96	7.17
289.5 - 336.5	2	0.37	97.03	30583407.9	0.69	7.86
336.5 - 391	3	0.56	97.59	77428911.7	1.75	9.60
391 - 454.4	3	0.56	98.14	124139063	2.80	12.40
454.4 - 528	3	0.56	98.70	200600405	4.52	16.92
528 - 614	1	0.19	98.89	106132639	2.39	19.32
614 - 713.8	1	0.19	99.07	136956367	3.09	22.40
713.8 - 829.8	1	0.19	99.26	257708518	5.81	28.21
829.8 - 964.7	2	0.37	99.63	691725571	15.59	43.80
964.7 - 1121.5	0	0.00	99.63	0	0.00	43.80
1121.5 - 1303.8	1	0.19	99.81	1102795013	24.86	68.66
1303.8 - 1515.7	1	0.19	100.00	1390254212	31.34	100.00
Total	539	100.00		4436397045	100.00	
Median (μm)			[redacted]			[redacted]

Table C.4.3. Size distribution of sample from system-Po on Dec. 2, 1996.

Size classes μm	Frequency	Frequency %	Cumulative frequency %	Spherical volume	Volume %	Cumulative volume %
< 8.3	0	0.00	0.00	0	0.00	0.00
8.3 - 9.6	0	0.00	0.00	0	0.00	0.00
9.6 - 11.1	0	0.00	0.00	0	0.00	0.00
11.1 - 12.9	0	0.00	0.00	0	0.00	0.00
12.9 - 15	0	0.00	0.00	0	0.00	0.00
15 - 17.4	0	0.00	0.00	0	0.00	0.00
17.4 - 20.1	3	0.69	0.69	10255.0953	0.00	0.00
20.1 - 23.3	4	0.92	1.61	19143.2026	0.00	0.00
23.3 - 27	16	3.69	5.30	132465.56	0.00	0.00
27 - 31.3	22	5.07	10.37	319164.992	0.00	0.01
31.3 - 36.3	22	5.07	15.44	459169.336	0.01	0.01
36.3 - 42.1	31	7.14	22.58	963392.27	0.01	0.03
42.1 - 48.8	35	8.06	30.65	1773866.23	0.03	0.05
48.8 - 56.6	36	8.29	38.94	2716880.09	0.04	0.09
56.6 - 65.6	31	7.14	46.08	3788374.13	0.06	0.15
65.6 - 76	46	10.60	56.68	8284412.01	0.12	0.27
76 - 88.1	46	10.60	67.28	13114763.5	0.19	0.46
88.1 - 102.1	35	8.06	75.35	15869342.9	0.23	0.69
102.1 - 118.4	29	6.68	82.03	20302705.9	0.30	0.99
118.4 - 137.5	21	4.84	86.87	23093772.6	0.34	1.33
137.5 - 158.8	15	3.46	90.32	23666265.7	0.35	1.68
158.8 - 184.5	11	2.53	92.86	29646597.8	0.43	2.11
184.5 - 214.5	7	1.61	94.47	28590983.5	0.42	2.53
214.5 - 249.2	4	0.92	95.39	26335194.6	0.39	2.91
249.2 - 289.5	3	0.69	96.08	29699241	0.43	3.35
289.5 - 336.5	4	0.92	97.00	65767351.4	0.96	4.31
336.5 - 391	0	0.00	97.00	0	0.00	4.31
391 - 454.4	0	0.00	97.00	0	0.00	4.31
454.4 - 528	5	1.15	98.16	302811329	4.43	8.74
528 - 614	0	0.00	98.16	0	0.00	8.74
614 - 713.8	2	0.46	98.62	282096074	4.13	12.86
713.8 - 829.8	0	0.00	98.62	0	0.00	12.86
829.8 - 964.7	0	0.00	98.62	0	0.00	12.86
964.7 - 1121.5	1	0.23	98.85	528607514	7.73	20.60
1121.5 - 1303.8	3	0.69	99.54	2653373133	38.81	59.41
1303.8 - 1515.7	2	0.46	100.00	2774633377	40.59	100.00
Total	434	100.00		6836074769	100.00	
Median (μm)			[redacted]			[redacted]

Table C.4.4. Size distribution of sample from system-Po on Jan. 20, 1997.

Size classes μm	Frequency	Frequency %	Cumulative frequency %	Spherical volume	Volume %	Cumulative volume %
< 8.3	0	0.00	0.00	0	0.00	0.00
8.3 - 9.6	4	0.71	0.71	1605.40676	0.00	0.00
9.6 - 11.1	10	1.79	2.50	6566.36632	0.00	0.00
11.1 - 12.9	7	1.25	3.75	6797.19844	0.00	0.01
12.9 - 15	14	2.50	6.25	19577.3997	0.01	0.01
15 - 17.4	16	2.86	9.11	36035.2203	0.02	0.03
17.4 - 20.1	21	3.75	12.86	72732.2296	0.03	0.06
20.1 - 23.3	41	7.32	20.18	207763.301	0.09	0.15
23.3 - 27	38	6.79	26.96	320974.511	0.14	0.29
27 - 31.3	47	8.39	35.36	586001.537	0.25	0.55
31.3 - 36.3	46	8.21	43.57	961711.759	0.42	0.96
36.3 - 42.1	44	7.86	51.43	1372167.13	0.59	1.56
42.1 - 48.8	47	8.39	59.82	2351005.41	1.02	2.58
48.8 - 56.6	34	6.07	65.89	2572982.68	1.12	3.69
56.6 - 65.6	40	7.14	73.04	4708015.03	2.04	5.73
65.6 - 76	26	4.64	77.68	4864073.1	2.11	7.84
76 - 88.1	25	4.46	82.14	7508183.76	3.26	11.10
88.1 - 102.1	21	3.75	85.89	9445471.62	4.10	15.19
102.1 - 118.4	28	5.00	90.89	19547095.6	8.47	23.67
118.4 - 137.5	17	3.04	93.93	18880544.5	8.19	31.85
137.5 - 158.8	13	2.32	96.25	21196300.4	9.19	41.04
158.8 - 184.5	9	1.61	97.86	21762150.3	9.44	50.48
184.5 - 214.5	5	0.89	98.75	19422532.8	8.42	58.90
214.5 - 249.2	5	0.89	99.64	30340232.2	13.15	72.05
249.2 - 289.5	0	0.00	99.64	0	0.00	72.05
289.5 - 336.5	0	0.00	99.64	0	0.00	72.05
336.5 - 391	1	0.18	99.82	21061630.6	9.13	81.18
391 - 454.4	1	0.18	100.00	43399507.1	18.82	100.00
454.4 - 528	0	0.00	100.00	0	0.00	100.00
528 - 614	0	0.00	100.00	0	0.00	100.00
614 - 713.8	0	0.00	100.00	0	0.00	100.00
713.8 - 829.8	0	0.00	100.00	0	0.00	100.00
829.8 - 964.7	0	0.00	100.00	0	0.00	100.00
964.7 - 1121.5	0	0.00	100.00	0	0.00	100.00
1121.5 - 1303.8	0	0.00	100.00	0	0.00	100.00
1303.8 - 1515.7	0	0.00	100.00	0	0.00	100.00
Total	560	100.00		230651657	100.00	
Median (μm)			[redacted]			[redacted]

Table C.4.5. Size distribution of sample from system-Po on Feb. 17, 1997.

Size classes µm	Frequency	Frequency %	Cumulative frequency %	Spherical volume	Volume %	Cumulative volume %
< 8.3	0	0.00	0.00	0	0.00	0.00
8.3 - 9.6	2	0.22	0.22	854.59162	0.00	0.00
9.6 - 11.1	9	0.99	1.21	5785.86226	0.00	0.00
11.1 - 12.9	9	0.99	2.20	8451.52748	0.00	0.00
12.9 - 15	15	1.65	3.85	20577.9062	0.00	0.01
15 - 17.4	16	1.76	5.60	35207.4118	0.01	0.01
17.4 - 20.1	29	3.19	8.79	103266.42	0.02	0.03
20.1 - 23.3	29	3.19	11.98	158540.162	0.03	0.06
23.3 - 27	29	3.19	15.16	245479.143	0.04	0.10
27 - 31.3	42	4.62	19.78	537482.582	0.09	0.19
31.3 - 36.3	44	4.84	24.62	903306.681	0.16	0.35
36.3 - 42.1	56	6.15	30.77	1806414.24	0.31	0.66
42.1 - 48.8	70	7.69	38.46	3376212.05	0.59	1.25
48.8 - 56.6	74	8.13	46.59	5813179.89	1.01	2.26
56.6 - 65.6	72	7.91	54.51	8452515.07	1.47	3.73
65.6 - 76	70	7.69	62.20	12948047	2.25	5.98
76 - 88.1	76	8.35	70.55	21754450.6	3.78	9.76
88.1 - 102.1	53	5.82	76.37	23840060	4.14	13.91
102.1 - 118.4	55	6.04	82.42	38752218.9	6.74	20.64
118.4 - 137.5	50	5.49	87.91	52942183.4	9.20	29.84
137.5 - 158.8	47	5.16	93.08	79233971.5	13.77	43.62
158.8 - 184.5	32	3.52	96.59	85572820.9	14.87	58.49
184.5 - 214.5	16	1.76	98.35	65738805.3	11.43	69.92
214.5 - 249.2	5	0.55	98.90	31927680.3	5.55	75.47
249.2 - 289.5	6	0.66	99.56	58250870.5	10.12	85.59
289.5 - 336.5	1	0.11	99.67	13273819.5	2.31	87.90
336.5 - 391	3	0.33	100.00	69620373	12.10	100.00
391 - 454.4	0	0.00	100.00	0	0.00	100.00
454.4 - 528	0	0.00	100.00	0	0.00	100.00
528 - 614	0	0.00	100.00	0	0.00	100.00
614 - 713.8	0	0.00	100.00	0	0.00	100.00
713.8 - 829.8	0	0.00	100.00	0	0.00	100.00
829.8 - 964.7	0	0.00	100.00	0	0.00	100.00
964.7 - 1121.5	0	0.00	100.00	0	0.00	100.00
1121.5 - 1303.8	0	0.00	100.00	0	0.00	100.00
1303.8 - 1515.7	0	0.00	100.00	0	0.00	100.00
Total	910	100.00		575322574	100.00	
Median (µm)			60.2			169.8

Table C.4.6. Size distribution of sample from system-Po on Mar. 31, 1997.

Size classes µm	Frequency	Frequency %	Cumulative frequency %	Spherical volume	Volume %	Cumulative volume %
< 8.3	0	0.00	0.00	0	0.00	0.00
8.3 - 9.6	4	0.52	0.52	1482.49838	0.00	0.00
9.6 - 11.1	4	0.52	1.04	2567.44365	0.00	0.00
11.1 - 12.9	9	1.17	2.21	8377.14623	0.00	0.00
12.9 - 15	12	1.56	3.77	17141.9368	0.00	0.00
15 - 17.4	17	2.21	5.98	41496.1594	0.01	0.01
17.4 - 20.1	16	2.08	8.06	54910.5293	0.01	0.02
20.1 - 23.3	38	4.94	13.00	193019.604	0.02	0.04
23.3 - 27	29	3.77	16.78	243139.246	0.03	0.07
27 - 31.3	37	4.81	21.59	475647.899	0.06	0.13
31.3 - 36.3	43	5.59	27.18	847674.398	0.10	0.23
36.3 - 42.1	55	7.15	34.33	1802989.83	0.22	0.45
42.1 - 48.8	45	5.85	40.18	2180660.77	0.26	0.71
48.8 - 56.6	57	7.41	47.59	4247348.12	0.51	1.22
56.6 - 65.6	37	4.81	52.41	4390826.65	0.53	1.76
65.6 - 76	48	6.24	58.65	8731507.79	1.06	2.81
76 - 88.1	54	7.02	65.67	15774352.2	1.91	4.72
88.1 - 102.1	39	5.07	70.74	17870879.3	2.16	6.88
102.1 - 118.4	55	7.15	77.89	38251586.7	4.63	11.51
118.4 - 137.5	37	4.81	82.70	41773861.2	5.06	16.57
137.5 - 158.8	39	5.07	87.78	66270559.6	8.02	24.59
158.8 - 184.5	38	4.94	92.72	96262762.8	11.65	36.24
184.5 - 214.5	22	2.86	95.58	88570856.1	10.72	46.96
214.5 - 249.2	19	2.47	98.05	120027539	14.53	61.48
249.2 - 289.5	6	0.78	98.83	60633014.5	7.34	68.82
289.5 - 336.5	4	0.52	99.35	65177993.8	7.89	76.71
336.5 - 391	3	0.39	99.74	71440525.7	8.65	85.35
391 - 454.4	0	0.00	99.74	0	0.00	85.35
454.4 - 528	2	0.26	100.00	121056217	14.65	100.00
528 - 614	0	0.00	100.00	0	0.00	100.00
614 - 713.8	0	0.00	100.00	0	0.00	100.00
713.8 - 829.8	0	0.00	100.00	0	0.00	100.00
829.8 - 964.7	0	0.00	100.00	0	0.00	100.00
964.7 - 1121.5	0	0.00	100.00	0	0.00	100.00
1121.5 - 1303.8	0	0.00	100.00	0	0.00	100.00
1303.8 - 1515.7	0	0.00	100.00	0	0.00	100.00
Total	769	100.00		826348938	100.00	
Median (µm)			[redacted]			[redacted]

Table C.4.7. Size distribution of sample from system-Po on Apr. 7, 1997.

Size classes μm	Frequency	Frequency %	Cumulative frequency %	Spherical volume	Volume %	Cumulative volume %
< 8.3	0	0.00	0.00	0	0.00	0.00
8.3 - 9.6	1	0.08	0.08	432.077772	0.00	0.00
9.6 - 11.1	5	0.42	0.50	2987.66177	0.00	0.00
11.1 - 12.9	6	0.50	1.00	6091.70239	0.00	0.00
12.9 - 15	16	1.34	2.34	22986.9076	0.00	0.00
15 - 17.4	34	2.85	5.19	78825.7606	0.01	0.02
17.4 - 20.1	34	2.85	8.03	115652.418	0.02	0.03
20.1 - 23.3	51	4.27	12.30	278304.587	0.04	0.08
23.3 - 27	67	5.61	17.91	577405.404	0.09	0.16
27 - 31.3	97	8.12	26.03	1227302.45	0.19	0.35
31.3 - 36.3	95	7.95	33.97	1901486.59	0.29	0.63
36.3 - 42.1	104	8.70	42.68	3213975.77	0.48	1.12
42.1 - 48.8	101	8.45	51.13	4866230.36	0.73	1.85
48.8 - 56.6	103	8.62	59.75	7928202.82	1.20	3.05
56.6 - 65.6	77	6.44	66.19	9145132.7	1.38	4.43
65.6 - 76	82	6.86	73.05	15237322	2.30	6.72
76 - 88.1	76	6.36	79.41	22194624.3	3.35	10.07
88.1 - 102.1	48	4.02	83.43	21033910.5	3.17	13.24
102.1 - 118.4	52	4.35	87.78	35631276.3	5.37	18.61
118.4 - 137.5	47	3.93	91.72	51810286.8	7.81	26.42
137.5 - 158.8	31	2.59	94.31	52294053.4	7.88	34.30
158.8 - 184.5	25	2.09	96.40	64169163.6	9.67	43.98
184.5 - 214.5	21	1.76	98.16	89305490.2	13.46	57.44
214.5 - 249.2	10	0.84	99.00	64622141.9	9.74	67.18
249.2 - 289.5	5	0.42	99.41	53013016.2	7.99	75.17
289.5 - 336.5	5	0.42	99.83	81132551.7	12.23	87.40
336.5 - 391	1	0.08	99.92	21080524.4	3.18	90.58
391 - 454.4	0	0.00	99.92	0	0.00	90.58
454.4 - 528	1	0.08	100.00	62480476	9.42	100.00
528 - 614	0	0.00	100.00	0	0.00	100.00
614 - 713.8	0	0.00	100.00	0	0.00	100.00
713.8 - 829.8	0	0.00	100.00	0	0.00	100.00
829.8 - 964.7	0	0.00	100.00	0	0.00	100.00
964.7 - 1121.5	0	0.00	100.00	0	0.00	100.00
1121.5 - 1303.8	0	0.00	100.00	0	0.00	100.00
1303.8 - 1515.7	0	0.00	100.00	0	0.00	100.00
Total	1195	100.00		663369855	100.00	
Median (μm)			[redacted]			[redacted]

Table C.4.8. Size distribution of sample from system-Po on Apr. 14, 1997.

Size classes μm	Frequency	Frequency %	Cumulative frequency %	Spherical volume	Volume %	Cumulative volume %
< 8.3	0	0.00	0.00	0	0.00	0.00
8.3 - 9.6	4	0.35	0.35	1466.08418	0.00	0.00
9.6 - 11.1	15	1.32	1.67	9886.61661	0.00	0.00
11.1 - 12.9	19	1.67	3.35	18269.1388	0.00	0.00
12.9 - 15	13	1.15	4.49	17594.8313	0.00	0.00
15 - 17.4	42	3.70	8.19	95149.784	0.01	0.01
17.4 - 20.1	55	4.85	13.04	193151.843	0.02	0.03
20.1 - 23.3	54	4.76	17.80	292493.408	0.03	0.06
23.3 - 27	49	4.32	22.11	416906.656	0.04	0.10
27 - 31.3	76	6.70	28.81	988822.049	0.09	0.19
31.3 - 36.3	73	6.43	35.24	1486612.02	0.14	0.33
36.3 - 42.1	72	6.34	41.59	2235599.98	0.21	0.53
42.1 - 48.8	91	8.02	49.60	4513846.89	0.42	0.95
48.8 - 56.6	85	7.49	57.09	6478390.17	0.60	1.55
56.6 - 65.6	92	8.11	65.20	10854123.5	1.00	2.55
65.6 - 76	75	6.61	71.81	13980226.8	1.29	3.84
76 - 88.1	76	6.70	78.50	21991608.7	2.03	5.87
88.1 - 102.1	66	5.81	84.32	29582720.6	2.73	8.60
102.1 - 118.4	41	3.61	87.93	29529909.9	2.73	11.33
118.4 - 137.5	41	3.61	91.54	43149601.8	3.98	15.31
137.5 - 158.8	37	3.26	94.80	62002823.1	5.72	21.04
158.8 - 184.5	14	1.23	96.04	36231819	3.35	24.38
184.5 - 214.5	22	1.94	97.97	91052211	8.41	32.79
214.5 - 249.2	3	0.26	98.24	18777147.2	1.73	34.52
249.2 - 289.5	6	0.53	98.77	60974793.8	5.63	40.15
289.5 - 336.5	11	0.97	99.74	177491202	16.39	56.54
336.5 - 391	0	0.00	99.74	0	0.00	56.54
391 - 454.4	2	0.18	99.91	88211160.4	8.14	64.68
454.4 - 528	0	0.00	99.91	0	0.00	64.68
528 - 614	0	0.00	99.91	0	0.00	64.68
614 - 713.8	0	0.00	99.91	0	0.00	64.68
713.8 - 829.8	0	0.00	99.91	0	0.00	64.68
829.8 - 964.7	1	0.09	100.00	382494290	35.32	100.00
964.7 - 1121.5	0	0.00	100.00	0	0.00	100.00
1121.5 - 1303.8	0	0.00	100.00	0	0.00	100.00
1303.8 - 1515.7	0	0.00	100.00	0	0.00	100.00
Total	1135	100.00		1083071827	100.00	
Median (μm)			[redacted]			[redacted]

Table C.4.9. Size distribution of sample from system-Po on Apr. 21, 1997.

Size classes μm	Frequency	Frequency %	Cumulative frequency %	Spherical volume	Volume %	Cumulative volume %
< 8.3	0	0.00	0.00	0	0.00	0.00
8.3 - 9.6	1	0.09	0.09	427.294811	0.00	0.00
9.6 - 11.1	13	1.11	1.19	8032.62319	0.00	0.00
11.1 - 12.9	10	0.85	2.04	9483.40478	0.00	0.00
12.9 - 15	10	0.85	2.89	14349.2518	0.00	0.00
15 - 17.4	25	2.13	5.02	56624.5825	0.01	0.01
17.4 - 20.1	36	3.06	8.09	120285.838	0.01	0.02
20.1 - 23.3	37	3.15	11.23	202758.174	0.02	0.04
23.3 - 27	42	3.57	14.81	356632.016	0.03	0.07
27 - 31.3	51	4.34	19.15	674929.411	0.07	0.14
31.3 - 36.3	56	4.77	23.91	1096306.8	0.11	0.25
36.3 - 42.1	65	5.53	29.45	2085425.22	0.20	0.45
42.1 - 48.8	81	6.89	36.34	4097267.69	0.40	0.85
48.8 - 56.6	78	6.64	42.98	6016256.28	0.59	1.44
56.6 - 65.6	82	6.98	49.96	9902261.25	0.97	2.40
65.6 - 76	108	9.19	59.15	19856357.5	1.94	4.34
76 - 88.1	78	6.64	65.79	22811448.5	2.23	6.57
88.1 - 102.1	81	6.89	72.68	36222200.4	3.53	10.10
102.1 - 118.4	72	6.13	78.81	51277428.7	5.00	15.10
118.4 - 137.5	81	6.89	85.70	89035766.4	8.69	23.79
137.5 - 158.8	58	4.94	90.64	95078886.1	9.28	33.06
158.8 - 184.5	45	3.83	94.47	119105748	11.62	44.68
184.5 - 214.5	35	2.98	97.45	146982809	14.34	59.02
214.5 - 249.2	13	1.11	98.55	81820785.9	7.98	67.00
249.2 - 289.5	8	0.68	99.23	75865771.2	7.40	74.41
289.5 - 336.5	3	0.26	99.49	47710280.7	4.65	79.06
336.5 - 391	5	0.43	99.91	129687575	12.65	91.71
391 - 454.4	0	0.00	99.91	0	0.00	91.71
454.4 - 528	0	0.00	99.91	0	0.00	91.71
528 - 614	1	0.09	100.00	84958988.2	8.29	100.00
614 - 713.8	0	0.00	100.00	0	0.00	100.00
713.8 - 829.8	0	0.00	100.00	0	0.00	100.00
829.8 - 964.7	0	0.00	100.00	0	0.00	100.00
964.7 - 1121.5	0	0.00	100.00	0	0.00	100.00
1121.5 - 1303.8	0	0.00	100.00	0	0.00	100.00
1303.8 - 1515.7	0	0.00	100.00	0	0.00	100.00
Total	1175	100.00		1025055085	100.00	
Median (μm)			[redacted]			[redacted]

Table C.4.10. Size distribution of sample from system-Po on Apr. 28, 1997.

Size classes μm	Frequency	Frequency %	Cumulative frequency %	Spherical volume	Volume %	Cumulative volume %
< 8.3	0	0.00	0.00	0	0.00	0.00
8.3 - 9.6	5	0.40	0.40	2136.47405	0.00	0.00
9.6 - 11.1	7	0.56	0.96	4516.34026	0.00	0.00
11.1 - 12.9	9	0.72	1.68	8618.62089	0.00	0.00
12.9 - 15	15	1.20	2.87	21161.0344	0.00	0.00
15 - 17.4	25	2.00	4.87	54157.7728	0.00	0.01
17.4 - 20.1	22	1.76	6.62	74116.6761	0.01	0.01
20.1 - 23.3	30	2.39	9.02	165142.552	0.01	0.03
23.3 - 27	36	2.87	11.89	293495.436	0.03	0.06
27 - 31.3	40	3.19	15.08	529912.766	0.05	0.10
31.3 - 36.3	52	4.15	19.23	1113593.4	0.10	0.20
36.3 - 42.1	66	5.27	24.50	2091420.96	0.19	0.39
42.1 - 48.8	77	6.15	30.65	3862034.03	0.35	0.74
48.8 - 56.6	92	7.34	37.99	7161806.56	0.64	1.38
56.6 - 65.6	107	8.54	46.53	12841126.4	1.15	2.53
65.6 - 76	113	9.02	55.55	20630499.4	1.85	4.37
76 - 88.1	119	9.50	65.04	34461403.8	3.08	7.46
88.1 - 102.1	93	7.42	72.47	40816531.1	3.65	11.11
102.1 - 118.4	101	8.06	80.53	69874844.2	6.25	17.36
118.4 - 137.5	80	6.38	86.91	87046552.2	7.79	25.15
137.5 - 158.8	50	3.99	90.90	86402513	7.73	32.88
158.8 - 184.5	57	4.55	95.45	143832047	12.87	45.76
184.5 - 214.5	25	2.00	97.45	103382748	9.25	55.01
214.5 - 249.2	11	0.88	98.32	68196681.8	6.10	61.11
249.2 - 289.5	7	0.56	98.88	77401390.6	6.93	68.04
289.5 - 336.5	5	0.40	99.28	83381002.8	7.46	75.50
336.5 - 391	6	0.48	99.76	143140185	12.81	88.31
391 - 454.4	2	0.16	99.92	72012926.7	6.44	94.75
454.4 - 528	1	0.08	100.00	58613963.7	5.25	100.00
528 - 614	0	0.00	100.00	0	0.00	100.00
614 - 713.8	0	0.00	100.00	0	0.00	100.00
713.8 - 829.8	0	0.00	100.00	0	0.00	100.00
829.8 - 964.7	0	0.00	100.00	0	0.00	100.00
964.7 - 1121.5	0	0.00	100.00	0	0.00	100.00
1121.5 - 1303.8	0	0.00	100.00	0	0.00	100.00
1303.8 - 1515.7	0	0.00	100.00	0	0.00	100.00
Total	1253	100.00		1117416529	100.00	
Median (μm)			68.6			198.3

APPENDIX D

DATA OF FLOC SHAPE

Table D.1.1. Distribution of floc shape of sample from system-Dm on Nov. 16, 1996.

Form Factor range	Frequency	Frequency %
0.1	3	0.30
0.2	20	1.99
0.3	31	3.08
0.4	48	4.77
0.5	103	10.24
0.6	276	27.44
0.7	225	22.37
0.8	185	18.39
0.9	111	11.03
1	4	0.40
Total	1006	100
Median		[illegible]

Aspect Ratio range	Frequency	Frequency %
2	806	83.44
3	136	14.08
4	21	2.17
5	3	0.31
6	0	0.00
7	0	0.00
8	0	0.00
9	0	0.00
10	0	0.00
11	0	0.00
12	0	0.00
Total	966	100.00
Median		[illegible]

Table D.1.2. Distribution of floc shape of sample from system-Dm on Nov. 20, 1996.

Form Factor range	Frequency	Frequency %
0.1	11	1.89
0.2	41	7.03
0.3	49	8.40
0.4	64	10.98
0.5	71	12.18
0.6	79	13.55
0.7	79	13.55
0.8	71	12.18
0.9	63	10.81
1	55	9.43
Total	583	100
Median		[illegible]

Aspect Ratio range	Frequency	Frequency %
2	304	52.14
3	196	33.62
4	63	10.81
5	9	1.54
6	0	0.00
7	2	0.34
8	1	0.17
9	4	0.69
10	4	0.69
11	0	0.00
12	0	0.00
Total	583	100.00
Median		[illegible]

Table D.1.3. Distribution of floc shape of sample from system-Dm on Dec. 4, 1996.

Form Factor range	Frequency	Frequency %
0.1	6	1.04
0.2	40	6.93
0.3	53	9.19
0.4	69	11.96
0.5	74	12.82
0.6	55	9.53
0.7	83	14.38
0.8	69	11.96
0.9	65	11.27
1	63	10.92
Total	577	100
Median		[illegible]

Aspect Ratio range	Frequency	Frequency %
2	311	53.90
3	198	34.32
4	44	7.63
5	15	2.60
6	4	0.69
7	3	0.52
8	1	0.17
9	1	0.17
10	0	0.00
11	0	0.00
12	0	0.00
Total	577	100.00
Median		[illegible]

Table D.1.4. Distribution of floc shape of sample from system-Dm on Dec. 10, 1996.

Form Factor range	Frequency	Frequency %
0.1	23	4.12
0.2	75	13.44
0.3	82	14.70
0.4	58	10.39
0.5	67	12.01
0.6	48	8.60
0.7	47	8.42
0.8	46	8.24
0.9	50	8.96
1	62	11.11
Total	558	100
Median		[illegible]

Aspect Ratio range	Frequency	Frequency %
2	303	54.30
3	202	36.20
4	33	5.91
5	10	1.79
6	4	0.72
7	1	0.18
8	1	0.18
9	3	0.54
10	0	0.00
11	0	0.00
12	1	0.18
Total	558	100.00
Median		[illegible]

Table D.1.5. Distribution of floc shape of sample from system-Dm on Jan. 22, 1997.

Form Factor range	Frequency	Frequency %
0.1	9	1.50
0.2	68	11.31
0.3	63	10.48
0.4	80	13.31
0.5	57	9.48
0.6	59	9.82
0.7	74	12.31
0.8	64	10.65
0.9	65	10.82
1	62	10.32
Total	601	100
Median		[illegible]

Aspect Ratio range	Frequency	Frequency %
2	337	56.17
3	202	33.67
4	39	6.50
5	15	2.50
6	2	0.33
7	3	0.50
8	2	0.33
9	0	0.00
10	0	0.00
11	0	0.00
12	0	0.00
Total	600	100.00
Median		[illegible]

Table D.1.6. Distribution of floc shape of sample from system-Dm on Jan. 29, 1997.

Form Factor range	Frequency	Frequency %
0.1	12	1.81
0.2	65	9.82
0.3	86	12.99
0.4	95	14.35
0.5	83	12.54
0.6	71	10.73
0.7	55	8.31
0.8	53	8.01
0.9	75	11.33
1	67	10.12
Total	662	100
Median		[illegible]

Aspect Ratio range	Frequency	Frequency %
2	397	59.97
3	201	30.36
4	39	5.89
5	12	1.81
6	4	0.60
7	6	0.91
8	2	0.30
9	0	0.00
10	1	0.15
11	0	0.00
12	0	0.00
Total	662	100.00
Median		[illegible]

Table D.1.7. Distribution of floc shape of sample from system-Dm on Feb. 4, 1997.

Form Factor range	Frequency	Frequency %
0.1	7	0.96
0.2	78	10.74
0.3	107	14.74
0.4	102	14.05
0.5	98	13.50
0.6	80	11.02
0.7	85	11.71
0.8	72	9.92
0.9	56	7.71
1	41	5.65
Total	726	100
Median		[illegible]

Aspect Ratio range	Frequency	Frequency %
2	422	58.13
3	245	33.75
4	42	5.79
5	7	0.96
6	3	0.41
7	3	0.41
8	2	0.28
9	0	0.00
10	1	0.14
11	0	0.00
12	0	0.00
13	0	0.00
14	1	0.14
Total	726	100.00
Median		[illegible]

Table D.1.8. Distribution of floc shape of sample from system-Dm on Feb. 12, 1997.

Form Factor range	Frequency	Frequency %
0.1	21	2.85
0.2	100	13.57
0.3	98	13.30
0.4	98	13.30
0.5	82	11.13
0.6	81	10.99
0.7	58	7.87
0.8	79	10.72
0.9	51	6.92
1	69	9.36
Total	737	100
Median		[illegible]

Aspect Ratio range	Frequency	Frequency %
2	447	60.65
3	229	31.07
4	45	6.11
5	8	1.09
6	2	0.27
7	5	0.68
8	1	0.14
9	0	0.00
10	0	0.00
11	0	0.00
12	0	0.00
13	0	0.00
14	0	0.00
Total	737	100.00
Median		[illegible]

Table D.2.1. Distribution of floc shape of sample from system-Py on Dec. 9, 1996.

Form Factor range	Frequency	Frequency %
0.1	11	2.4
0.2	36	7.8
0.3	30	6.5
0.4	66	14.3
0.5	49	10.6
0.6	46	10.0
0.7	51	11.1
0.8	54	11.7
0.9	56	12.1
1	62	13.4
Total	461	100
Median		0.587

Aspect Ratio range	Frequency	Frequency %
2	220	47.7
3	152	33.0
4	48	10.4
5	19	4.1
6	3	0.7
7	7	1.5
8	4	0.9
9	5	1.1
10	1	0.2
11	0	0.0
12	2	0.4
Total	461	100
Median		2.02

Table D.2.2. Distribution of floc shape of sample from system-Py on Jan. 13, 1997.

Form Factor range	Frequency	Frequency %
0.1	16	2.94
0.2	67	12.32
0.3	61	11.21
0.4	56	10.29
0.5	59	10.85
0.6	53	9.74
0.7	61	11.21
0.8	47	8.64
0.9	61	11.21
1	63	11.58
Total	544	100
Median		0.52

Aspect Ratio range	Frequency	Frequency %
2	270	49.63
3	200	36.76
4	51	9.38
5	11	2.02
6	3	0.55
7	5	0.92
8	2	0.37
9	1	0.18
10	1	0.18
11	0	0
12	0	0
Total	544	100
Median		2.01

Table D.2.3. Distribution of floc shape of sample from system-Py on Jan. 28, 1997.

Form Factor range	Frequency	Frequency %
0.1	16	2.97
0.2	58	10.78
0.3	70	13.01
0.4	63	11.71
0.5	64	11.90
0.6	43	7.99
0.7	54	10.04
0.8	48	8.92
0.9	63	11.71
1	59	10.97
Total	538	100
Median		0.5

Aspect Ratio range	Frequency	Frequency %
2	292	53.68
3	191	35.11
4	31	5.70
5	11	2.02
6	2	0.37
7	3	0.55
8	4	0.74
9	3	0.55
10	1	0.18
11	0	0.00
12	0	0.00
Total	538	98.90
Median		1.95

Table D.2.4. Distribution of floc shape of sample from system-Py on Feb. 11, 1997.

Form Factor range	Frequency	Frequency %
0.1	20	3.34
0.2	65	10.87
0.3	81	13.55
0.4	84	14.05
0.5	71	11.87
0.6	58	9.70
0.7	53	8.86
0.8	39	6.52
0.9	61	10.20
1	66	11.04
Total	598	100
Median		[illegible]

Aspect Ratio range	Frequency	Frequency %
2	336	56.19
3	208	34.78
4	31	5.18
5	13	2.17
6	3	0.50
7	3	0.50
8	3	0.50
9	1	0.17
10	0	0.00
11	0	0.00
12	0	0.00
Total	598	100.00
Median		[illegible]

Table D.2.5. Distribution of floc shape of sample from system-Py on Feb. 25, 1997.

Form Factor range	Frequency	Frequency %
0.1	26	2.54
0.2	100	9.78
0.3	125	12.23
0.4	124	12.13
0.5	133	13.01
0.6	129	12.62
0.7	115	11.25
0.8	97	9.49
0.9	103	10.08
1	70	6.85
Total	1022	100
Median		[illegible]

Aspect Ratio range	Frequency	Frequency %
2	533	52.15
3	330	32.29
4	89	8.71
5	29	2.84
6	7	0.68
7	15	1.47
8	12	1.17
9	4	0.39
10	1	0.10
11	0	0.00
12	2	0.20
Total	1022	100.00
Median		[illegible]

Table D.2.6. Distribution of floc shape of sample from system-Py on Apr. 1, 1997.

Form Factor range	Frequency	Frequency %
0.1	10	1.39
0.2	70	9.72
0.3	102	14.17
0.4	111	15.42
0.5	73	10.14
0.6	95	13.19
0.7	71	9.86
0.8	74	10.28
0.9	65	9.03
1	49	6.81
Total	720	100
Median		[illegible]

Aspect Ratio range	Frequency	Frequency %
2	393	54.58
3	248	34.44
4	50	6.94
5	14	1.94
6	4	0.56
7	7	0.97
8	2	0.28
9	2	0.28
10	0	0.00
11	0	0.00
12	0	0.00
Total	720	100.00
Median		[illegible]

Table D.2.7. Distribution of floc shape of sample from system-Py on Apr. 8, 1997.

Form Factor range	Frequency	Frequency %
0.1	23	2.21
0.2	85	8.17
0.3	121	11.63
0.4	112	10.77
0.5	133	12.79
0.6	114	10.96
0.7	129	12.40
0.8	111	10.67
0.9	101	9.71
1	111	10.67
Total	1040	100
Median		[illegible]

Aspect Ratio range	Frequency	Frequency %
2	510	49.04
3	328	31.54
4	105	10.10
5	39	3.75
6	12	1.15
7	21	2.02
8	9	0.87
9	7	0.67
10	3	0.29
11	0	0.00
12	4	0.38
13	1	0.10
14	0	0.00
15	0	0.00
16	1	0.10
Total	1040	100.00
Median		[illegible]

Table D.2.8. Distribution of floc shape of sample from system-Py on Apr. 15, 1997.

Form Factor range	Frequency	Frequency %
0.1	15	1.37
0.2	69	6.30
0.3	144	13.15
0.4	131	11.96
0.5	132	12.05
0.6	130	11.87
0.7	125	11.42
0.8	108	9.86
0.9	122	11.14
1	119	10.87
Total	1095	100
Median		[illegible]

Aspect Ratio range	Frequency	Frequency %
2	615	56.16
3	380	34.70
4	70	6.39
5	21	1.92
6	3	0.27
7	3	0.27
8	2	0.18
9	0	0.00
10	1	0.09
11	0	0.00
12	0	0.00
Total	1095	100.00
Median		[illegible]

Table D.2.9. Distribution of floc shape of sample from system-Py on Apr. 22, 1997.

Form Factor range	Frequency	Frequency %
0.1	13	1.01
0.2	72	5.60
0.3	125	9.72
0.4	142	11.04
0.5	147	11.43
0.6	155	12.05
0.7	198	15.40
0.8	160	12.44
0.9	138	10.73
1	136	10.58
Total	1286	100
Median		[illegible]

Aspect Ratio range	Frequency	Frequency %
2	718	55.83
3	426	33.13
4	96	7.47
5	25	1.94
6	2	0.16
7	14	1.09
8	5	0.39
9	0	0.00
10	0	0.00
11	0	0.00
12	0	0.00
Total	1286	100.00
Median		[illegible]

Table D.3.1. Distribution of floc shape of sample from system-Pm on Oct. 15, 1996.

Form Factor range	Frequency	Frequency %
0.1	40	3.97
0.2	24	2.38
0.3	34	3.38
0.4	42	4.17
0.5	70	6.95
0.6	216	21.45
0.7	192	19.07
0.8	237	23.54
0.9	147	14.60
1	5	0.50
Total	1007	100
Median		[illegible]

Aspect Ratio range	Frequency	Frequency %
2	800	83.68
3	116	12.13
4	27	2.82
5	6	0.63
6	2	0.21
7	3	0.31
8	0	0.00
9	0	0.00
10	1	0.10
11	1	0.10
12	0	0.00
Total	956	100.00
Median		[illegible]

Table D.3.2. Distribution of floc shape of sample from system-Pm on Oct. 29, 1996.

Form Factor range	Frequency	Frequency %
0.1	60	6.01
0.2	63	6.31
0.3	77	7.72
0.4	114	11.42
0.5	123	12.32
0.6	131	13.13
0.7	131	13.13
0.8	170	17.03
0.9	128	12.83
1	1	0.10
Total	998	100
Median		[illegible]

Aspect Ratio range	Frequency	Frequency %
2	782	81.37
3	152	15.82
4	19	1.98
5	5	0.52
6	2	0.21
7	0	0.00
8	1	0.10
9	0	0.00
10	0	0.00
11	0	0.00
12	0	0.00
Total	961	100.00
Median		[illegible]

Table D.3.3. Distribution of floc shape of sample from system-Pm on Nov. 26, 1996.

Form Factor range	Frequency	Frequency %
0.1	25	5.57
0.2	52	11.58
0.3	50	11.14
0.4	51	11.36
0.5	40	8.91
0.6	46	10.24
0.7	48	10.69
0.8	60	13.36
0.9	40	8.91
1	37	8.24
Total	449	100
Median		[illegible]

Aspect Ratio range	Frequency	Frequency %
2	252	56.12
3	159	35.41
4	25	5.57
5	11	2.45
6	0	0.00
7	0	0.00
8	0	0.00
9	0	0.00
10	1	0.22
11	0	0.00
12	1	0.22
Total	449	100.00
Median		[illegible]

Table D.3.4. Distribution of floc shape of sample from system-Pm on Apr. 3, 1997.

Form Factor range	Frequency	Frequency %
0.1	46	3.23
0.2	128	8.99
0.3	184	12.92
0.4	160	11.24
0.5	161	11.31
0.6	181	12.71
0.7	145	10.18
0.8	134	9.41
0.9	135	9.48
1	150	10.53
Total	1424	100
Median		0.52

Aspect Ratio range	Frequency	Frequency %
2	685	48.10
3	525	36.87
4	149	10.46
5	38	2.67
6	3	0.21
7	18	1.26
8	4	0.28
9	2	0.14
10	0	0.00
11	0	0.00
12	0	0.00
Total	1424	100.00
Median		2.04

Table D.3.5. Distribution of floc shape of sample from system-Pm on Apr. 24, 1997.

Form Factor range	Frequency	Frequency %
0.1	31	2.77
0.2	154	13.74
0.3	162	14.45
0.4	158	14.09
0.5	144	12.85
0.6	115	10.26
0.7	114	10.17
0.8	77	6.87
0.9	89	7.94
1	77	6.87
Total	1121	100
Median		0.42

Aspect Ratio range	Frequency	Frequency %
2	591	52.72
3	369	32.92
4	96	8.56
5	25	2.23
6	2	0.18
7	20	1.78
8	6	0.54
9	6	0.54
10	4	0.36
11	0	0.00
12	1	0.09
13	1	0.09
Total	1121	100.00
Median		1.95

Table D.3.6. Distribution of floc shape of sample from system-Pm on May 1, 1997.

Form Factor range	Frequency	Frequency %
0.1	22	2.25
0.2	100	10.24
0.3	136	13.92
0.4	150	15.35
0.5	111	11.36
0.6	114	11.67
0.7	96	9.83
0.8	69	7.06
0.9	89	9.11
1	90	9.21
Total	977	100
Median		0.65

Aspect Ratio range	Frequency	Frequency %
2	567	58.03
3	300	30.71
4	69	7.06
5	21	2.15
6	4	0.41
7	11	1.13
8	3	0.31
9	2	0.20
10	0	0.00
11	0	0.00
12	0	0.00
Total	977	100.00
Median		1.89

Table D.3.7. Distribution of floc shape of sample from system-Pm on May 8, 1997.

Form Factor range	Frequency	Frequency %
0.1	5	0.44
0.2	69	6.12
0.3	128	11.35
0.4	163	14.45
0.5	160	14.18
0.6	142	12.59
0.7	122	10.82
0.8	123	10.90
0.9	105	9.31
1	111	9.84
Total	1128	100
Median		0.52

Aspect Ratio range	Frequency	Frequency %
2	649	57.54
3	370	32.80
4	78	6.91
5	18	1.60
6	2	0.18
7	4	0.35
8	6	0.53
9	1	0.09
10	0	0.00
11	0	0.00
12	0	0.00
Total	1128	100.00
Median		1.88

Table D.4.1. Distribution of floc shape of sample from system-Po on Nov. 18, 1996.

Form Factor range	Frequency	Frequency %
0.1	8	1.48
0.2	19	3.53
0.3	27	5.01
0.4	46	8.53
0.5	52	9.65
0.6	60	11.13
0.7	78	14.47
0.8	80	14.84
0.9	86	15.96
1	83	15.40
Total	539	100
Median		[illegible]

Aspect Ratio range	Frequency	Frequency %
2	309	57.33
3	168	31.17
4	44	8.16
5	8	1.48
6	0	0.00
7	3	0.56
8	1	0.19
9	4	0.74
10	1	0.19
11	0	0.00
12	1	0.19
Total	539	100.00
Median		[illegible]

Table D.4.2. Distribution of floc shape of sample from system-Po on Dec. 2, 1996.

Form Factor range	Frequency	Frequency %
0.1	7	1.61
0.2	16	3.69
0.3	21	4.84
0.4	53	12.21
0.5	44	10.14
0.6	54	12.44
0.7	58	13.36
0.8	61	14.06
0.9	58	13.36
1	62	14.29
Total	434	100
Median		[illegible]

Aspect Ratio range	Frequency	Frequency %
2	189	43.55
3	167	38.48
4	45	10.37
5	12	2.76
6	3	0.69
7	8	1.84
8	4	0.92
9	4	0.92
10	1	0.23
11	0	0.00
12	1	0.23
Total	434	100.00
Median		[illegible]

Table D.4.3. Distribution of floc shape of sample from system-Po on Jan. 20, 1997.

Form Factor range	Frequency	Frequency %
0.1	2	0.36
0.2	22	3.93
0.3	29	5.18
0.4	62	11.07
0.5	55	9.82
0.6	56	10.00
0.7	66	11.79
0.8	85	15.18
0.9	86	15.36
1	97	17.32
Total	560	100
Median		[illegible]

Aspect Ratio range	Frequency	Frequency %
2	289	51.61
3	195	34.82
4	39	6.96
5	14	2.50
6	2	0.36
7	12	2.14
8	5	0.89
9	0	0.00
10	1	0.18
11	1	0.18
12	2	0.36
Total	560	100.00
Median		[illegible]

Table D.4.4. Distribution of floc shape of sample from system-Po on Feb. 17, 1997.

Form Factor range	Frequency	Frequency %
0.1	2	0.22
0.2	32	3.52
0.3	74	8.13
0.4	104	11.43
0.5	141	15.49
0.6	124	13.63
0.7	131	14.40
0.8	113	12.42
0.9	108	11.87
1	81	8.90
Total	910	100
Median		[illegible]

Aspect Ratio range	Frequency	Frequency %
2	519	57.03
3	280	30.77
4	65	7.14
5	20	2.20
6	5	0.55
7	8	0.88
8	4	0.44
9	8	0.88
10	1	0.11
11	0	0.00
12	0	0.00
Total	910	100.00
Median		[illegible]

Table D.4.5. Distribution of floc shape of sample from system-Po on Mar. 31, 1997.

Form Factor range	Frequency	Frequency %
0.1	2	0.26
0.2	47	6.11
0.3	67	8.71
0.4	93	12.09
0.5	115	14.95
0.6	86	11.18
0.7	83	10.79
0.8	94	12.22
0.9	103	13.39
1	79	10.27
Total	769	100
Median		[illegible]

Aspect Ratio range	Frequency	Frequency %
2	420	54.76
3	252	32.86
4	58	7.56
5	20	2.61
6	2	0.26
7	7	0.91
8	2	0.26
9	4	0.52
10	1	0.13
11	0	0.00
12	1	0.13
13	0	0.00
14	0	0.00
15	0	0.00
16	0	0.00
17	0	0.00
18	1	0.13
19	0	0.00
20	0	0.00
21	0	0.00
22	0	0.00
23	0	0.00
24	1	0.13
Total	767	100.26
Median		[illegible]

Table D.4.6. Distribution of floc shape of sample from system-Po on Apr. 7, 1997.

Form Factor range	Frequency	Frequency %
0.1	7	0.59
0.2	25	2.09
0.3	83	6.95
0.4	119	9.96
0.5	150	12.55
0.6	174	14.56
0.7	152	12.72
0.8	175	14.64
0.9	152	12.72
1	158	13.22
Total	1195	100
Median		[illegible]

Aspect Ratio range	Frequency	Frequency %
2	666	55.78
3	386	32.33
4	99	8.29
5	25	2.09
6	3	0.25
7	8	0.67
8	4	0.34
9	0	0.00
10	0	0.00
11	0	0.00
12	1	0.08
13	0	0.00
14	0	0.00
15	0	0.00
16	0	0.00
17	1	0.08
18	0	0.00
19	0	0.00
20	0	0.00
21	0	0.00
22	0	0.00
23	1	0.08
Total	1194	100.00
Median		[illegible]

Table D.4.7. Distribution of floc shape of sample from system-Po on Apr. 14, 1997.

Form Factor range	Frequency	Frequency %
0.1	5	0.44
0.2	47	4.14
0.3	85	7.49
0.4	134	11.81
0.5	133	11.72
0.6	148	13.04
0.7	164	14.45
0.8	164	14.45
0.9	123	10.84
1	132	11.63
Total	1135	100
Median		[illegible]

Aspect Ratio range	Frequency	Frequency %
2	612	53.92
3	377	33.22
4	82	7.22
5	34	3.00
6	5	0.44
7	13	1.15
8	3	0.26
9	5	0.44
10	4	0.35
11	0	0.00
12	0	0.00
Total	1135	100.00
Median		[illegible]

Table D.4.8. Distribution of floc shape of sample from system-Po on Apr. 21, 1997.

Form Factor range	Frequency	Frequency %
0.1	4	0.34
0.2	53	4.51
0.3	116	9.87
0.4	137	11.66
0.5	164	13.96
0.6	138	11.74
0.7	148	12.60
0.8	156	13.28
0.9	140	11.91
1	119	10.13
Total	1175	100
Median		[illegible]

Aspect Ratio range	Frequency	Frequency %
2	700	59.57
3	343	29.19
4	81	6.89
5	29	2.47
6	4	0.34
7	13	1.11
8	4	0.34
9	0	0.00
10	1	0.09
11	0	0.00
12	0	0.00
Total	1175	100.00
Median		[illegible]

Table D.4.9. Distribution of floc shape of sample from system-Po on Apr. 28, 1997.

Form Factor range	Frequency	Frequency %
0.1	5	0.40
0.2	37	2.95
0.3	80	6.38
0.4	123	9.82
0.5	178	14.21
0.6	157	12.53
0.7	195	15.56
0.8	185	14.76
0.9	177	14.13
1	116	9.26
Total	1253	100
Median		[illegible]

Aspect Ratio range	Frequency	Frequency %
2	826	65.92
3	321	25.62
4	68	5.43
5	16	1.28
6	4	0.32
7	12	0.96
8	2	0.16
9	0	0.00
10	0	0.00
11	0	0.00
12	1	0.08
13	1	0.08
14	1	0.08
15	0	0.00
16	0	0.00
17	1	0.08
Total	1253	100.00
Median		[illegible]

APPENDIX E

DATA OF SETTLING VELOCITY MEASUREMENT

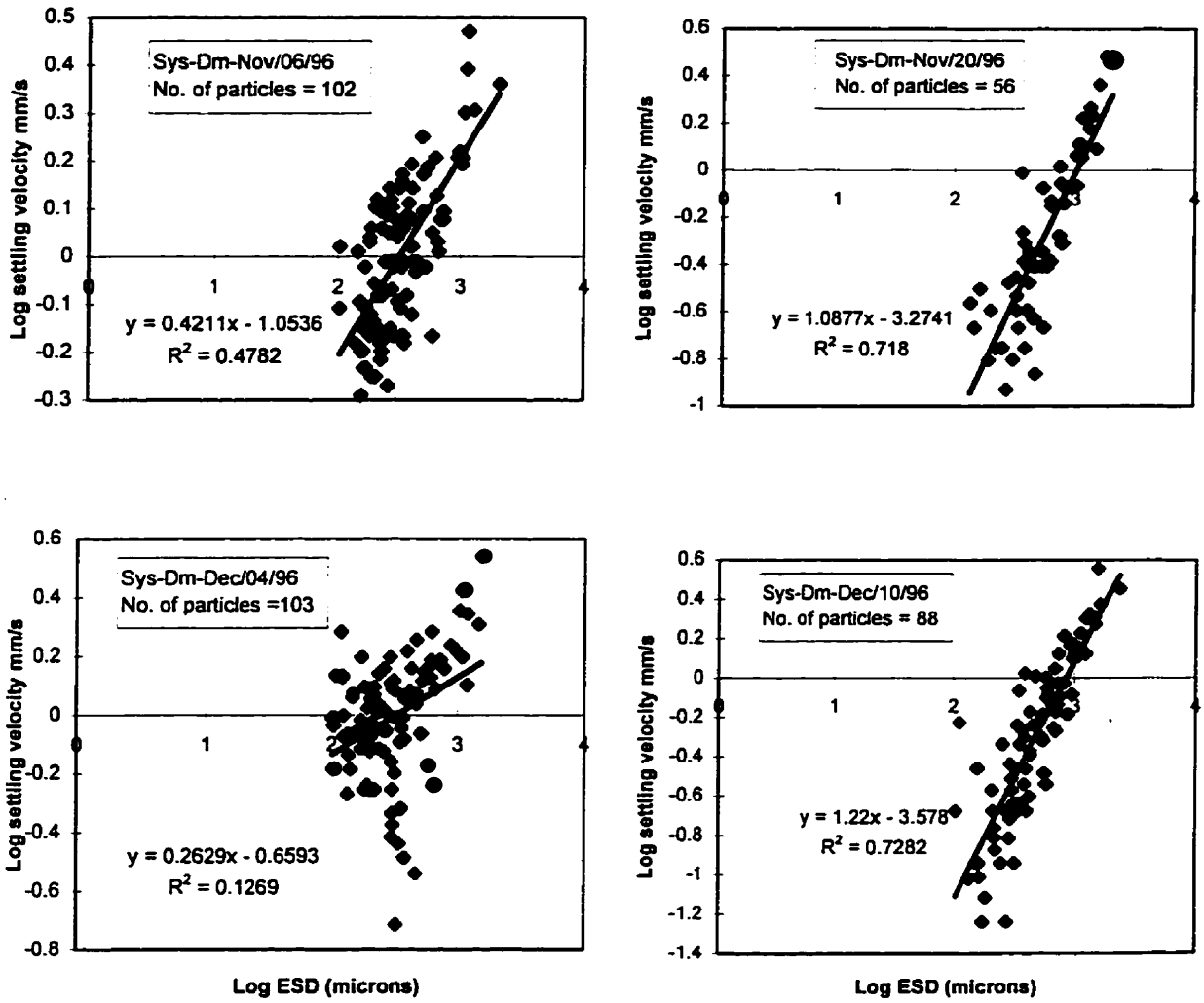

Figure E.1. The settling velocity as a function of ESD of sludge flocs from municipal wastewater treatment plant (system-Dm).

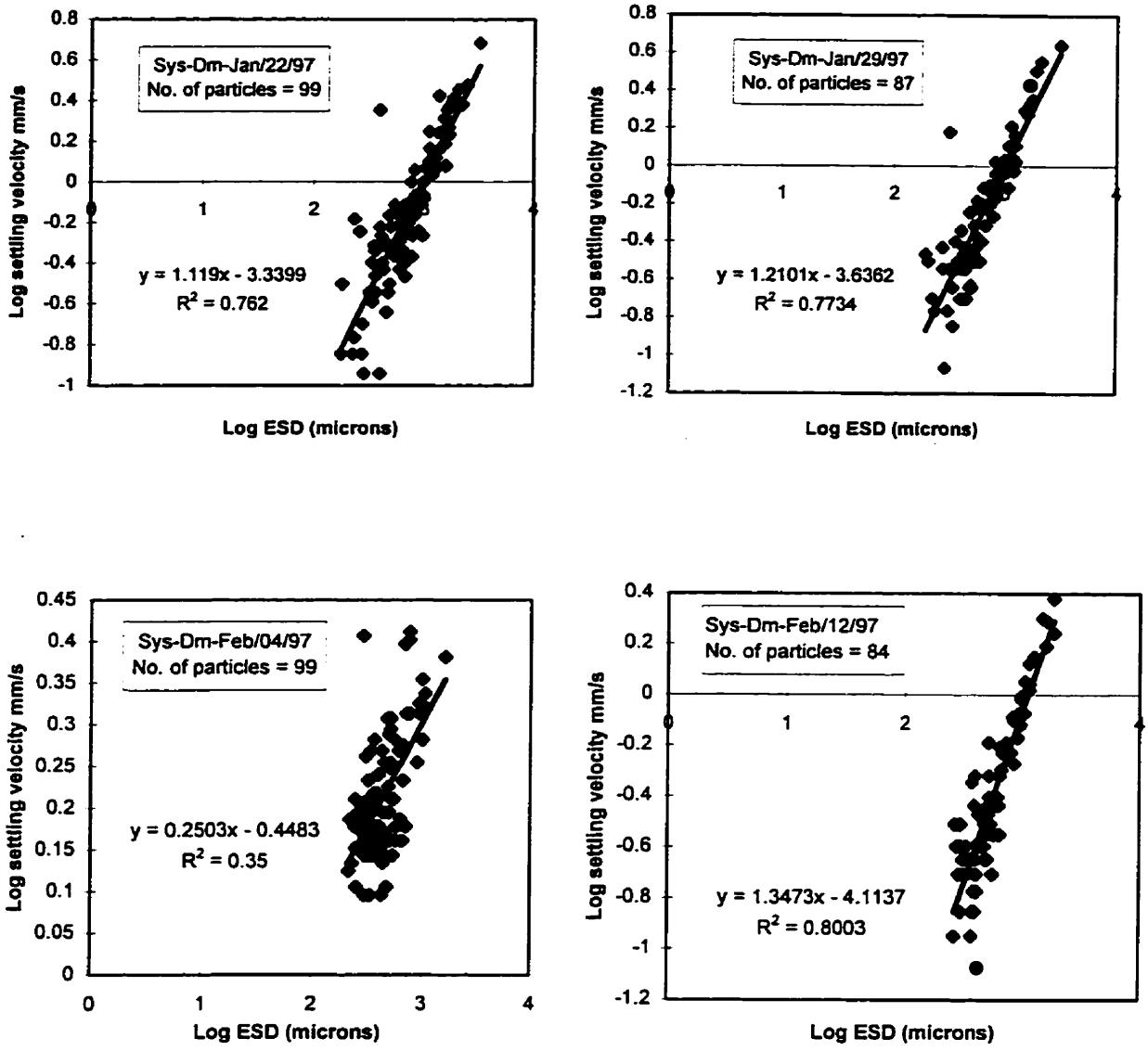

Figure E.1 (continued). The settling velocity as a function of ESD of sludge flocs from municipal wastewater treatment plant (system-Dm).

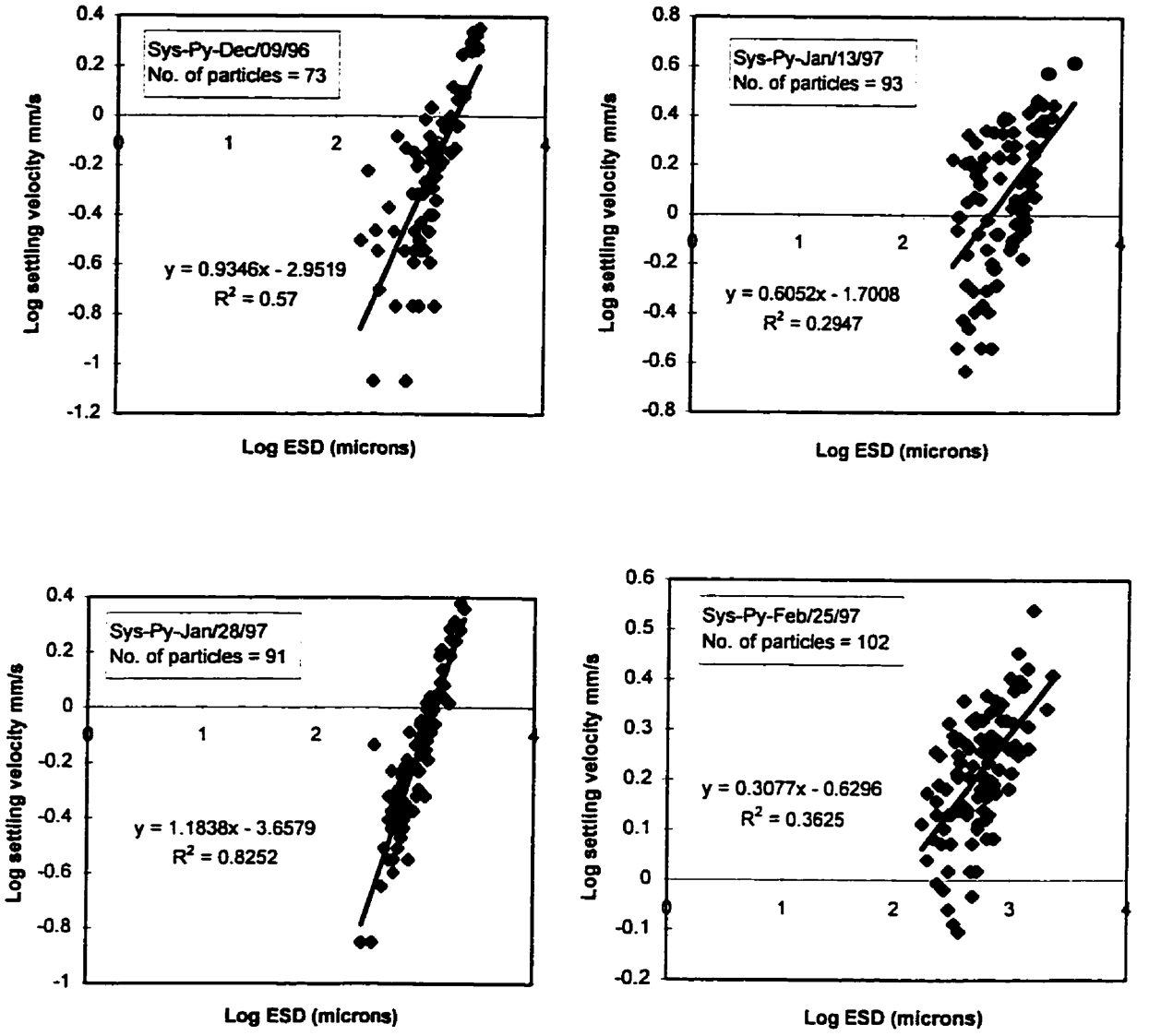

Figure E.2. The settling velocity as a function of ESD of sludge flocs from poultry processing wastewater treatment plant (system-Py).

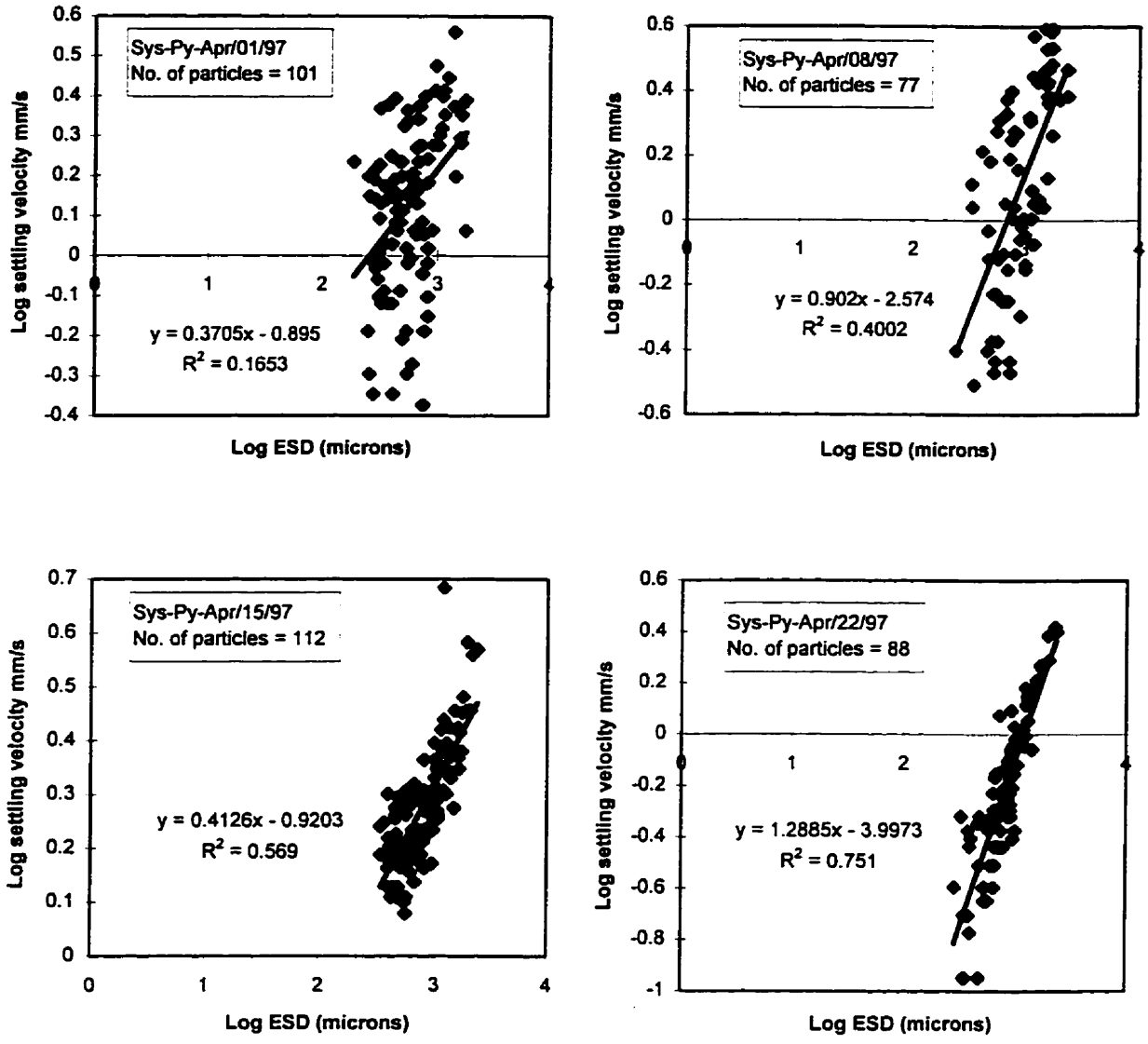

Figure E.2 (continued). The settling velocity as a function of ESD of sludge flocs from poultry processing wastewater treatment plant (system-Py).

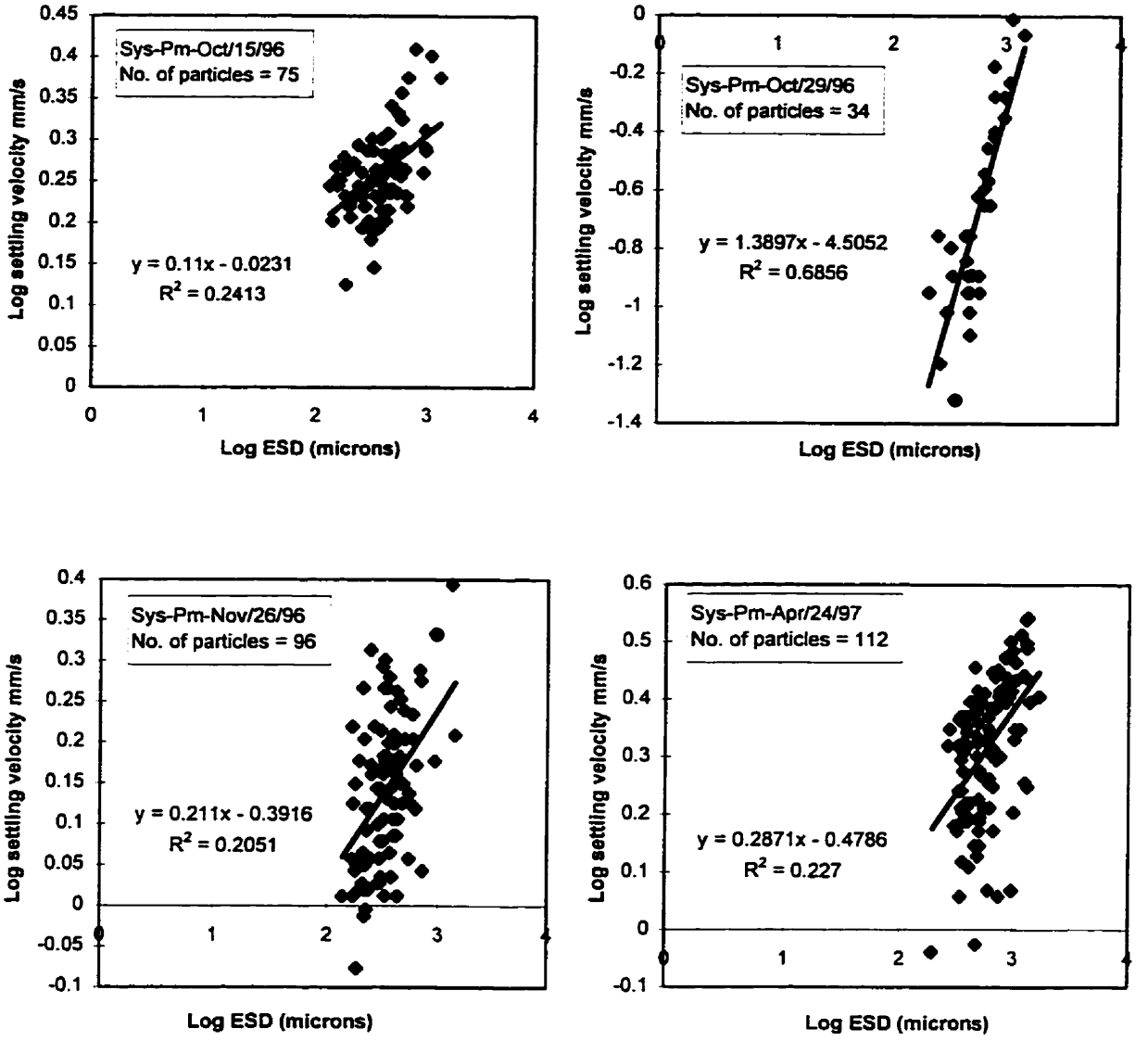

Figure E.3. The settling velocity as a function of ESD of sludge flocs from petroleum refinery wastewater treatment plant (system-Pm).

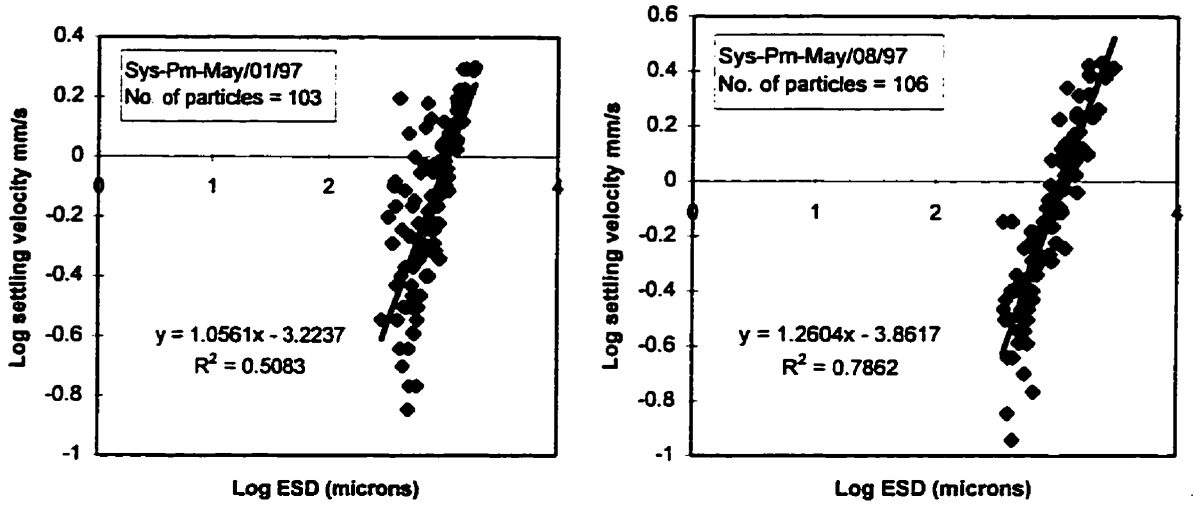

Figure E.3 (continued). The settling velocity as a function of ESD of sludge flocs from petroleum refinery wastewater treatment plant (system-Pm).

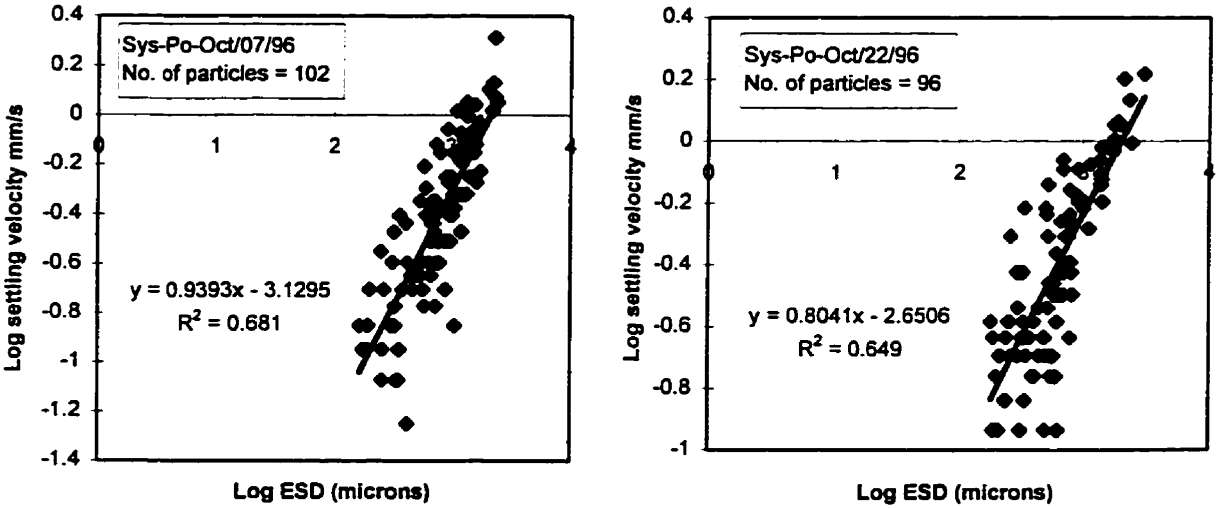

Figure E.4. The settling velocity as a function of ESD of sludge flocs from potato processing wastewater treatment plant (system-Po).

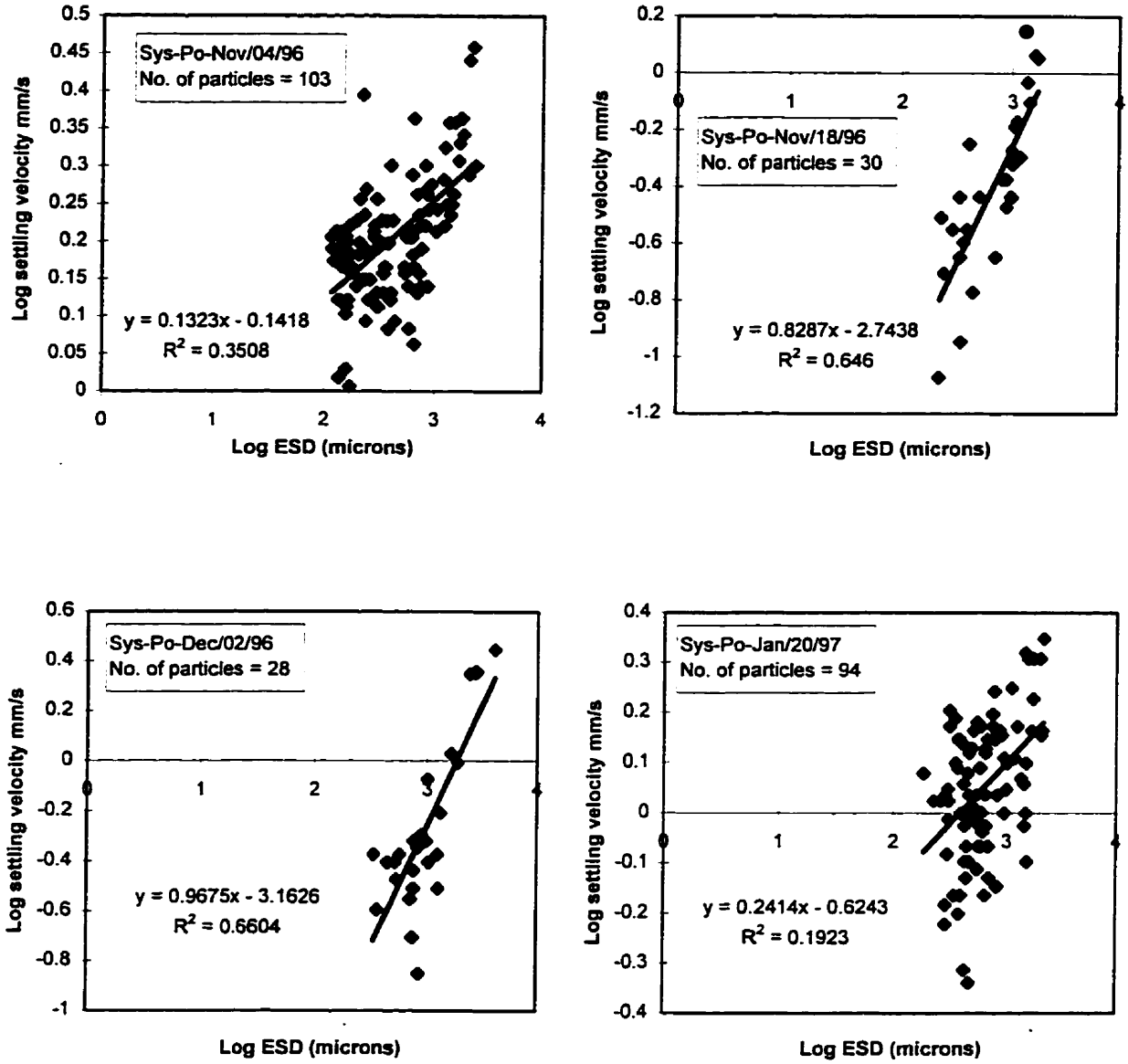

Figure E.4 (continued). The settling velocity as a function of ESD of sludge flocs from potato processing wastewater treatment plant (system-Po).

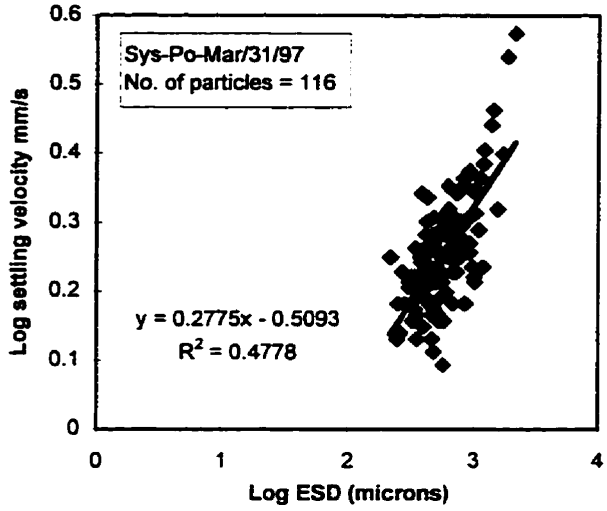

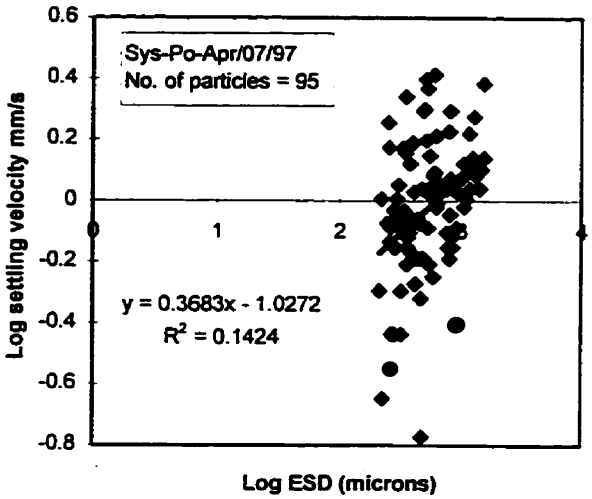

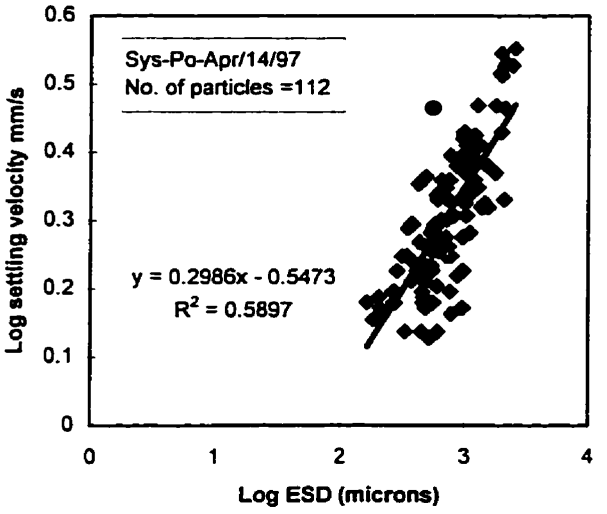

Figure E.4 (continued). The settling velocity as a function of ESD of sludge flocs from potato processing wastewater treatment plant (system-Po).

APPENDIX F

DATA OF EFFECTIVE DENSITY MEASUREMENT

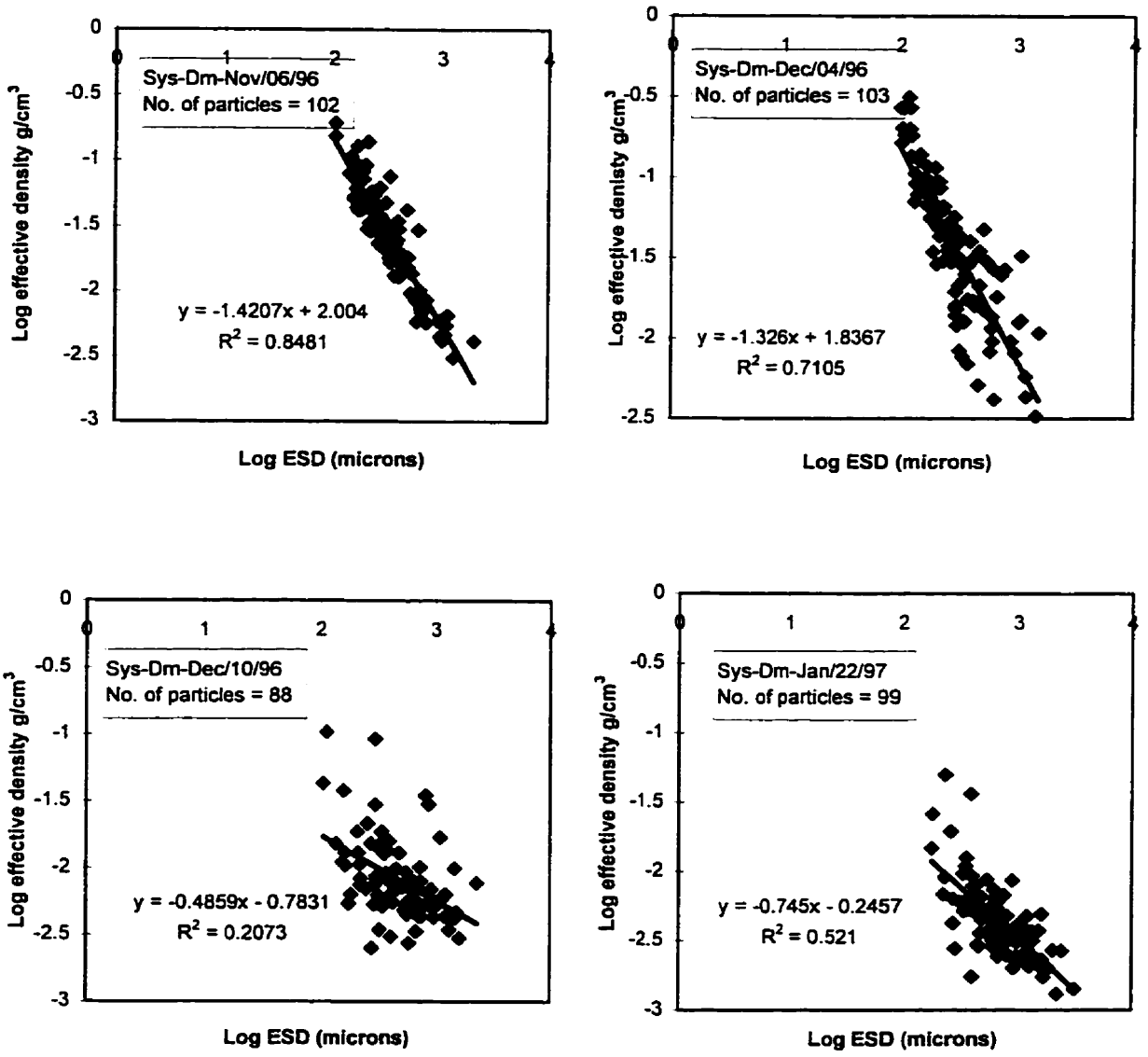

Figure F.1. The effective density as a function of ESD of sludge flocs from municipal wastewater treatment plant (system-Dm).

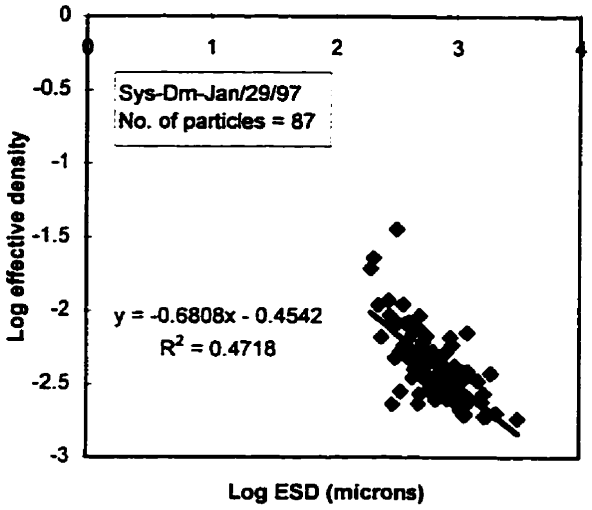

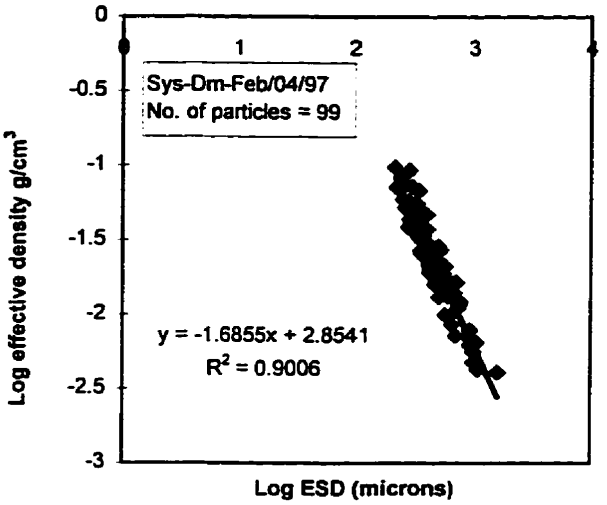

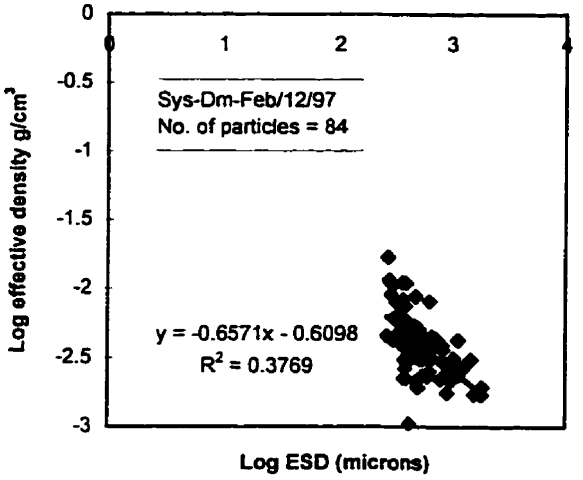

Figure F.1(continued). The effective density as a function of ESD of sludge flocs from municipal wastewater treatment plant (system-Dm).

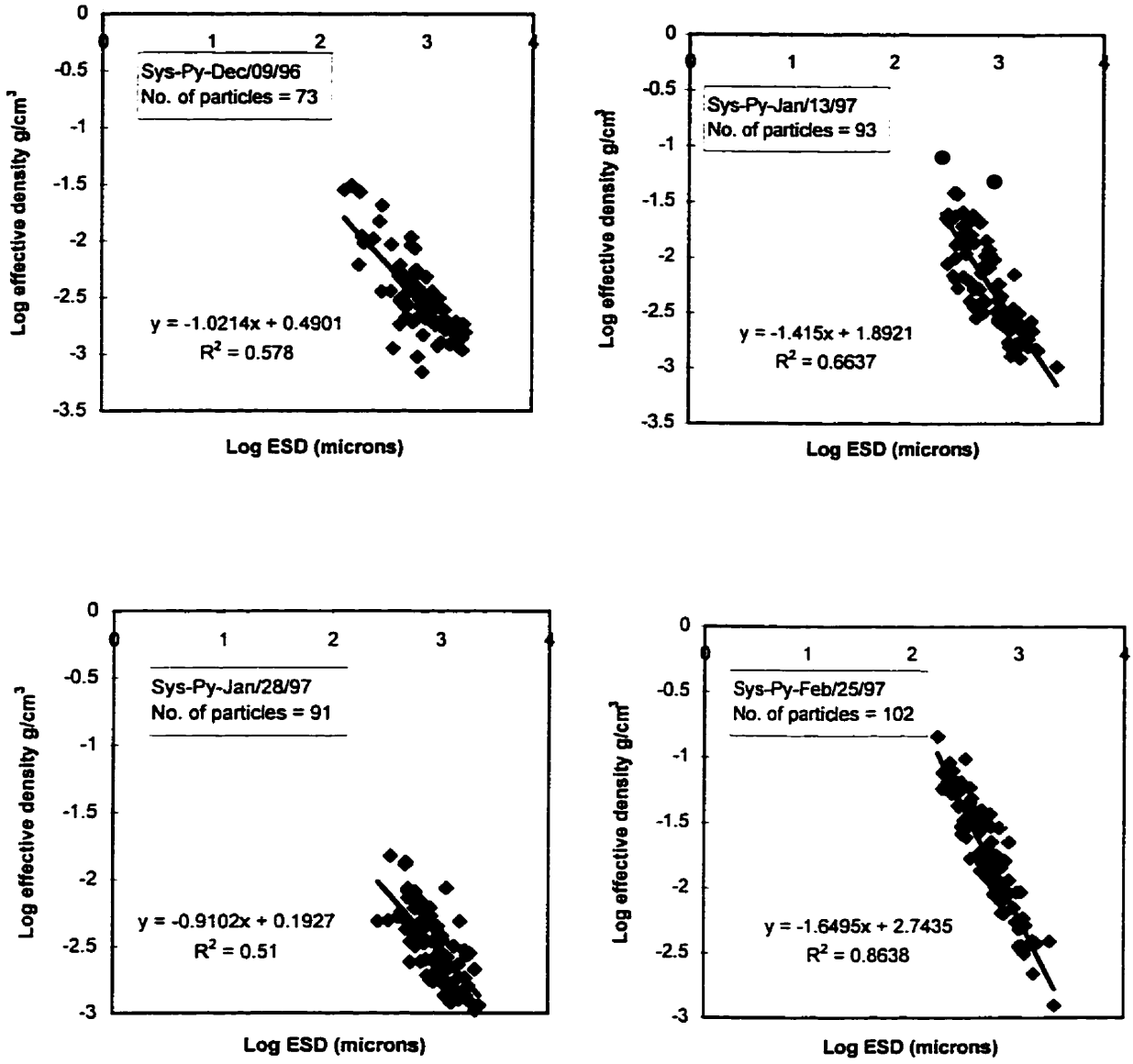

Figure F.2. The effective density as a function of ESD of sludge flocs from poultry processing wastewater treatment plant (system-Py).

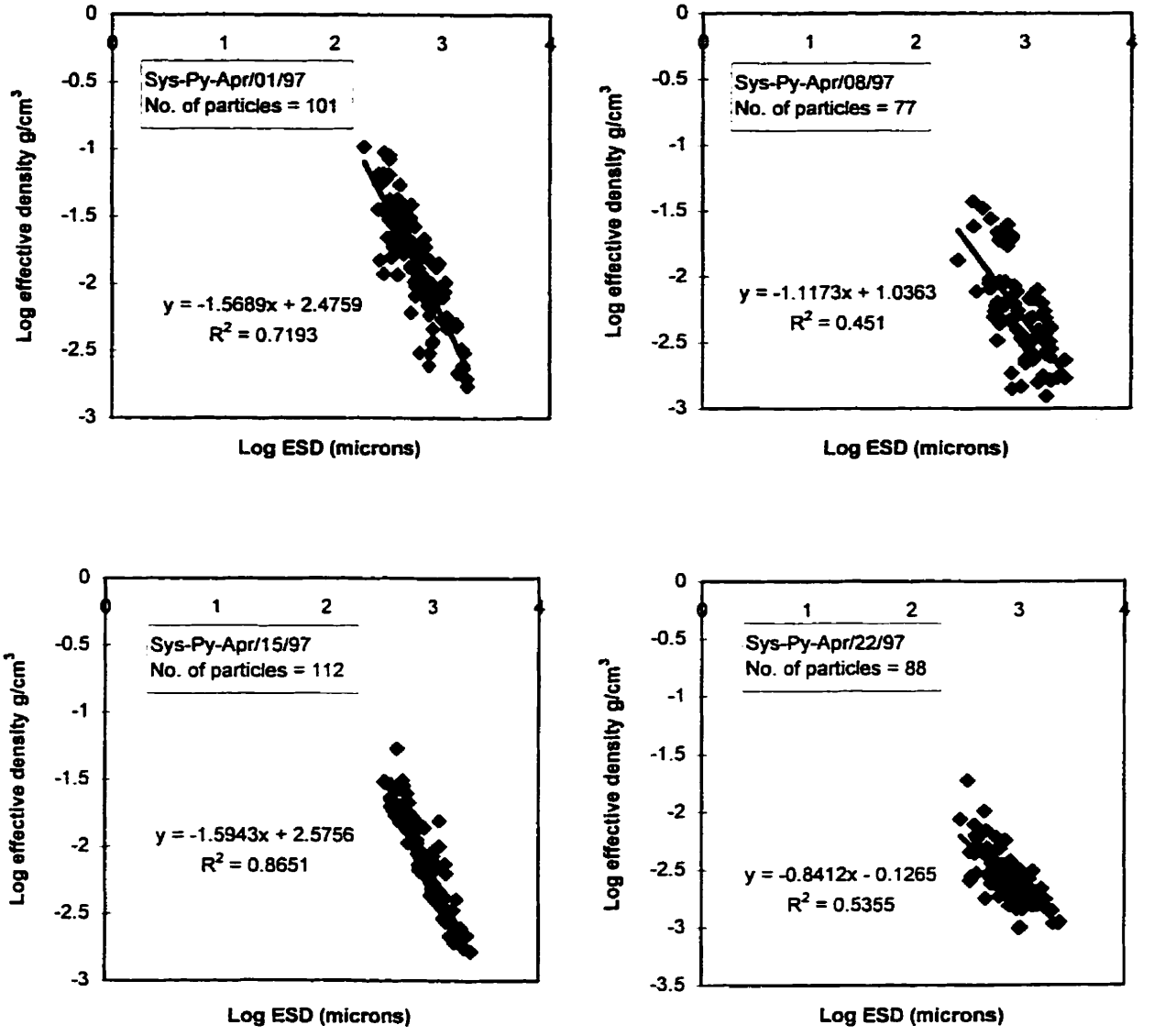

Figure F.2 (continued). The effective density as a function of ESD of sludge flocs from poultry processing wastewater treatment plant (system-Py).

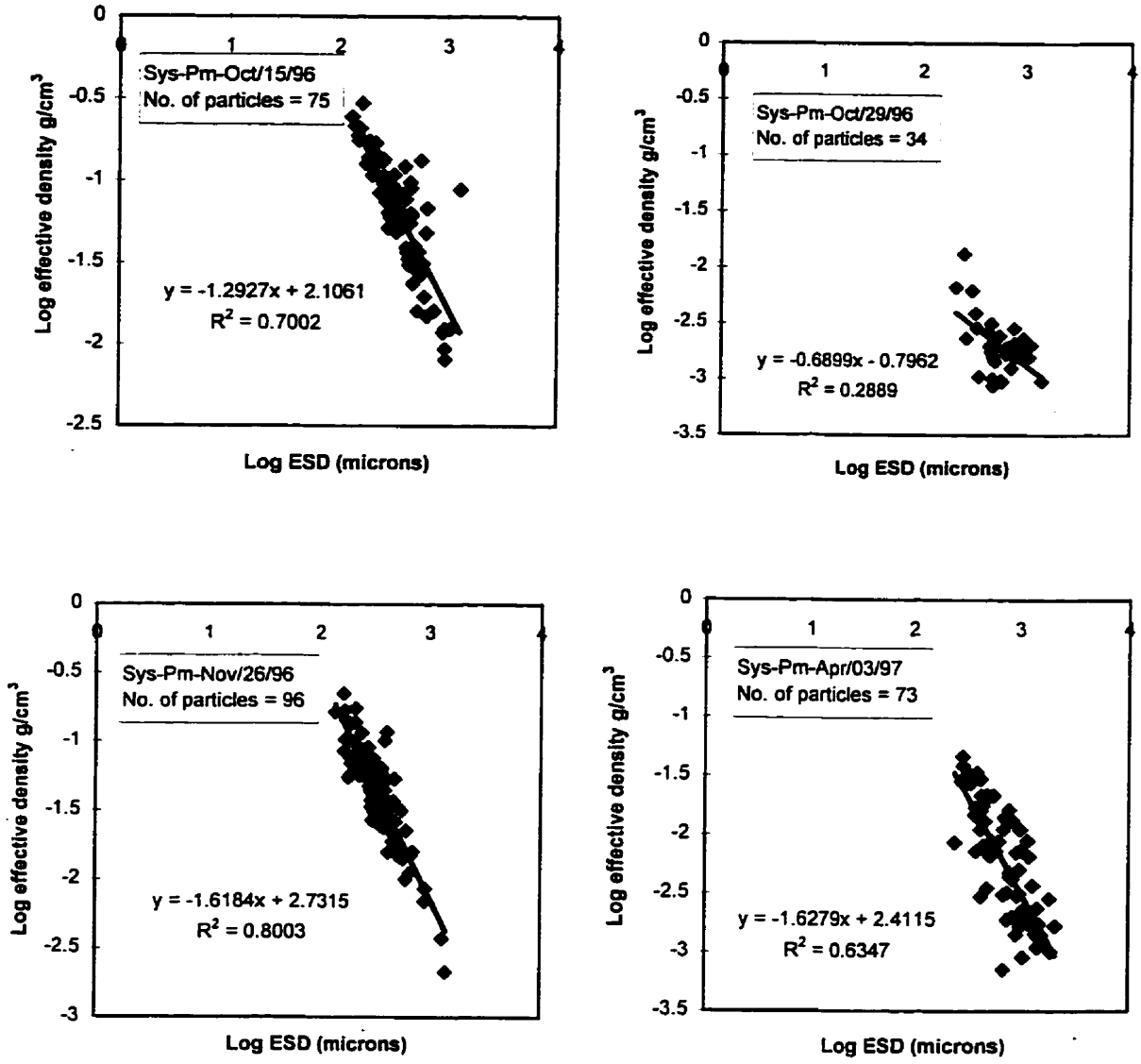

Figure F.3. The effective density as a function of ESD of sludge flocs from petroleum refinery wastewater treatment plant (system-Pm).

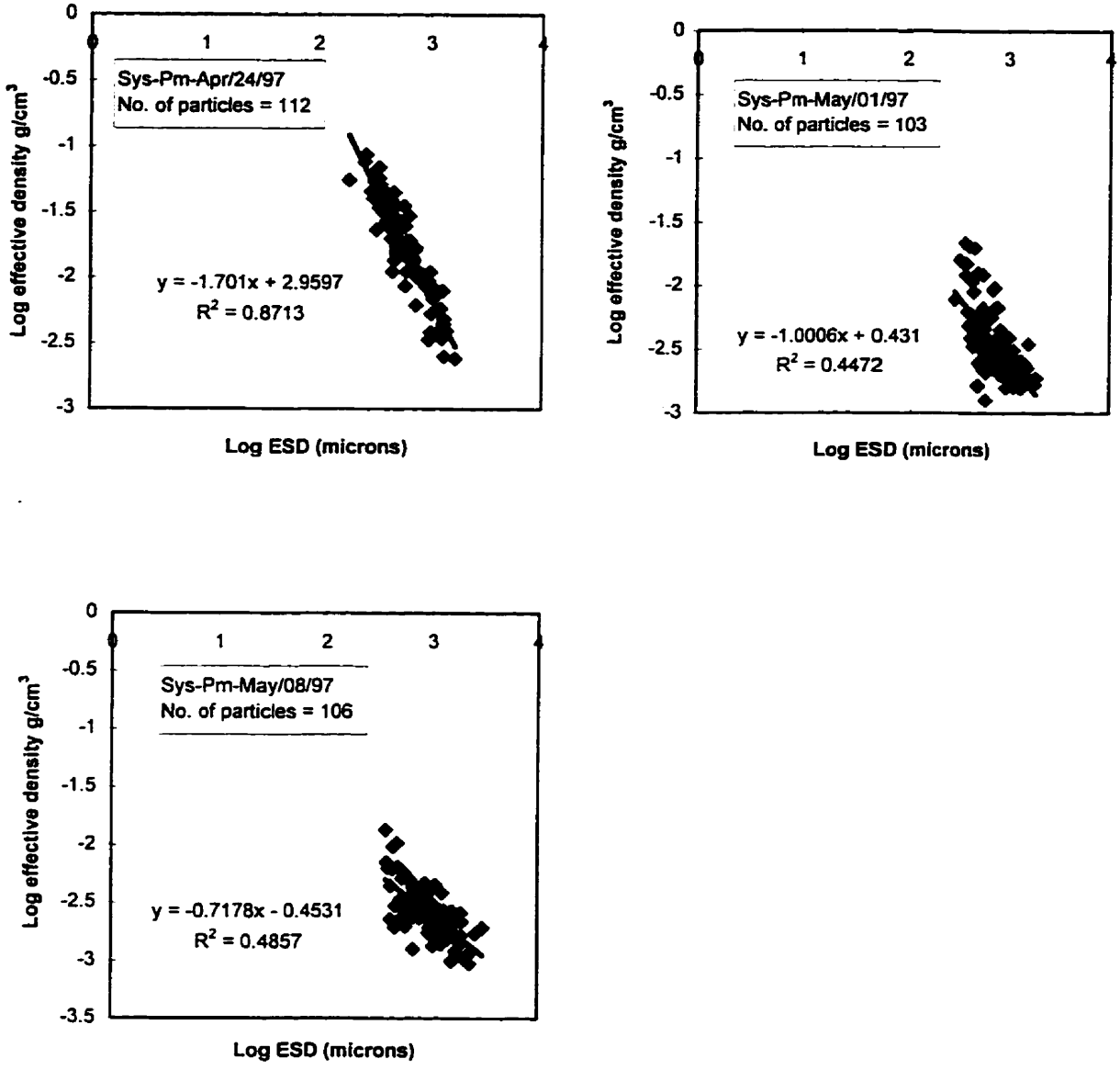

Figure F.3 (continued). The effective density as a function of ESD of sludge flocs from petroleum refinery wastewater treatment plant (system-Pm).

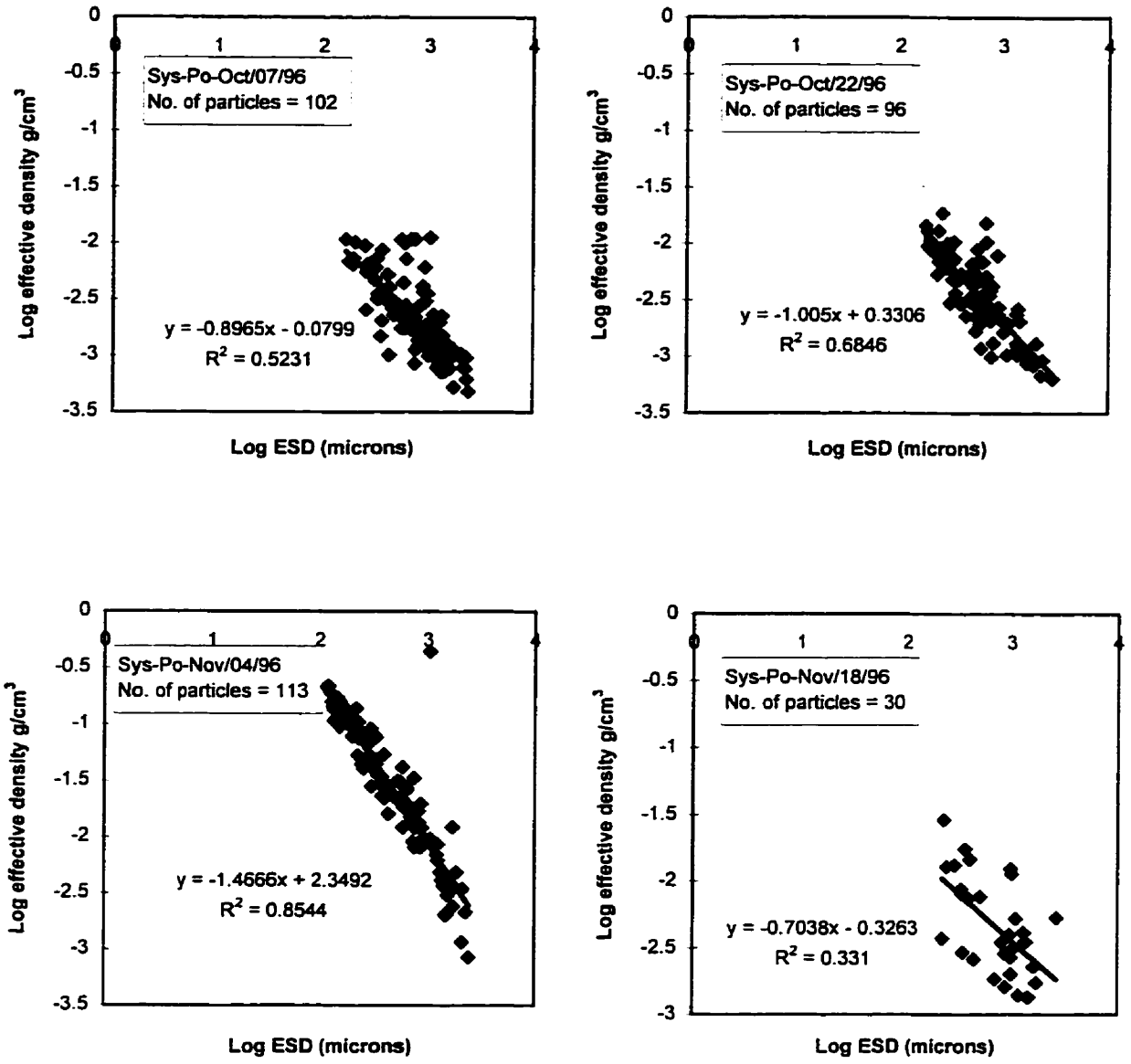

Figure F.4. The effective density as a function of ESD of sludge flocs from potato processing wastewater treatment plant (system-Po).

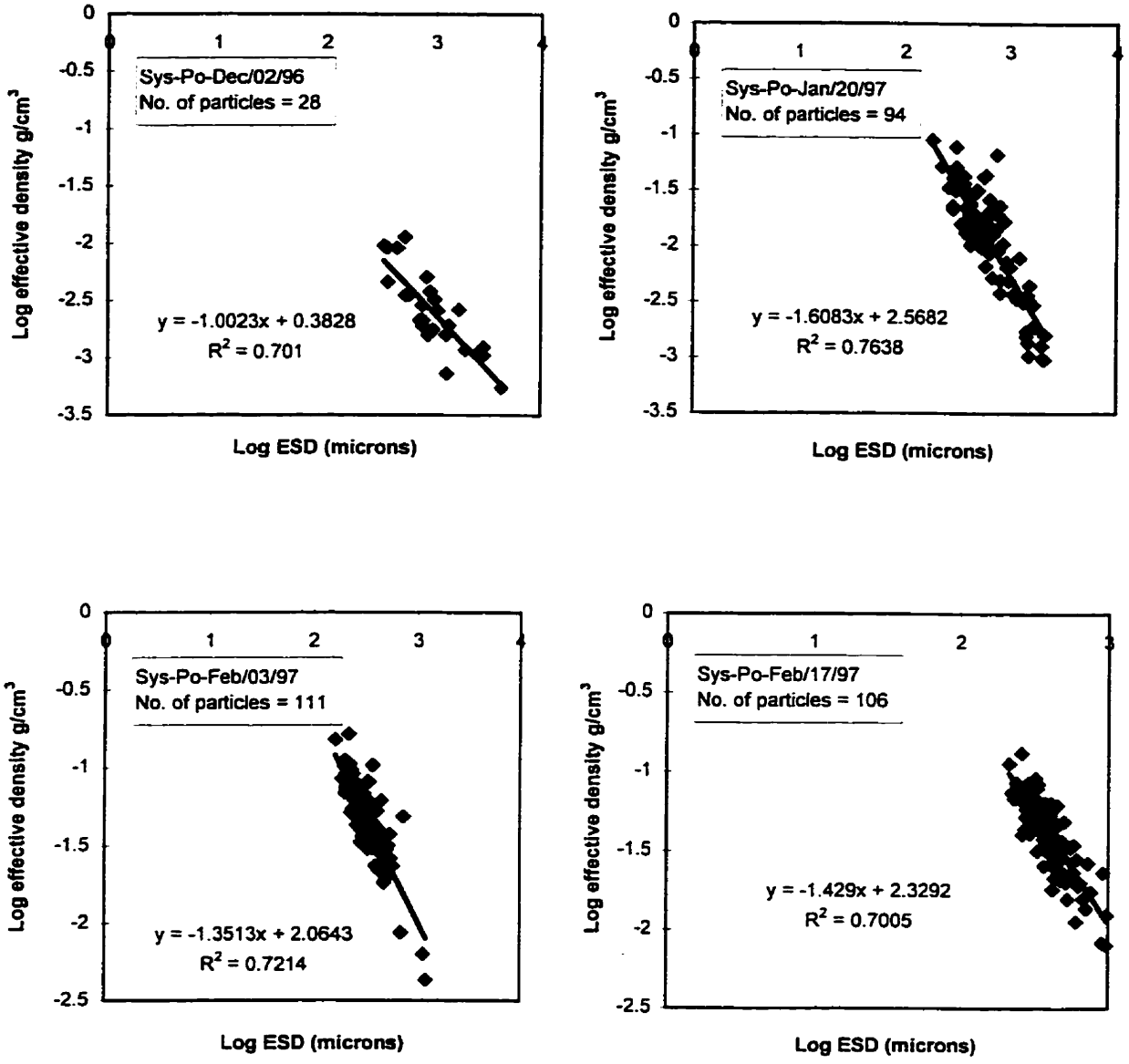

Figure F.4 (continued). The effective density as a function of ESD of sludge flocs from potato processing wastewater treatment plant (system-Po).

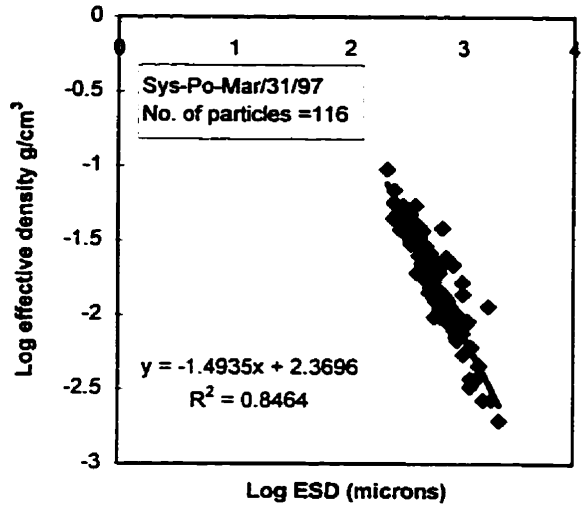

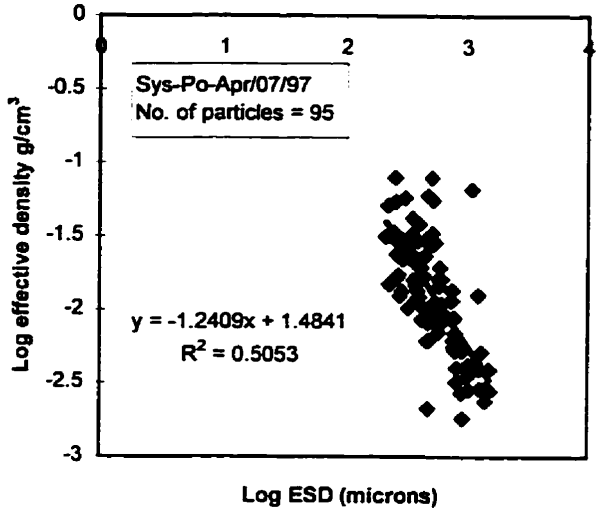

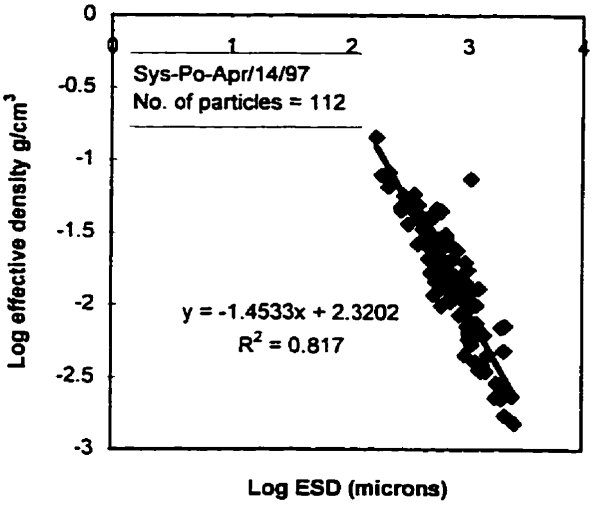

Figure F.4 (continued). The effective density as a function of ESD of sludge flocs from potato processing wastewater treatment plant (system-Po).

APPENDIX G

OPERATING DATA OF TREATMENT PLANTS

Table G.1. Operating data from municipal wastewater treatment plant.

Sampling date	Influent BOD mg/l	Ave. influent flow x 10^3 m^3/d	HRT[1] h	F/M d^{-1}
Nov/06/96	322	646	5.9	0.72
Nov/20/96	296	757	5.0	0.58
Feb/12/97	130	632	6.0	0.53
Feb/19/97	144	981	3.9	0.60
Mar/24/97	na	713	5.3	na
Apr/07/97	na	732	5.2	na
Apr/11/97	na	697	5.4	na
Apr/14/97	na	687	5.5	na
Apr/16/97	139	718	5.3	0.50
Apr/23/97	185	664	5.7	0.54
Apr/28/97	na	799	4.7	na
May/07/97	154	687	5.5	0.57
May/12/97	na	830	4.6	na
May/14/97	261	701	5.4	0.87
May/16/97	na	706	5.4	na
May/21/97	197	661	5.7	0.60
May/23/97	na	660	5.7	na

na : not available

[1] HRT = total volume of aeration tanks / influent flow per h = 17,522 x 9 / (Ave. influent flow x 1000 / 24)

Table G.2. Operating data from poultry processing wastewater treatment plant.

Sampling date	Influent BOD mg/l	HRT d	MCRT d	DO uptake mg/l/h	F/M d^{-1}
Dec/09/96	508	3.5	28	7	0.05
Jan/13/97	600	3.5	28	9	0.06
Jan/28/97	715	3.5	28	13	0.08
Feb/11/97	643	3.5	28	9	0.07
Feb/25/97	1299	3.5	28	10	0.15
Apr/01/97	744	3.5	28	10	0.07
Apr/15/97	1024	3.5	28	11	0.09
Apr/22/97	1125	3.5	28	9	0.15

Table G.3. Operating data from potato processing wastewater treatment plant

Sampling date	[1] Influent [2] COD mg/l	Hydraulic retention time (HRT) days	Mean cell residence time (MCRT) days
Oct/07/96	4728	1.2	10
Oct/22/96	5325	1.2	8
Nov/04/96	4811	1.0	8
Nov/18/96	5193	1.3	8
Dec/02/96	5252	1.1	10
Jan/20/97	6110	1.1	10
Feb/03/97	6017	1.1	10
Feb/17/97	4229	1.1	8
Mar/31/97	3889	1.1	8
Apr/07/97	4776	1.0	10
Apr/14/97	3880	1.0	9
Apr/21/97	4727	1.1	9
Apr/28/97	4700	1.2	9
May/05/97	5854	1.2	9
May/12/97	4405	1.2	8

[1] Influent of system, not bioreactors.
[2] COD = 2 x BOD

APPENDIX H

FILAMENTS IDENTIFICATION

Table H.1. Filament identification of sludge sample from poultry processing wastewater treatment plant.

Type of sample:	Mixed liquor - Poultry processing wastewater treatment plant				
Sampling date:	Feb/03/97				
Filament No.	A	B	C	D	E
Location	E	E	E	E	E
Filament shape	Irregular	SC	SC	SC	SC
Length, µm	40	80 - 100	40	40	20
Diameter, µm	1.6	1.6	0.8	0.8	0.8
Cell shape	unclear	rectangle	unclear	rod-chain	rectangle
Cell size	-	1.6 x 2	-	0.8 x 1.2	0.8 x 1.3
Septa	Yes	Yes	-	Yes	Yes
Indentations	Yes	No	No	Yes	No
Branching	No	No	No	No	-
Sheath					
Epiphytic growth	No	No	No	No	No
Sulphur Granules		Not in situ		Not in situ	Not in situ
Other Granules	No	No	No	No	No
Gram stain	-	-			
Neisser Trichome	+				
Neiseer Granules					
Rel. Abundance	80%				
Rank	1				
Identification	N. limicola	Thiothrix 1			

Filament location: E - extending from floc, F - free in bulk solution, I - inside floc.
Filament shape: SC - smoothcurved, ST - straight, I - irregular, C - coiled

Table H.2. Filament identification of sludge sample from petroleum refinery wastewater treatment plant.

Type of sample:	Mixed liquor - Petroleum refinery wastewater treatment plant				
Sampling date:	Mar/07/97				
Filament No.	A	B	C	D	E
Location	E	E	E	E	I
Filament shape	SC, ST	ST	SC	SC	SC
Length, μm	50 - 100	100 - 200	30	50 - 100	300
Diameter, μm	1.8 - 2.0	1.5 - 1.8	<1.0	1 - 1.5	>1.0
Cell shape	rectangle	rounded rod	oval/rod	rod	unclear
Cell size	2 x 2.5	1.5 x 3.5	1 x 1.5	1 x 3	-
Septa	Yes	Yes	Yes/chain	Yes	No
Indentations	No	Yes	Yes	Yes	No
Branching	No	Yes	No	No	No
Sheath	Yes	-			
Epiphytic growth	No	No	No	No	
Sulphur Granules	No	No			
Other Granules	No	No	No	No	No
Gram stain	-	-	-	-	-
Neisser Trichome		-	-		
Neiseer Granules	Yes				
Rel. Abundance	5%	5%			
Rank			1		
Identification	Thiothrix 1	S. natans			

Filament location: E - extending from floc, F - free in bulk solution, I - inside floc.
Filament shape: SC - smoothcurved, ST - straight, I - irregular, C - coiled

APPENDIX I

STATISTICAL ANALYSIS

Table I.1. The statistical comparison of settling properties, sludge characteristics and EPS composition of sludge from different treatment systems.[1]

Treatment systems	Settling properties				Sludge properties							
	SVI		30-min settling		MLSS		MLVSS		VSS/SS %		CHO-sludge	
	t-test[2,3]		t-test		t-test		t-test		t-test		t-test	
Dm-Py	8.44E-06	sd	1.77E-06	sd	2.51E-06	sd	1.2E-07	sd	3.9E-14	sd	0.008118	sd
Dm-Pm	0.000689	sd	5.02E-07	sd	0.009566	sd	0.00235	sd	1.7E-07	sd	0.316082	nsd
Dm-Po	0.00017	sd	0.000701	sd	0.038192	sd	0.00015	sd	1.7E-16	sd	0.421505	nsd
Py-Pm	0.923321	nsd	0.439721	nsd	0.254142	nsd	0.10385	nsd	0.00029	sd	0.315493	nsd
Py-Po	0.884543	nsd	0.133693	nsd	0.002242	sd	0.01419	sd	6.2E-07	sd	0.066703	nsd
Pm-Po	0.966947	nsd	0.051438	nsd	0.03165	sd	0.02138	sd	0.20658	nsd	0.201678	nsd

Treatment systems	EPS composition											
	Protein-EPS		CHO-EPS		DNA-EPS		Acidic Poly.-EPS		Total EPS		Extractable CHO	
	t-test		t-test		t-test		t-test		t-test		t-test	
Dm-Py	2.42E-08	sd	0.0009	sd	0.610292	nsd	2.4E-05	sd	6.4E-09	sd	0.046132	sd
Dm-Pm	0.001592	sd	0.070011	nsd	0.002276	sd	0.00209	sd	0.00053	sd	0.23081	nsd
Dm-Po	0.002985	sd	0.984875	nsd	0.037417	sd	0.26815	nsd	0.00493	sd	0.21765	nsd
Py-Pm	0.058551	nsd	0.094829	nsd	0.005315	sd	0.3843	nsd	0.06243	nsd	0.563358	nsd
Py-Po	0.013622	sd	0.008088	sd	0.069593	nsd	0.00067	sd	0.00626	sd	0.291266	nsd
Pm-Po	0.59496	nsd	0.110799	nsd	0.474926	nsd	0.018	sd	0.32345	nsd	0.855661	nsd

[1] No. of sludge samples analyzed are as follows: Dm (17), Py (8), Pm (7) and Po (10).

[2] sd: significant difference of the means between two systems using 2-tailed t-test at $\alpha = 0.05$.

[3] nsd: no significant difference of the means between two systems using 2-tailed t-test at $\alpha = 0.05$.

Table I.2. The statistical comparison of percentage composition of EPS of sludge from different treatment systems.[1]

Treatment systems	Percentage composition of EPS							
	Protein-EPS		CHO-EPS		DNA-EPS		Acidic Poly.-EPS	
	t-test[2,3]		t-test		t-test		t-test	
Dm-Py	0.0439	sd	0.2226	nsd	0.003	sd	0.0929	nsd
Dm-Pm	0.9304	nsd	0.3031	nsd	0.5924	nsd	0.1668	nsd
Dm-Po	0.1679	nsd	0.0861	nsd	0.5541	nsd	0.205	nsd
Py-Pm	0.0785	nsd	0.9792	nsd	0.0024	sd	0.9094	nsd
Py-Po	0.8495	nsd	0.3384	nsd	0.0017	sd	0.0174	sd
Pm-Po	0.2125	nsd	0.354	nsd	0.9997	nsd	0.0387	sd

[1] No. of sludge samples analyzed are as follows: Dm (17), Py (8), Pm (7) and Po (10).
[2] sd: significant difference of the means between two systems using 2-tailed t-test at $\alpha = 0.05$.
[3] nsd: no significant difference of the means between two systems using 2-tailed t-test at $\alpha = 0.05$.

Table I.3 The statistical comparison of settling properties, sludge characteristics and EPS composition of sludge from potato processing wastewater treatment system during functional and dysfunctional period.

1 Anova: Single Factor

SUMMARY

Groups	Count	Sum	Average	Variance
SVI (Functional)	7	1380	197.143	3443.81
SVI (Dysfunctional)	3	772	257.333	5504.333

ANOVA

Source of Variation	SS	df	MS	F	P-value	F crit
Between Groups	7608.1	1	7608.08	1.921746	0.2031	5.3176
Within Groups	31672	8	3958.94			
Total	39280	9				

2 Anova: Single Factor

SUMMARY

Groups	Count	Sum	Average	Variance
30-MIN (Functional)	7	364	52	460.6667
30-MIN (Dysfunctional)	3	297	99	1

ANOVA

Source of Variation	SS	df	MS	F	P-value	F crit
Between Groups	4638.9	1	4638.9	13.41692	0.0064	5.3176
Within Groups	2766	8	345.75			
Total	7404.9	9				

3 Anova: Single Factor

SUMMARY

Groups	Count	Sum	Average	Variance
MLSS (Functional)	7	17.77	2.53857	0.130224
MLSS (Dysfunctional)	3	10.18	3.39333	0.213733

ANOVA

Source of Variation	SS	df	MS	F	P-value	F crit
Between Groups	1.5343	1	1.5343	10.15412	0.0129	5.3176
Within Groups	1.2088	8	0.1511			
Total	2.7431	9				

4 Anova: Single Factor

SUMMARY

Groups	Count	Sum	Average	Variance
MLVSS (Functional)	7	14.614	2.08771	0.082
MLVSS (Dysfunctional)	3	8.123	2.70767	0.17399

ANOVA

Source of Variation	SS	df	MS	F	P-value	F crit
Between Groups	0.8071	1	0.80712	7.68726	0.0242	5.3176
Within Groups	0.84	8	0.10499			
Total	1.6471	9				

5 Anova: Single Factor

SUMMARY

Groups	Count	Sum	Average	Variance
VSS % (Functional)	7	575	82.1429	1.47619
VSS % (Dysfunctional)	3	240	80	4

ANOVA

Source of Variation	SS	df	MS	F	P-value	F crit
Between Groups	9.6429	1	9.64286	4.57627	0.0649	5.3176
Within Groups	16.857	8	2.10714			
Total	26.5	9				

6 Anova: Single Factor

SUMMARY

Groups	Count	Sum	Average	Variance
CHO in sludge (Functional)	6	1186.2	197.7	11226
CHO in sludge (Dysfunctional)	3	943.8	314.6	12981.7

ANOVA

Source of Variation	SS	df	MS	F	P-value	F crit
Between Groups	27331	1	27331.2	2.33049	0.1707	5.5915
Within Groups	82094	7	11727.7			
Total	109425	8				

Table I.3 (continued).

7 Anova: Single Factor

SUMMARY

Groups	*Count*	*Sum*	*Average*	*Variance*
CHO in EPS (Functional)	7	59.781	8.54014	9.005025
CHO in EPS (Dysfunctional)	3	43.76	14.5867	13.36373

ANOVA

Source of Variation	*SS*	*df*	*MS*	*F*	*P-value*	*F crit*
Between Groups	76.777	1	76.7769	7.605667	0.0248	5.3176
Within Groups	80.758	8	10.0947			
Total	157.53	9				

8 Anova: Single Factor

SUMMARY

Groups	Count	Sum	Average	Variance
Acidic P. in EPS (Functional)	7	22.683	3.24043	1.113063
Acidic P. in EPS (Dysfunctional)	3	12.218	4.07267	1.890409

ANOVA

Source of Variation	SS	df	MS	F	P-value	F crit
Between Groups	1.4545	1	1.4545	1.112516	0.3223	5.3176
Within Groups	10.459	8	1.3074			
Total	11.914	9				

9 Anova: Single Factor

SUMMARY

Groups	Count	Sum	Average	Variance
Protein in EPS (Functional)	7	333.1	47.5857	101.3254
Protein in EPS (Dysfunctional)	3	222.79	74.2633	418.3744

ANOVA

Source of Variation	SS	df	MS	F	P-value	F crit
Between Groups	1494.6	1	1494.56	8.276094	0.0206	5.3176
Within Groups	1444.7	8	180.588			
Total	2939.3	9				

10 Anova: Single Factor

SUMMARY

Groups	Count	Sum	Average	Variance
DNA in EPS (Functional)	7	17.514	2.50206	2.7686
DNA in EPS (Dysfunctional)	3	9.4289	3.14297	5.69538

ANOVA

Source of Variation	SS	df	MS	F	P-value	F crit
Between Groups	0.8626	1	0.86261	0.24644	0.6329	5.3176
Within Groups	28.002	8	3.5003			
Total	28.865	9				

11 Anova: Single Factor

SUMMARY

Groups	Count	Sum	Average	Variance
Total EPS (Functional)	7	433.08	61.8683	92.0775
Total EPS (Dysfunctional)	3	288.2	96.0656	422.381

ANOVA

Source of Variation	SS	df	MS	F	P-value	F crit
Between Groups	2455.9	1	2455.85	14.0613	0.0056	5.3176
Within Groups	1397.2	8	174.653			
Total	3853.1	9				

12 Anova: Single Factor

SUMMARY

Groups	*Count*	*Sum*	*Average*	*Variance*
Extractable CHO (Functional)	6	25.498	4.24975	1.39359
Extractable CHO (Dysfunctional)	3	14.305	4.76821	0.6015

ANOVA

Source of Variation	*SS*	*df*	*MS*	*F*	*P-value*	*F crit*
Between Groups	0.5376	1	0.5376	0.46056	0.5192	5.5915
Within Groups	8.171	7	1.16728			
Total	8.7086	8				

Table I.4. The statistical comparison of percentage composition of EPS of sludge from potato processing wastewater treatment system during functional and dysfunctional period.

1 Anova: Single Factor

SUMMARY

Groups	Count	Sum	Average	Variance
Carbohydrate % (Dysfunctio	7	100.53	14.36176	46.96065
Carbohydrate % (Functional)	3	47.303	15.76757	31.14484

ANOVA

Source of Variation	SS	df	MS	F	P-value	F crit
Between Groups	4.1503	1	4.150261	0.096503	0.76401	5.3176
Within Groups	344.05	8	43.0067			
Total	348.2	9				

2 Anova: Single Factor

SUMMARY

Groups	Count	Sum	Average	Variance
Acidic Poly.% (Functional)	7	36.657	5.236775	2.448635
Acidic Poly.% (Dysfunctional)	3	12.755	4.251583	1.034575

ANOVA

Source of Variation	SS	df	MS	F	P-value	F crit
Between Groups	2.0383	1	2.038269	0.972865	0.35285	5.3176
Within Groups	16.761	8	2.09512			
Total	18.799	9				

3 Anova: Single Factor

SUMMARY

Groups	Count	Sum	Average	Variance
Protein% (Functional)	7	535.38	76.4827	83.05069
Protein% (Dysfunctional)	3	229.95	76.6491	71.07085

ANOVA

Source of Variation	SS	df	MS	F	P-value	F crit
Between Groups	0.0582	1	0.05818	0.000727	0.9792	5.3176
Within Groups	640.45	8	80.0557			
Total	640.5	9				

4 Anova: Single Factor

SUMMARY

Groups	Count	Sum	Average	Variance
DNA% (Functional)	7	27.431	3.91876	5.730225
DNA% (Dysfunctional)	3	9.9951	3.3317	5.273488

ANOVA

Source of Variation	SS	df	MS	F	P-value	F crit
Between Groups	0.7237	1	0.72375	0.128872	0.7289	5.3176
Within Groups	44.928	8	5.61604			
Total	45.652	9				

APPENDIX J

INDEX PRINTS OF SCLM IMAGES

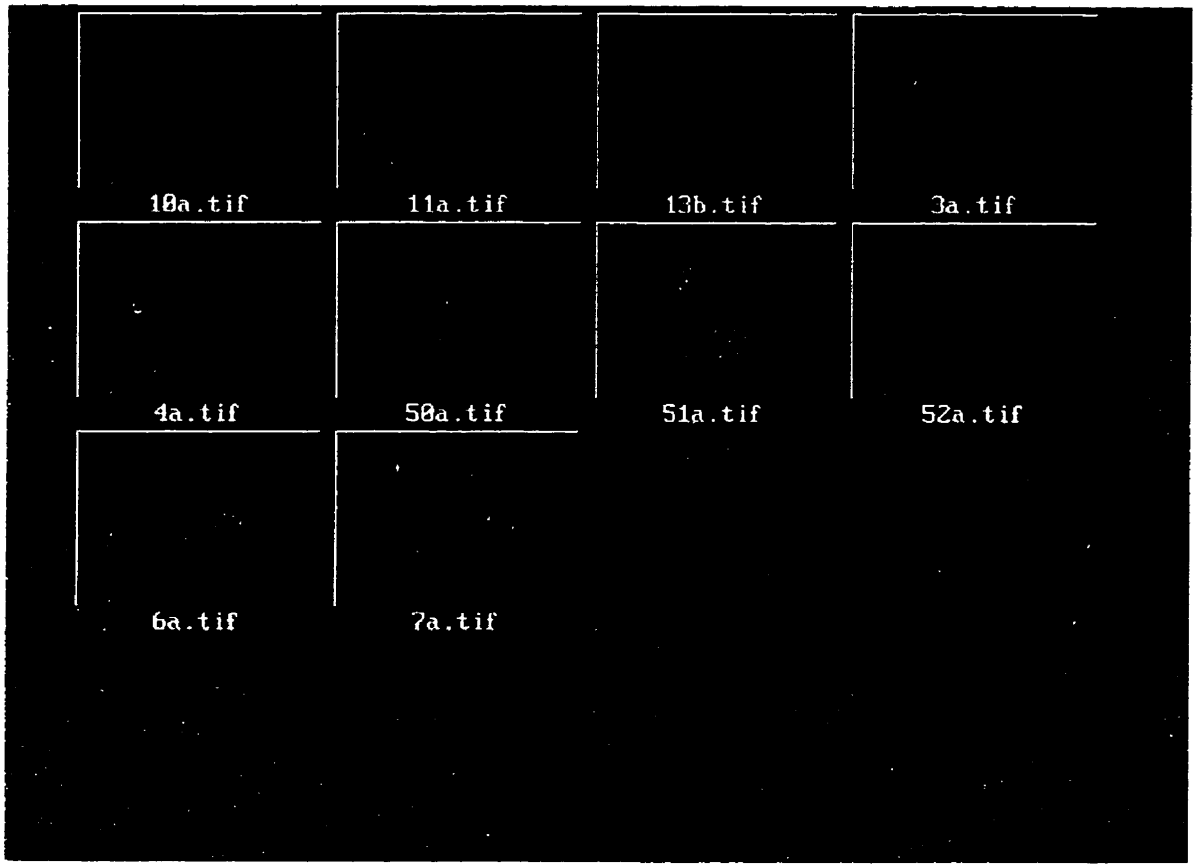

No.	Stain	Oil immersion lens	Zoom	Filter	Magnification	Remark
3a	Live/Dead	63x	30x	FITC	3780x	* live cells
4a	Live/Dead	63x	30x	TR	3780x	*dead cells
6a	FITC	40x	20x		1600x	
7a	FITC	63x	20x		2520x	
10a	ConA	40x	20x	FITC	1600x	
11a	ConA	40x	20x	FITC	1600x	
13b	WGA	40x	20x	TR	1600x	
50	FITC	40x	20x		1600x	washed again
51	WGA	40x	20x	TR	1600x	washed again
52	ConA	40x	20x	FITC	1600x	washed again

Figure J.1. Index print of SCLM images of flocs from municipal wastewater treatment system.

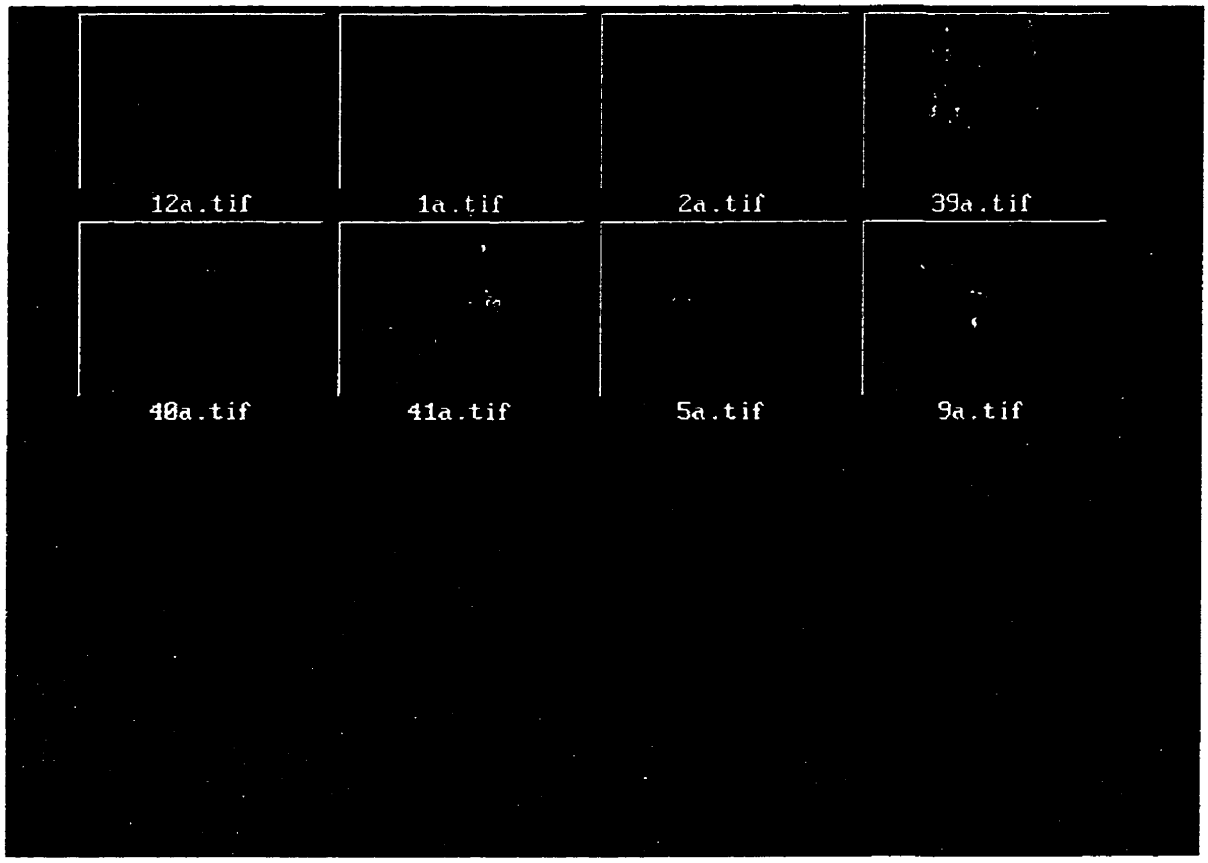

No.	Stain	Oil immersion lens	Zoom	Filter	Magnification	Remark
1a	Live/Dead	63x	20x	FITC	2520x	* live cells
2a	Live/Dead	63x	20x	TR	2520x	*dead cells
5a	FITC	40x	20x		1600x	
9a	ConA	40x	20x	FITC	1600x	
12a	WGA	40x	20x	TR	1600x	
39	FITC	40x	20x		1600x	*z-series - overlapping 38 images, 2μm distance per image
40	WGA	40x	20x	TR	1600x	washed again
41	ConA	40x	20x	FITC	1600x	washed again

Figure J.2. Index print of SCLM images of flocs from poultry processing wastewater treatment system.

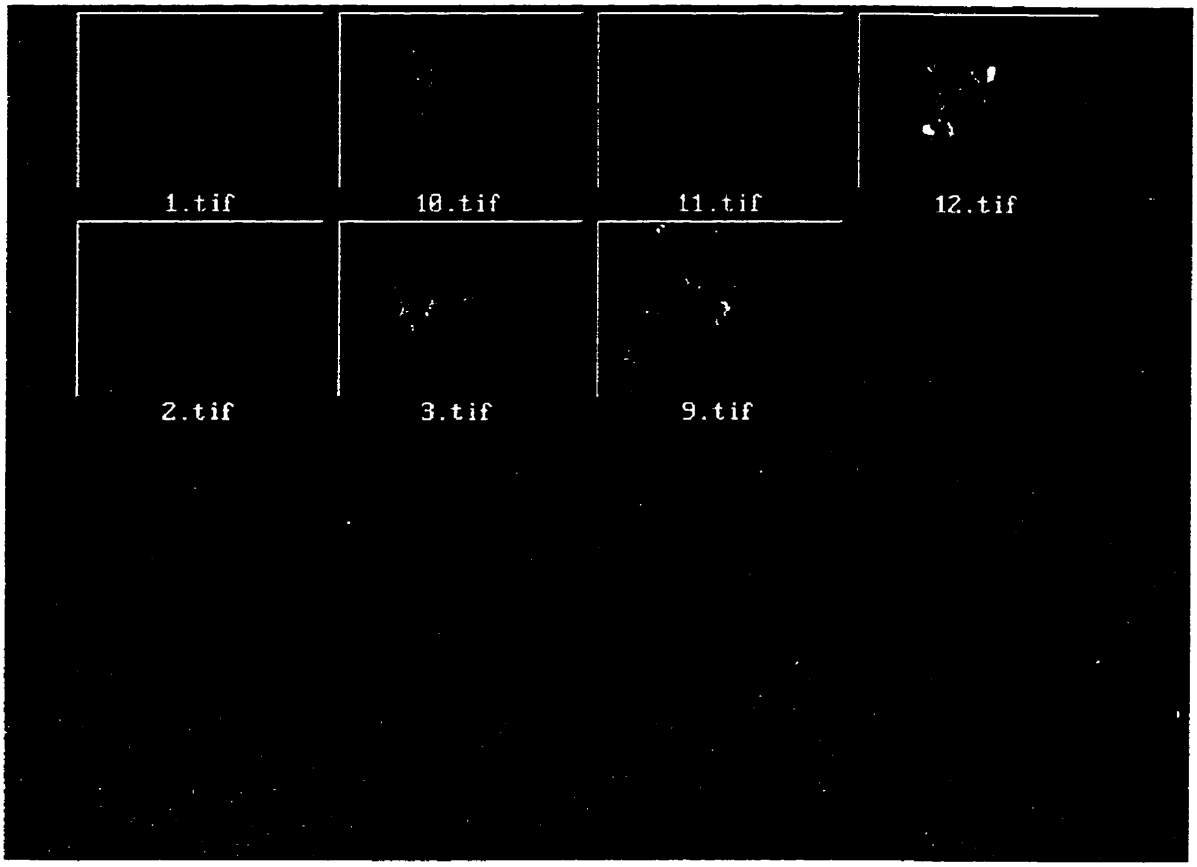

No.	Stain	Filter
1	Live/Dead	FITC
2	Gram stain	
3	FITC	
9	ConA	FITC
10	ConA	FITC
11	ConA	FITC
12	WGA	TR

Figure J.3. Index print of SCLM images of flocs from petroleum refinery wastewater treatment system.

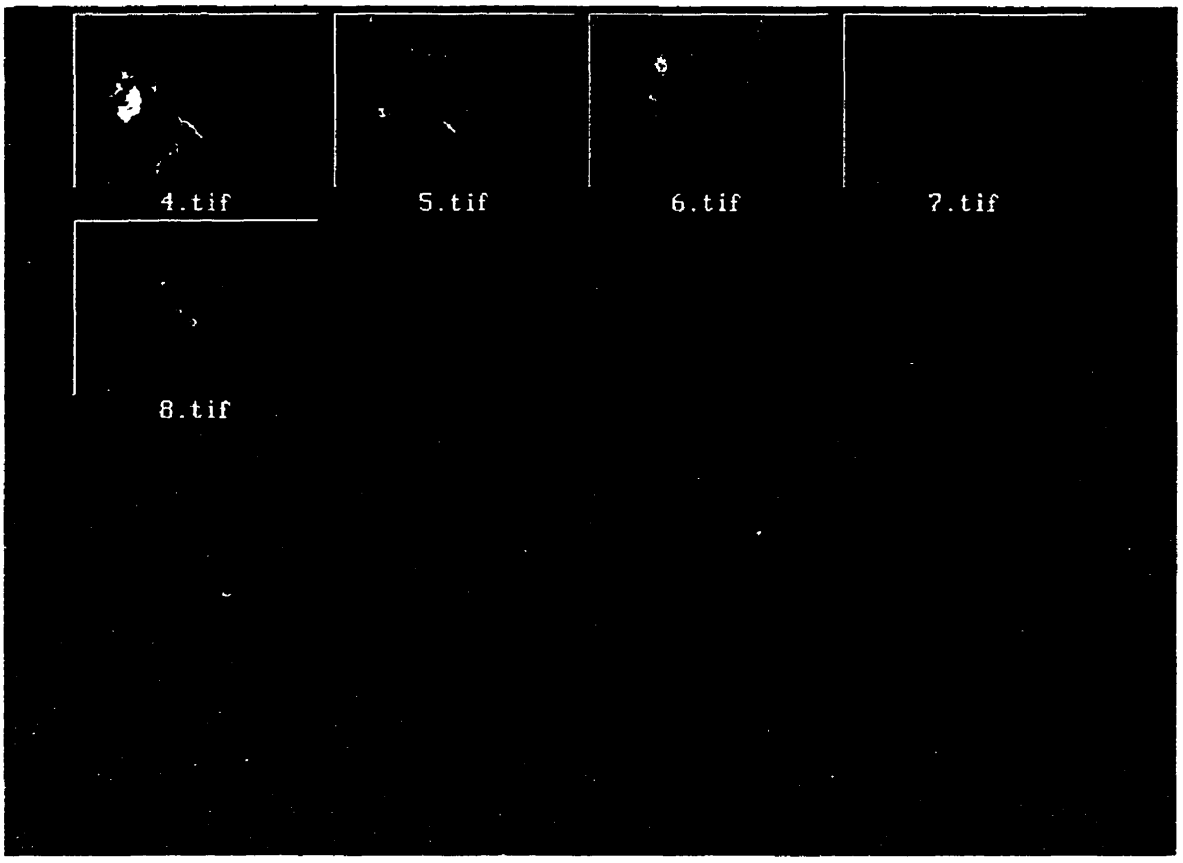

No.	Stain	Filter
4	FITC	
5	FITC	
6	ConA	FITC
7	ConA	FITC
8	WGA	TR

Figure J.4. Index print of SCLM images of flocs from potato processing wastewater treatment system.

APPENDIX K

CHARACTERIZATION OF MICROBIAL COMMUNITY (USING BIOLOG PLATES)

Table K.1. The microbial activities data of sludge from municipal wastewater treatment plant (system-Dm) and poultry processing wastewater treatment plant (system-Py).

Carbon sources in Biolog GN plate	Dm-1/0514/25	Dm-2/0507/25	Py-1/0506/50	Py-2/0429/50
Water	0.190	0.120	0.185	0.121
α-Cyclodextrin	1.053	0.903	0.953	0.244
Dextrin	2.089	2.633	3.107	2.420
Glycogen	1.883	2.171	2.611	2.505
Tween 40	0.353	0.371	1.426	1.052
Tween 80	0.440	0.575	1.099	0.747
N-Acetyl-D-galactosamine	0.760	0.845	1.019	1.177
N-Acetyl-D-glucosamine	2.280	2.434	2.804	2.882
Adonitol	0.817	0.673	0.594	0.698
L-Arabinose	1.495	1.335	1.290	1.298
D-Arabitol	1.045	0.844	0.947	0.906
Cellobiose	2.042	1.614	1.221	0.953
i-Erythritol	0.343	0.300	0.231	0.255
D-Fructose	1.934	2.038	1.807	1.132
L-Fucose	0.719	1.206	1.205	0.881
D-Galactose	1.886	2.032	1.403	1.460
Gentiobiose	1.421	1.303	0.770	0.877
α-D-Glucose	2.374	2.452	2.747	2.309
m-Inositol	0.570	0.627	0.526	0.564
α-D-Lactose	2.334	2.291	1.152	1.215
Lactulose	1.071	1.277	0.373	1.259
Maltose	2.382	2.398	2.236	2.336
D-Minnitol	1.933	1.984	1.637	1.960
D-Mannose	1.513	1.599	1.150	1.333
D-Melibiose	1.615	1.593	1.137	1.312
β-Methyl-D-glucoside	2.326	2.587	2.794	2.992
D-Psicose	0.723	0.790	0.913	0.813
D-Raffinose	1.531	1.379	0.751	0.928
L-Rhamnose	0.928	0.748	0.751	0.675
D-Sorbitol	1.346	1.129	1.054	1.210
Sucrose	2.391	2.790	2.897	3.073
D-Trehalose	2.444	2.727	2.551	3.154
Turanose	0.851	0.673	0.630	0.562
Xylitol	0.421	0.403	0.288	0.240
Methylpyruvate	1.245	1.097	1.213	1.056
Mono-methylsuccinate	0.635	0.414	0.645	0.688
Acetic acid	0.410	0.563	0.869	0.625
cis-Aconitic acid	1.526	1.347	0.630	0.996
Citric acid	1.166	1.181	0.739	0.707
Formic acid	0.349	0.361	0.327	0.391
D-Galactonic acid lactone	1.526	0.988	0.679	1.014
D-Galacturonic acid	1.773	1.294	1.523	1.495
D-Gluconic acid	2.045	2.332	2.247	3.002
D-Glucosaminic acid	0.520	0.362	0.587	0.890
D-Glucuronic acid	1.603	1.101	0.923	1.293

Table K.1(continued). The microbial activities data of sludge from system-Dm and system-Py.

Carbon sources in Biolog GN plate	Dm-1/0514/25	Dm-2/0507/25	Py-1/0506/50	Py-2/0429/50
α-Hydroxybutyric acid	0.182	0.264	0.378	0.297
β-Hydroxybutyric acid	0.323	0.523	1.168	0.562
γ-Hydroxybutyric acid	0.359	0.542	1.170	0.345
p-Hydroxyphenylacetic acid	0.413	0.342	0.326	0.349
Itaconic acid	0.225	0.218	0.127	0.263
α-Ketobutyric acid	0.119	0.103	0.163	0.138
α-Ketoglutaric acid	0.899	0.954	0.356	0.259
α-Ketovaleric acid	0.134	0.128	0.281	0.224
D,L-Lactic acid	1.493	1.487	1.384	1.233
Malonic acid	0.201	0.315	0.634	0.400
Propionic acid	0.382	0.393	0.684	0.605
Quinic acid	1.568	1.430	1.147	0.582
D-Saccharic acid	1.074	0.901	0.432	0.783
Sebacic acid	0.147	0.132	0.174	0.299
Succinic acid	1.106	0.944	0.932	1.056
Bromosuccinic acid	0.636	1.035	1.022	0.828
Succinamic acid	0.326	0.450	0.751	0.782
Glucuronamide	0.582	0.686	0.671	0.947
Alaninamide	0.329	0.332	0.522	0.498
D-Alanine	0.452	0.533	0.873	0.694
L-Alanine	0.428	0.431	0.705	0.608
L-Alanyl-glycine	0.399	0.394	0.561	0.576
L-Aspargine	1.663	1.170	1.164	0.900
L-Aspartic acid	0.772	0.878	0.953	1.064
L-Glutamic acid	0.903	1.052	0.915	1.200
Glycyl-L-aspartic acid	0.787	0.801	1.087	0.900
Glycyl-L-glutamic acid	0.580	0.583	0.622	0.733
L-Histidine	0.710	0.681	0.917	0.826
Hydroxy-L-proline	0.916	0.537	0.233	0.479
L-Leucine	0.222	0.226	0.263	0.277
L-Ornithine	0.298	0.348	0.584	0.540
L-Phenylalanine	0.177	0.230	0.468	0.532
L-Proline	0.516	0.512	0.770	0.763
L-Pyroglutamic acid	0.291	0.490	0.472	0.213
D-Serine	1.495	1.222	1.096	1.194
L-Serine	0.954	1.006	1.013	0.966
L-Threonine	0.333	0.257	0.465	0.417
D,L-Carnitine	0.285	0.301	0.459	0.180
γ-aminobutyric acid	0.849	0.924	0.699	0.651
Urocanic acid	0.567	0.537	0.577	0.624
Inosine	1.579	1.685	1.625	1.310
Uridine	0.911	1.035	0.969	1.312
Thymidine	0.677	0.716	0.662	0.900
Phenylethylamine	0.084	0.075	0.137	0.095
Putrescine	0.758	0.602	0.490	0.323
2-Aminoethanol	0.146	0.175	0.263	0.249
2,3-Butanediol	0.477	0.302	0.693	0.457
Glycerol	1.201	1.200	1.380	1.311
D,L-alpha-Glycerol phosphate	1.078	1.273	1.450	1.976
Glucose-1-phosphate	1.867	1.926	1.567	1.819
Glucose-6-phosphate	2.016	1.954	2.090	2.884

Table K.2. The microbial activities data of sludge from petroleum refinery wastewater treatmnet plant (system-Pm) and potato processing wastewater treatement plant (system-Po).

Carbon sources in Biolog GN plate	Pm-1/0508/100	Pm-2/0501	Po-1/0428/50	Po-2/0512/50
Water	0.132	0.165	0.133	0.419
α-Cyclodextrin	0.762	0.252	0.294	0.633
Dextrin	4.651	3.196	1.632	1.239
Glycogen	5.051	2.073	1.964	0.825
Tween 40	1.052	1.315	0.885	0.632
Tween 80	1.217	2.155	1.326	0.614
N-Acetyl-D-galactosamine	0.630	1.311	0.744	0.713
N-Acetyl-D-glucosamine	3.880	3.245	1.644	2.159
Adonitol	0.206	0.240	0.547	1.091
L-Arabinose	0.631	1.043	1.481	1.885
D-Arabitol	0.193	0.249	0.737	1.560
Cellobiose	0.163	0.294	1.270	2.163
i-Erythritol	0.220	0.290	0.251	0.529
D-Fructose	2.111	1.240	1.727	2.156
L-Fucose	0.663	1.214	1.219	0.787
D-Galactose	0.695	0.627	1.234	1.947
Gentiobiose	0.319	0.716	0.828	1.845
α-D-Glucose	3.879	3.647	1.865	2.319
m-Inositol	0.236	0.200	0.887	0.854
α-D-Lactose	0.131	0.197	0.962	2.065
Lactulose	0.207	0.227	0.238	0.601
Maltose	3.387	2.660	1.671	1.950
D-Minnitol	1.902	0.975	1.571	1.855
D-Mannose	1.235	0.826	0.912	2.132
D-Melibiose	0.220	0.295	1.482	2.163
β-Methyl-D-glucoside	3.260	1.684	1.176	2.097
D-Psicose	0.209	0.285	1.153	0.875
D-Raffinose	0.131	0.177	1.325	2.094
L-Rhamnose	0.152	0.207	0.903	1.264
D-Sorbitol	0.264	0.343	1.321	2.124
Sucrose	1.527	1.651	2.094	2.320
D-Trehalose	4.230	2.484	1.538	2.293
Turanose	0.282	0.707	0.494	0.615
Xylitol	0.181	0.290	0.241	0.554
Methylpyruvate	1.312	1.472	1.117	1.230
Mono-methylsuccinate	0.633	0.565	0.633	0.597
Acetic acid	0.727	1.628	0.880	0.438
cis-Aconitic acid	0.540	1.910	1.658	0.939
Citric acid	1.463	0.865	1.252	1.081
Formic acid	0.369	0.491	0.314	0.429
D-Galactonic acid lactone	0.122	0.232	1.313	1.616
D-Galacturonic acid	0.399	0.825	1.493	1.806
D-Gluconic acid	2.587	1.457	2.602	1.837
D-Glucosaminic acid	0.146	0.178	0.464	0.612
D-Glucuronic acid	0.581	0.150	1.136	1.703

Table K.2 (continued). The microbial activities data of sludge from system-Pm and system-Po.

Carbon sources in Biolog GN plate	Pm-1/0508/100	Pm-2/0501/100	Po-1/0428/50	Po-2/0512/50
α-Hydroxybutyric acid	0.088	0.101	0.183	0.170
β-Hydroxybutyric acid	0.718	1.150	0.904	0.625
γ-Hydroxybutyric acid	0.884	1.346	1.111	0.246
p-Hydroxyphenylacetic acid	0.415	0.389	0.658	0.597
Itaconic acid	0.291	0.269	0.312	0.314
α-Ketobutyric acid	0.052	0.148	0.082	0.143
α-Ketoglutaric acid	1.304	1.133	1.206	0.625
α-Ketovaleric acid	0.105	0.177	0.440	0.239
D,L-Lactic acid	1.212	1.469	1.342	1.038
Malonic acid	0.314	0.673	0.577	0.514
Propionic acid	0.513	1.007	0.761	0.497
Quinic acid	2.164	1.515	2.080	0.949
D-Saccharic acid	1.477	1.056	1.693	1.217
Sebacic acid	0.150	0.577	0.552	0.168
Succinic acid	1.100	1.770	1.304	0.843
Bromosuccinic acid	1.170	2.268	1.145	0.866
Succinamic acid	0.703	1.321	0.807	0.247
Glucuronamide	0.418	0.450	0.882	0.592
Alaninamide	0.538	0.687	0.603	0.350
D-Alanine	0.968	1.736	0.951	0.757
L-Alanine	0.735	1.394	0.743	0.687
L-Alanyl-glycine	0.727	0.965	0.654	0.659
L-Aspargine	1.652	1.325	1.243	0.990
L-Aspartic acid	1.391	0.988	0.885	0.668
L-Glutamic acid	1.665	1.649	1.214	0.807
Glycyl-L-aspartic acid	0.148	0.521	0.314	0.439
Glycyl-L-glutamic acid	0.524	0.695	0.537	0.395
L-Histidine	1.034	2.327	1.439	0.742
Hydroxy-L-proline	0.836	0.552	0.587	0.610
L-Leucine	0.244	0.280	0.231	0.229
L-Ornithine	0.552	0.281	0.496	0.597
L-Phenylalanine	0.124	0.359	0.456	0.559
L-Proline	1.009	1.546	0.813	0.678
L-Pyroglutamic acid	0.731	1.086	0.712	0.257
D-Serine	1.090	1.001	1.111	1.390
L-Serine	2.256	1.076	0.578	0.553
L-Threonine	0.087	0.087	0.294	0.399
D,L-Carnitine	0.534	0.779	0.704	0.284
γ-aminobutyric acid	0.780	2.187	1.133	0.743
Urocanic acid	0.091	1.193	1.447	0.541
Inosine	2.685	3.999	0.927	0.923
Uridine	0.474	0.583	0.924	1.731
Thymidine	0.970	0.512	0.800	0.794
Phenylethylamine	0.091	0.216	0.209	0.077
Putrescine	0.776	0.807	0.946	0.548
2-Aminoethanol	0.443	0.204	0.297	0.274
2,3-Butanediol	0.671	1.095	0.536	0.571
Glycerol	1.341	0.630	0.952	1.023
D,L-alpha-Glycerol phosphate	2.221	0.255	1.406	1.008
Glucose-1-phosphate	1.682	0.964	2.104	1.741
Glucose-6-phosphate	0.095	0.115	2.241	1.842

Table K.3. The statistical factor analysis for the principal components.

STAT. FACTOR ANALYSIS	Factor Scores (data.sta) Rotation: Varimax raw Extraction: Principal components		
Case	Factor 1	Factor 2	Factor 3
1	-.78555	-.66394	-1.21744
2	.10938	-.36173	-1.62107
3	1.02740	3.46668	-.98720
4	.88472	2.97429	-.87240
5	-.63668	.69560	-.33527
6	-1.31525	1.07726	1.47121
7	-.26395	.29609	-.41795
8	1.56911	2.59974	-.40717
9	.15981	-.92643	-.69415
10	.77179	-.64560	1.20990
11	.65301	-1.10938	-.43810
12	1.50970	-1.59709	.73513
13	-.64001	-.62150	-1.00777
14	1.22676	.04608	1.02917
15	-.31382	.14858	.67761
16	1.60121	-.88272	.06100
17	.79677	-1.04145	.11119
18	1.17026	2.63268	.79000
19	-.25532	-.87846	.13874
20	2.07361	-1.61088	-.33126
21	.52722	-.68282	-1.92584
22	1.38663	1.84174	.10331
23	1.53396	-.00042	.09599
24	1.29120	-.55449	-.48716
25	1.37399	-1.52152	1.04096
26	2.57509	1.44064	-2.31099
27	-.05703	-.78282	.46071
28	1.08124	-1.71693	1.09193
29	.23347	-1.10451	.13031
30	1.05039	-1.40385	.84781
31	2.52066	.34172	.56105
32	2.25609	2.15355	-1.33545
33	-.31491	-.35512	-.63669
34	-.54634	-.64771	-1.04739
35	.06865	.34206	.34314
36	-.43208	-.24171	-.58979
37	-1.11367	.61116	.44876
38	-.46594	.05822	2.46680
39	-.03765	-.09668	.63237
40	-.70391	-.34312	-.97358
41	.69283	-1.45495	1.03095
42	1.07230	-.81217	.95863

Table K.3 (continued).

STAT. FACTOR ANALYSIS	Factor Scores (data.sta) Rotation: Varimax raw Extraction: Principal components		
Case	Factor 1	Factor 2	Factor 3
43	1.67348	.70953	1.52043
44	-.17502	-.66424	-1.09355
45	1.09382	-1.20987	.05584
46	-.72551	-.53123	-1.42399
47	-.79544	.30555	.16120
48	-1.22142	.62556	.72405
49	-.69824	-.55581	-.15345
50	-.86293	-.51575	-.90098
51	-.93058	-.55635	-1.38683
52	-.85342	.11793	1.14462
53	-.94820	-.58923	-.62723
54	.24984	.37001	.59961
55	-.83629	-.22474	-.34527
56	-.87388	.05642	.04072
57	-.41010	.58324	2.47894
58	-.41568	-.19425	2.00533
59	-1.20767	-.32760	-.14812
60	-.52448	.52717	1.13519
61	-.91784	.98513	1.09936
62	-1.07809	.51092	.03167
63	-.28206	-.41801	-.19722
64	-.86635	-.08188	-.42415
65	-.99660	.62020	.62760
66	-.91850	.31399	.16721
67	-.77136	.02650	-.20942
68	.09077	.39321	.45100
69	-.23122	.40525	-.53205
70	-.43884	.79710	.47866
71	.03588	-.22281	-1.64530
72	-.50839	-.08254	-.79865
73	-1.24532	.91767	1.99504
74	-.44068	-.35394	-.47316
75	-.83643	-.42754	-1.17381
76	-.48220	-.40693	-.92476
77	-.64994	-.54475	-.70467
78	-.87556	.55045	.15908
79	-1.23228	.24607	.13807
80	.54706	-.20744	.14283
81	-.11960	.95872	-1.62670

Table K.3 (continued).

STAT. FACTOR ANALYSIS	Factor Scores (data.sta) Rotation: Varimax raw Extraction: Principal components		
Case	Factor 1	Factor 2	Factor 3
82	-.51532	-.66416	-1.21677
83	-1.15727	-.05848	.09159
84	-1.05074	.65809	1.46551
85	-1.09127	-.24631	2.01651
86	-.65790	2.87559	.24210
87	.69662	-.81394	-.16691
88	-.15253	-.23080	-.51599
89	-1.09267	-.49275	-1.03243
90	-.76124	-.17018	.49644
91	-.86273	-.40814	-1.11151
92	-.84853	.16442	-.38765
93	.59845	.04319	-.90042
94	.86991	.24872	-.90004
95	1.15905	-.18498	1.56704
96	2.21029	-1.29405	1.18540

STAT. FACTOR ANALYSIS	Factor Loadings (Varimax raw) (data.sta) Extraction: Principal components (Marked loadings are > .700000)		
Variable	Factor 1	Factor 2	Factor 3
MN1	.894985 *	.261811	.259054
CF1	.905074 *	-.001734	.299813
ML1	.734180 *	.613587	.111571
MN2	.869239 *	.400600	.206131
PC1	.415499	.862977 *	.010536
CF2	.580817	.340426	.695500
ML2	.830726 *	.454032	.080195
PC2	.076324	.899030 *	.320967
Expl.Var	4.120670	2.480537	.805217
Prp.Totl	.515084	.310067	.100652

STAT. FACTOR ANALYSIS	Eigenvalues (data.sta) Extraction: Principal components			
Value	Eigenval	% total Variance	Cumul. Eigenval	Cumul. %
1	5.926241	74.07802	5.926241	74.07802
2	1.111390	13.89238	7.037632	87.97040
3	.368792	4.60990	7.406424	92.58030

IMAGE EVALUATION
TEST TARGET (QA-3)

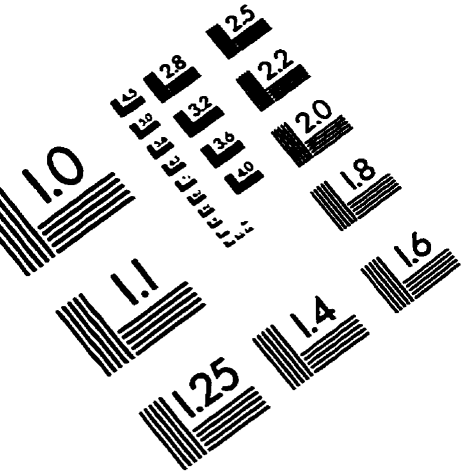

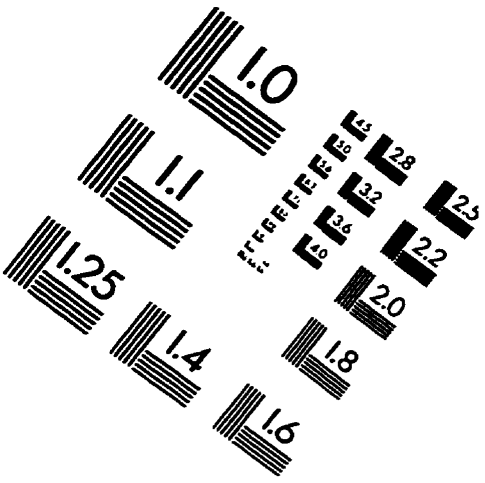

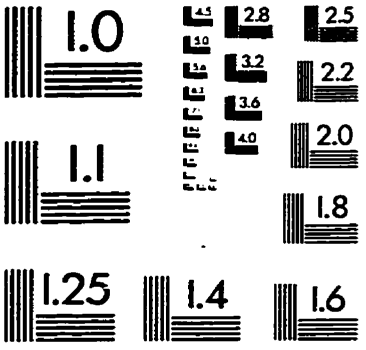

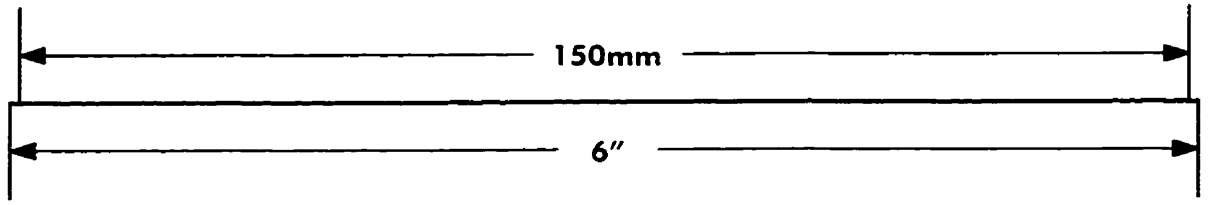

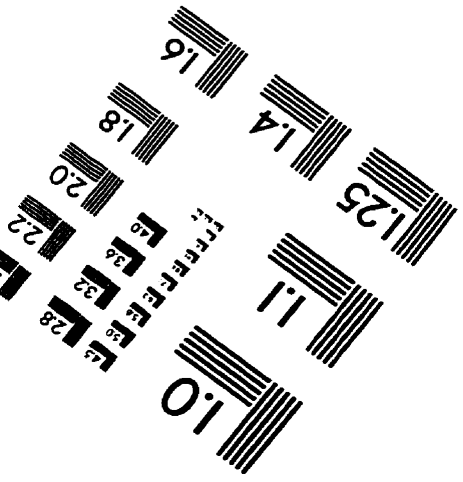

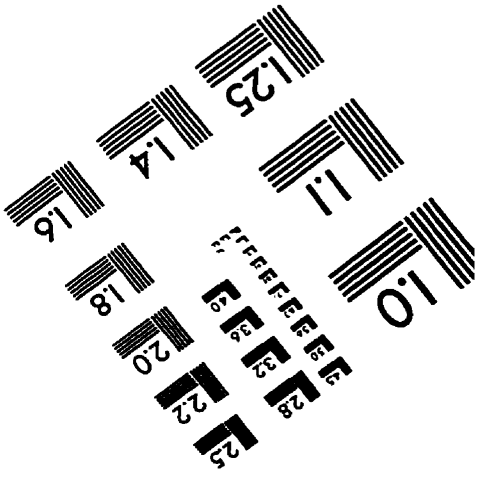

APPLIED IMAGE, Inc
1653 East Main Street
Rochester, NY 14609 USA
Phone: 716/482-0300
Fax: 716/288-5989